

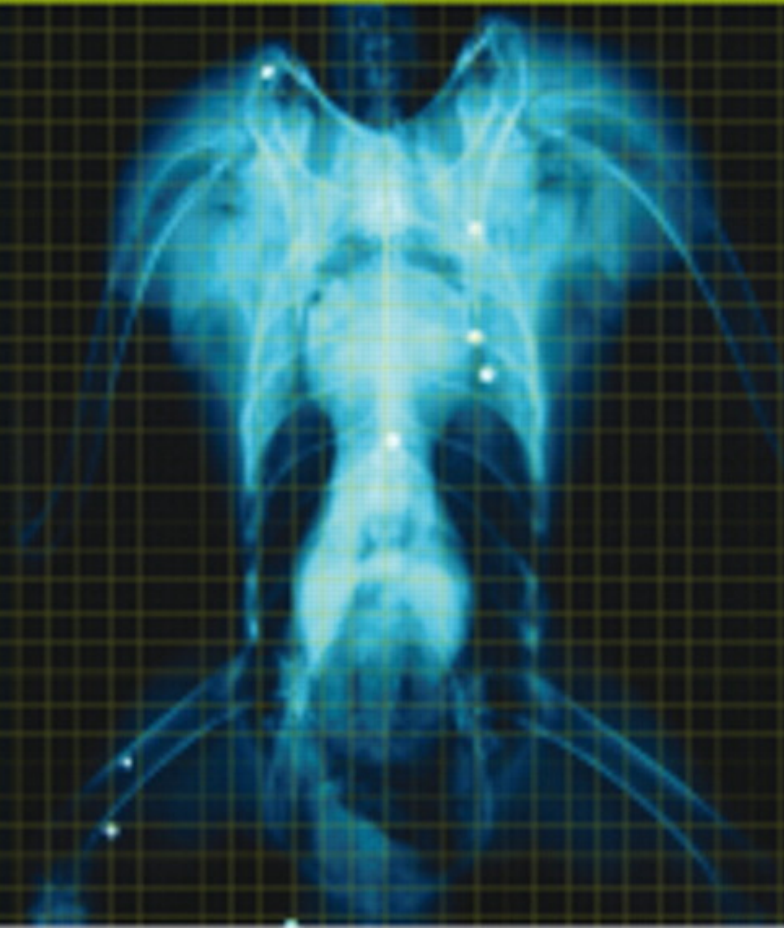
Anatomical and Clinical Radiology of Birds of Prey

including interactive
advanced anatomical imaging

Jaime H. Samour
Jesus L. Naldo



SAUNDERS
ELSEVIER



Anatomical and Clinical Radiology of Birds of Prey

For Elsevier:

Commissioning Editor: Joyce Rodenhuis

Development Editor: Rita Demetriou-Swanwick

Project Manager: David Fleming, Christine Johnston

Designer: Andy Chapman

Illustrations Manager: Bruce Hogarth

Illustrator: Samantha Elmhurst

6670 -
100. 8. 19

#1307655

636.686937
A435
2007

Anatomical and Clinical Radiology of Birds of Prey

including interactive advanced anatomical imaging

Jaime H. Samour MVZ, PhD, Dip ECAMS

Jesus L. Naldo DVM

Wrsan, Wildlife Division
PO Box 77338
Abu Dhabi
United Arab Emirates



嘉義大學新民圖書館



E 0072350

SAUNDERS
ELSEVIER

An imprint of Elsevier Limited

© 2007, Elsevier Limited. All rights reserved.

No part of this publication may be reproduced, stored in a retrieval system, or transmitted in any form or by any means, electronic, mechanical, photocopying, recording or otherwise, without the prior permission of the Publishers. Permissions may be sought directly from Elsevier's Health Sciences Rights Department, 1600 John F. Kennedy Boulevard, Suite 1800, Philadelphia, PA 19103-2899, USA; phone: (+1) 215 239 3804; fax: (+1) 215 239 3805; or, e-mail: healthpermissions@elsevier.com. You may also complete your request on-line via the Elsevier homepage (<http://www.elsevier.com>), by selecting 'Support and contact' and then 'Copyright and Permission'.

First published 2007

ISBN-13: 978 0 7020 2802 1

ISBN-10: 0 7020 2802 9

British Library Cataloguing in Publication Data

A catalogue record for this book is available from the British Library

Library of Congress Cataloging in Publication Data

A catalog record for this book is available from the Library of Congress

Notice

Knowledge and best practice in this field are constantly changing. As new research and experience broaden our knowledge, changes in practice, treatment and drug therapy may become necessary or appropriate. Readers are advised to check the most current information provided (i) on procedures featured or (ii) by the manufacturer of each product to be administered, to verify the recommended dose or formula, the method and duration of administration, and contraindications. It is the responsibility of the practitioner, relying on their own experience and knowledge of the patient, to make diagnoses, to determine dosages and the best treatment for each individual patient, and to take all appropriate safety precautions. To the fullest extent of the law, neither the publisher nor the author assumes any liability for any injury and/or damage.

The Publisher

Printed in Spain

ELSEVIER

your source for books,
journals and multimedia
in the health sciences

www.elsevierhealth.com

Working together to grow
libraries in developing countries

www.elsevier.com | www.bookaid.org | www.sabre.org

ELSEVIER

BOOK AID
International

Sabre Foundation

The
publisher's
policy is to use
paper manufactured
from sustainable forests

Contents

Contributors vii

Foreword ix

Preface xi

Acknowledgements xiii

Dedications xv

Chapter 1 Introduction 1

Chapter 2 Radiographic procedures 3

Section 1: Restraint and positioning 3

Section 2: Conventional radiography 8

Section 3: Magnification radiography 9

Section 4: Contrast radiography 12

Chapter 3 Radiographic anatomy – general considerations 21

Section 1: Musculoskeletal system 21

Section 2: Gastrointestinal system 22

Section 3: Liver 23

Section 4: Spleen 23

Section 5: Respiratory system 23

Section 6: Heart and vascular system 24

Section 7: Urinary system 24

Section 8: Reproductive system 24

Section 9: Radiographic species catalog 25

Saker falcon (*Falco cherrug*) 25

Gyr falcon (*Falco rusticolus*) 46

Steppe eagle (*Aquila nipalensis*) 65

Palm nut vulture (*Gypohierax angolensis*) 83

Eurasian honey buzzard (*Pernis apivorus*) 103

Northern goshawk (*Accipiter gentilis*) 119

Red kite (*Milvus milvus*) 139

Common barn owl (*Tyto alba*) 159

Eurasian eagle owl (*Bubo bubo*) 175

Chapter 4 Clinical and pathological conditions 197

Section 1: Trauma-related medical conditions 197

Section 2: Management-related diseases 218

Section 3: Infectious diseases 230

Section 4: Degenerative diseases 249

Section 5: Neoplastic diseases 251

Chapter 5 Common diagnostic mistakes 253

Chapter 6 Advanced clinical anatomy imaging 261

Section 1: The importance of advanced diagnostic imaging in veterinary medicine 261

Section 2: Material and methods 262

Section 3: The Digital Imaging and Communications in Medicine standard (DICOM) 264

Section 4: Advanced diagnostic imaging techniques 266

Index 275

Contributors

Jaime Samour MVZ, PhD, Dip ECAMS

Wrsan, Wildlife Division
PO Box 77338
Abu Dhabi
United Arab Emirates

Jesus L. Naldo DVM

Wrsan, Wildlife Division
PO Box 77338
Abu Dhabi
United Arab Emirates

Paolo Zucca DVM, PhD

Laboratory of Animal Cognition and Comparative
Neuroscience
Department of Psychology, University of Trieste
via S. Anastasio, 12 - 34100 Trieste
Italy

Professor Roberto Pozzi-Mucelli MD, PhD

Department of Morphological-Biomedical Science
Faculty of Medicine, University of Verona
P. le Scuro 10, Policlinico Borgo Roma, Verona
Italy

Donatella Gelli DVM

Department of Clinical Sciences
Faculty of Veterinary Medicine
University of Padua, Viale dell'Università 16
Agripolis, 35020 Legnaro (PD)
Italy

Mauro Delogu DVM, PhD

Department of Public Veterinary Health and Animal Pathology
Faculty of Veterinary Medicine
University of Bologna
via Tolara di Sopra 50 - 40064
Ozzano Emilia, Bologna
Italy

Foreword

Veterinary science is an exciting, ever-changing and expanding subject. It seems that almost daily more and more is known about an ever greater range of creatures. Birds of prey have fascinated mankind for millennia as can be seen from the mummified remains of falcons found in ancient Egypt. Veterinary interest in this group of birds was first encapsulated by John Cooper in 1978 when he produced his first book: *Veterinary Aspects of Captive Birds of Prey*. Since then there have been many books and conferences centered on this group of birds. Dedicated falcon hospitals have been pioneered in the Middle East and the group of veterinarians that work in these hospitals has made many contributions to our knowledge.

However, in spite of nearly 30 years of veterinary research, there are still huge gaps in our basic knowledge about raptors. These gaps are not easily addressed in this day and age: conferences and research institutes require the presentation of 'cutting-edge topics' and there is the constant quest to present 'new' topics based on small numbers of cases. It is, therefore, refreshing (as well as invaluable) that two well-known and well-respected specialist falcon veterinarians, Jaime Samour and Jesus Naldo, have produced this book – *Anatomical and Clinical Radiology of Birds of Prey* – which is dedicated to filling a major gap in our

knowledge with fundamental information. It is virtually impossible to appreciate the abnormal without a comprehensive knowledge of the normal, especially in the group of birds lumped together as birds of prey. Comprehensive sets of radiographs are shown of clinically normal representative species from hawks, falcons and owls, nine different species are illustrated. The publication contains well-produced radiographs accompanied by line drawings, with adequate sets of labels to show the anatomy, are an incredibly useful resource. Within this book, these illustrations are the building block for understanding the pathology associated with the multitude of diseases seen in these birds. In the second part of this book, the most common disease processes that affect birds of prey are depicted through color photographs. Each disease has accompanying radiographs taken of that particular case, which is extremely useful.

I hope that the many veterinarians interested in treating birds of prey will enjoy and make as much use of this book, as I know I will.

Nigel Harcourt-Brown
November 2006
Harrogate, UK

Preface

Modern raptor medicine, as we know it today, started with the publication of the book entitled *Veterinary Aspects of Captive Birds of Prey* by Professor J. E. Cooper in 1978. This was the culmination of years of interest and dedication to raptors by a man with an unselfish and almost pathological passion to teach and share his knowledge with others. Today raptor medicine is one of the fastest developing specialties of avian medicine with well-established raptor research institutions, raptor rescue and rehabilitation centers throughout the world, and highly specialized falcon hospitals continuing to sprout across the Middle East. *Anatomical and Clinical Radiology of Birds of Prey*, including interactive advanced anatomical imaging, intends to contribute to the increasing demand for specialist text books in raptor medicine. Our intention was to produce a reference atlas that can be used by students, professionals and aspiring specialists to evaluate

health and disease in raptors. The book offers the reader several attractive features. In addition to all the anatomical and clinical imaging presented, color photographs, for instance, are used liberally to demonstrate radiographic procedures, the species depicted in the anatomical section and the clinical and pathological conditions included. For the first time, we also offer interactive advanced clinical anatomy using ultrasonography, computed axial tomography and magnetic resonance imaging of two different birds of prey. We sincerely hope that this book will go a long way to help promoting raptor medicine as a specialty and to continue the mission started by a man with an unselfish and almost pathological passion...

Jaime H Samour, Jesus L Naldo
Abu Dhabi, United Arab Emirates
November 2006

Acknowledgements

The authors would like to thank HRH Prince Fahad bin Sultan bin Abdulaziz Al Saud for continuing support to the clinical and research program of the Hospital; to all the technical staff for assistance provided in handling the birds and obtaining the radiographs; to Generoso G. Quiambao for his commendable technical support in preparing the photographs displayed in the book.

Also we would like to thank Dr Paolo Zucca, Laboratory of Animal Cognition and Comparative Neuroscience, Department of Psychology, University of Trieste, Trieste, Italy; Dr Donatella Gelli, Department of Clinical Sciences, Faculty of Veterinary Medicine, University of Padua, Legnaro (PD), Italy; Dr Mauro Delogu, Department of Public Veterinary Health and Animal Pathology, Faculty of Veterinary Medicine,

University of Bologna, Bologna, Italy; Professor Jean-Michel Hatt, Division of Zoo Animals and Exotic Pets, Vetsuisse Faculty, University of Zürich, Zürich, Switzerland; Dr Marino García-Montijano, T. Álvarez and P. Prieto, Consejería de Medio Ambiente y Ordenación del Territorio, Comunidad de Madrid, Spain; Dr Tom Bailey, Dubai Falcon Hospital, Dubai, UAE; Dr Jorge García de la Fuente, Dr Angel Luis Sánchez and the Unidad de Cirugía y Radiología (Departamento de Patología Animal: Medicina Animal) de la Facultad de Veterinaria de León, Spain for the photographic and radiographic materials they provided.

Lastly, the authors would like to thank all the staff at Elsevier, especially Rita Demetriou-Swanwick, Joyce Rodenhuis, David Fleming and Christine Johnston.

Dedications

J. Samour: To my sons, Omar and Adam and daughters, Miriam and Yasmeeen with all my love and to my wife Merle for her unwavering support over the years and for inspiring me to be a better man.

J. Naldo: This book is dedicated with love to my wife Cristina for standing by me throughout the years, to my wonderful children, Michael John, Jesse Gabriel and Bea Kristine and to my parents for the upbringing and education they provided me.

Chapter 1 Introduction

The history of X-rays

The history of radiography begins with Wilhelm Conrad Röntgen, born on 27th March 1845 in Lennep in the German Rhineland. At the early age of 3, his parents move to Apeldoorn in The Netherlands. Later, the young Röntgen began studying at a technical school in Utrecht, where he was expelled after refusing to name a fellow student who had drawn a caricature of a teacher. In early 1865, Röntgen attended the University of Utrecht, but not as a regular student, since he lacked the necessary qualifications. Later that year, he became a full-time student of mechanical engineering at the Zurich Polytechnic School in Switzerland. At this Polytechnic School he became the protégé of Augustus Kundt, the Professor of Physics at the School, who inspired him to follow a career in physics. Röntgen became his assistant and later moved with him to the newly created University of Strasbourg. Between 1875 and 1888 he took different posts at the Hohenheim Agricultural Academy in Wurtemberg, University of Strasbourg and Giessen University. In 1888 he became Professor of Physics and Director of the Institute of the University of Wurzburg. In this new post, Röntgen, in common with many other scientists of that era, turned his attention to the study of cathode rays.

Working late in his laboratory the evening of 8th November 1895, he had a Crookes tube (a cathode-ray generator vacuum tube invented by Sir William Crookes, 1832–1919) covered with black card to mask the fluorescent glow on the glass. When the tube was connected, he noticed that some crystals of barium platino-cyanide on a nearby table became fluorescent. He then observed that a screen coated with barium platino-cyanide held near the tube fluoresced all over, but if a metallic object was placed between the tube and the screen, it cast a shadow. Further investigation demonstrated that some unknown rays were generated at the point of contact of the cathode-ray beam on the interior of the vacuum tube, that these were not deflected by magnetic fields and that these could penetrate solid matter. Using the same procedure, 1 week later he obtained an image of the hand of his wife that clearly showed her wedding ring and the bones. This was the first radiograph ever obtained of a human being. Röntgen himself used the term X-rays (X-strahlen in German) because of the

nature of the rays was uncertain. He submitted the first paper on X-rays to the President of the Physical Medical Society of Wurzburg on 28th December 1895. In January 1896, Röntgen was invited to give a lecture of his discovery to the Physical Medical Society of Wurzburg. During the meeting, Röntgen obtained an X-ray photograph of the hand of the anatomist A. von Kolliker, who was in the audience. After completing the image, von Kolliker proposed that the new rays should be called Röntgen-rays. In Germany the name Röntgen-rays was adopted almost immediately and remains in use even to this day.

In 1900, Röntgen moved from Wurzburg to take charge of the Physical Institute of the University of Munich. In 1901 he became the first Nobel laureate for physics. At his new post in Munich, he resumed his work on the physical properties of crystals. After his retirement in 1920, he was granted permission to use two rooms at the Institute where he continued working until a few days before his death on 10th February 1923.

Radiography as a diagnostic tool

Today, radiography is one of the most important diagnostic tools available to veterinary surgeons in the diagnosis of musculoskeletal disorders and diseases of the celomic cavity. Great advances have been made in the application of radiographic techniques to avian medicine in the past 25 years. This has been parallel to the development of high-frequency ultralight radiographic units, cassettes with high-definition screens, fast films and automatic developers. Radiographic techniques are useful in avian medicine for the primary diagnosis and as an adjunct to other diagnostic procedures, such as endoscopy and hematology, contributing to the differential diagnosis. In addition, radiography can prove valuable for the monitoring of the progression of diseases and in evaluating the efficiency of therapeutic regimens. This non-invasive diagnostic technique can be used with patients of all sizes and with the advent of safe and efficient inhalation anesthetic agents, such as isoflurane, radiography in birds is now an uneventful procedure.

Reference

Bowers B 1970 X-rays their discovery and applications. HMSO, Science Museum of London, London, UK

Chapter 2 Radiographic procedures

SECTION 1 Restraint and positioning

Anesthesia

Adequate restraint for radiography is critical if high-quality diagnostic radiographs are to be obtained. Inhalation anesthesia with isoflurane (IsoFlo, Abbott Laboratories, North Chicago, IL 60064, USA) is the safest method of restraining birds of prey.

Whole-body ventrodorsal and lateral positions (Figs 2.1 & 2.2)

Survey radiographs of the whole body in the ventrodorsal and lateral views are taken of each bird. Detailed radiograph of an extremity (head, neck, wing, foot) is obtained when indicated. Perfect positioning for a whole-body projection can be achieved with the following procedure (Baumgartner 1991, Harcourt-Brown 1996, Krautwald-Junghanns 1996, Krautwald-Junghanns & Trinka 2000, McMillan 1994, Naldo 2000, Romagnano 1997, Smith & Smith 1997).

In the ventrodorsal view:

- the bird is placed on dorsal recumbency
- the keel should be superimposed over the vertebral column
- both wings are slightly extended laterally and secured with masking tape
- both legs are pulled backwards, positioned symmetrically and secured with masking tape on the tarsometatarsus
- center the primary beam over the patient at the point of the sternum and collimate to reduce scatter.

In the lateral view:

- the bird is usually placed on left-to-right lateral recumbency
- the hip and shoulder joints should be superimposed
- the wings should be extended dorsally, with the lower wing placed slightly cranial to the upper wing to permit differentiation of right from left
- the upper wing is secured with masking tape across the carpometacarpal joints



Fig. 2.1 Positioning technique for a ventrodorsal survey radiograph of a saker falcon (*Falco cherrug*). The bird is placed on dorsal recumbency. The keel should be superimposed over the vertebral column. The legs are pulled backwards and secured with masking tape on the tarsometatarsus. Both wings are slightly extended and may be secured with masking tape.

- foam padding should be placed between the wings to prevent over-extension
- both legs can be extended caudally or the dependent leg can be positioned cranially to the contralateral leg and secured at the tarsometatarsus with masking tape
- the X-ray beam is centered on the midline cranial to the caudal tip of the sternum.

SECTION 1 RESTRAINT AND POSITIONING



Fig. 2.2 Positioning technique for a lateral survey radiograph of a saker falcon (*Falco cherrug*). The bird is placed on right lateral recumbency. The legs are extended caudally with the dependent leg positioned cranially to the other leg and secured with masking tape on the tarsometatarsus. Both wings are extended dorsally and secured with masking tape.



Fig. 2.3 Positioning technique for ventrodorsal radiograph of the wing of a gyr falcon (*Falco rusticolus*). The bird is placed on dorsal recumbency. The legs are pulled backwards and secured with masking tape on the tarsometatarsus. The wing is fully extended and secured with masking tape.

SECTION 1 RESTRAINT AND POSITIONING

Wing: ventrodorsal position (Fig. 2.3)

A detailed radiograph of the wing can be taken in the ventrodorsal, 'stressed' and craniocaudal position.

In the ventrodorsal position:

- the bird is placed on dorsal recumbency
- both legs are pulled backwards, positioned symmetrically and secured with masking tape on the tarsometatarsus
- the affected wing is fully extended laterally and secured with masking tape on the metacarpals.

Wing: 'stressed' position (Figs 2.4–2.6)

A detailed radiograph of the wing in 'stressed' position may be beneficial to evaluate fractures or damage to the humerus, clavicle, coracoid or scapula:

- the bird is placed on dorsal recumbency
- both legs are pulled backwards, positioned symmetrically and secured with masking tape on the tarsometatarsus
- both wings are fully extended laterally, 'stressed' cranially, positioned symmetrically and secured with masking tape on the metacarpals.

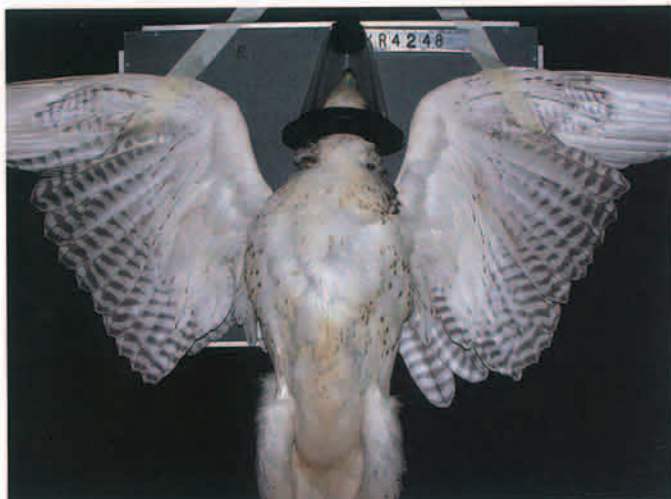


Fig. 2.4 Positioning technique for ventrodorsal radiograph of the shoulders of a gyrfalcon (*Falco rusticolus*). The bird is placed on dorsal recumbency. The legs are pulled backwards and secured with masking tape on the tarsometatarsus. The wings are extended and 'stressed' cranially and secured with masking tape on the metacarpals.

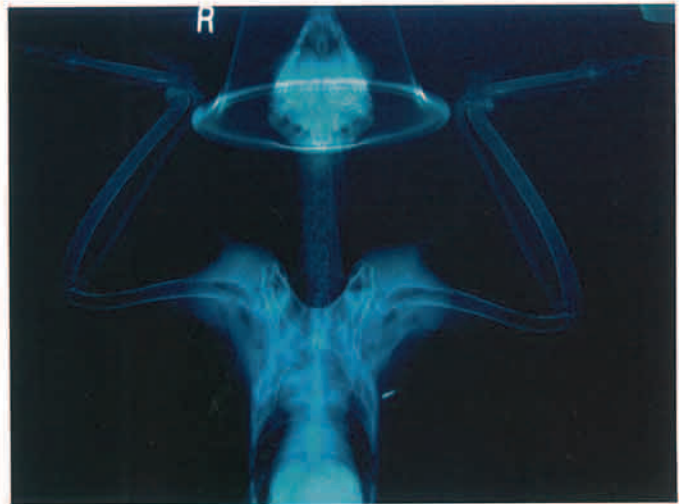


Fig. 2.5 Ventrodorsal radiograph of the shoulders of a lanner falcon (*Falco biarmicus*) in a 'stressed' position. Note the enhanced visualization of the structures of the shoulder joint.

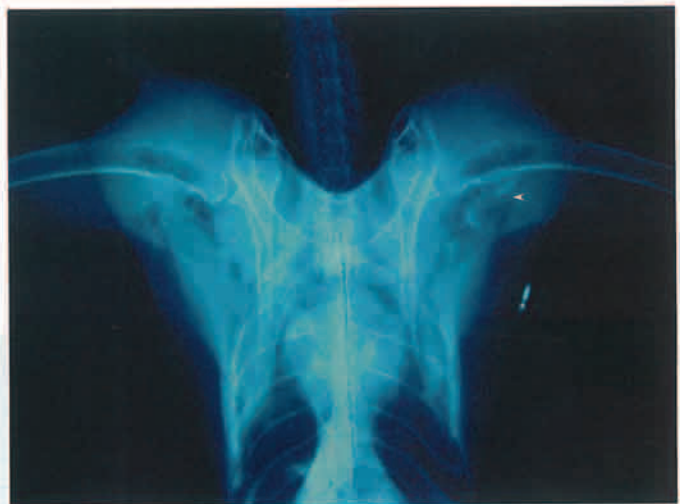


Fig. 2.6 Ventrodorsal radiograph of the shoulders of a saker falcon (*Falco cherrug*) in a 'stressed' position. The bird was presented because of drooped left wing. There is a fracture of the ventral tubercle of the left humerus (arrowhead). The radiopaque object on the pectoral muscle is a passive induce transponder (PIT) identification chip.

SECTION 1 RESTRAINT AND POSITIONING

Craniocaudal position

Pectoral girdle and pectoral limb (Fig. 2.7):

- the craniocaudal view may be beneficial, particularly to evaluate fractures of the wing or damage to the clavicle, coracoid, scapula or humerus
- rotate the head of the radiographic machine to center the horizontal beam between the radius and the ulna. A cassette holder or a stand with foam pads may help achieve this positioning
- an alternative method is to have an adequately protected technician hold the bird with the affected wing fully extended and head to the side
- true craniocaudal positioning results in superimposition of the antebrachial bones and all digits. This projection can also be achieved in an oblique position, which permits separation of the radius and ulna as well as the alular digits
- evidence of the pectoral muscles extending toward the humerus indicates the ventral surface of the wing.

Pelvic limb:

- the craniocaudal view of the pelvic limb is taken with the bird placed on dorsal recumbency
- both legs are pulled backwards, positioned symmetrically and secured with masking tape on the tarsometatarsus
- individual digits must be extended and secured with masking tape.

Caudoplantar position (Fig. 2.8)

- the caudoplantar view of the foot is beneficial to evaluate the digits, metatarsophalangeal joints and the sesamoid bone between the metatarsophalangeal joint of digit II and the flexor tendons. It is particularly useful in assessing chronic bumblefoot infection
- the bird is placed on ventral recumbency over a rolled towel
- the foot is positioned with the plantar surface as close as possible to the cassette
- all digits are secured with masking tape
- center the primary beam at the point of the metatarsophalangeal joint of digit I (hallux).

Standing position (Figs 2.9 & 2.10)

Survey radiographs of hooded birds of prey that cannot be anesthetized for some reason, e.g. anesthetic risks or simply because the owner refuses anesthesia, can be taken with the bird standing on a perch:

- radiographs can be obtained in the ventrodorsal or lateral positions
- a cassette should be placed on the holder or stand positioned as close as possible to the patient.



Fig. 2.7 Positioning technique for craniocaudal radiograph of the wing of a gyrfalcon (*Falco rusticolus*). The bird is held with the wing fully extended and the head to the side.

SECTION 1 RESTRAINT AND POSITIONING

- rotate the head of the radiographic machine to center the horizontal beam over the patient and collimate to reduce scatter
- this technique has its limitations and it can be used only on selected cases, e.g. some musculoskeletal disorders, lead pellets or fragments in the ventriculus, impaction and detection of a passive induced transponder (PIT).



Fig. 2.8 Positioning technique for caudoplantar radiograph of the foot of a gyrfalcon (*Falco rusticolus*). The bird is placed on ventral recumbency over a rolled towel. The foot is positioned with the plantar surface as close as possible to the cassette. All digits are secured with masking tape. Center the primary beam at the point of the metatarsophalangeal joint of digit I.



Fig. 2.9 Positioning technique for a survey radiograph of a saker falcon (*Falco cherrug*) in a standing position. The bird is placed standing on a custom-built stand or perch. A cassette is placed on a holder positioned as close as possible to the bird. This technique is used for birds that cannot be anesthetized; however, its use offer only limited diagnostic value.

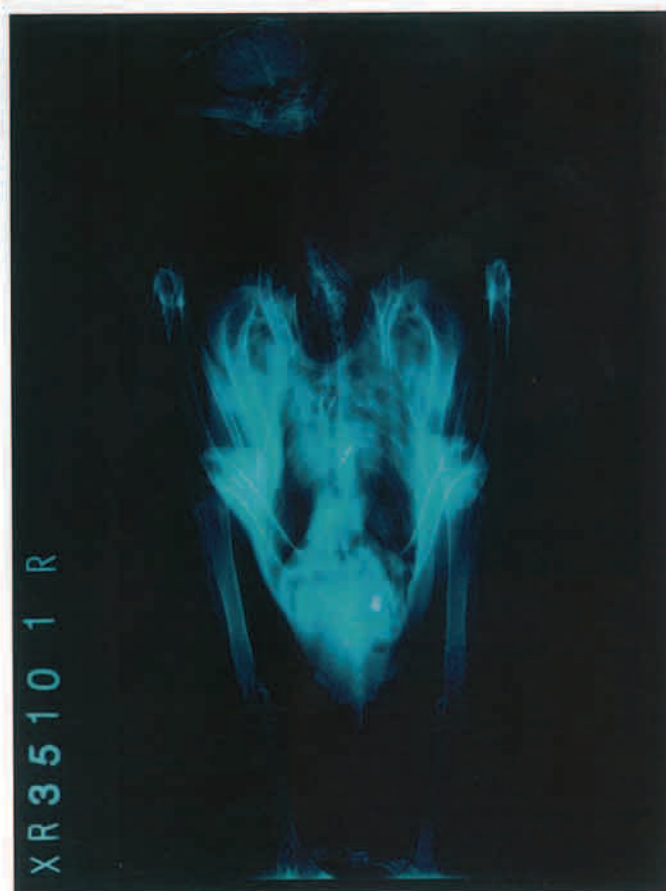


Fig. 2.10 Survey radiograph of a falcon taken in standing position. The bird was presented because of reduced appetite and drooped wings. Note the presence of a lead pellet in the ventriculus.

SECTION 2 Conventional radiography

Most survey radiographs included in this book were taken with a portable radiographic unit (ATOMSCOPE HF 80, Mikasa X-ray Co., Ltd., 13-2, Hongo 3-Chome, Bunkyo-ku, Tokyo 113, Japan). This unit has an X-ray tube voltage of 50–80 kV (5 kV step), fixed 15 mA current, exposure time of 0.02–1.98 s (0.02 s step), and focal spot of 1.0 mm. Screen films (MG-SR, Konica Medical Film, Konica Corp. No. 26-2, Nishishinjuku 1-Chome, Shinjuku-ku, Tokyo 163-0512, Japan) and cassettes (HR-Regular, Veterinary X-Rays, Seer Green, Beaconsfield, Bucks HP9 2QZ, England)

were used. The exposure settings used in all birds examined were 50–60 kV, 15 mA, and 0.04 s, with the exception of the golden eagle, where the exposure time was increased to 0.06 s. As a standard procedure, whole body (plus neck and proximal limbs) survey radiographs were taken in both ventrodorsal and left-to-right lateral positions. Detailed extremity (head, wing, leg) view was taken using 50–55 kV, 15 mA, and 0.04 s exposure settings (Table 2.1).

Table 2.1 Exposure guidelines for conventional radiography*

Species	Subject	Bodyweight (g)	kV	mA	Seconds	FFD
Steppe eagle	Whole body, proximal limbs	2500–3500	60	15	0.04	26 inches
Steppe eagle	Head, distal limbs	2500–3500	55–60	15	0.04	23.5–26 inches
Large-sized raptors	Whole body	1400–1500	55–60	15	0.04	23.5 inches
Medium-sized raptors	Whole body	800–1300	55	15	0.04	23.5 inches
Small-sized raptors	Whole body	<800	50	15	0.04	23.5 inches
Large-sized raptors	Extremities – head, feet, wing	1000–1500	55	15	0.04	23.5 inches
Small-to-medium-sized raptors	Extremities – head, feet, wing	<1000	50	15	0.04	23.5 inches

**Radiographs were recorded on standard double emulsion films (MG-SR, Konica Medical Film, Japan) in high definition screens in cassettes (HR-Regular, Veterinary X-rays, UK)
kV – kilovoltage; mA – milliAmpere (the ATOMSCOPE HF 80 Portable X-ray equipment has a constant setting of 15 mA); FFD – focal-to-film distance*

SECTION 3 Magnification radiography

Magnification or augmented radiography (Figs 2.11–2.14) will enhance visualization of special areas of interest (e.g. the infraorbital sinus, limbs, joints). The cost of magnification is a reduction in the spatial resolution or image sharpness, which is inversely proportional to the degree of magnification (Tell et al 2003).

Indications include:

- evaluating the nature and extent of craniofacial soft tissue or musculoskeletal abnormalities
- evaluating sinuses

- evaluating ocular and ear abnormalities
- evaluating limbs and joints.

Table-top technique (Table 2.2)

- the film cassette is placed on the top of the table
- the object to film distance (OFD) is increased by placing the patient on styrofoam blocks
- the focal to film distance (FFD) is decreased by lowering the tube housing closer to the film cassette.



Fig. 2.11 Positioning technique for obtaining a magnified view of the hips of a saker falcon (*Falco cherrug*). The object-to-film distance (OFD) was 12 inches and the focal-to-film distance (FFD) was 20 inches. The OFD was increased by placing the falcon on a styrofoam block.



Fig. 2.12 Positioning technique for obtaining a magnified view of the head of a gyr falcon (*Falco rusticolus*). The object-to-film distance (OFD) was 8 inches and the focal-to-film distance (FFD) was 20 inches. The OFD was increased by placing the falcon on a styrofoam block.

SECTION 3 MAGNIFICATION RADIOGRAPHY

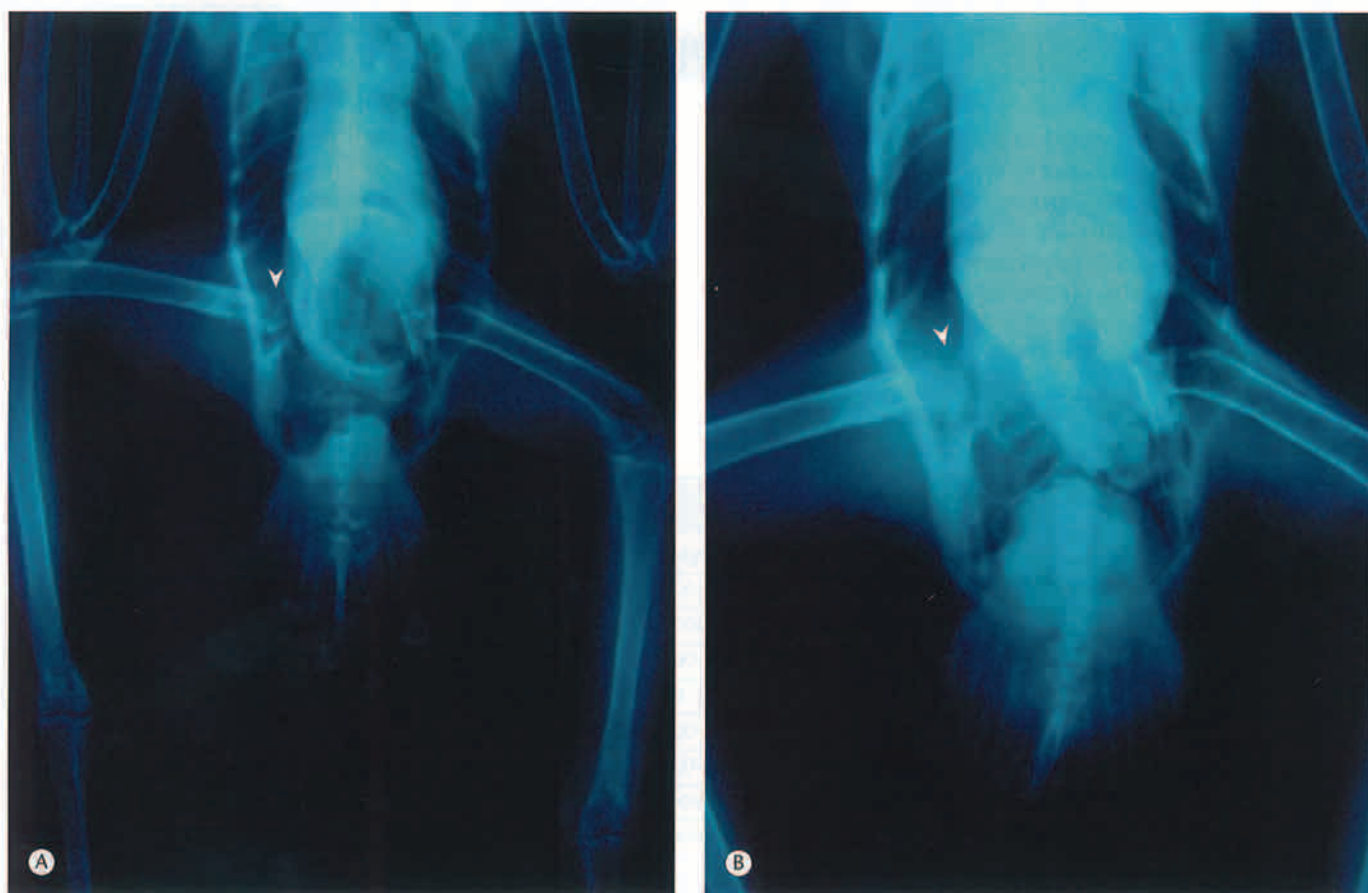


Fig. 2.13 (A) Non-magnified and (B) magnified ventrodorsal radiograph of the hips of a saker falcon (*Falco cherrug*), showing the typical signs of osteolysis of the right coxofemoral joint (arrowhead). The magnified view was obtained with an object-to-film distance (OFD) of 8 inches and focal-to-film distance (FFD) of 20 inches.

SECTION 3 MAGNIFICATION RADIOGRAPHY

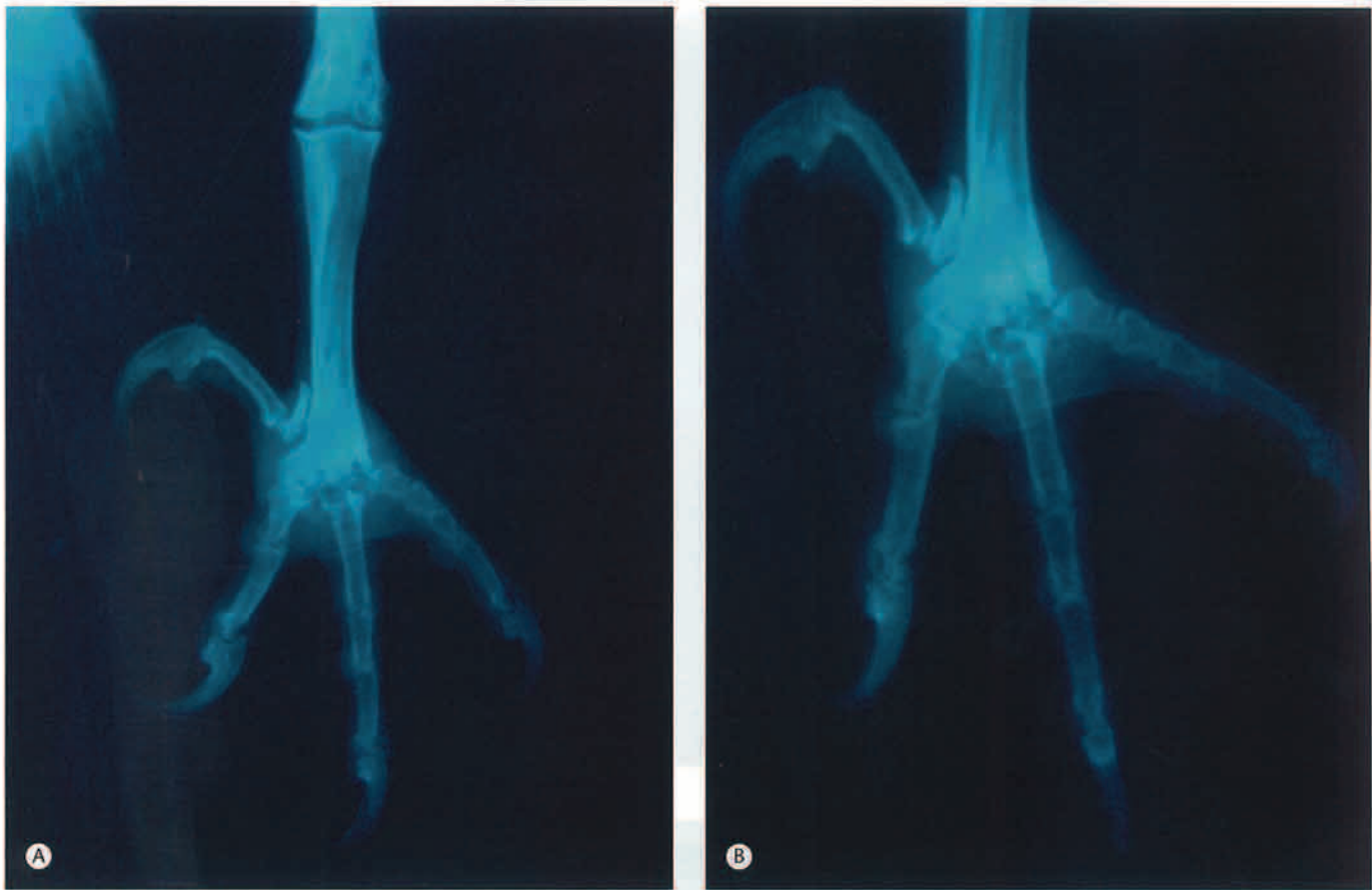


Fig. 2.14 (A) Non-magnified and (B) magnified craniocaudal radiograph of the foot of a saker falcon (*Falco cherrug*), showing typical changes associated with chronic bumblefoot infection. The magnified view was obtained with an object-to-film distance (OFD) of 8 inches and focal-to-film distance (FFD) of 20 inches.

Table 2.2 Exposure guidelines for magnification radiography*

Subject	Bodyweight (g)	kV	mA	Seconds	OFD	FFD
Whole body	1400–1500	55–60	15	0.04	12 inches	20 inches
Whole body	800–1300	55	15	0.04	12 inches	20 inches
Whole body	<800	50	15	0.04	12 inches	20 inches
Extremities – head, feet, wing	1000–1500	55	15	0.04	12 inches	20 inches
Extremities – head, feet, wing	<1000	50	15	0.04	12 inches	20 inches

*Radiographs were recorded on standard double emulsion films (MG-SR, Konica Medical Film, Japan) in high definition screens in cassettes (HR-Regular, Veterinary X-rays; UK)
 kV – kilovoltage; mA – milliAmpere (the ATOMSCOPE HF 80 Portable X-ray equipment has a constant setting of 15 mA); OFD – object-to-film distance; FFD – focal-to-film distance

SECTION 4 Contrast radiography

Contrast studies may be performed for the examination of the following:

- organ size
- organ shape
- organ position
- abnormal contents
- outline of an organ against neighboring organs
- determination of organ function
- thickness and condition of the wall of hollow structures.

Gastrointestinal contrast radiography

(Figs 2.15 & 2.16)

Indications for gastrointestinal contrast studies include:

- regurgitation
- persistent diarrhea

- constipation
- abnormal abdominal palpation
- abdominal enlargement
- abnormalities observed on survey radiographs.

Until recently, anesthesia was not recommended in contrast studies of the gastrointestinal tract, because it may lead to cessation of gastrointestinal motility. However, studies by Lennox and Crosta (2005) showed no significant differences in the progression of barium sulphate between radiographs collected with isoflurane and manual restraint alone.

The common contrast techniques used in avian gastrointestinal tract radiography include:

- gastrointestinal contrast with 25–45% barium sulphate, administered directly into the esophagus with a dosage of 20 ml/kg bodyweight. The contrast medium will be in the proventriculus and ventriculus within a few minutes and will reach the intestines in 30–60 min (Table 2.3). If the area of interest is the



Fig. 2.15 Lateral survey radiograph of a saker falcon (*Falco cherrug*) that was admitted because of vomiting, reduced appetite and constipation. Note the gaseous distention of the intestines (i). Proventriculus (p) and ventriculus (v).

SECTION 4 CONTRAST RADIOGRAPHY

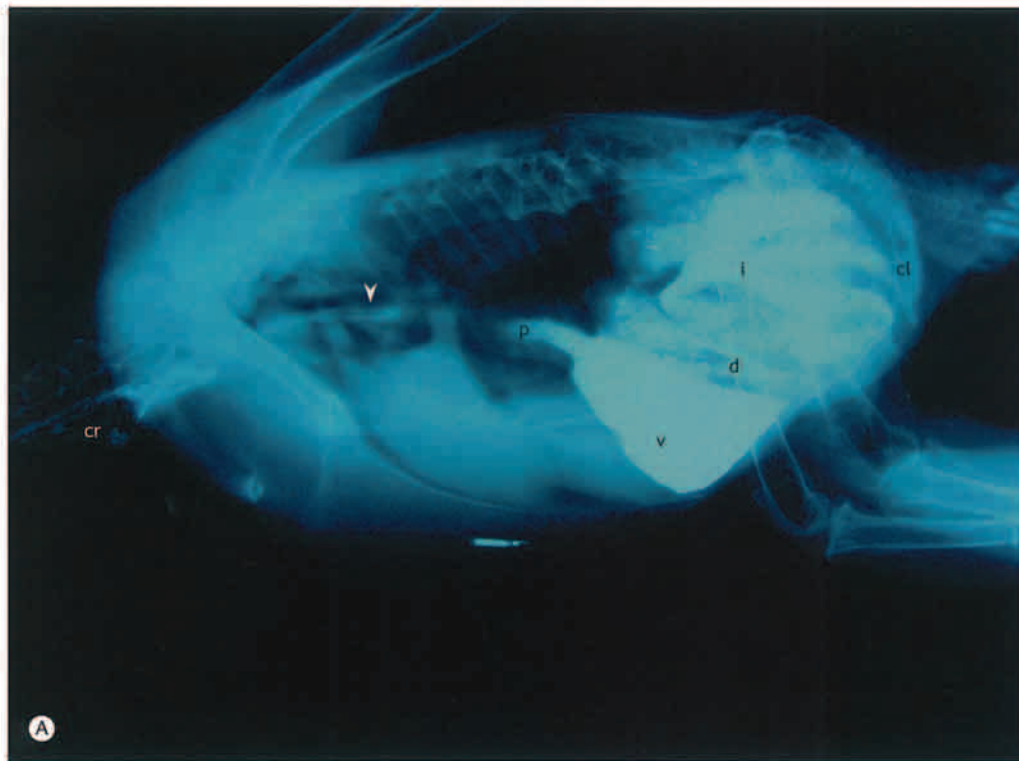
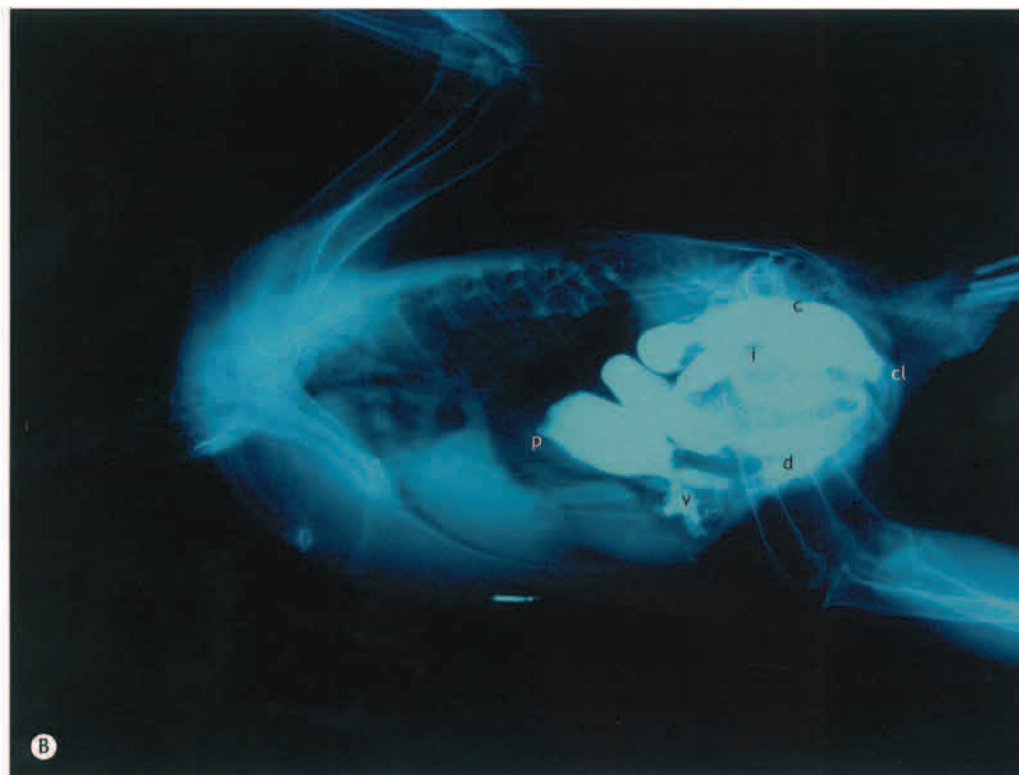


Fig. 2.16 Lateral gastrointestinal contrast radiograph of the same bird as in Figure 2.15 taken (A) 1 h, (B) 3 h.



SECTION 4 CONTRAST RADIOGRAPHY

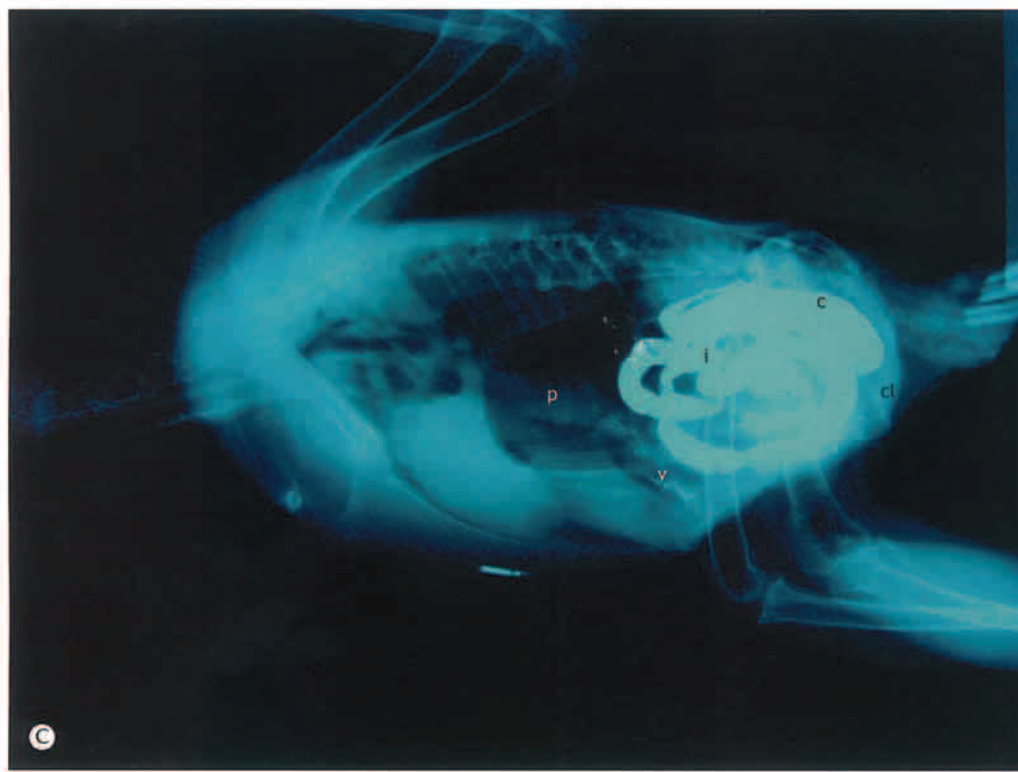


Fig. 2.16 (Cont'd) Lateral gastrointestinal contrast radiograph of the same bird as in Figure 2.15 taken (C) 9 h, and (D) 24 h after barium sulphate was administered by stomach gavage. There is delayed passage of the contrast media into the cloaca. In normal falcons, the contrast media should be present in the cloaca within 2–4 h and completely empty after 8 h. Crop (cr), proventriculus (p), ventriculus (v), duodenum (d), ilium and jejunum (i), colon (c), cloaca (cl) and thoracic esophagus (arrowhead).



SECTION 4 CONTRAST RADIOGRAPHY

Table 2.3 Barium sulphate transit times in hawk (Smith & Smith 1997)

Crop	0 min	Large intestine	1–1.5 h
Crop–stomach	10 min	Cloaca	2–4 h
Stomach	15 min	Empty	8 h
Small intestine	30 min		

lower gastrointestinal tract, the contrast medium can be administered directly to the ventriculus (Krautwald-Junghanns & Trinkaus 2000)

- double contrast with 25% barium sulphate (positive contrast medium), with a dosage of 10 ml/kg bodyweight given either oral or cloacal. Air (negative contrast medium) is introduced immediately after the administration of barium sulphate at 20 ml/kg bodyweight (Krautwald-Junghanns & Trinkaus 2000). This technique is useful for demonstration of the thickness and condition of the wall of the gastrointestinal tract and demonstration of the cloaca
- iohexol, a nonionic, low-osmolar, water-soluble, iodinated contrast medium may be used as an alternative to barium sulphate suspension for gastrointestinal-tract contrast studies. It should be used in suspected cases of intestinal perforation because iodine is less likely to cause peritonitis than barium sulphate. If aspirated, iohexol is absorbed from the celomic cavity with minimal tissue reaction. Iohexol has a rapid transit time through the avian gastrointestinal tract when compared with barium. However, iohexol studies often produce uneven luminal coverage and bubbles (Romagnano & Love 2000, Smith & Smith 1997).

Radiographic abnormalities may be defined by gastrointestinal contrast studies (McMillan 1994) showing:

- changes in the location, size or shape of abdominal organs
- the differentiation between the gastrointestinal tract and other organs
- increased or decreased motility
- increased or decreased luminal diameter
- mucosal irregularities
- filling defects
- changes in wall thickness
- extravasation of contrast media
- dilution of contrast with mucous or fluid.

Positive pressure insufflation contrast radiography (Figs 2.17 & 2.18)

In an anesthetized, intubated bird, air sacs can be insufflated manually to increase total air sac area, thus using air as a negative contrast medium to improve visualization of internal organs and their borders on radiographs (Sherrill et al 2001):

- once anesthetized, birds are intubated with a semiflexible silicone endotracheal tube and maintained at a surgical plane of anesthesia
- a rebreathing circuit fitted with a ventilation bag (1L) and a manometer (units in cm of water) is used
- whole-body radiographs are taken without and then with positive pressure insufflation (PPI)
- PPI at 20 cm of water pressure is applied manually to the ventilating bag of a closed rebreathing circuit while radiograph is taken.

Urography (Figs 2.19 & 2.20)

There are very few indications for urography in birds, because gross and histologic characteristics of the kidney cause the resulting images to provide relatively little useful information. However, it can be used to define renal dimensions or masses. Indications for urography include polyuria/polydipsia and non-specific clinical signs of leg paresis or joint swelling (Smith & Smith 1997).

For urogenital tract contrast radiography the agent used is 70–80% organic iodine compound or a compound with 300–400 mg iodine/ml with a dosage of 700–800 mg iodine/kg bodyweight, which is warmed to body temperature and injected intravenously. Ventrodorsal and lateral radiographs are obtained immediately and at 1-, 2-, 5-, 10- and 20-minute intervals (Krautwald-Junghanns & Trinkaus 2000, McMillan 1994).

Angiography (Fig. 2.21)

Angiography could be an important diagnostic tool for the detection of cardiovascular disease in birds. It had been used in the diagnosis of aneurysm of the right coronary artery in a white cockatoo (*Cacatua alba*) (Vink-Nootebom et al 1998) and atherosclerosis of the aorta and brachiocephalic arteries in a severe macaw (*Ara severa*) (Phalen et al 1996). Fluorescein angiography was used to examine the blood supply of the eyes of various raptors (Korbel et al 2000).

SECTION 4 CONTRAST RADIOGRAPHY

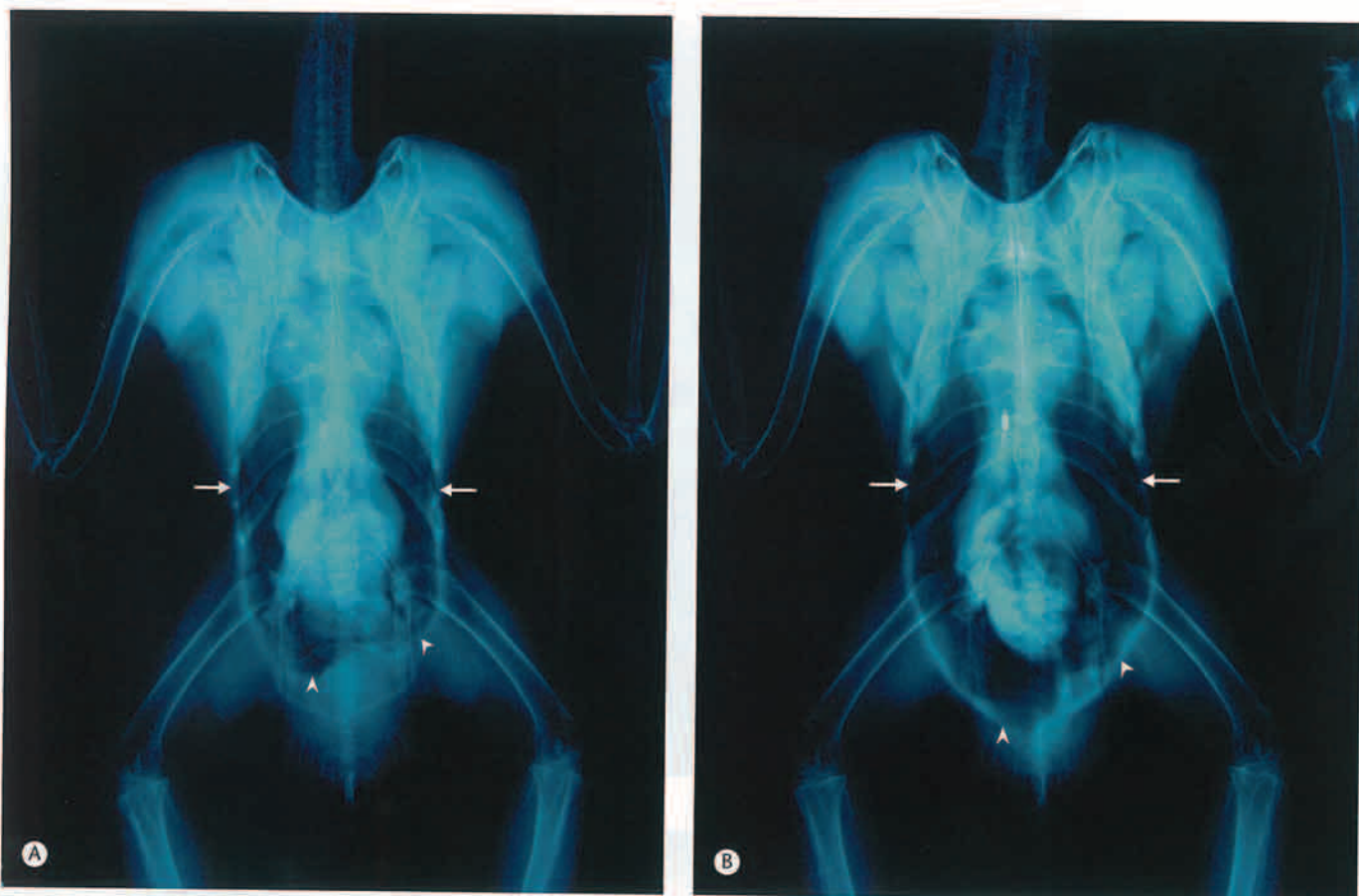


Fig. 2.17 (A) Ventrodorsal survey radiograph and (B) ventrodorsal positive-pressure insufflation (PPI) radiograph of an anesthetized, intubated saker falcon (*Falco cherrug*). Note enhanced visualization of internal structures, including the thoracic (arrows) and abdominal (arrowheads) airsacs, as a result of PPI.

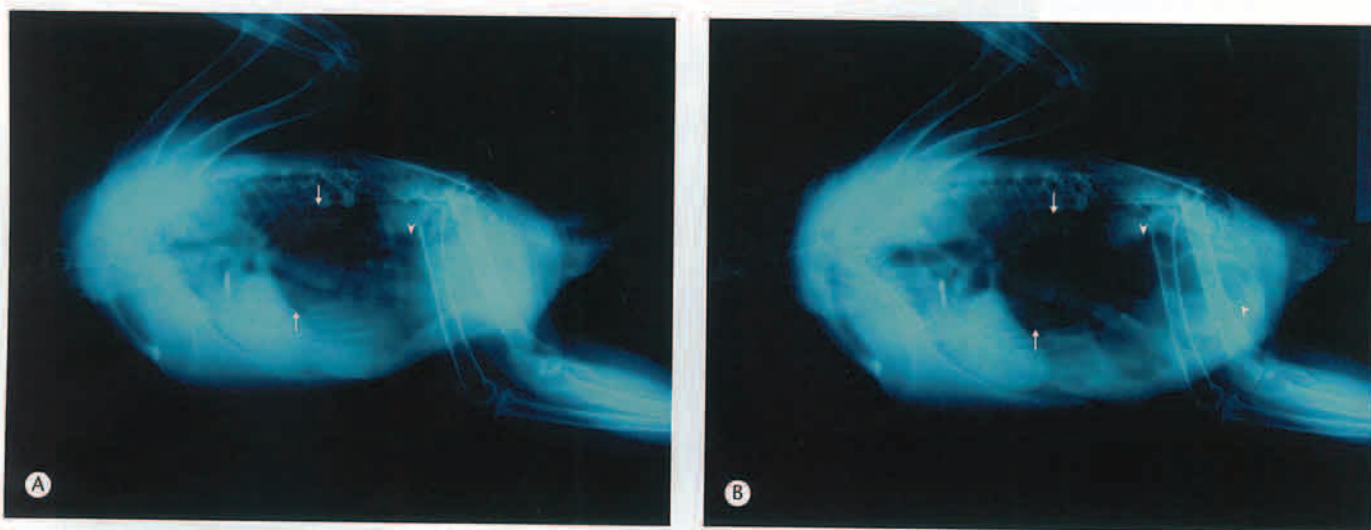


Fig. 2.18 (A) Lateral survey radiograph and (B) lateral PPI radiograph of an anesthetized, intubated saker falcon (*Falco cherrug*). Note enhanced visualization of internal structures, including the thoracic (arrows) and abdominal (arrowhead) airsacs, as a result of PPI.

SECTION 4 CONTRAST RADIOGRAPHY

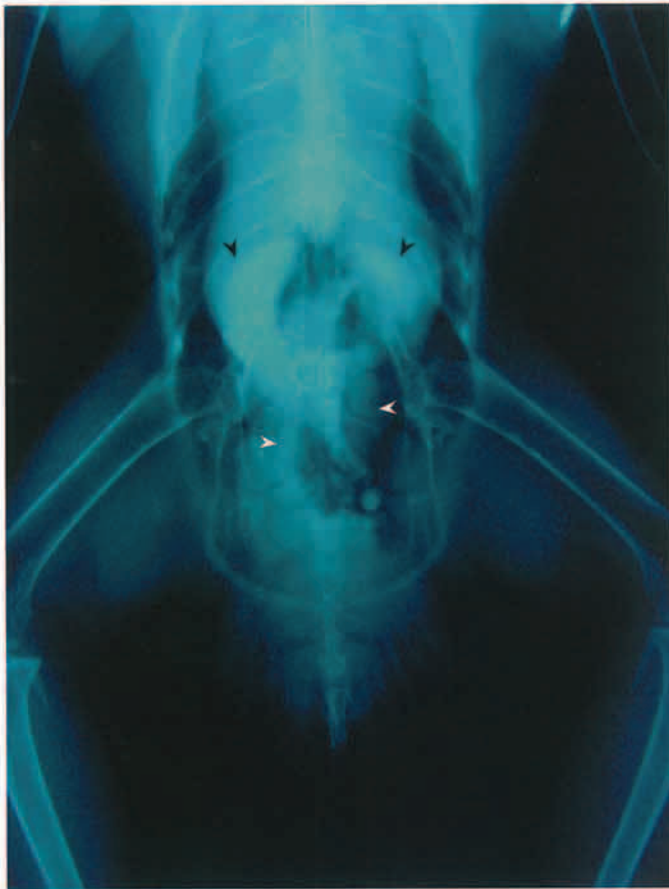


Fig. 2.19 Ventrodorsal survey radiograph of a clinically normal peregrine falcon (*Falco peregrinus*). Kidney, cranial portion (black arrowheads); kidney, caudal portion (white arrowheads).

Myelography (Fig. 2.22)

Abnormalities that can be detected by myelography include spinal cord compression, spinal trauma, or space occupying masses. Patients must be anesthetized for this procedure. A 25-gauge spinal needle is carefully inserted

at the thoracosynsacral junction and 0.8–1.2 ml/kg of non-ionic iodinated material is injected into the subarachnoid space (Harr et al 1997). Alternatively, contrast material can be injected directly into the cerebellar medullary cistern (McMillan 1994).

Radiographic interpretation

A systematic approach to film interpretation is important in order to reach a correct diagnosis. Develop your own standard procedure for evaluating films so that you do not just focus on the most obvious lesion and perhaps overlook more subtle changes. A useful technique is to first assess the film for overall radiographic quality from a technical viewpoint, then work sequentially through each body system. The authors use an organ to organ-system approach, proceeding from cranial to caudal, evaluating the head and neck, skeletal system, respiratory, cardiovascular, gastrointestinal, other celomic organs, and genitourinary systems.

Silverman (1990) recommends the following analysis:

- skeletal – skull, spine, pectoral girdle, pelvic girdle, wings and legs
- cardiovascular – heart and greater vessels
- respiratory – nasal sinuses, mouth, trachea, syrinx, lungs and air sacs
- gastrointestinal – mouth, crop, esophagus, proventriculus, ventriculus, intestines and cloaca
- genitourinary – pelvic region, kidneys, abdomen and cloaca
- accessory organs – liver and spleen.

The radiographs are scrutinized according to the following criteria (Baumgartner 1991):

- size of the organ
- density of organs and parts of organs
- structure of organs
- evaluation of the contents of the gastrointestinal tract.

SECTION 4 CONTRAST RADIOGRAPHY

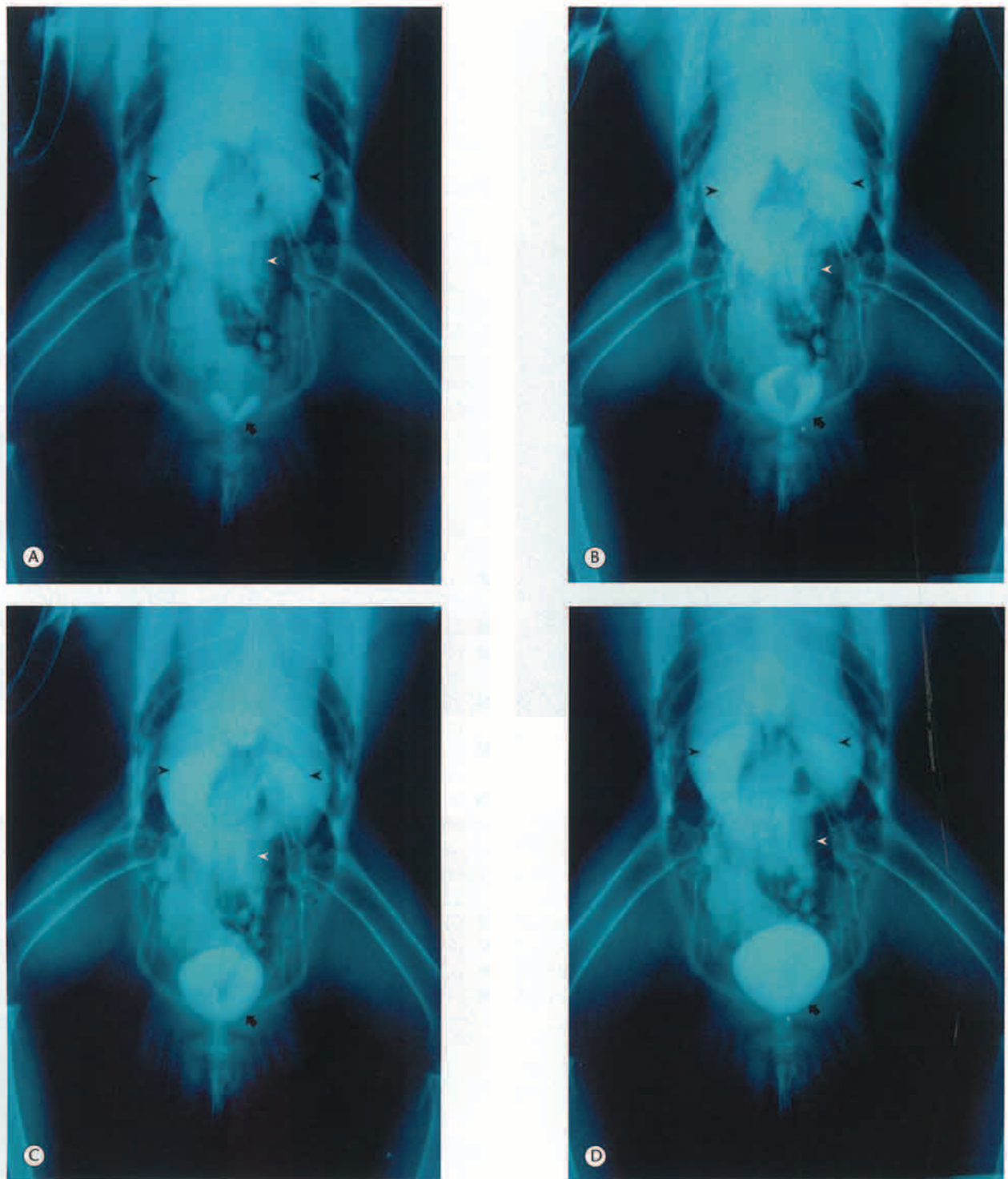


Fig. 2.20 Urogenital tract contrast radiography of the same bird as in Figure 2.19 taken (A) 1 min, (B) 4 min, (C) 9 min, and (D) 20 min after an iodine compound (300 mg iodine/ml) was administered intravenously at a dose rate of 800 mg iodine/kg bodyweight. Kidney, cranial portion (black arrowheads); kidney, caudal portion (white arrowheads) and cloaca (thick black arrow).

SECTION 4 CONTRAST RADIOGRAPHY



Fig. 2.21 Angiography of the patagium of an Eurasian buzzard (*Buteo buteo*). The radiograph was obtained using 100 kVp, 300 mA and 5/10 s (courtesy of M Delogu).



Fig. 2.22 Myelography of a juvenile northern long-eared owl (*Asio otus*). (A) Lateral whole body projection and (B) ventrodorsal projection of the synsacrum highlighting the *sinus rhomboidalis*. The radiograph was obtained using 80 kVp, 200 mA and 2/10 s (courtesy of M Delogu).



SECTION 4 CONTRAST RADIOGRAPHY

References

- Baumgartner R 1991 Radiology in birds. Proceedings of European Association of Avian Veterinarians, March 13–16, Vienna, Austria, pp. 405–409
- Harr KE, Kollias GV, Rendano V et al 1997 A Myelographic technique for avian species. *Veterinary Radiology Ultrasound* 38:187–192
- Harcourt-Brown NH 1996 Radiology. In: Beynon PH (ed.) *Manual of Raptors, Pigeons and Waterfowl*. British Small Animal Veterinary Association, Gloucestershire, pp. 89–97
- Korbel RT, Nell B, Redig RT et al 2000 Video fluorescein angiography in the eyes of various raptors and mammals. Proceedings of Association of Avian Veterinarians, August 30–September 1, Portland, Oregon, pp. 89–95
- Krautwald-Junghanns ME 1996 Avian Radiology. In: Roskopf W, Woerpel R (eds.) *Diseases of Cage and Aviary Birds*. Williams and Wilkins, Baltimore, Maryland, pp. 630–663
- Krautwald-Junghanns ME, Trinkaus K 2000 Imaging techniques. In: Tully TN, Lawton MPC, Dorrestein GM (eds) *Avian Medicine*. Butterworth-Heinemann, Oxford, pp. 52–73
- Lennox AM, Crosta L 2005 The effects of isoflurane anaesthesia on gastrointestinal transit time. Proceedings of European Association of Avian Veterinarians, April 24–30, Arles, France, pp. 207–210
- McMillan MC 1994 Imaging techniques. In: Ritchie BW, Harrison GJ, Harrison LR (eds) *Avian Medicine: Principles and Application*. Wingers Publishing, Lake Worth, Florida, pp. 246–326
- Naldo JL 2000 Radiology. In: Samour JH (ed.) *Avian Medicine*. Harcourt Publishers, London, pp. 50–60
- Phalen DN, Hays HB, Filippich LJ et al 1996 Heart failure in a macaw with atherosclerosis of the aorta and brachiocephalic arteries. *Journal of American Veterinary Medical Association* 209(8):1435–1440
- Romagnano A 1997 Radiology. Proceedings of Association of Avian Veterinarians, September 9–13, Reno, Nevada, pp. 551–561
- Romagnano A, Love NE 2000 Imaging interpretation. In: Olsen GH, Orosz SE (eds) *Manual of Avian Medicine*. Mosby, St. Louis, Missouri, pp. 391–423
- Sherrill J, Ware LH, Lynch WE et al 2001 Contrast radiography with positive-pressure insufflation in northern pintails (*Anas acuta*). *Journal of Avian Medicine and Surgery* 15(3):178–186
- Silverman S 1990 Basic avian radiology. Proceedings of Association of Avian Veterinarians, September 10–15, Phoenix, Arizona, pp. 334–338
- Smith BJ, Smith SA 1997 Radiology. In: Altman RB, Clubb SL, Dorrestein GM, Quesenberry K (eds) *Avian Medicine and Surgery*. WB Saunders, Philadelphia, pp. 170–199
- Tell L, Silverman S, Wisner E 2003 Imaging techniques for evaluating the head of birds, reptiles and small exotic mammals. *Exotic DVM* 5(2):31–37
- Vink-Nooteboom M, Schoemaker NJ, Kik MJ et al 1998 Clinical diagnosis of aneurysm of the right coronary artery in a white cockatoo (*Cacatua alba*). *Journal of Small Animal Practice* 39(11):533–537

Further reading

- Krautwald ME, Tellhelm B, Hummel GH et al 1992 *Atlas of Radiographic Anatomy and Diagnosis of Cage Birds*. Paul Parrey, Berlin
- Rubel GA, Isenbugel E, Wolvekamp P 1991 *Atlas of Diagnostic Radiology of Exotic Pets*. WB Saunders, Philadelphia

Chapter 3

Radiographic anatomy – general considerations

SECTION 1 Musculoskeletal system

The skull of birds of prey, in common with other avian species, has different reptilian features, including a single occipital condyle, movable quadrate and pterygoid bones, the quadrate bone articulating with an articular bone forming part of the lower jaw and a lower jaw comprising of six small bones instead of a single one (King & McLelland 1984). In addition, the skull of birds comprises the infraorbital sinus that includes several diverticula extending into the periorbital areas. A salient anatomical characteristic of the skull of most birds of prey is that the lacrimal bone extends laterally and caudally to form a ledge over the eye. This appears to be involved in providing a shade to shield the eye from sunlight. The osprey (*Pandion haliaetus*) is a notable exception, since it has a smaller lacrimal bone that does not project over the eye (Smith & Smith 1992). The bill and the skull of the barn owl (*Tyto alba*) are elongated and narrow resembling more the skull of a vulture than that of an owl. The interorbital septum is complete and thick in contrast to the thin and often perforated septum in other raptors (Smith & Smith 1992).

There are about 14 or 15 cervical vertebrae in most birds. The first thoracic vertebra is the first vertebra that provides base to the first pair of ribs that articulate with the sternum. The first two to five thoracic vertebrae are fused to form a single bone called the notarium. In most species, this is followed by a free thoracic vertebra. The synsacrum is integrated by 10 to 23 thoracic, lumbar, sacral and caudal vertebrae to form a single bone. There are five to eight free caudal vertebrae followed by the pygostyle. This is a single upturned flattened bone that provides support to the rectrices or tail feathers (King & McLelland 1984). During the course of this study, the authors, in common with other authors (Richardson 1972), found that all the falcons species studied, including gyr (*Falco rusticolus*), saker (*Falco cherrug*), peregrine (*Falco peregrinus*) and lanner (*Falco biarmicus*) falcons, and gyr-peregrine (*Falco rusticolus-peregrinus*) and gyr-saker (*Falco rusticolus-cherrug*) hybrid falcons, have two small accessory bones ventrolaterally to the base of the pygostyle. Most birds of prey have six or seven pairs of ribs integrated by two sections, the vertebral and the sternal sections. The sternum is a large single bone that provides support to some of the internal organs and together with the ribs act as bellows during respiration.

The ventral aspect of the sternum possesses a prominent longitudinal median keel or carina.

In most avian species, the clavicles fuse ventrally to form the furcula. In owls this fusion is only by a cartilage or fibrous tissue (King & McLelland 1984). The wings of *Buteo* and *Accipiter* possess two unique bones that are absent in most other birds of prey, the humeroscapular bone and an additional carpal bone, the *os prominens* (Smith & Smith 1992). The humeroscapular bone is a small bone dorsal to the shoulder joint on the deep surface of the major deltoid muscle. It is present in the red-tailed hawk (*Buteo jamaicensis*) and most owls except the barn owl (Smith & Smith 1992). Among the different species studied by the authors, the humeroscapular bone is present in the honey buzzard (*Pernis apivorus*), eagle owl (*Bubo bubo*), red-naped shaheen (*Falco pelegrinoides babylonicus*), sparrowhawk (*Accipiter nisus*), goshawk (*Accipiter gentilis*), red kite (*Milvus milvus*), black kite (*Milvus migrans*), gyr falcon, and gyr-peregrine and gyr-saker hybrid falcons. The second unique bone of the wing is a small additional carpal bone, the *os prominens*, located cranially and medially to the radial carpal bone. In hawks, the great horned owl (*Bubo virginianus*), barred owl (*Strix varia*) and screech owl (*Otus asio*), the bone is elliptical in shape (Smith & Smith 1992). This bone is absent in the peregrine (*Falco peregrinus*) and prairie falcons (*Falco mexicanus*), American kestrel (*Falco sparverius*) and barn owl (Smith & Smith 1992). This observation was supported by the work of Zucca and Cooper (2000) who reported that the additional carpal bone was certainly absent in the peregrine falcon, but also in the lanner falcon, Eurasian hobby (*Falco subbuteo*) and common kestrel (*Falco tinnunculus*). During the course of our studies, this bone was also observed to be absent in the peregrine and lanner falcons, but also in the barn owl, European kestrel, palm nut vulture (*Gypohierax angolensis*), red-naped shaheen and Barbary (*Falco pelegrinoides*), saker, gyr, and gyr-saker and gyr-peregrine hybrid falcons. The additional carpal bone is present in the honey buzzard, Harris hawk (*Parabuteo unicinctus*), goshawk, sparrowhawk, steppe eagle (*Aquila nipalensis*), golden eagle (*Aquila chrysaetos*), red kite, black kite and eagle owl.

Intratendinous ossifications (*tendo ossificans*) are located on the inside of the tendon of the *m. extensor longus digiti majoris* in the region of the carpometacarpus and the

SECTION 1 MUSCULOSKELETAL SYSTEM

proximal phalanx of the major digit in the peregrine and lanner falcon, Eurasian hobby and common kestrel (Zucca & Cooper 2000). In our studies, these bony structures were found in the red-naped shaheen, eagle owl, barn owl and gyr, saker, peregrine and lanner falcons and in gyr-peregrine and gyr-saker hybrid falcons. Two sesamoid bones are present in the metacarpophalangeal joint and one sesamoid bone in the interphalangeal joint of the major digit in the peregrine and lanner falcon, Eurasian hobby and common kestrel (Zucca & Cooper 2000). In our studies, these sesamoid bones were observed in the kestrel, red-naped shaheen, goshawk, sparrowhawk, Harris hawk, red kite, black kite, honey buzzard and gyr, saker, peregrine and lanner falcons, and gyr-peregrine and gyr-saker hybrid falcons. The wing claw on the first digit of the manus is present in the peregrine, lanner, laggar (*Falco jugger*), saker, and gyr falcon, lesser and common kestrel, and Eurasian hobby (Zucca & Cooper 2000).

Most birds of prey have anisodactyl feet, meaning three digits pointing forward and one digit or hallux (digit No 1) pointing backwards. Owls and the osprey have zygodactyl feet, implying that two digits pointing forwards and two digits pointing backwards. However, these species are able

to move the outer or fourth digit from the backwards to the forward position (King & McLelland 1984). The radiographic differences in the pelvic limb of hawks and of falcons have been well documented (Harcourt-Brown 2000, 2001). Five ossifications in soft tissues were seen in the pelvic limbs of falcons and not in hawks. These were: an ossification in the medial head of *m. flexor hallucis longus*; an ossification of part of tibial cartilage; an ossification in the medial ligament that attaches the tibial cartilage to the medial hypotarsal crest (*ligamentum cartilagometatarsale mediale*); intratendinous ossifications in *m. flexor hallucis longus* and *flexor digitorum longus*; and a sesamoid bone at the metatarsophalangeal junction involved in restraining the digital flexor tendons that supply digit II. Fifteen different falcon species and a large number of various falcon hybrids studied by Harcourt-Brown (2001) showed the same radiographic features. Hawks had a smaller medial hypotarsal crest than falcons, a sesamoid in *ansa iliofibularis*, and a fused or immobile first phalangeal joint in digit II (Harcourt-Brown 2000, 2001). In the eagle owl, intratendinous ossifications occur in the tendon of the extensor and flexor muscles in the tibiotarsal and tarsometatarsal regions.

SECTION 2 Gastrointestinal system

In falcons and falconets, the cutting edge of the maxillary rhamphotheca has a well-defined projecting triangular structure on both sides, commonly known as tomial tooth. The esophagus has two sections: the cervical, which is very short, and the thoracic, which is the longest section. The ingluvies or crop is a dilatation of the esophagus and it is present in all raptors with the exception of owls. The esophagus leads to the proventriculus without any particular anatomical boundary. The proventriculus or true stomach is relatively small and is interconnected to the thin-walled ventriculus or gizzard.

The intermediate zone between the proventriculus and the ventriculus is denominated the isthmus. On radiological examination it is relatively common to observe in the ventriculus casting material such as feathers, fur and bones, or foreign objects such as sand and lead pellets. The intestinal tract is located in the caudal most portion of the abdominal cavity. The end section of the gastrointestinal system is the cloaca. The cloaca is not visible radiographically, unless it is filled with air or if it contains an egg, or a large amount of urates and feces.

SECTION 3 Liver

The liver is composed of two lobes that join cranially in the midline. The liver extends into the thoracic cavity surrounding the apex of the heart. The right lobe is larger than the left. A gallbladder is present in all birds of prey. The shadow formed by the heart and the liver, and, indirectly, the ventriculus, creates an hour-glass shape as observed on a ventrodorsal radiographic view. This is commonly denominated the cardiohepatic waist. Loss of

cardiohepatic waist is commonly found in specimens with an enlarged liver. Conversely, the cardiohepatic waist may be lost if the ventriculus is partially or totally full with either ingesta or casting material. The barn owl does not appear to have a well-developed cardiohepatic waist so this feature does not have any clinical relevance in this species. This radiographic feature may be also common in other owls.

SECTION 4 Spleen

The spleen is a relatively small round organ located on the right side of the intersection between the proventriculus and the ventriculus. In most species, the spleen can be easily observed radiographically in the lateral view immediately above the caudal aspect of the proventriculus.

Observation of the spleen on radiology examination is made easier if the digestive tract is relatively empty. An enlarged spleen can sometimes be observed in the ventrodorsal view.

SECTION 5 Respiratory system

The nostrils or nares are rounded in Falconidae with a centrally positioned tubercle denominated the operculum. In *Accipiter*, *Buteo*, eagles and owls the nares are oval in shape and with a less prominent operculum (Fox 1995). The nasal cavities are separated by the nasal septum and contain the rostral, middle and caudal conchae. The infra-orbital sinus is a large triangular cavity located immediately under the skin below the eye. The sinus is intercommunicated to several diverticula located in the periorbital area. The larynx is integrated by four cartilages partially ossified. The laryngeal opening to the trachea is a narrow slit between the two arytenoids cartilages called the rima

glottis. The trachea is located towards the right side of the neck and is formed by a series of complete signet-shaped cartilaginous rings. Most avian species have a tracheobronchial syrinx, since this is located in both the trachea and the bronchi. Owls have a bronchial syrinx. The syrinx is integrated by partially ossified cartilages and vibrating membranes. The lungs are quadrilateral in shape and are positioned dorsally within the thoracic cavity, partially embedded in the intercostal spaces. The air-sac system is integrated by a single cervical and a single clavicular air sac, and paired cranial thoracic, paired caudal thoracic and paired abdominal air sacs.

SECTION 6 Heart and the vascular system

The heart is situated centrally in the thoracic cavity. The caudal most part or apex is surrounded by the lobes of the liver. The great blood vessels are easily observed at the base or cranial most part of the heart on lateral radio-

graphic views. In this view, it is also feasible to assess the shape and measure the length and width of the heart during radiological examination.

SECTION 7 Urinary System

The avian kidneys are divided into the cranial, middle and caudal divisions. They are located dorsally and are embedded deep into the fosae of the pelvic bones, parti-

cularly the middle and caudal divisions. Most of the cranial division is visible radiographically on the lateral view.

SECTION 8 Reproductive system

In most avian species, only the left ovary and left oviducts are functional. However, in many birds of prey the right ovary and oviduct are partially developed. The shape changes with age and activity ranging from an elongated 'V' to semitriangular to quadrilateral in shape. The testes are tubular in shape and are located cranially and ventrally

to the cranial division of the kidney. During the breeding season it is possible to observe the reproductive tract in the lateral position. Radiologically, it is possible to observe large and developing follicles and testes, and fully form eggs within the oviduct.

SECTION 9 Radiographic species catalog

**Saker falcon** (*Falco cherrug*, Gray, 1834, India)

The saker falcon is a large desert species traditionally used for falconry throughout the Middle East since ancient times. The body weight of males ranges from 730 to 990 g and females from 970 to 1300 g. The length of the body is between 45 and 55 cm, with a wingspan of 102–129 cm. The color of the plumage is variable ranging from dark gray-black to white-cream. Two subspecies are currently recognized. *F. c. cherrug* is found in central Europe, east through southwest Russia, Ukraine and Iran to river Yenisey and the foothills of the Altai mountain range. *F. c. milvipes* is found in southeast Siberia, north Mongolia and north China south to west and central China. Sakers live in steppe, open woodland and rocky outcrops feeding mainly on rodents and other small mammals. Birds and reptiles are also consumed to a lesser extent.

SECTION 9 RADIOGRAPHIC SPECIES CATALOG

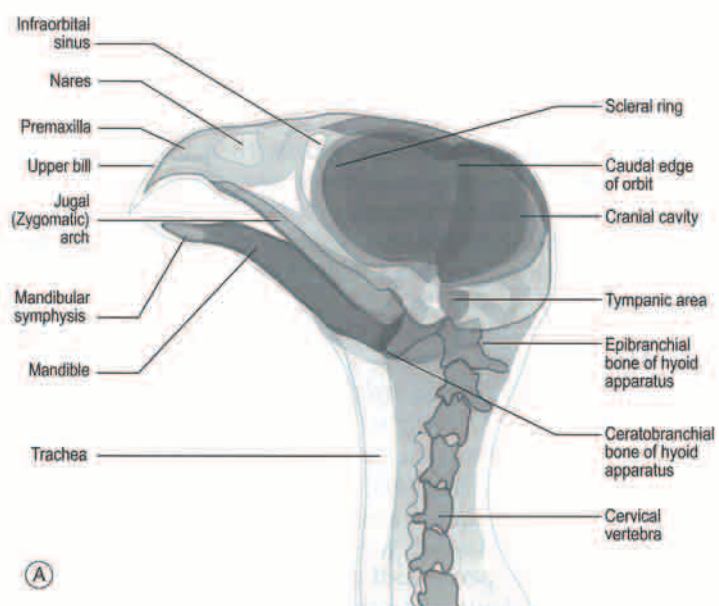


Fig. 3.1 (A and B) Lateral (Le-Rt) view of the head of the saker falcon.

SECTION 9 RADIOGRAPHIC SPECIES CATALOG

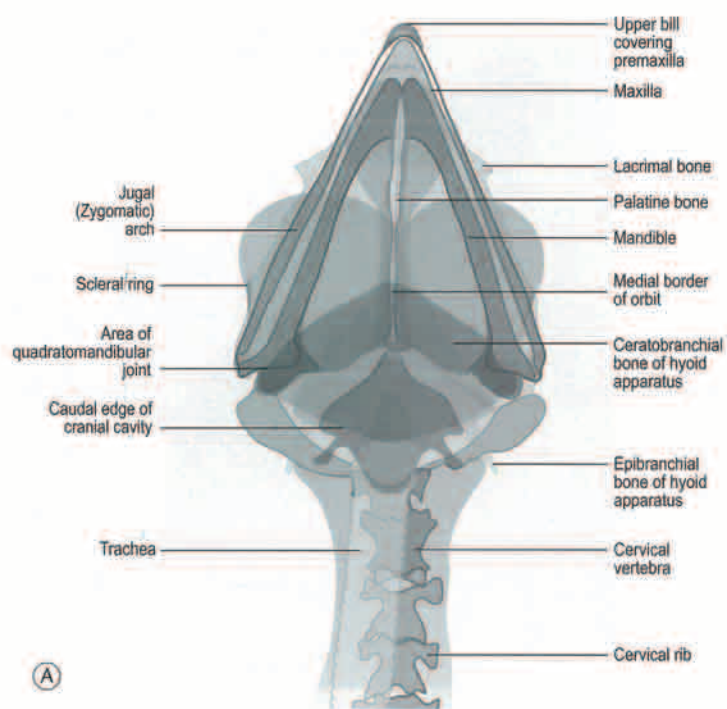


Fig. 3.2 (A and B) Ventrodorsal view of the head of the saker falcon.

SECTION 9 RADIOGRAPHIC SPECIES CATALOG

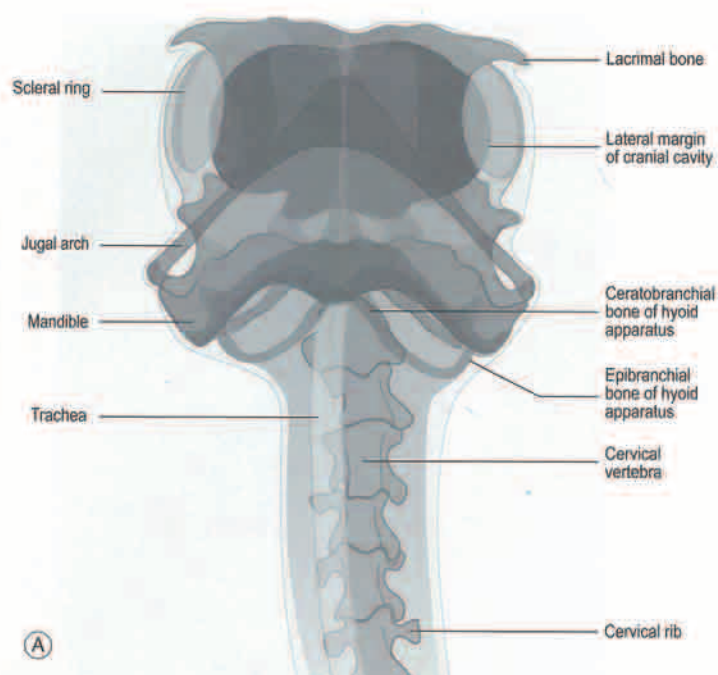


Fig. 3.3 (A and B) Rostrocaudal view of the head of the saker falcon. Note the prominent lacrimal bone.

SECTION 9 RADIOGRAPHIC SPECIES CATALOG

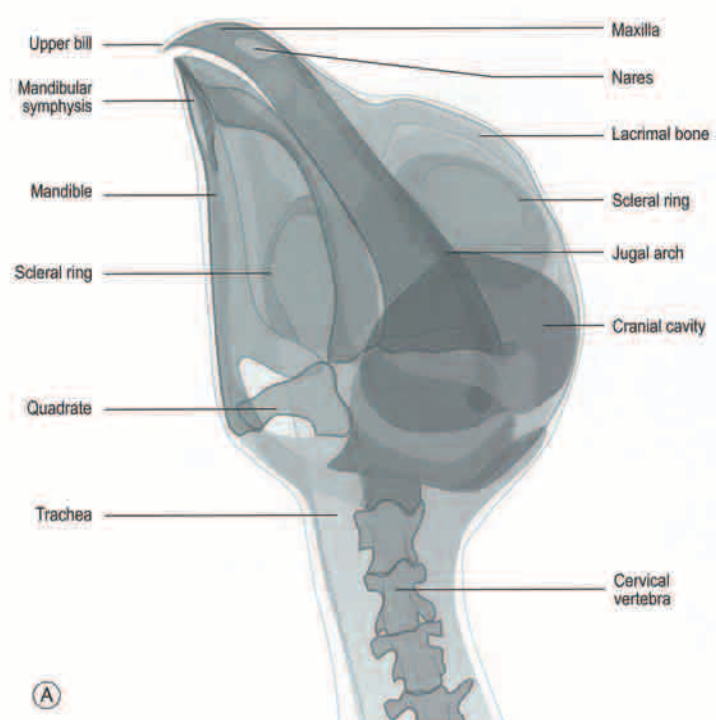


Fig. 3.4 (A and B) Oblique (LeD-RtVO) view of the head of the saker falcon.

SECTION 9 RADIOGRAPHIC SPECIES CATALOG

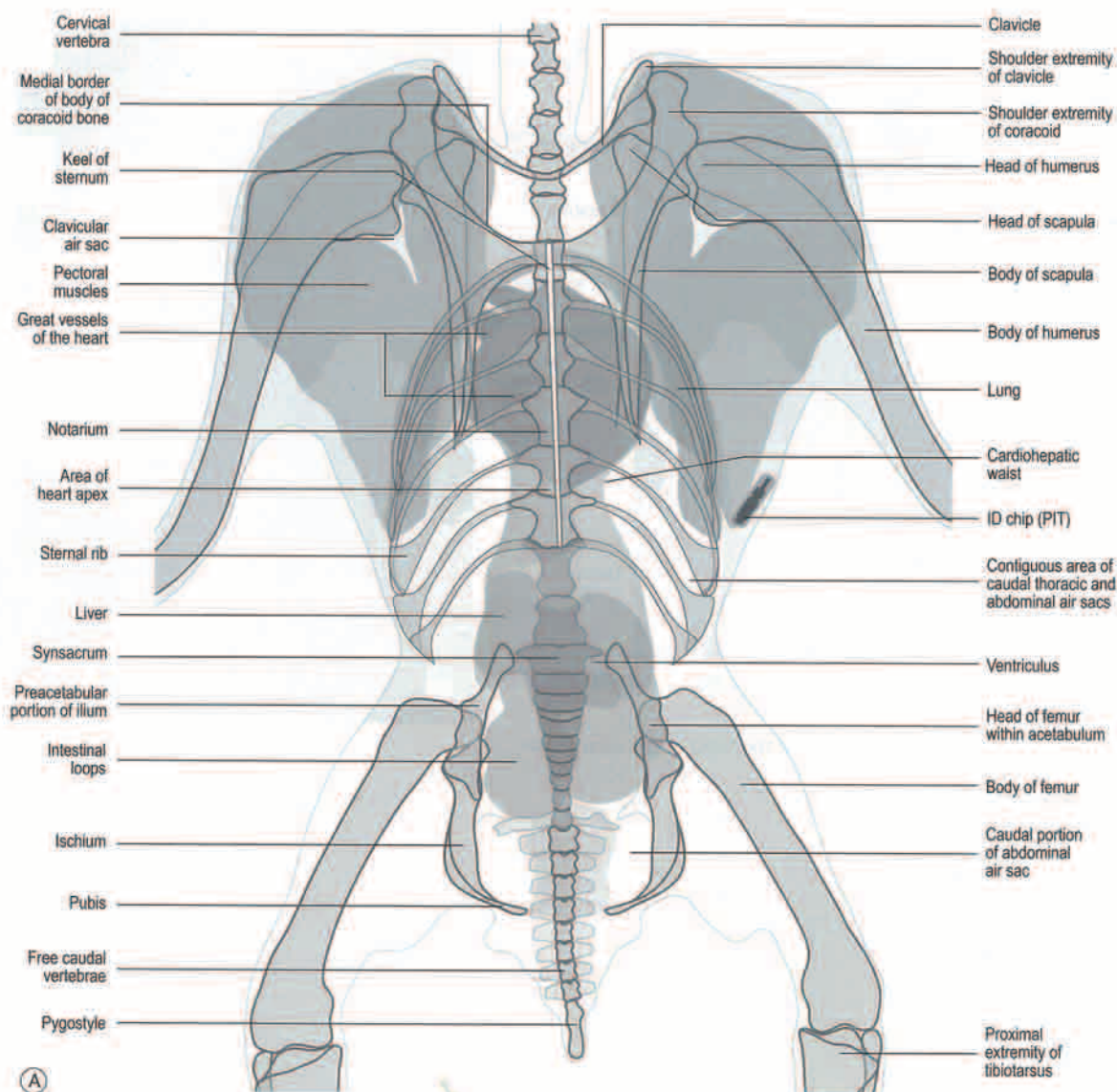


Fig. 3.5 (A and B) Ventrodorsal view of the body of the saker falcon. Note the typical hourglass cardiohepatic waist.

SECTION 9 RADIOGRAPHIC SPECIES CATALOG



Fig. 3.5 (Cont'd).

SECTION 9 RADIOGRAPHIC SPECIES CATALOG

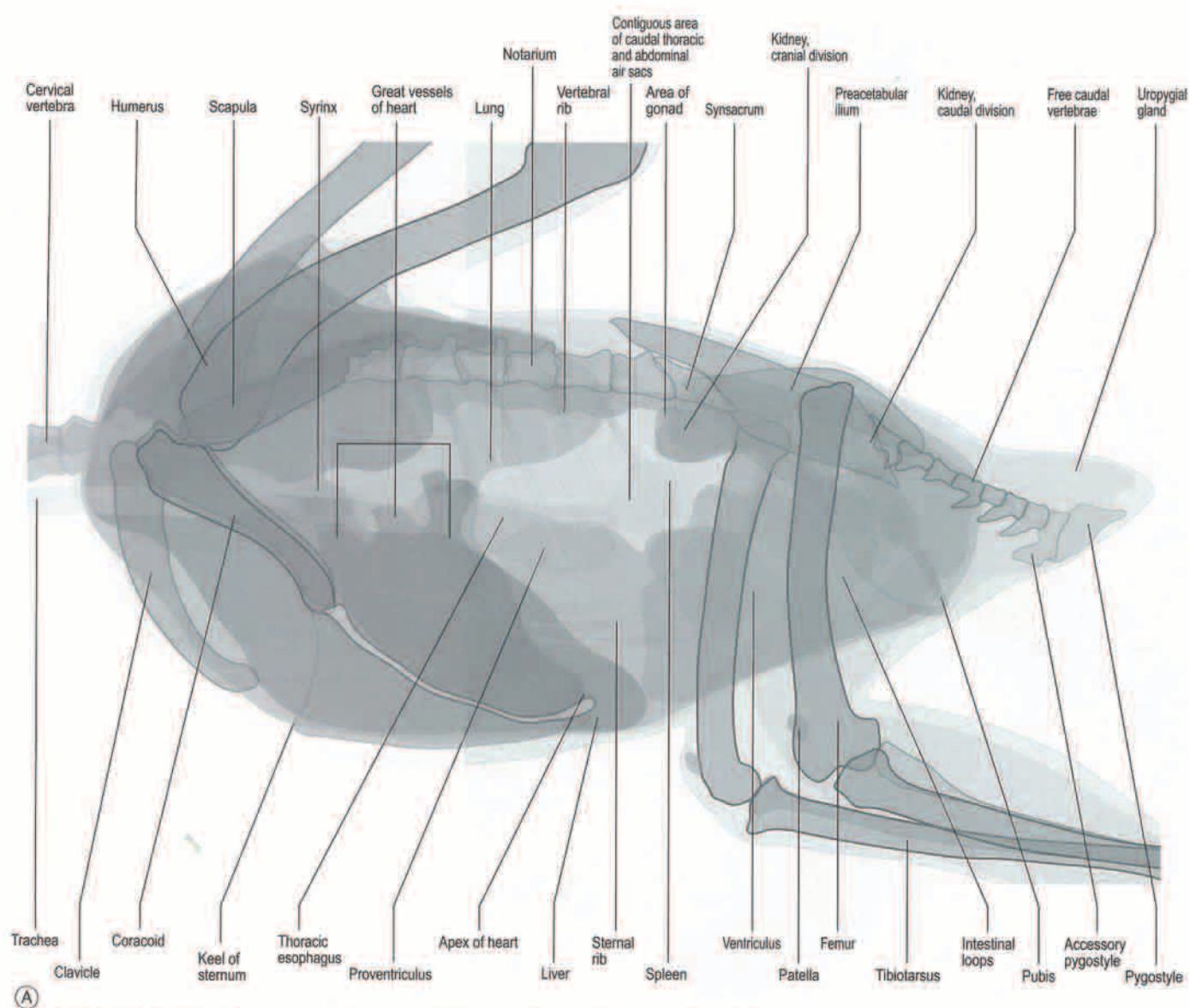


Fig. 3.6 (A and B) Lateral (Le-Rt) view of the body of the saker falcon. Note the characteristic stippled appearance of the lungs. Also note the accessory pygostyle bone, which is best observed in the lateral view.

SECTION 9 RADIOGRAPHIC SPECIES CATALOG



Fig. 3.6 (Cont'd).

SECTION 9 RADIOGRAPHIC SPECIES CATALOG

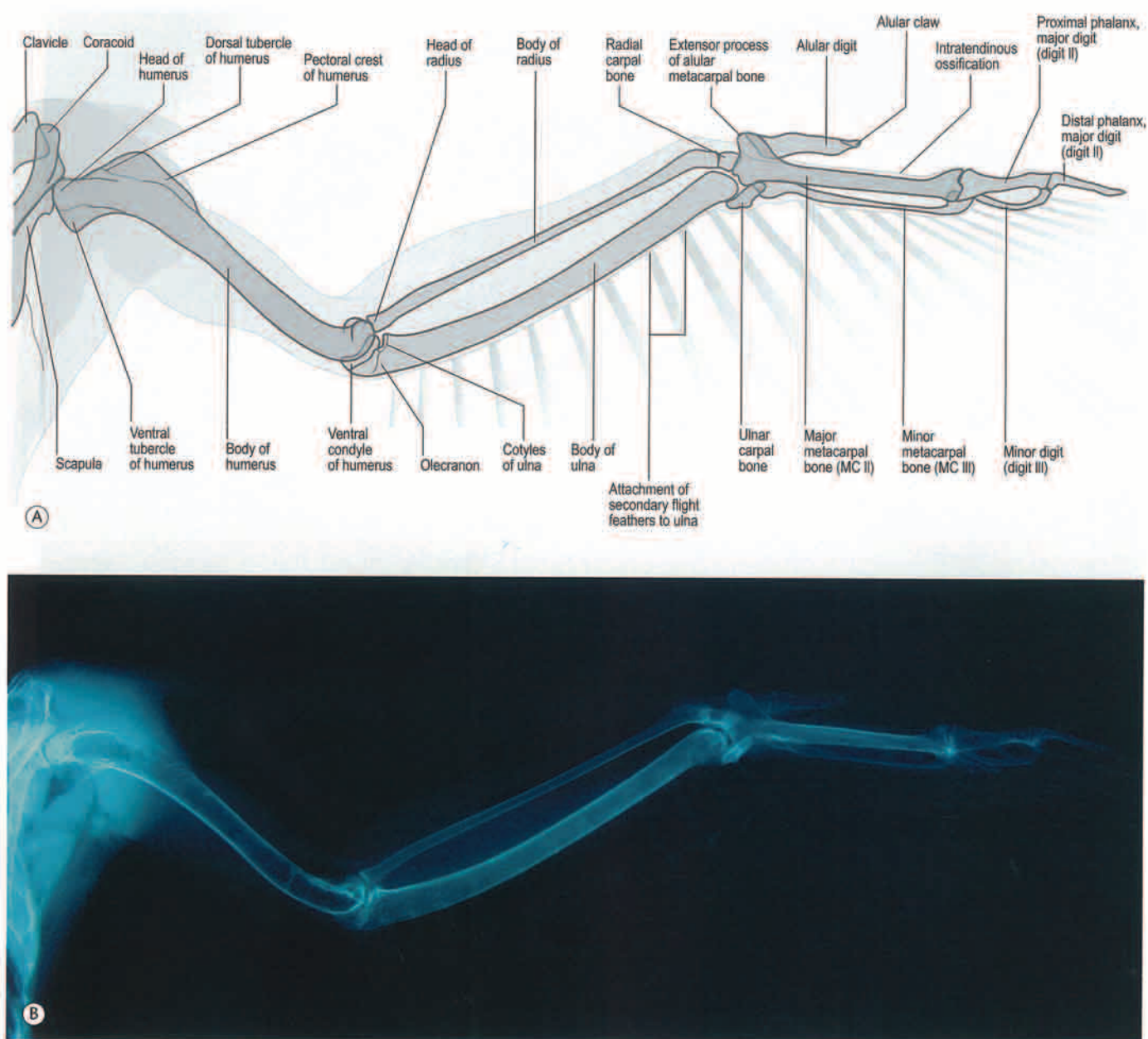


Fig. 3.7 (A and B) Ventrodorsal view of the wing of the saker falcon. The shoulder joint is comprised of the humerus, coracoid, scapula and clavicle. The minor digit (digit III) is composed of one phalanx; the major digit (digit II) is composed of a proximal and a distal phalanx. Note the presence of the alular claw and intratendinous ossification. The additional carpal bone, which is present in some species of raptors is absent in the saker and other falcons.

SECTION 9 RADIOGRAPHIC SPECIES CATALOG

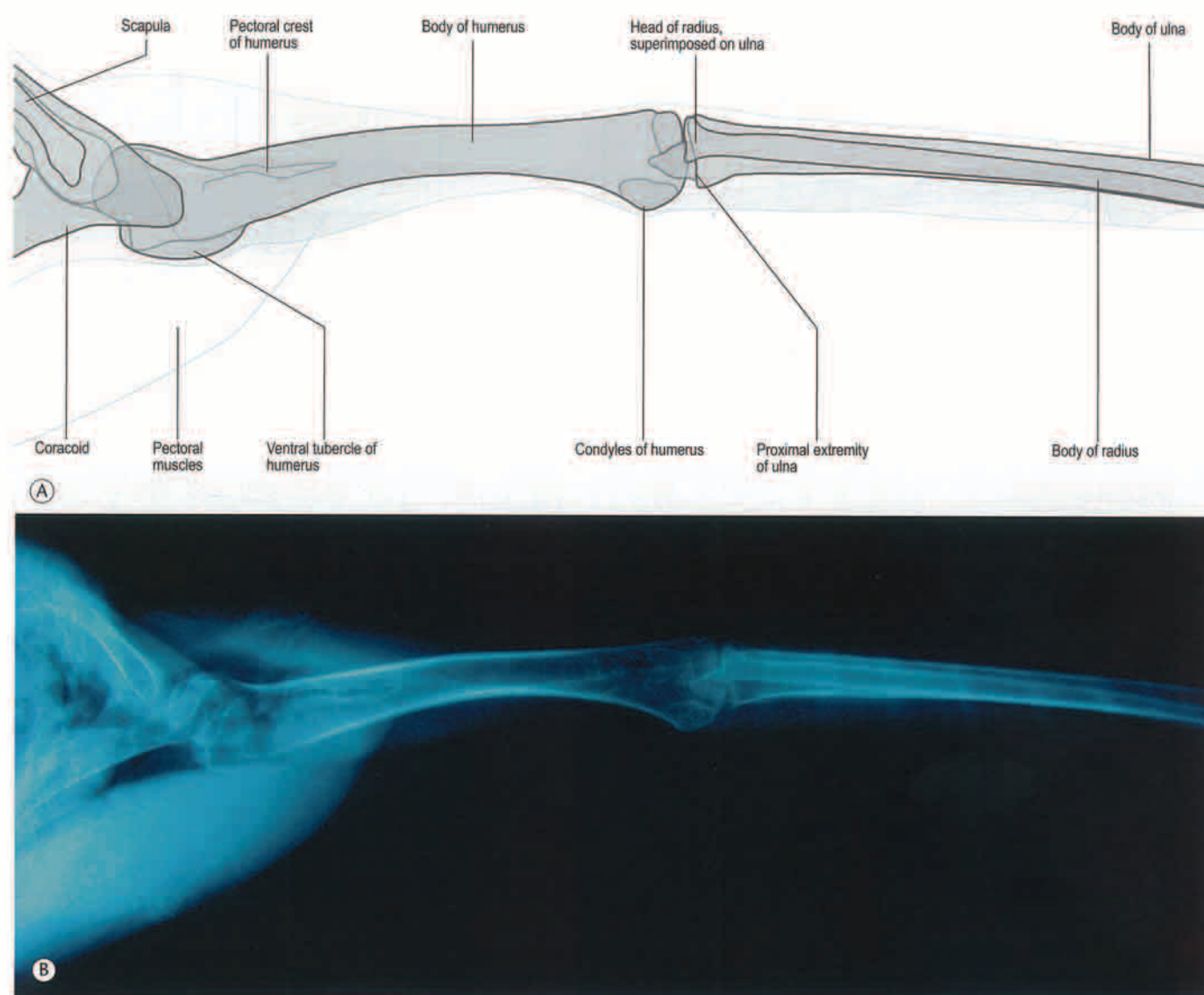


Fig. 3.8 (A and B) Craniocaudal view of the proximal wing of the saker falcon. The humeroscapular bone of the shoulder, which is present in other species of raptors is absent in the saker falcon. Evidence of the pectoral muscles extending toward the humerus indicates the ventral surface of the wing.

SECTION 9 RADIOGRAPHIC SPECIES CATALOG

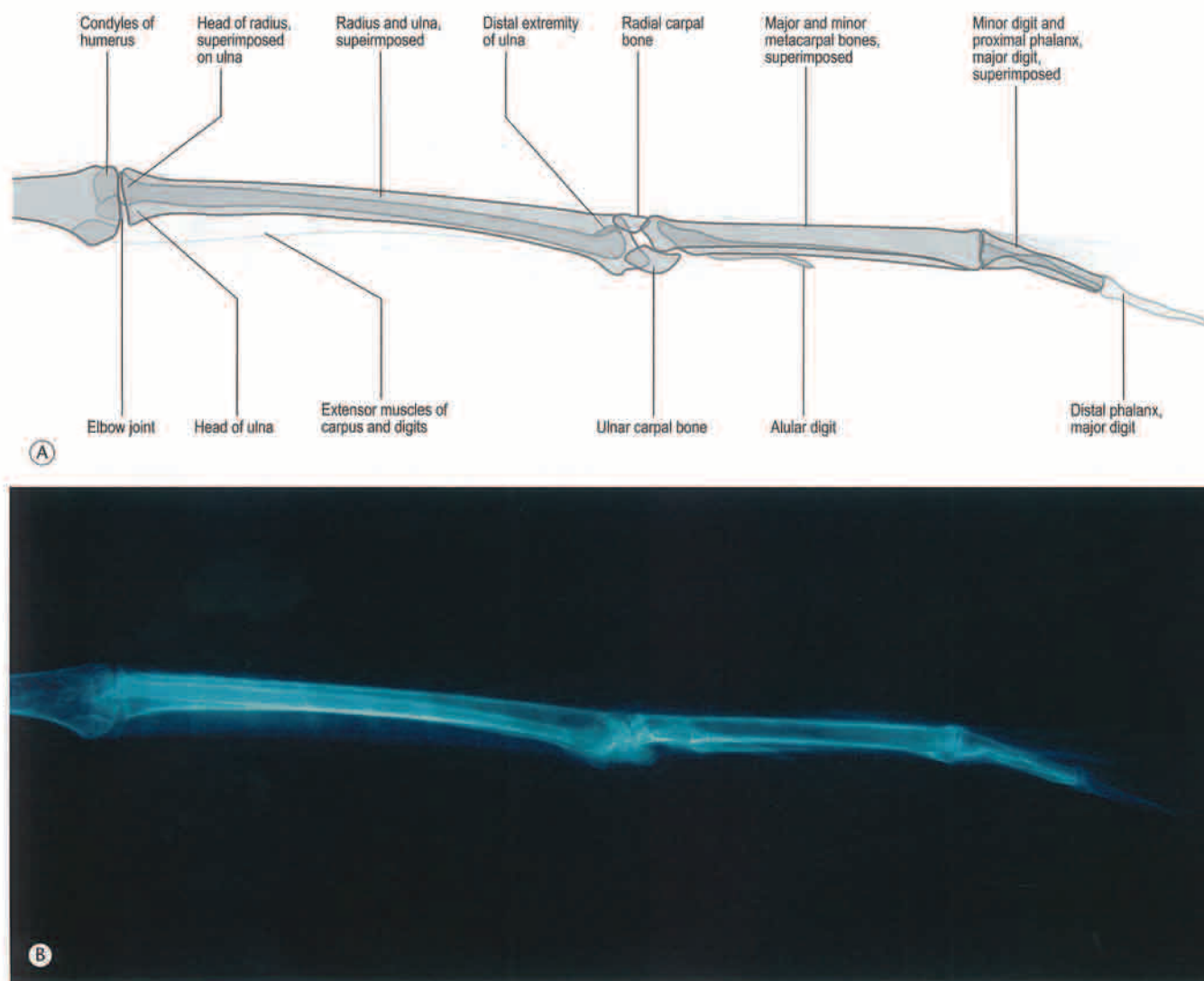


Fig. 3.9 (A and B) Craniocaudal view of the distal wing of the saker falcon. True craniocaudal positioning results in superimposition of the antebrachial bones and all digits.

SECTION 9 RADIOGRAPHIC SPECIES CATALOG

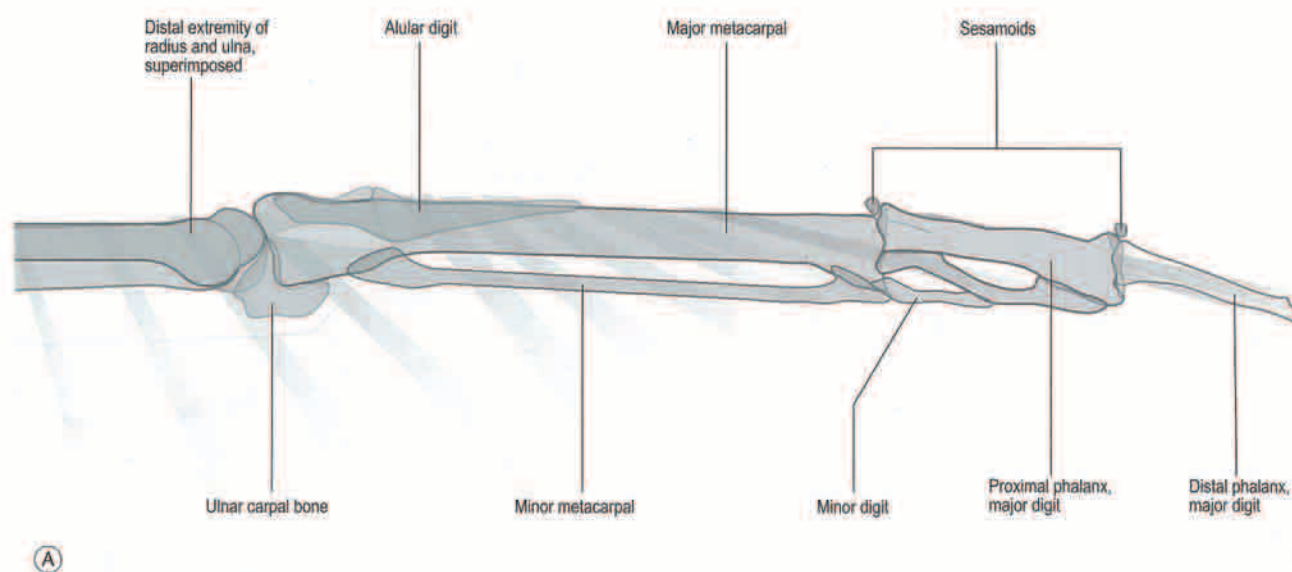


Fig. 3.10 (A and B) Oblique view of the distal wing of the saker falcon. To be able to achieve this position the tip of the wing is rotated slightly out of its craniocaudal orientation. Note the presence of sesamoid bones in the metacarpophalangeal joint and interphalangeal joint of the major digit. The second, smaller sesamoid bone in the metacarpophalangeal joint is not visible in the radiograph.

SECTION 9 RADIOGRAPHIC SPECIES CATALOG

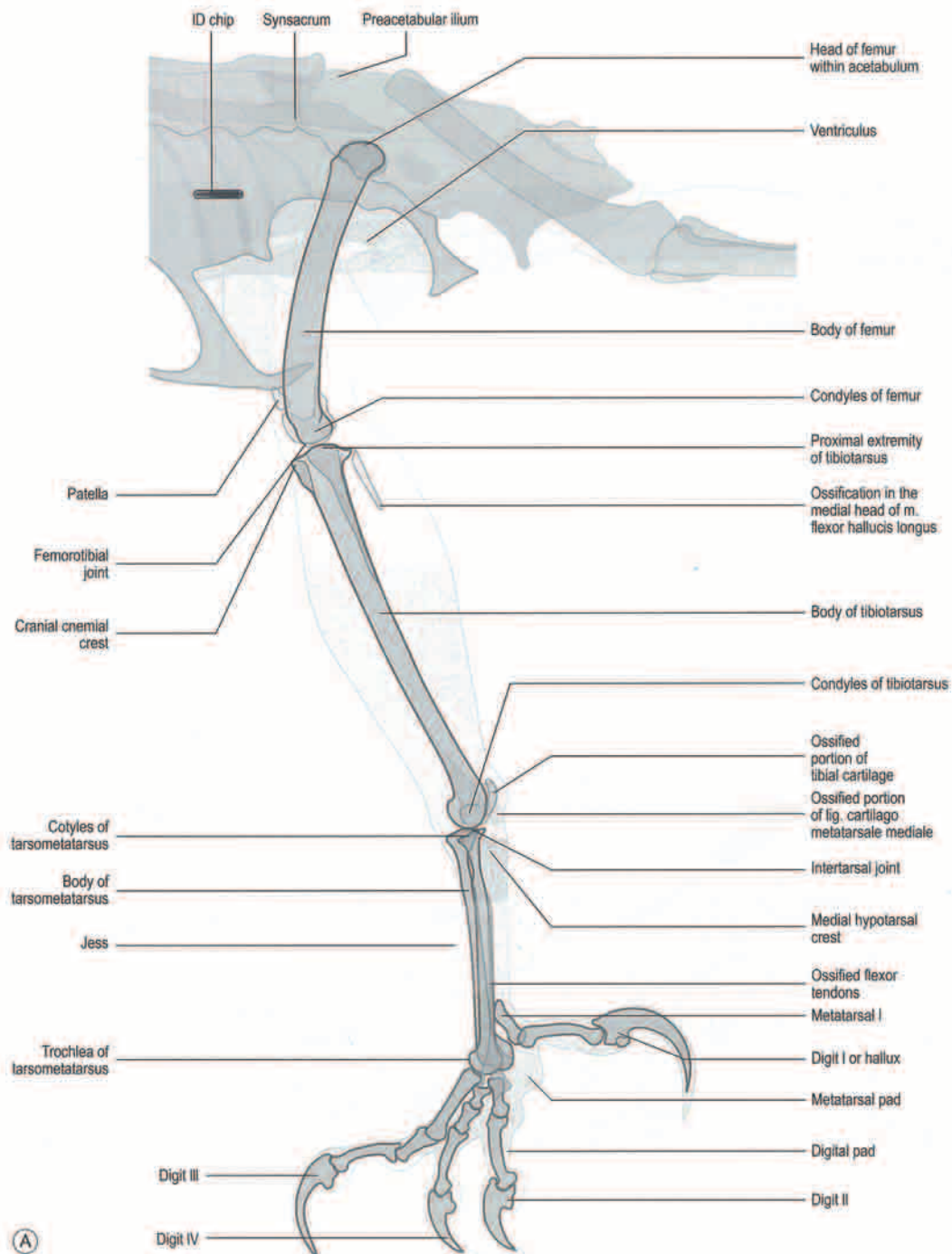


Fig. 3.11 (A and B) Mediolateral view of the pelvic limb of the saker falcon. *Falco* spp. have well-developed medial hypotarsal crest and movable phalangeal joints in digit II. Also, they have five ossifications in soft tissues namely, the ossified spike of bone in the origin of the medial head of *m. flexor hallucis longus*, the ossified portion of tibial cartilage, the ossified portion of *lig. cartilago-metatarsale mediale*, the intratendinous ossification of flexor tendons in the tarsometatarsus and the sesamoid between the metatarsophalangeal joint of digit II and the flexor tendons.

SECTION 9 RADIOGRAPHIC SPECIES CATALOG



Fig. 3.11 (Cont'd).

SECTION 9 RADIOGRAPHIC SPECIES CATALOG

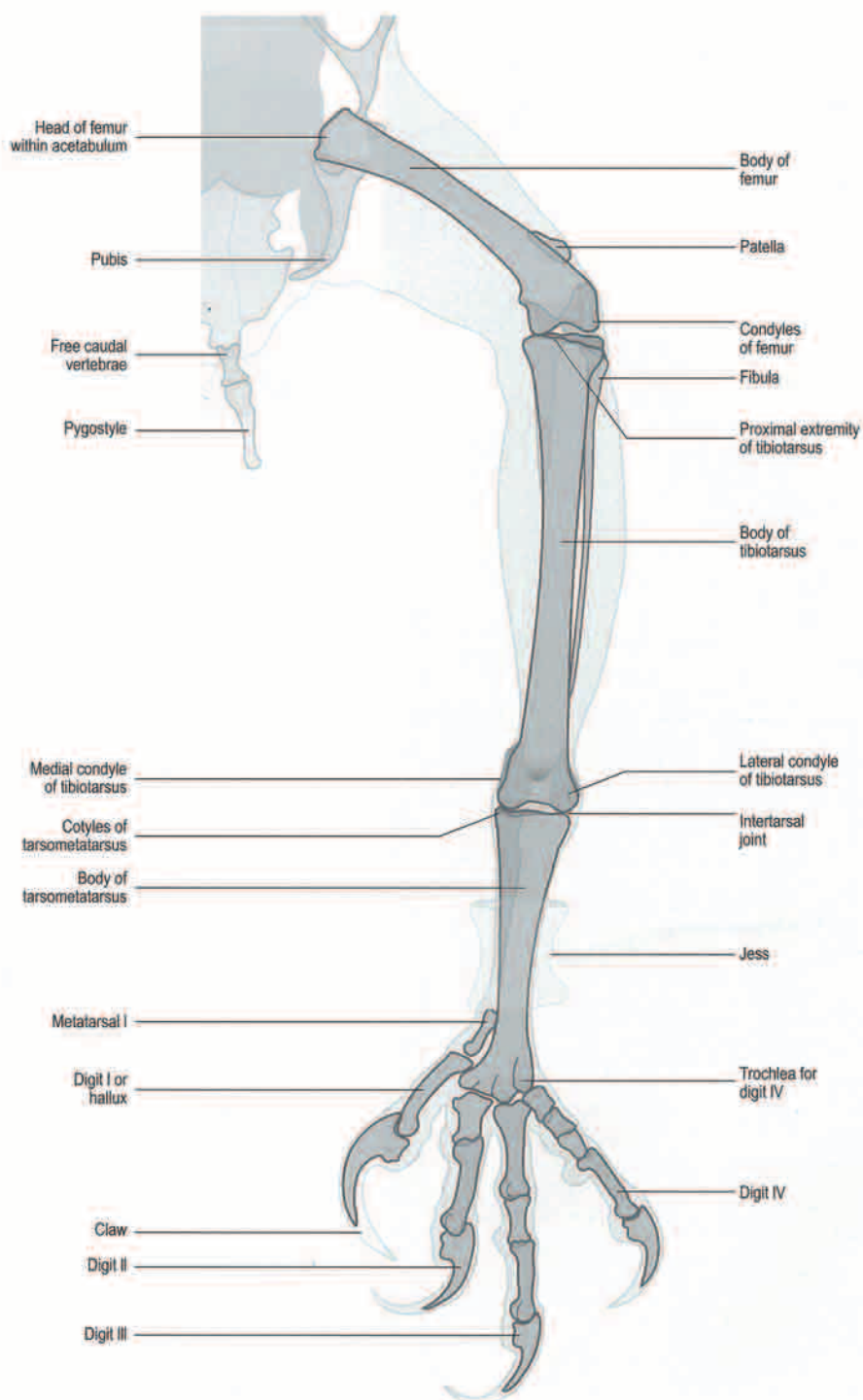


Fig. 3.12 (A and B) Craniocaudal view of the pelvic limb of the saker falcon. Note that digit I possesses two phalanges, digit II possesses three phalanges, digit III possesses four phalanges and digit IV possesses five phalanges.

SECTION 9 RADIOGRAPHIC SPECIES CATALOG



Fig. 3.12 (Cont'd).

SECTION 9 RADIOGRAPHIC SPECIES CATALOG

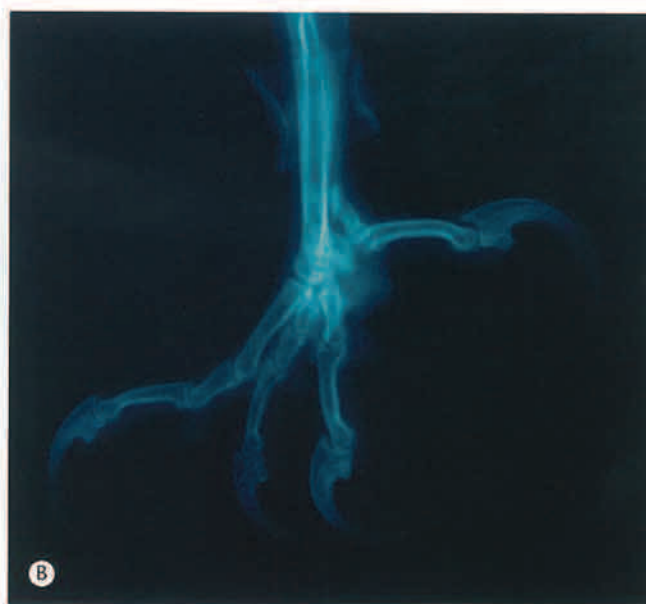
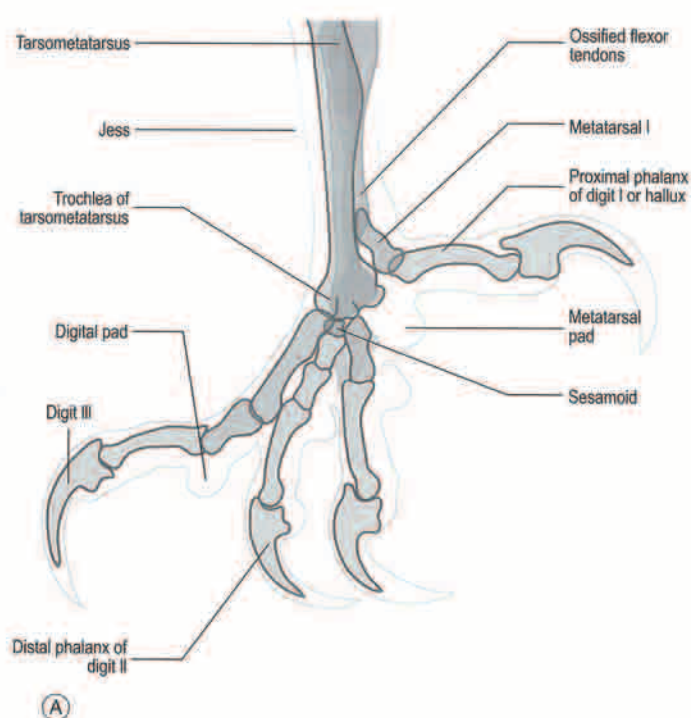


Fig. 3.13 (A and B) Mediolateral close-up of the foot of the saker falcon. The distal phalanx of each digit is covered by a horny claw. Note the ossified flexor tendons of the tarsometatarsus and the sesamoid bone between the metatarsophalangeal joint of digit II and the flexor tendons.

SECTION 9 RADIOGRAPHIC SPECIES CATALOG

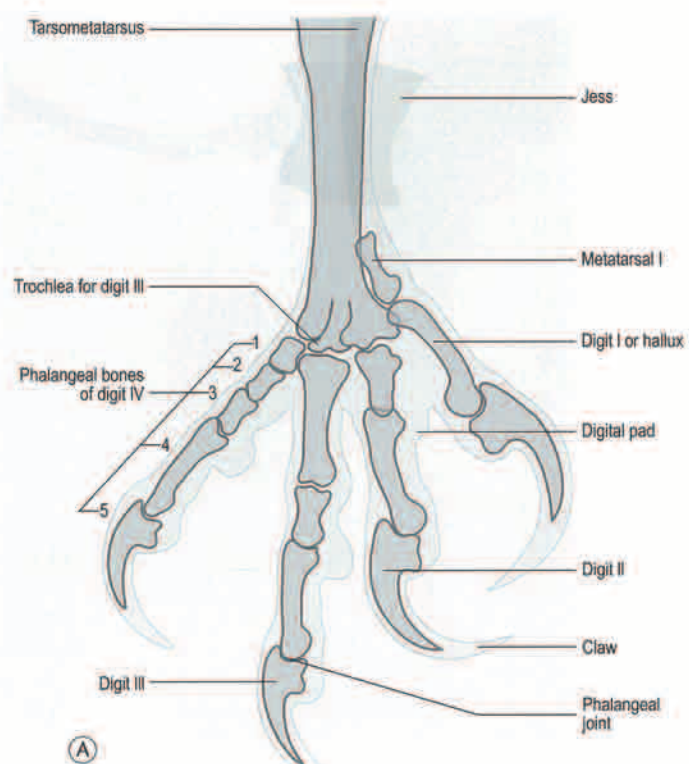


Fig. 3.14 (A and B) Craniocaudal close-up of the foot of the saker falcon, with digit I flexed.

SECTION 9 RADIOGRAPHIC SPECIES CATALOG

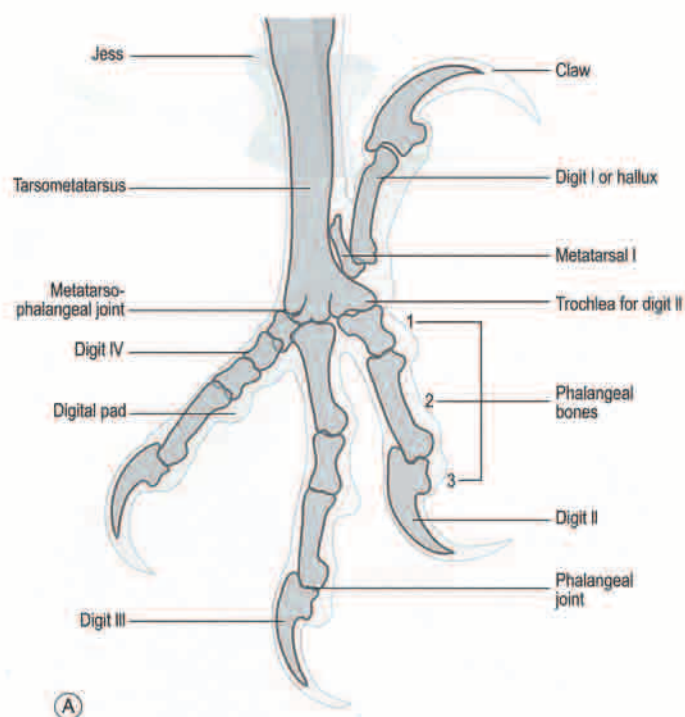


Fig. 3.15 (A and B) Craniocaudal close-up of the foot of the saker falcon, with digit I extended.

SECTION 9 RADIOGRAPHIC SPECIES CATALOG

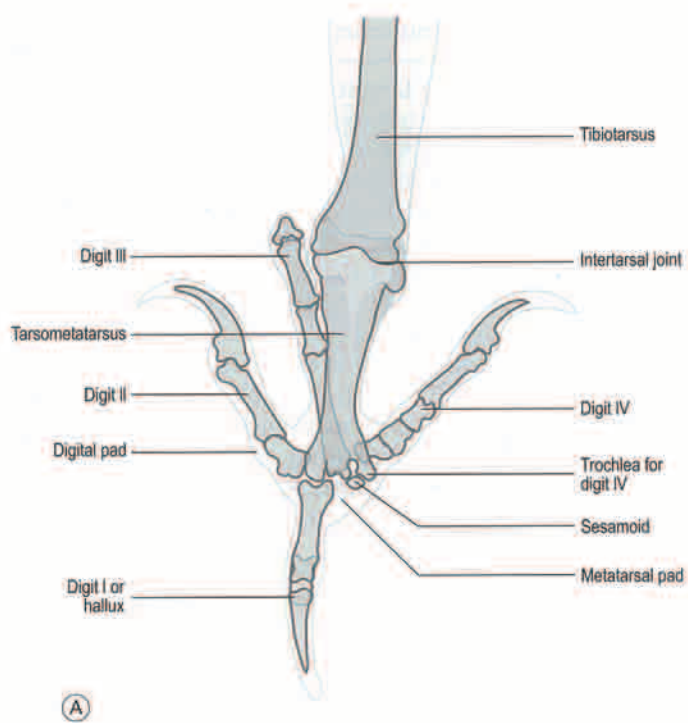


Fig. 3.16 (A and B) Caudoplantar close-up of the foot of the saker falcon. Note the sesamoid bone between the metatarsophalangeal joint of digit II and the flexor tendons.

**Gyr falcon** (*Falco rusticolus*, Linnaeus, 1758, Sweden)

The gyr falcon is the largest falcon species in the world. This is a favorite species amongst falconers all over the world due to its large size and strength. The length of the body is between 48 and 60 cm. The body weight of males ranges from 961 to 1321 g and females from 1262 to 2100 g, with a wingspan of 120–135 cm. The species is highly polymorphic with three main colors, white, gray and black. Streaked or barred markings on upperparts and underparts. Four races are recognized: *F. r. rusticolus* from Europe, *F. r. obsoletus* from Asia and parts of North America, *F. r. candicans* from the high Arctic of North America and Greenland and *F. r. islandicus* from Iceland. Gyrs inhabit three types of habitats, maritime, riverine and montane, feeding on mammals and birds. Found throughout tundra and taiga from sea level to 1400 m altitude.

SECTION 9 RADIOGRAPHIC SPECIES CATALOG

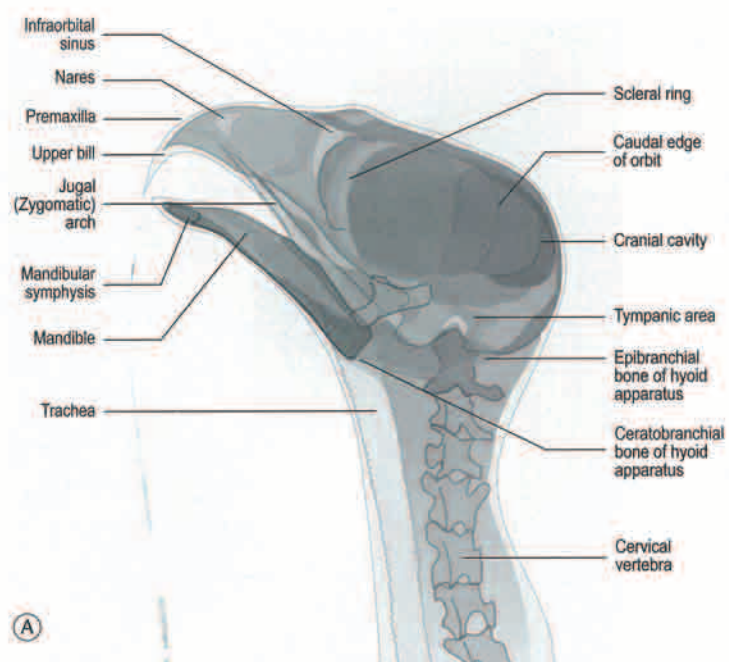


Fig. 3.17 (A and B) Lateral (Le-Rt) view of the head of the gyr falcon.

SECTION 9 RADIOGRAPHIC SPECIES CATALOG

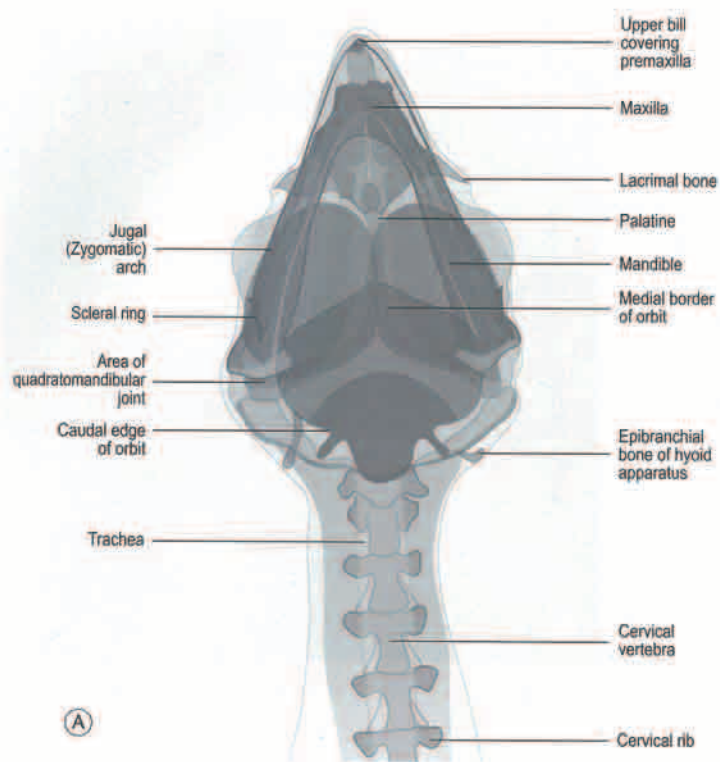


Fig. 3.18 (A and B) Ventrodorsal view of the head of the gyr falcon.

SECTION 9 RADIOGRAPHIC SPECIES CATALOG

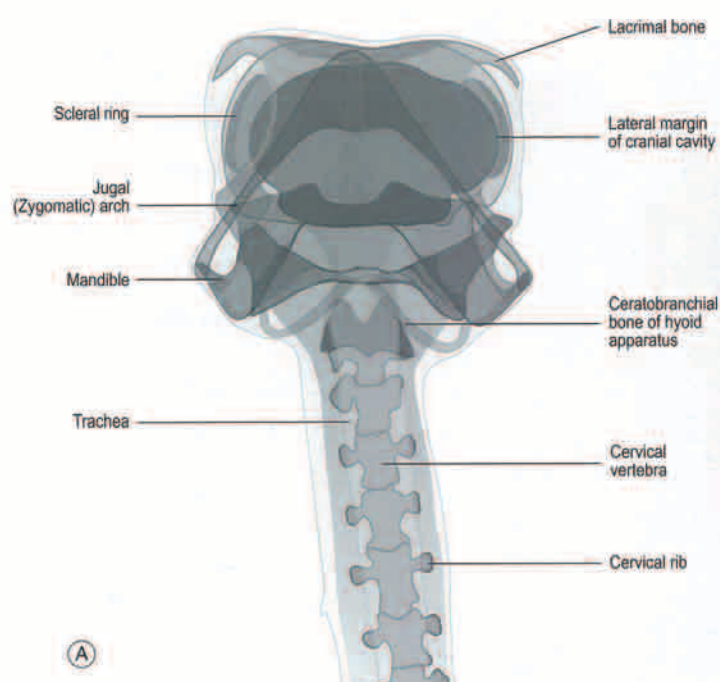


Fig. 3.19 (A and B) Rostrocaudal view of the head of the gyr falcon.

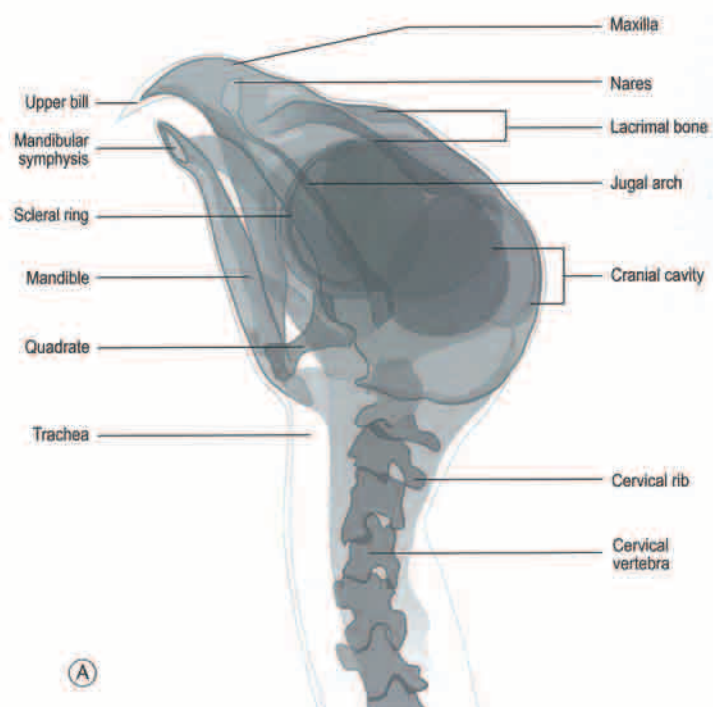


Fig. 3.20 (A and B) Oblique (LeD-RtVO) view of the head of the gyr falcon.

SECTION 9 RADIOGRAPHIC SPECIES CATALOG

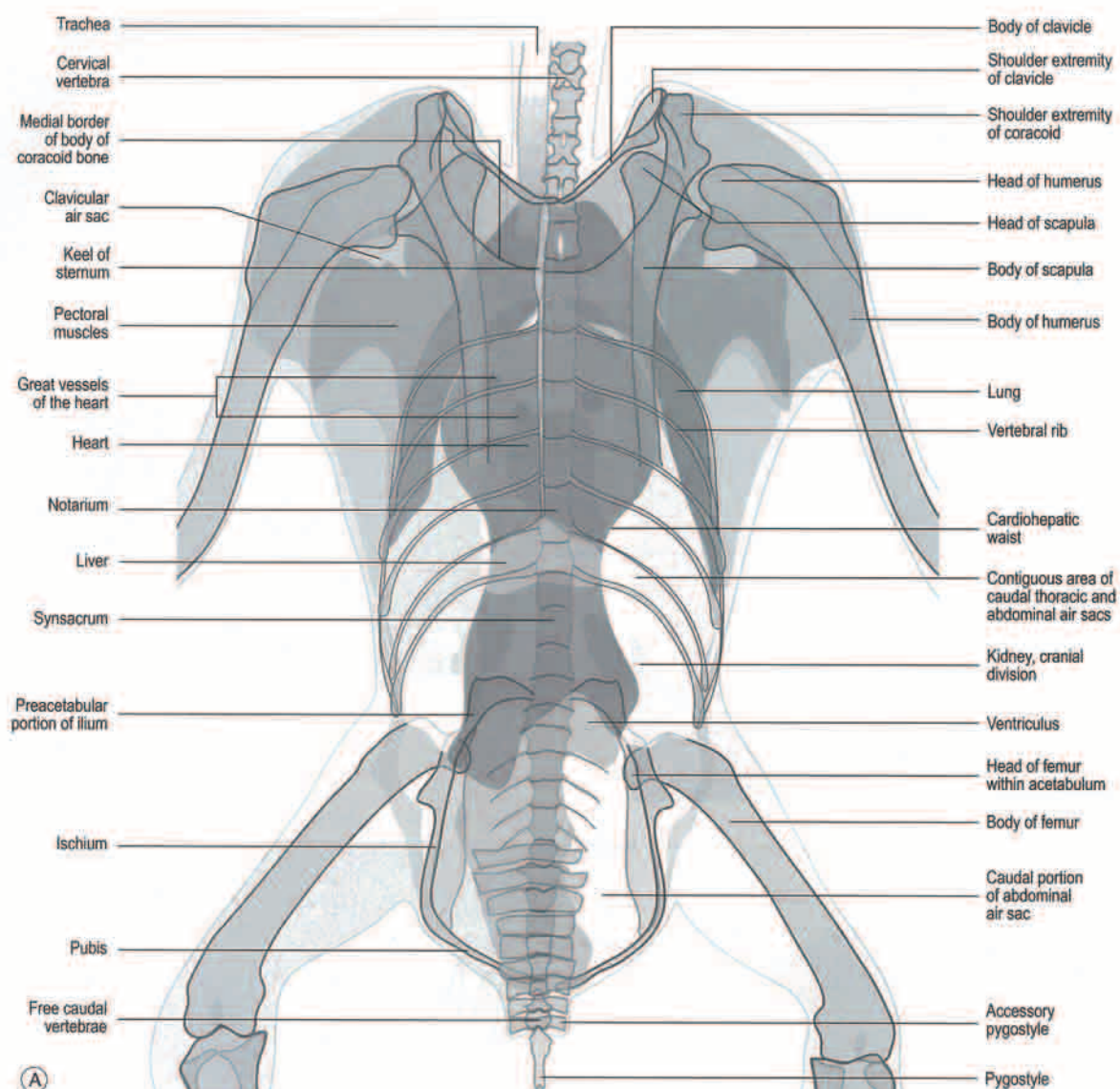


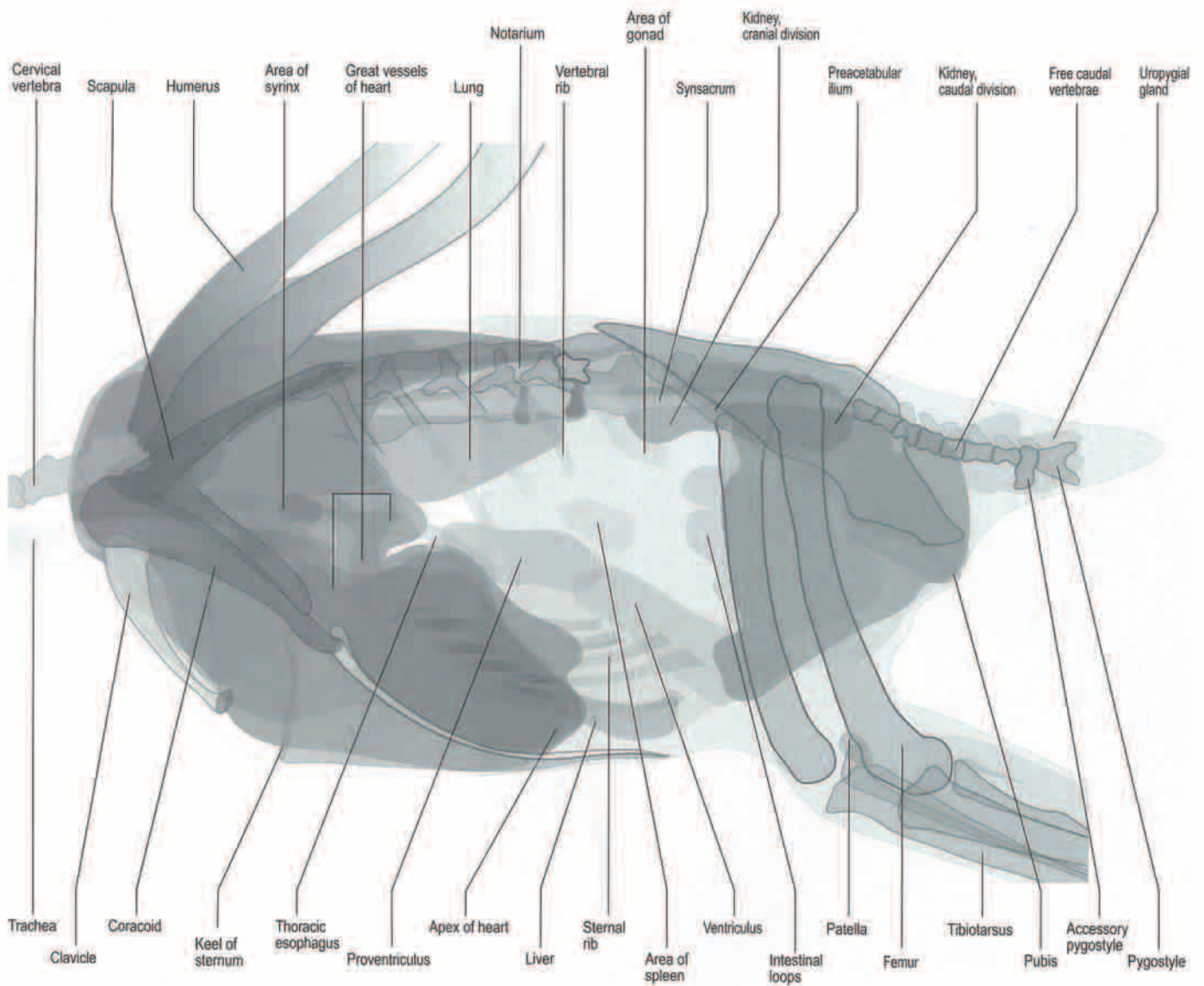
Fig. 3.21 (A and B) Ventrordorsal view of the body of the gyr falcon. Note the typical hourglass cardiohepatic waist.

SECTION 9 RADIOGRAPHIC SPECIES CATALOG



Fig. 3.21 (Cont'd).

SECTION 9 RADIOGRAPHIC SPECIES CATALOG



(A)

Fig. 3.22 (A and B) Lateral (Le-Rt) view of the body of the gyr falcon. Note the accessory pygostyle bone.

SECTION 9 RADIOGRAPHIC SPECIES CATALOG



Fig. 3.22 (Cont'd).

SECTION 9 RADIOGRAPHIC SPECIES CATALOG

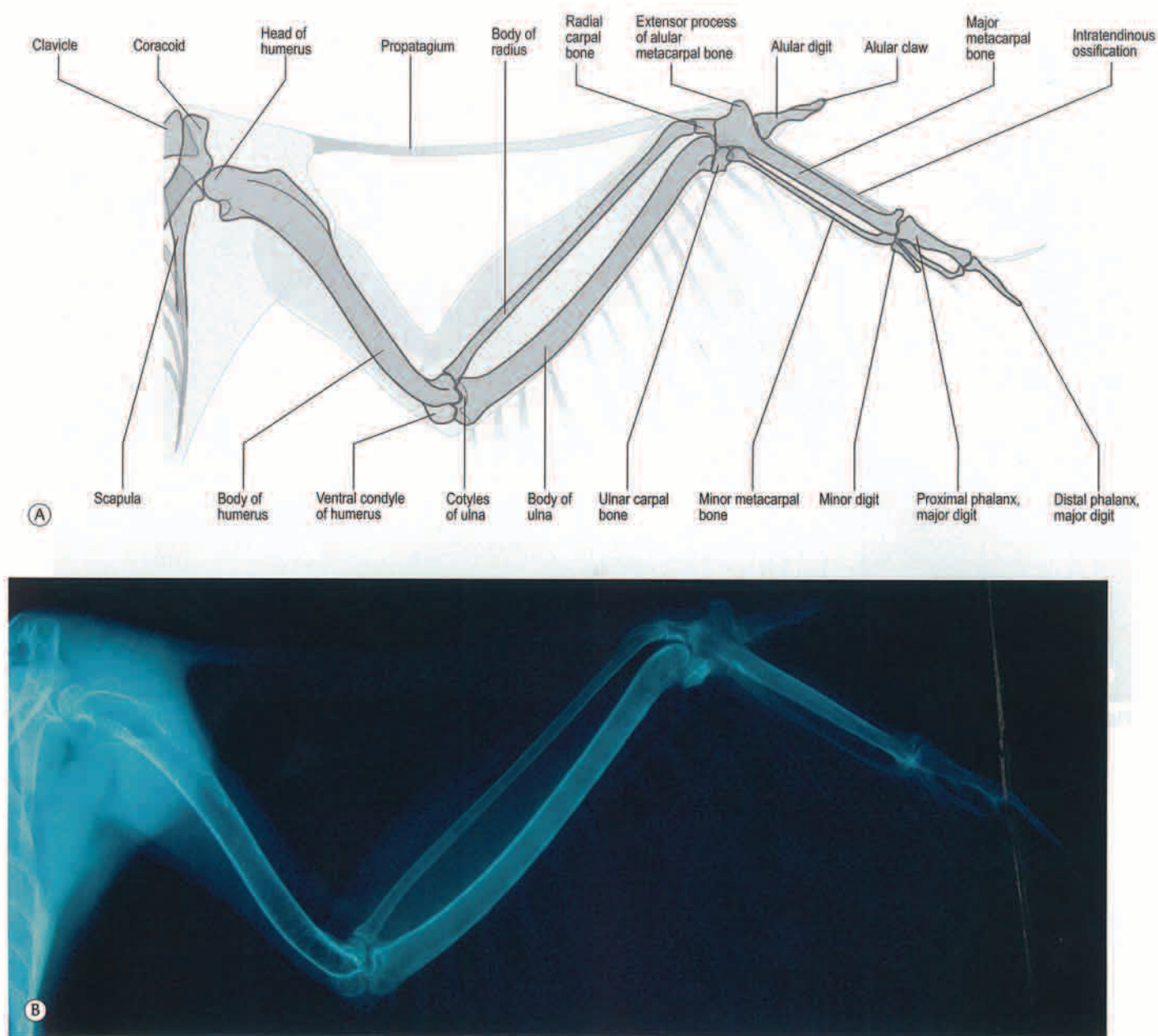


Fig. 3.23 (A and B) Ventrodorsal view of the wing of the gyr falcon. Note the presence of the alular claw and intratendinous ossification. The additional carpal bone, which is present in some species of raptors is absent in the gyr and other falcons.

SECTION 9 RADIOGRAPHIC SPECIES CATALOG

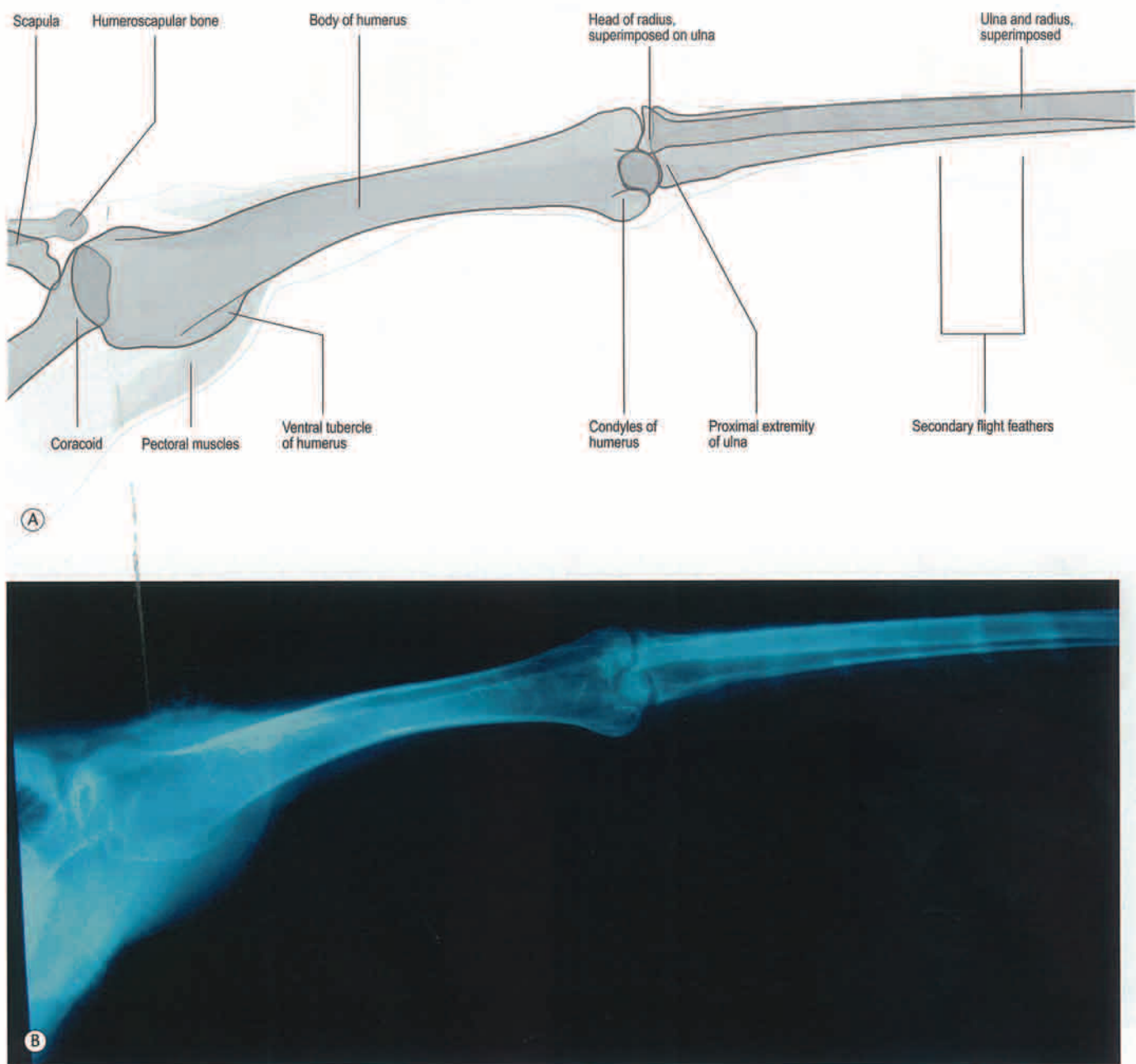
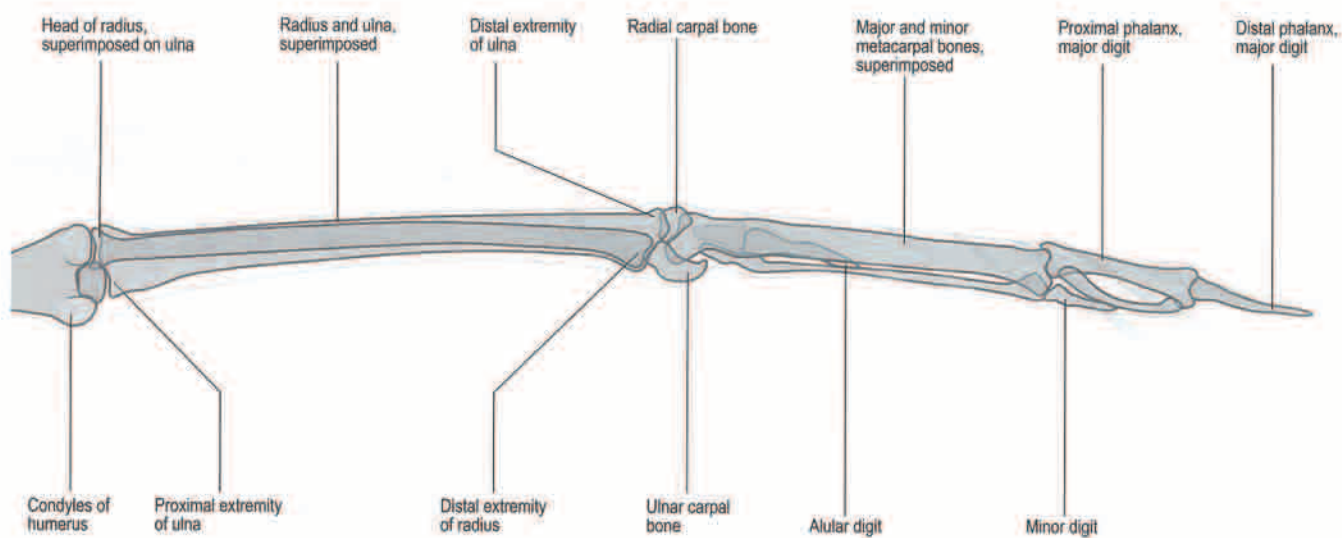


Fig. 3.24 (A and B) Craniocaudal view of the proximal wing of the gyr falcon. Note the presence of the humeroscapular bone. This bone is also present in the gyr-peregrine hybrid and gyr-saker hybrid falcons.

SECTION 9 RADIOGRAPHIC SPECIES CATALOG



(A)



(B)

Fig. 3.25 (A and B) Craniocaudal view of the distal wing of the gyr falcon.

SECTION 9 RADIOGRAPHIC SPECIES CATALOG

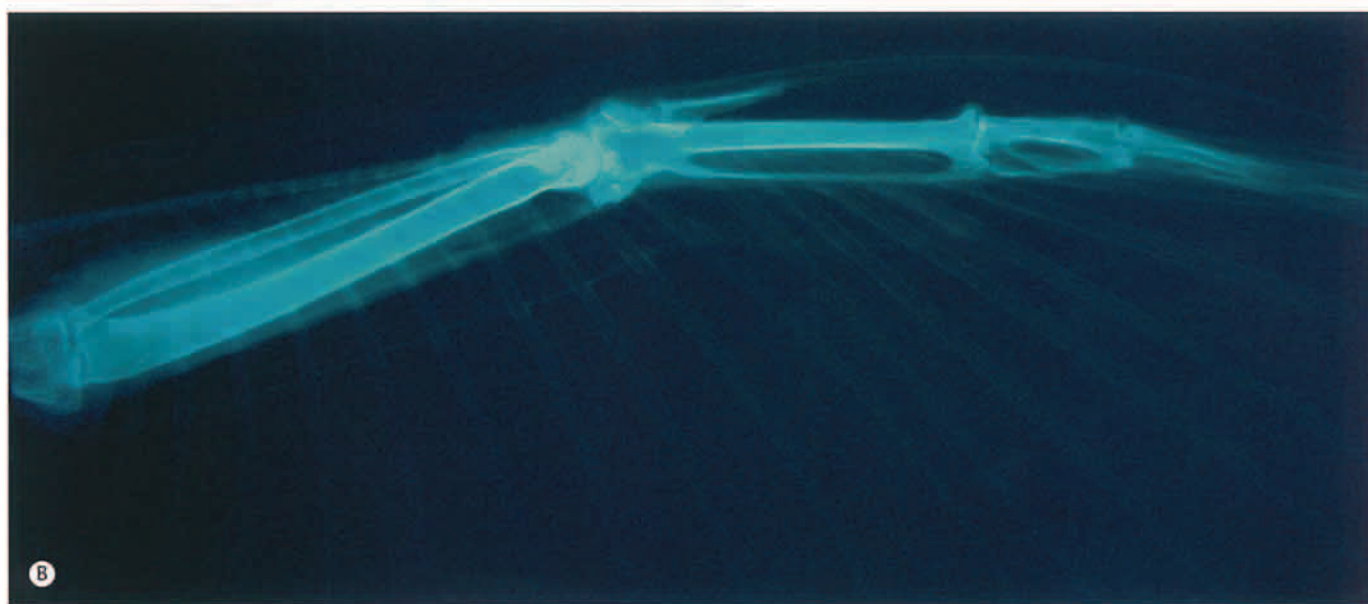
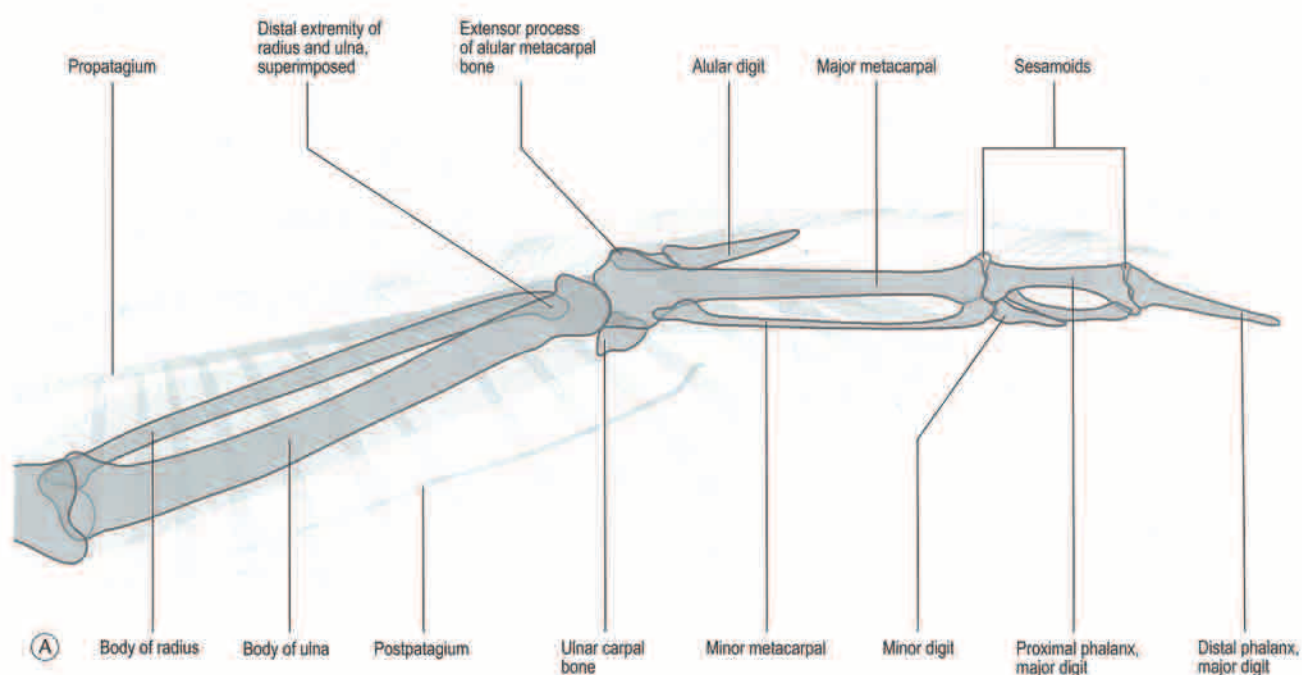


Fig. 3.26 (A and B) Oblique view of the distal wing of the gyr falcon. To be able to achieve this position the tip of the wing is rotated slightly out of its craniocaudal orientation. Note the presence of sesamoid bones. The second, smaller sesamoid bone in the metacarpophalangeal joint is not visible in the radiograph.

SECTION 9 RADIOGRAPHIC SPECIES CATALOG

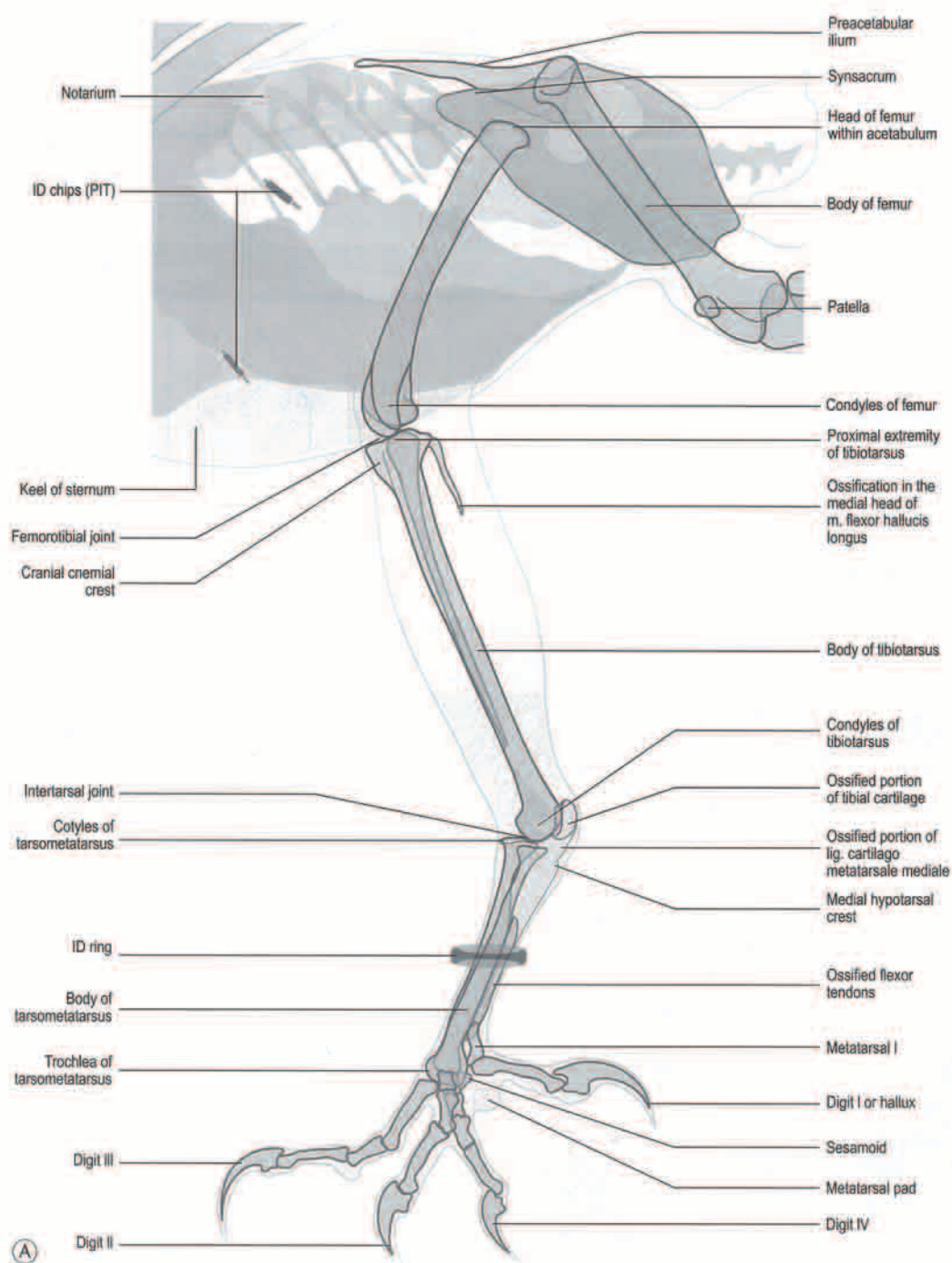


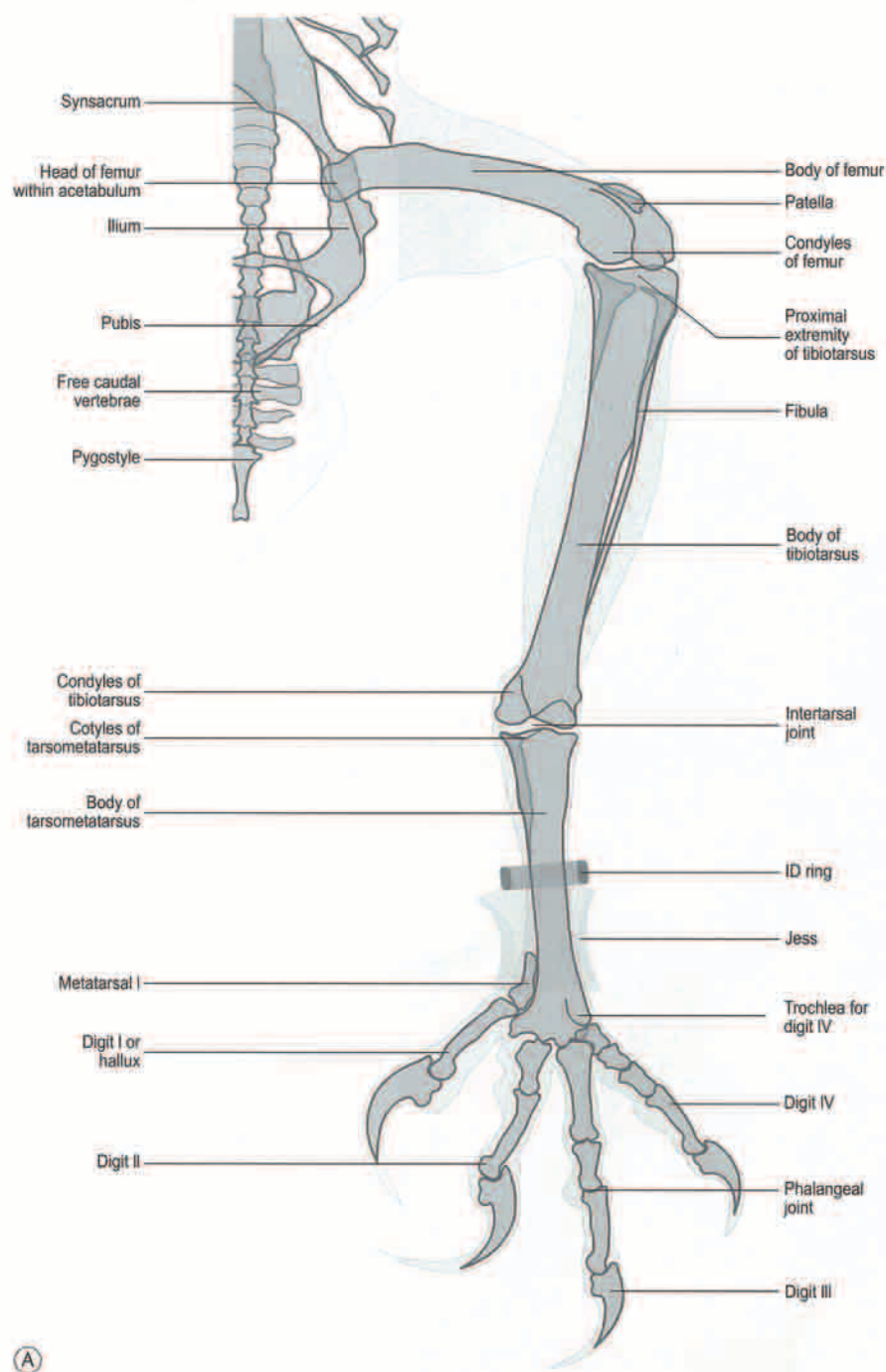
Fig. 3.27 (A and B) Mediolateral view of the pelvic limb of the gyr falcon. Note the ossified spike of bone in the origin of the medial head of *m. flexor hallucis longus*, the ossified portion of tibial cartilage, the ossified portion of *lig. cartilago-metatarsale mediale*, the intratendinous ossification of flexor tendons in the tarsometatarsus and the sesamoid between the metatarsophalangeal joint of digit II and the flexor tendons.

SECTION 9 RADIOGRAPHIC SPECIES CATALOG



Fig. 3.27 (Cont'd).

SECTION 9 RADIOGRAPHIC SPECIES CATALOG



(A)

Fig. 3.28 (A and B) Craniocaudal view of the pelvic limb of the gyr falcon.

SECTION 9 RADIOGRAPHIC SPECIES CATALOG



Fig. 3.28 (Cont'd).

SECTION 9 RADIOGRAPHIC SPECIES CATALOG

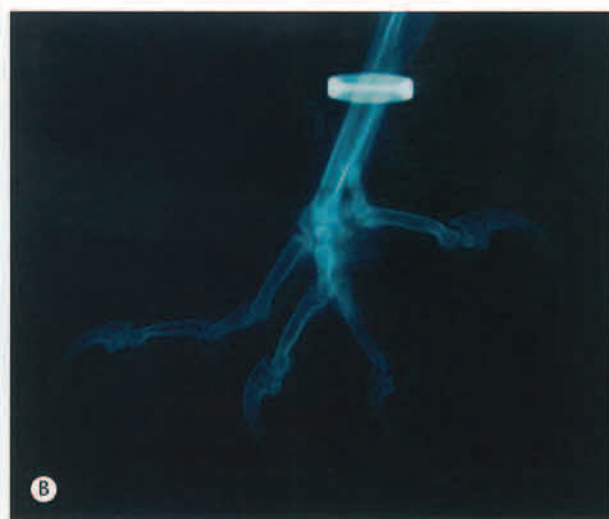
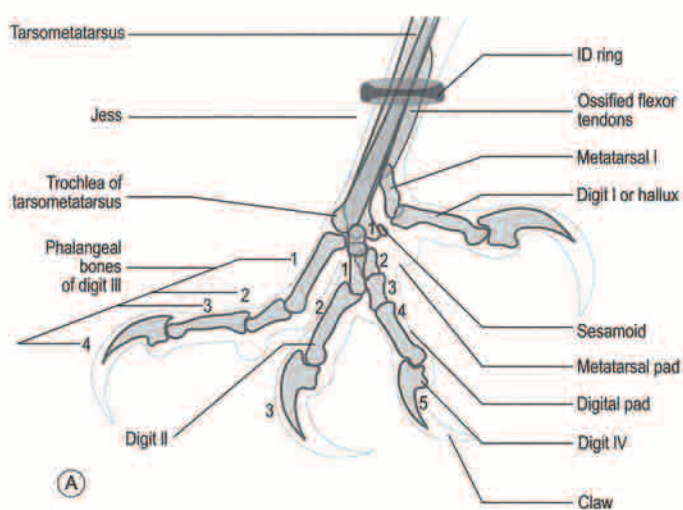


Fig. 3.29 (A and B) Mediolateral close-up of the foot of the gyr falcon. Note the ossified flexor tendons of the tarsometatarsus and the sesamoid bone between the metatarsophalangeal joint of digit II and the flexor tendons.

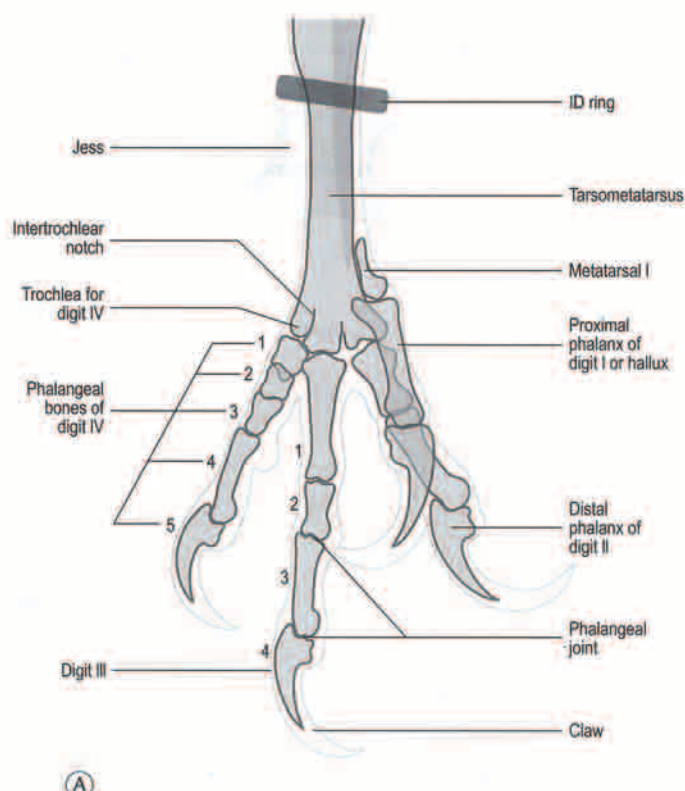


Fig. 3.30 (A and B) Craniocaudal close-up of the foot of the gyr falcon, with digit I flexed.

SECTION 9 RADIOGRAPHIC SPECIES CATALOG

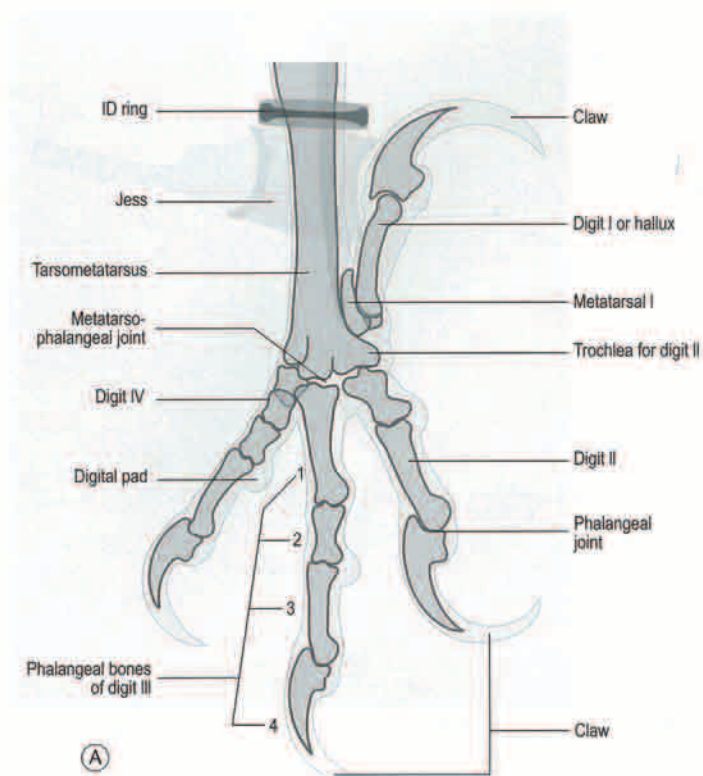


Fig. 3.31 (A and B) Craniocaudal close-up of the foot of the gyr falcon, with digit I extended.

SECTION 9 RADIOGRAPHIC SPECIES CATALOG

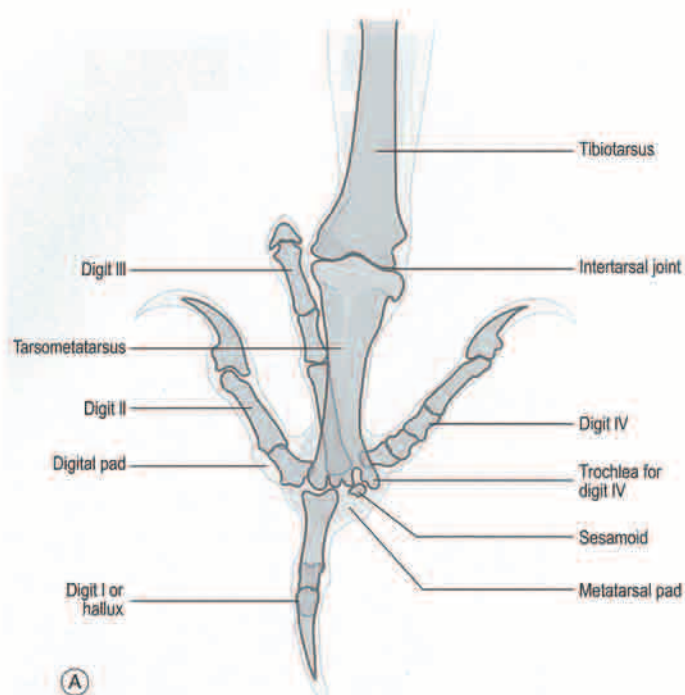


Fig. 3.32 (A and B) Caudoplantar close-up of the foot of the gyr falcon. Note the sesamoid bone between the metatarsophalangeal joint of digit II and the flexor tendons.

SECTION 9 RADIOGRAPHIC SPECIES CATALOG

**Steppe eagle** (*Aquila nipalensis*, Hodgson, 1833, Nepal)

The steppe eagle is a medium-to-large size species measuring 72–81 cm in length with a wingspan of 160–200 cm. The body weight of an individual ranges from 2400 to 3900 g. Overall plumage color is dark brown with adults displaying a prominent rufous nape patch. The female is considerably larger than males. Juvenile and immature individuals display a conspicuous broad white band along

greater underwing coverts. Two subspecies have currently been identified: *A. n. orientalis* from southeast European Russia east to Lake Balkhash and east Kazakhstan wintering in the Middle East, Arabia and East and South Africa, and *A. n. nipalensis* from Altai and Tibet east to Manchuria wintering in south Asia. Steppe inhabit semidesert habitats feeding chiefly on mammals. Immature specimens usually take carrion during migration and wintering.

SECTION 9 RADIOGRAPHIC SPECIES CATALOG

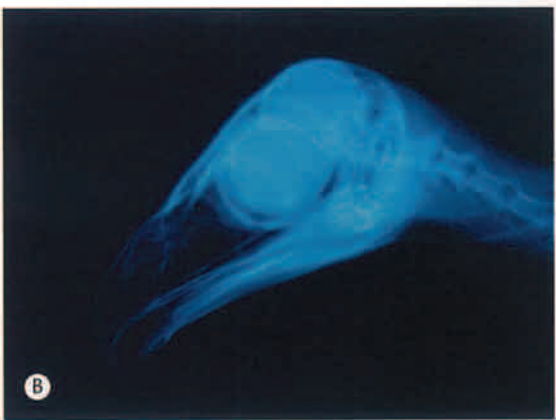
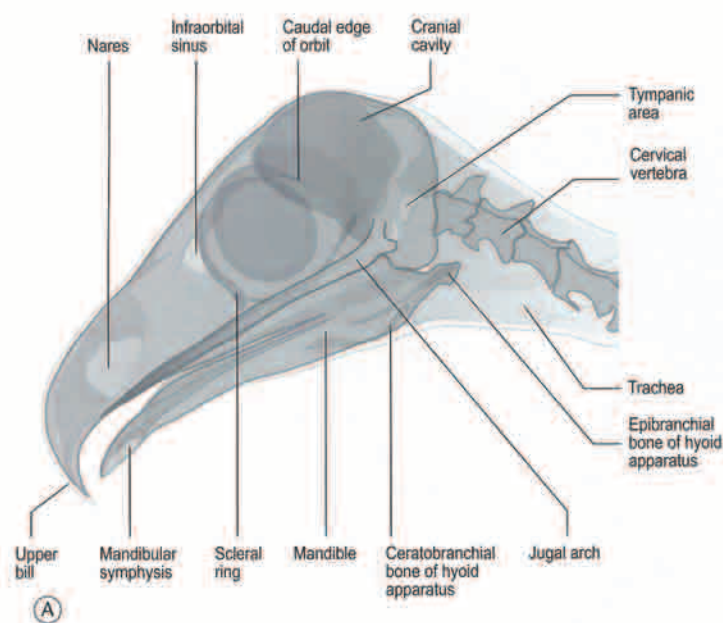


Fig. 3.33 (A and B) Lateral (Le-Rt) view of the head of the steppe eagle.

SECTION 9 RADIOGRAPHIC SPECIES CATALOG

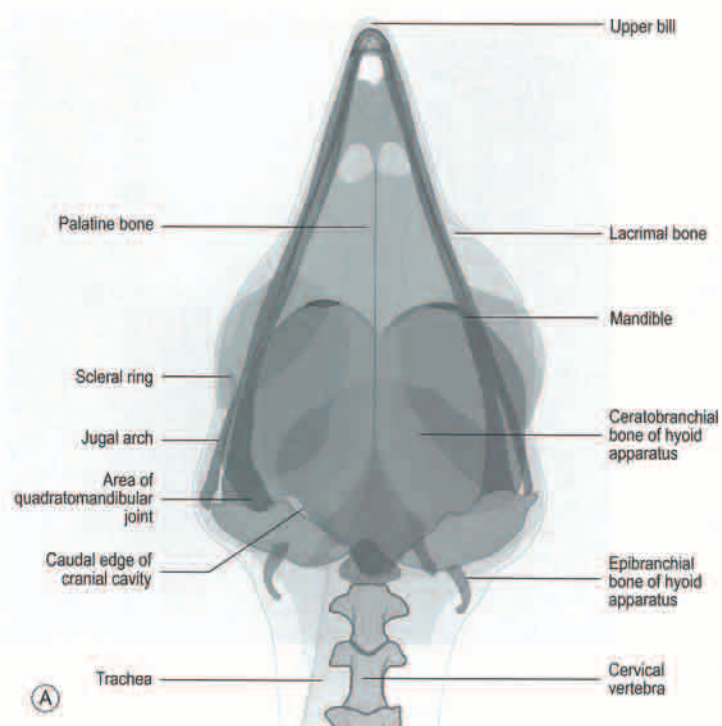


Fig. 3.34 (A and B) Ventrodorsal view of the head of the steppe eagle.

SECTION 9 RADIOGRAPHIC SPECIES CATALOG

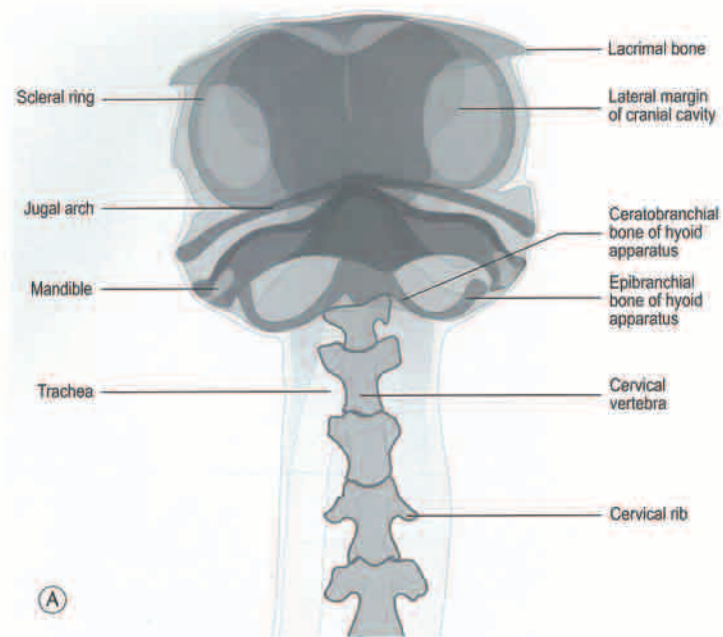


Fig. 3.35 (A and B) Rostrocaudal view of the head of the steppe eagle.

SECTION 9 RADIOGRAPHIC SPECIES CATALOG

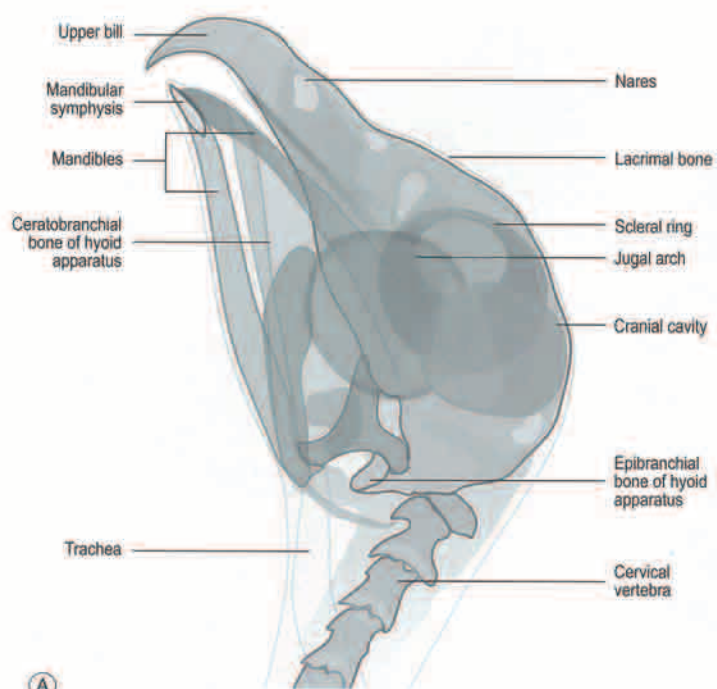


Fig. 3.36 (A and B) Oblique (LeD-RtVO) view of the head of the steppe eagle.

SECTION 9 RADIOGRAPHIC SPECIES CATALOG

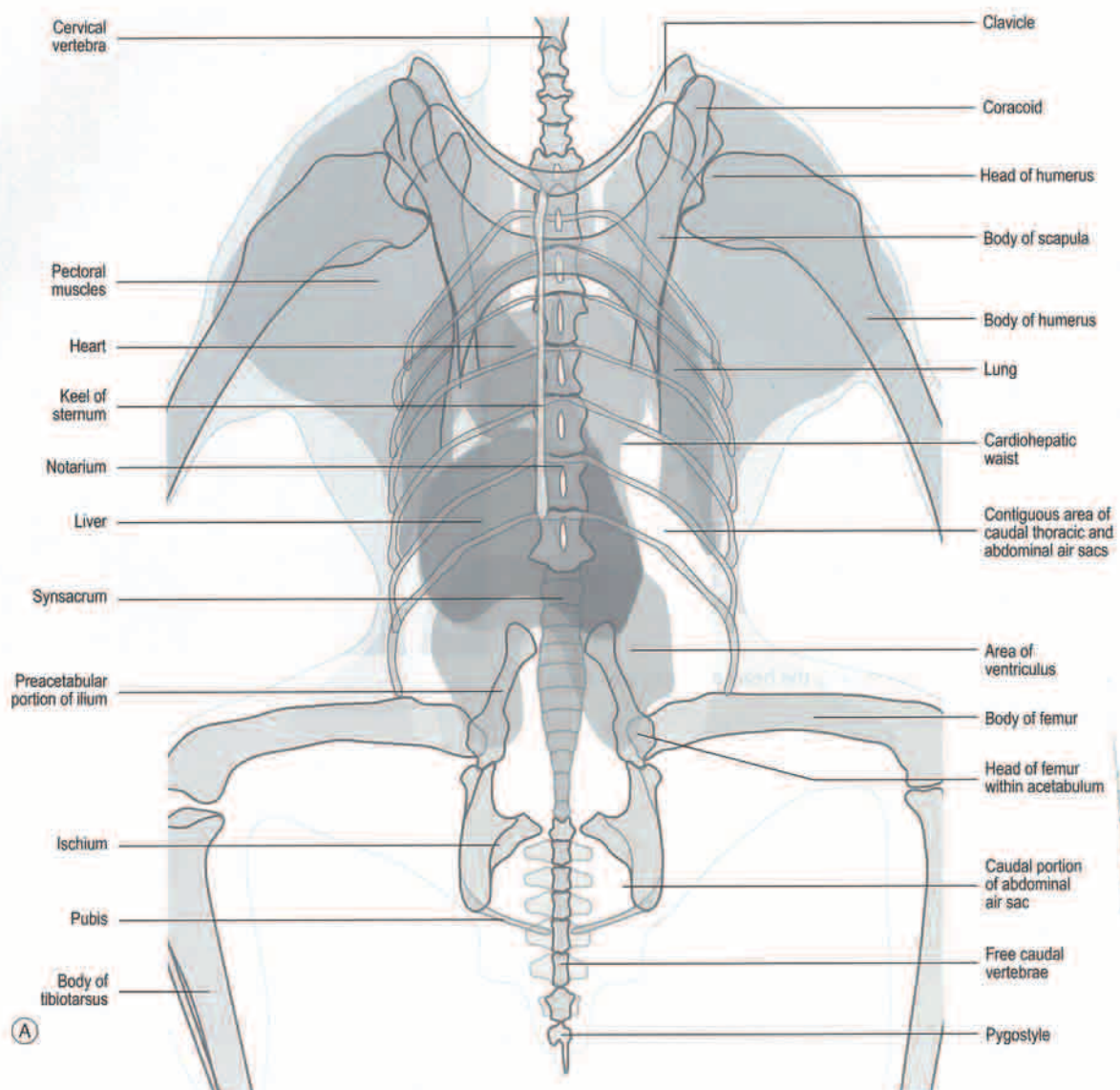


Fig. 3.37 (A and B) Ventrodorsal view of the body of the steppe eagle.

SECTION 9 RADIOGRAPHIC SPECIES CATALOG



Fig. 3.37 (Cont'd).

SECTION 9 RADIOGRAPHIC SPECIES CATALOG

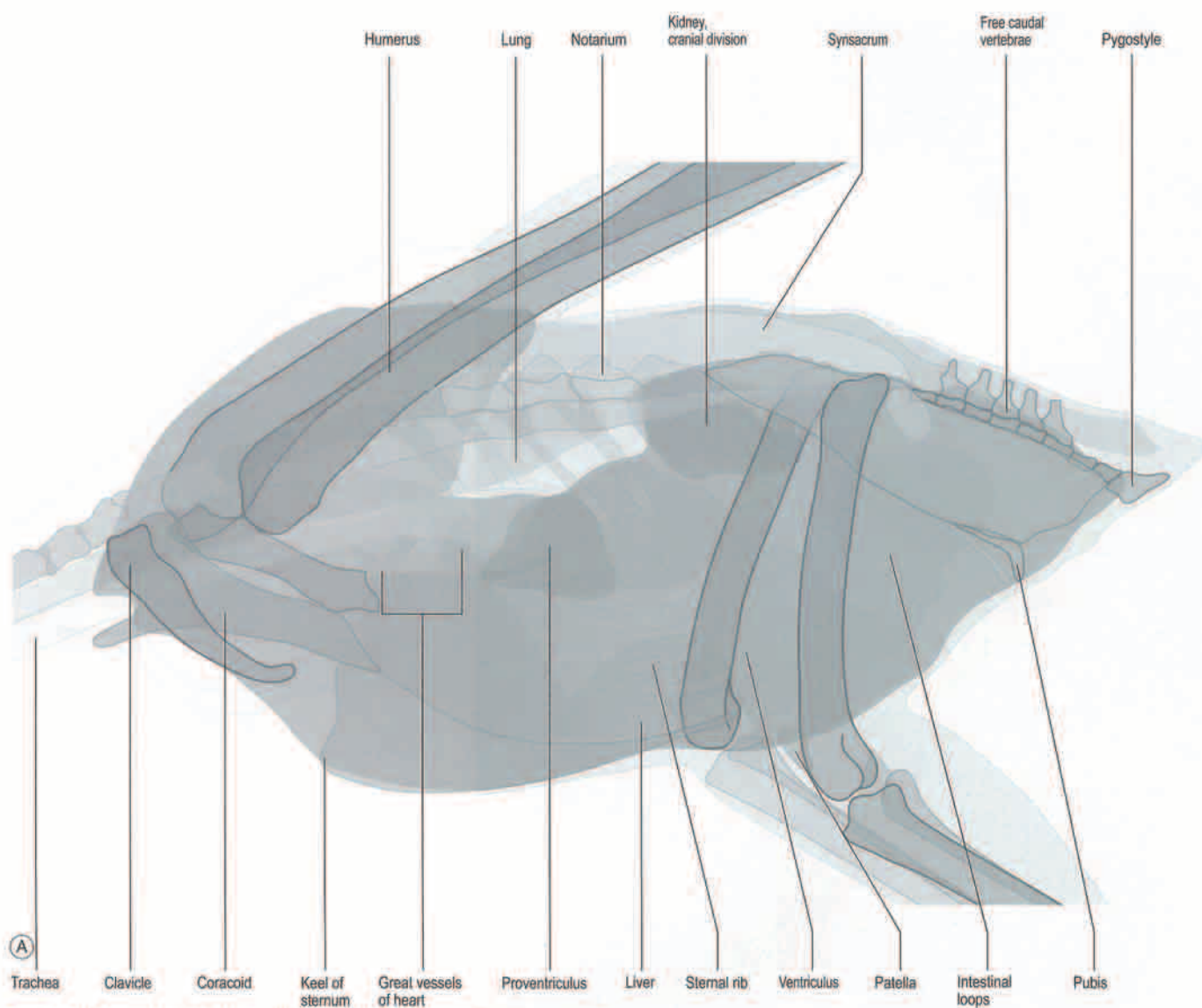


Fig. 3.38 (A and B) Lateral (Le-Rt) view of the body of the steppe eagle.

SECTION 9 RADIOGRAPHIC SPECIES CATALOG

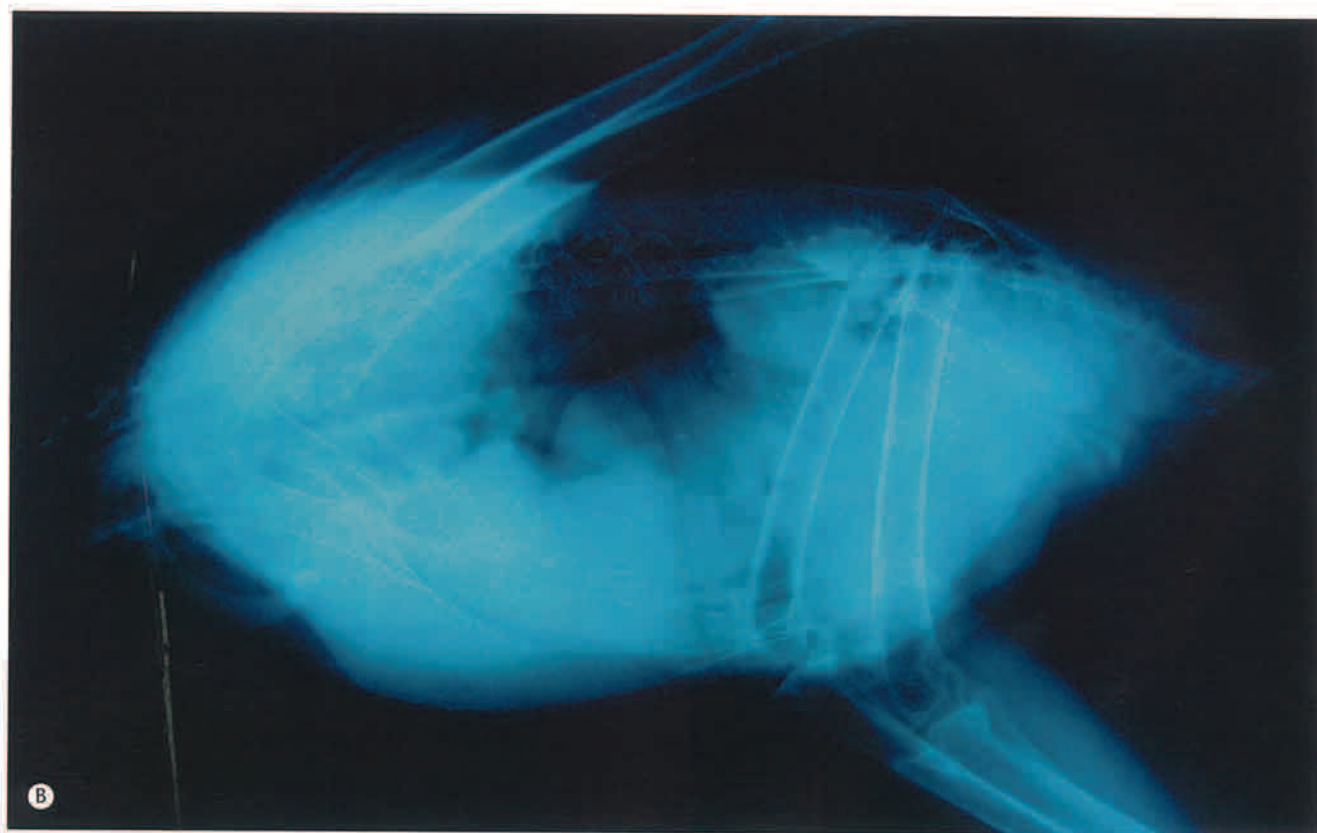


Fig. 3.38 (Cont'd).

SECTION 9 RADIOGRAPHIC SPECIES CATALOG

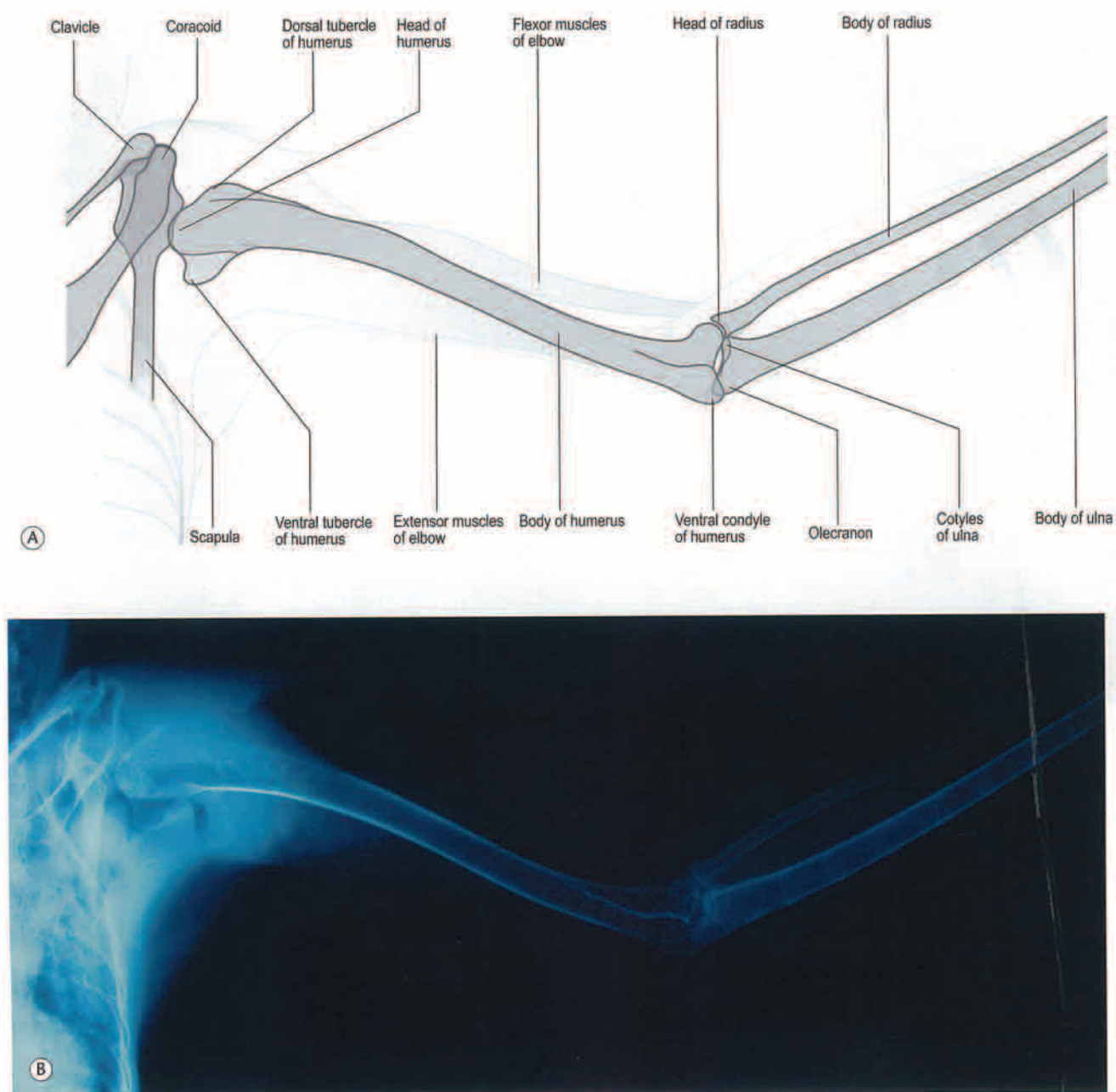


Fig. 3.39 (A and B) Ventrodorsal view of the proximal wing of the steppe eagle.

SECTION 9 RADIOGRAPHIC SPECIES CATALOG

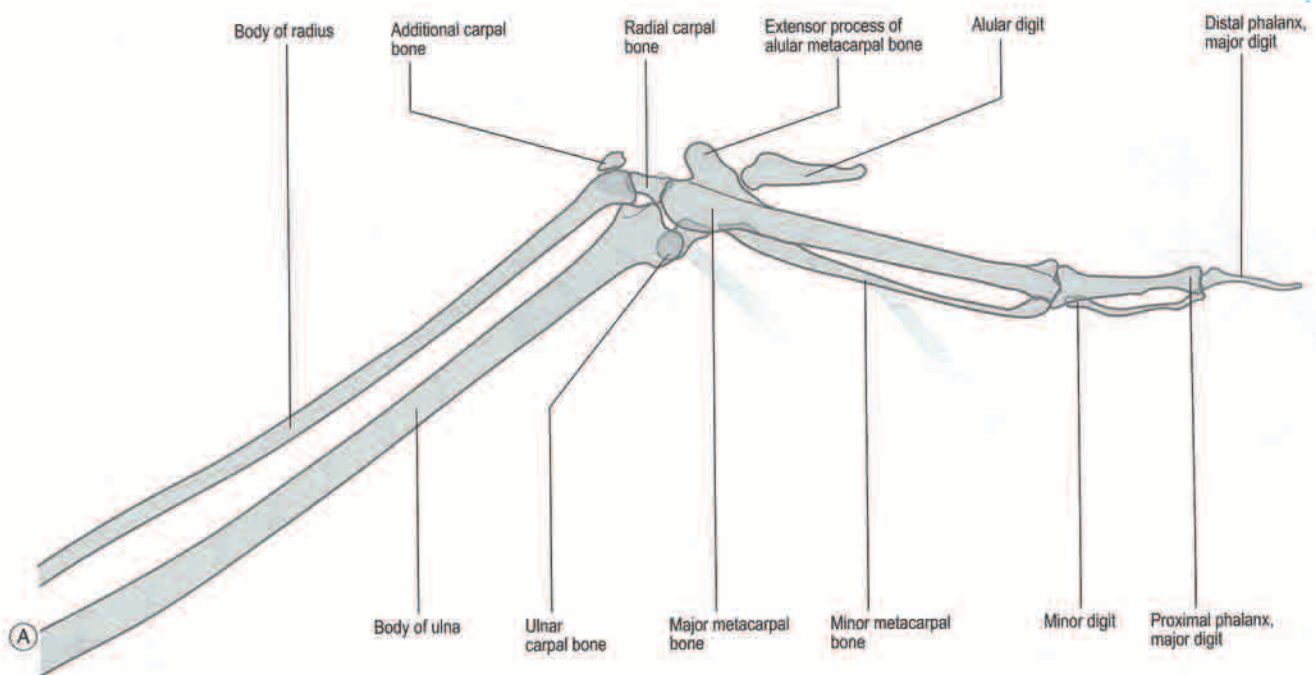


Fig. 3.40 (A and B) Ventrodorsal view of the distal wing of the steppe eagle. Note the presence of the additional carpal bone.

SECTION 9 RADIOGRAPHIC SPECIES CATALOG

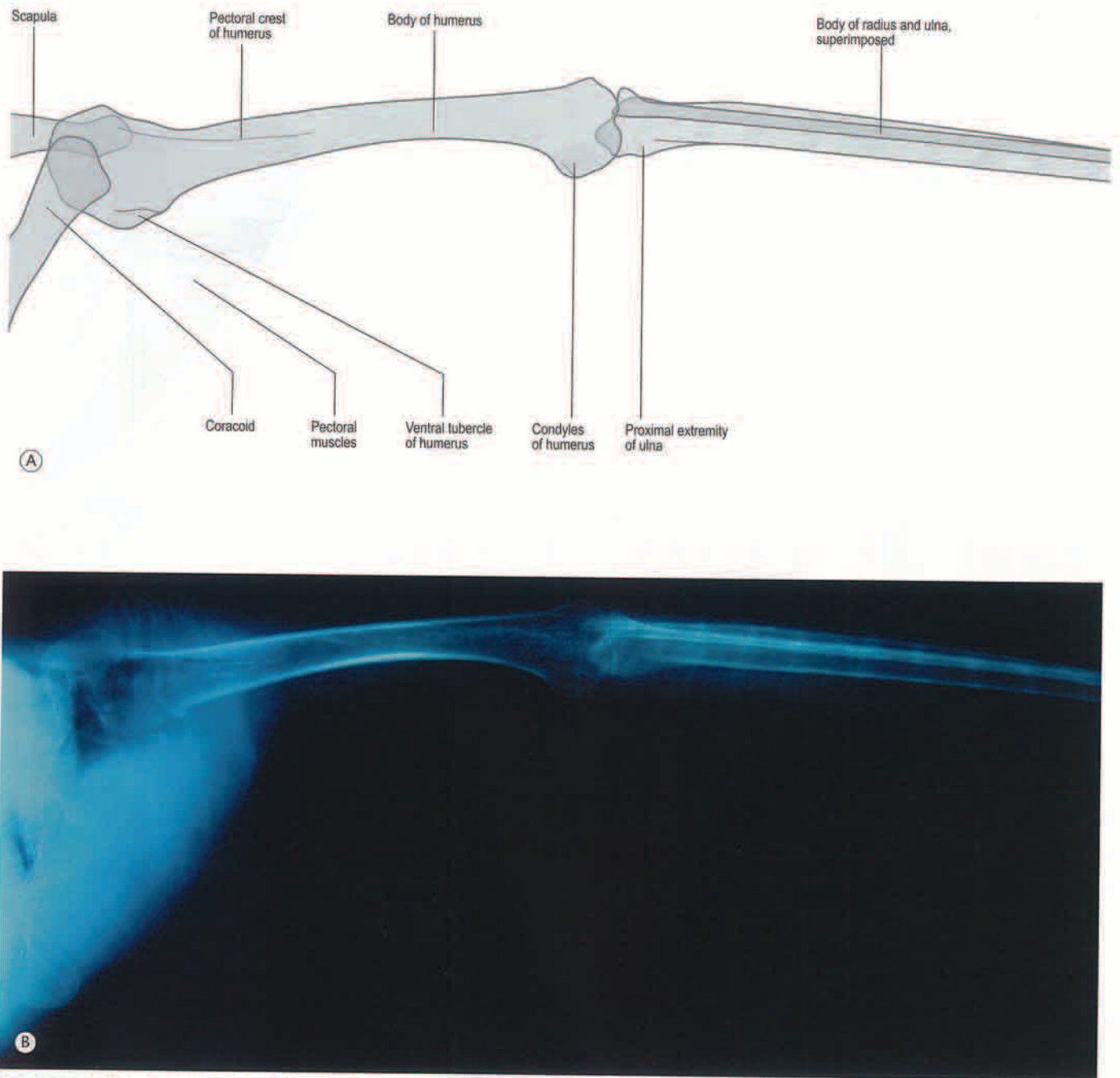


Fig. 3.41 (A and B) Craniocaudal view of the proximal wing of the steppe eagle. Note the absence of the humeroscapular bone.

SECTION 9 RADIOGRAPHIC SPECIES CATALOG

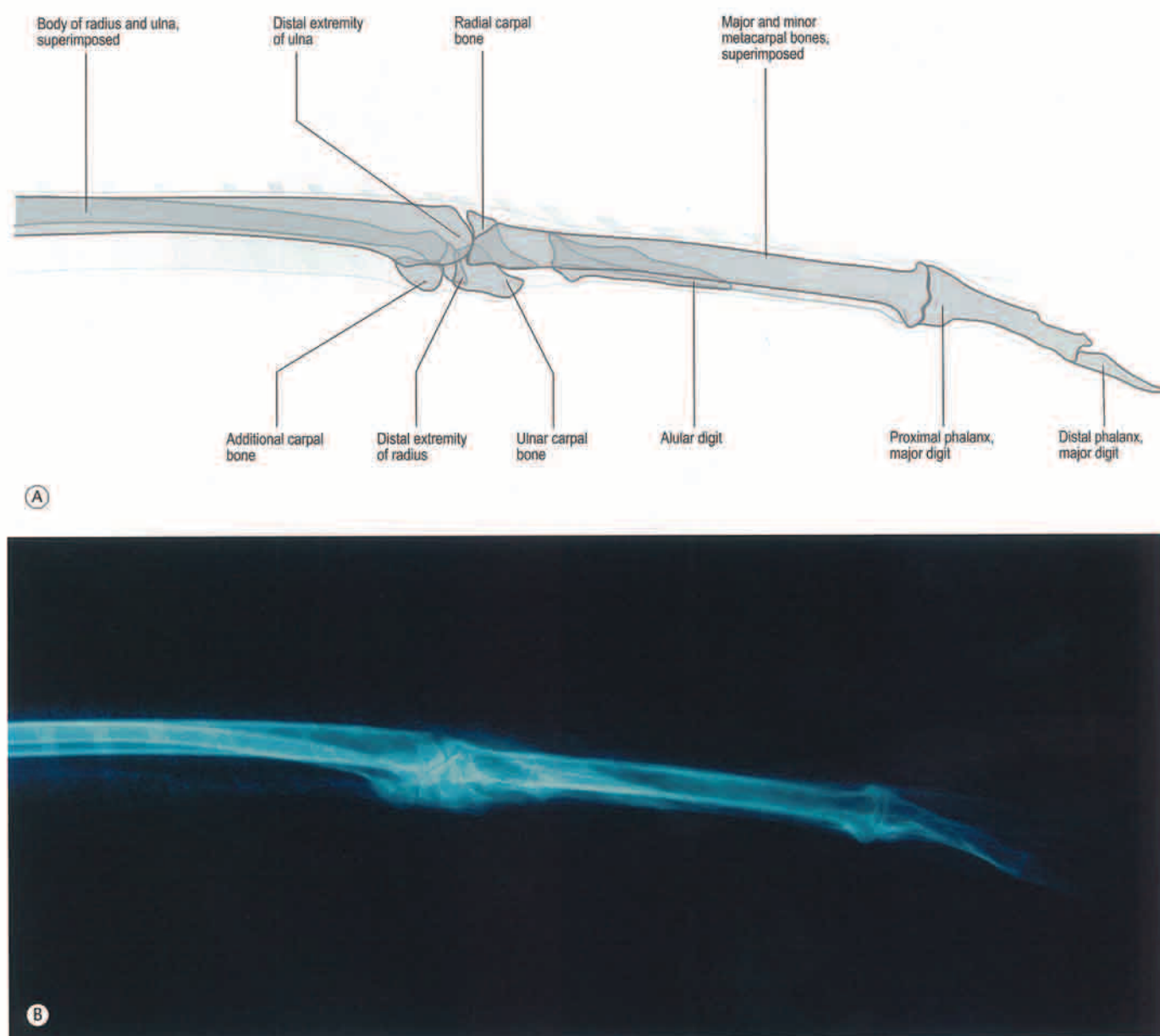


Fig. 3.42 (A and B) Craniocaudal view of the distal wing of the steppe eagle. Note the presence of the additional carpal bone.

SECTION 9 RADIOGRAPHIC SPECIES CATALOG

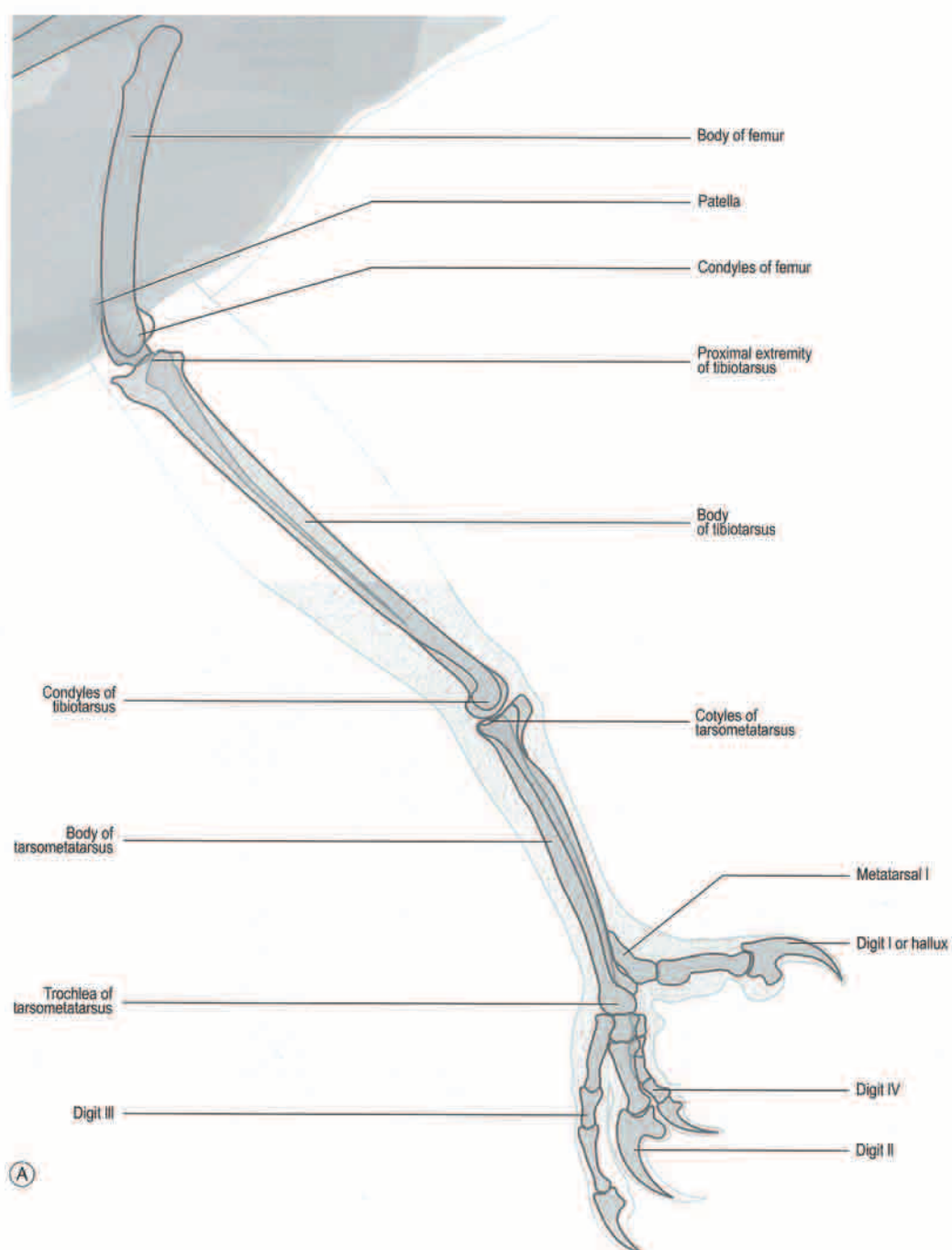


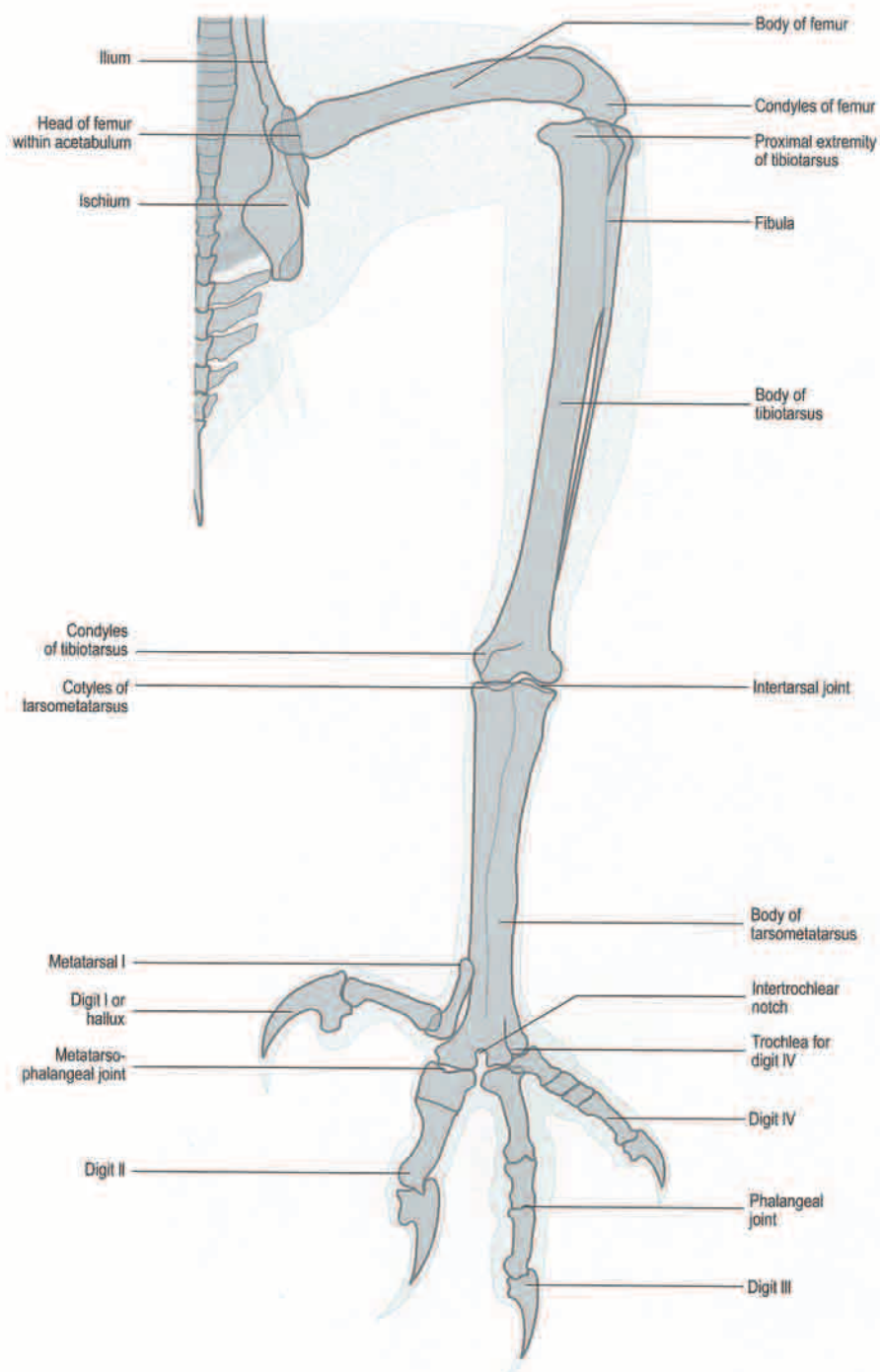
Fig. 3.43 (A and B) Mediolateral view of the pelvic limb of the steppe eagle.

SECTION 9 RADIOGRAPHIC SPECIES CATALOG



Fig. 3.43 (Cont'd).

SECTION 9 RADIOGRAPHIC SPECIES CATALOG



(A)

Fig. 3.44 (A and B) Craniocaudal view of the pelvic limb of the steppe eagle.

SECTION 9 RADIOGRAPHIC SPECIES CATALOG



Fig. 3.44 (Cont'd).

SECTION 9 RADIOGRAPHIC SPECIES CATALOG

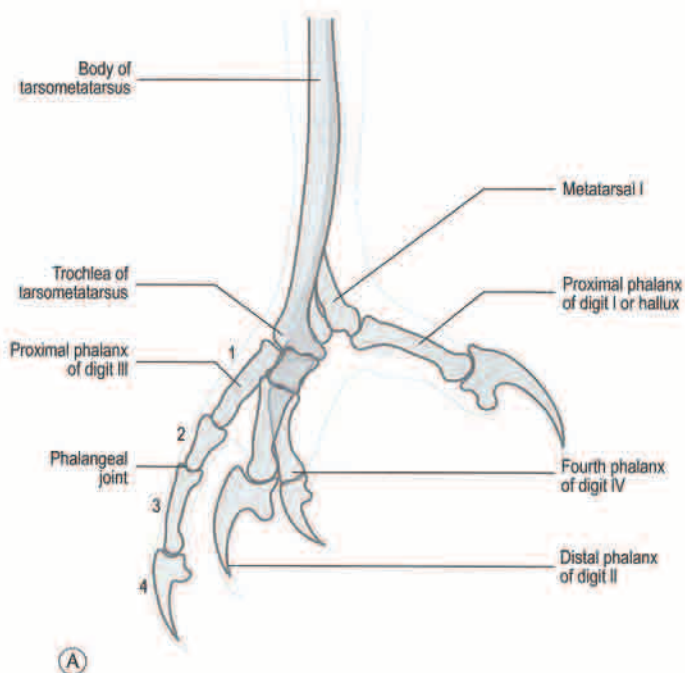


Fig. 3.45 (A and B) Mediolateral close-up of the foot of the steppe eagle.

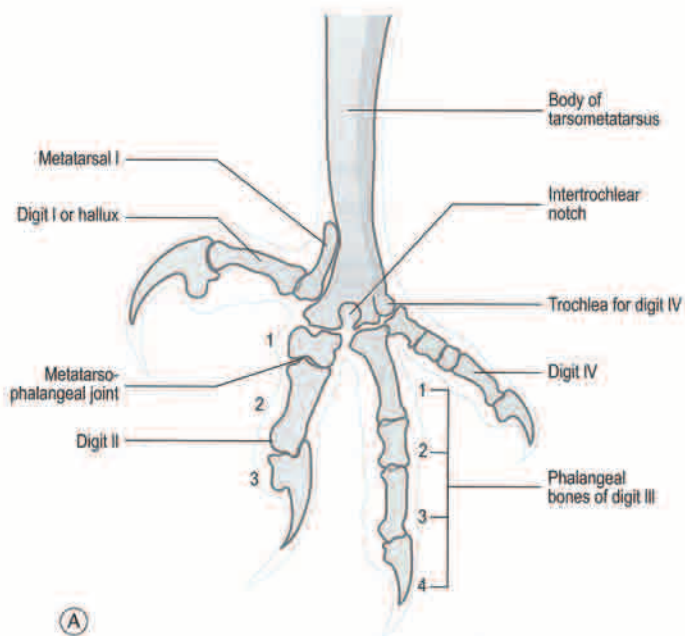


Fig. 3.46 (A and B) Craniocaudal close-up of the foot of the steppe eagle.

SECTION 9 RADIOGRAPHIC SPECIES CATALOG



Palm nut vulture (*Gypohierax angolensis*, Gmelin, 1788, Angola)

The palm nut vulture is a relatively small species. Individuals weigh between 1361 and 1712 g. The length of the body is 60 cm with a wingspan of 150 cm. The species is monotypic with black back including secondary feathers and primary tips and short black tail with white tip. The face has a distinct bare red patch with white neck, breast, shoulders and thighs. The species is found in Senegambia east to Kenya coast and south to Angola and northeast South Africa. It lives on the edges of tropical forest, large rivers, lakes, estuaries and seashore feeding mainly on the fleshy pericarp of *Elaeis guineensis* and *Raphia* sp. palm fruits. Other food items could be included in the diet in particular, invertebrates, fish, crabs, amphibian, mollusks and even medium-sized birds and mammals.

SECTION 9 RADIOGRAPHIC SPECIES CATALOG

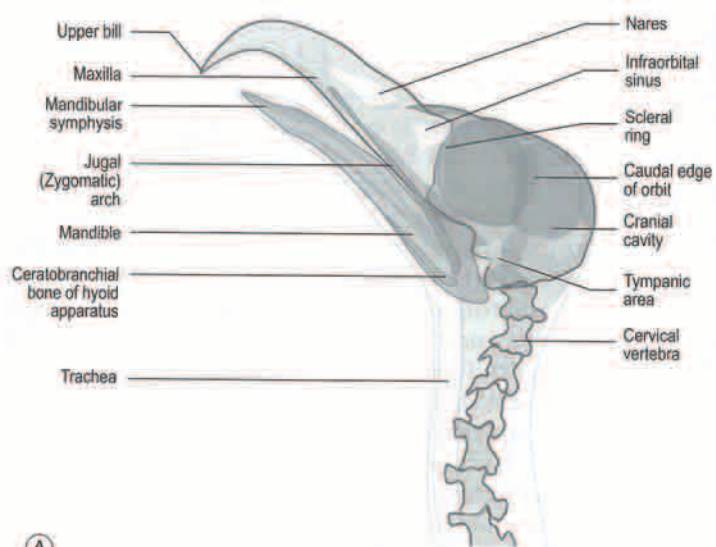


Fig. 3.47 (A and B) Lateral (Le-Rt) view of the head of the palm nut vulture.

SECTION 9 RADIOGRAPHIC SPECIES CATALOG

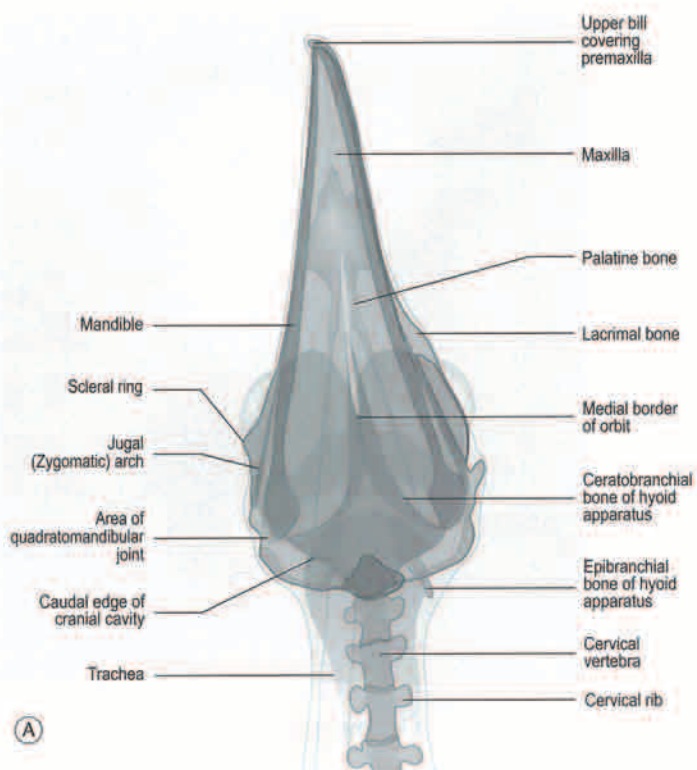


Fig. 3.48 (A and B) Ventrodorsal view of the head of the palm nut vulture.

SECTION 9 RADIOGRAPHIC SPECIES CATALOG

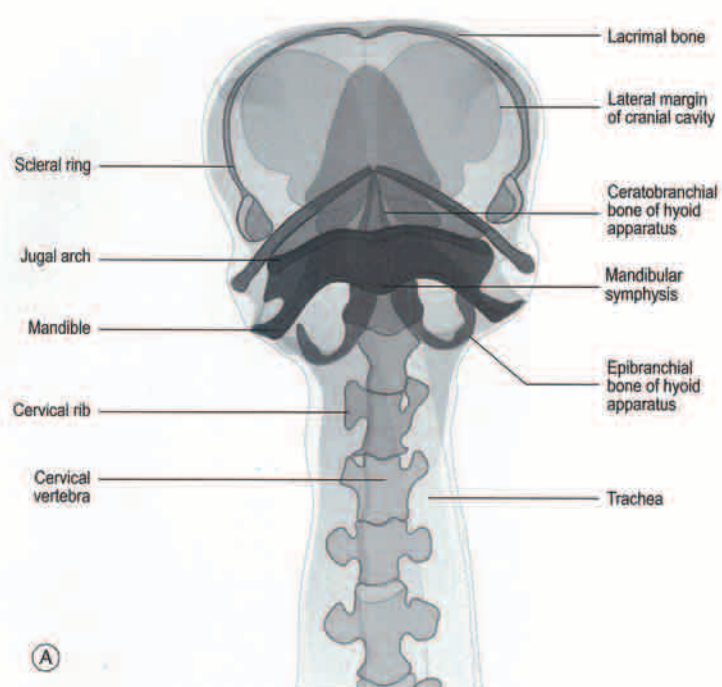


Fig. 3.49 (A and B) Rostrocaudal view of the head of the palm nut vulture. Note the less prominent lacrimal bone.

SECTION 9 RADIOGRAPHIC SPECIES CATALOG

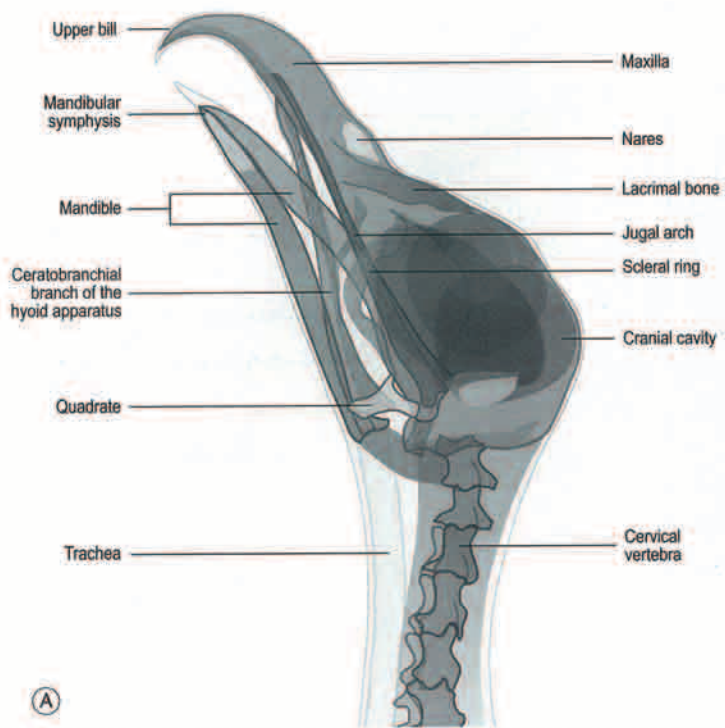


Fig. 3.50 (A and B) Oblique (LeD-RtVO) view of the head of the palm nut vulture.

SECTION 9 RADIOGRAPHIC SPECIES CATALOG

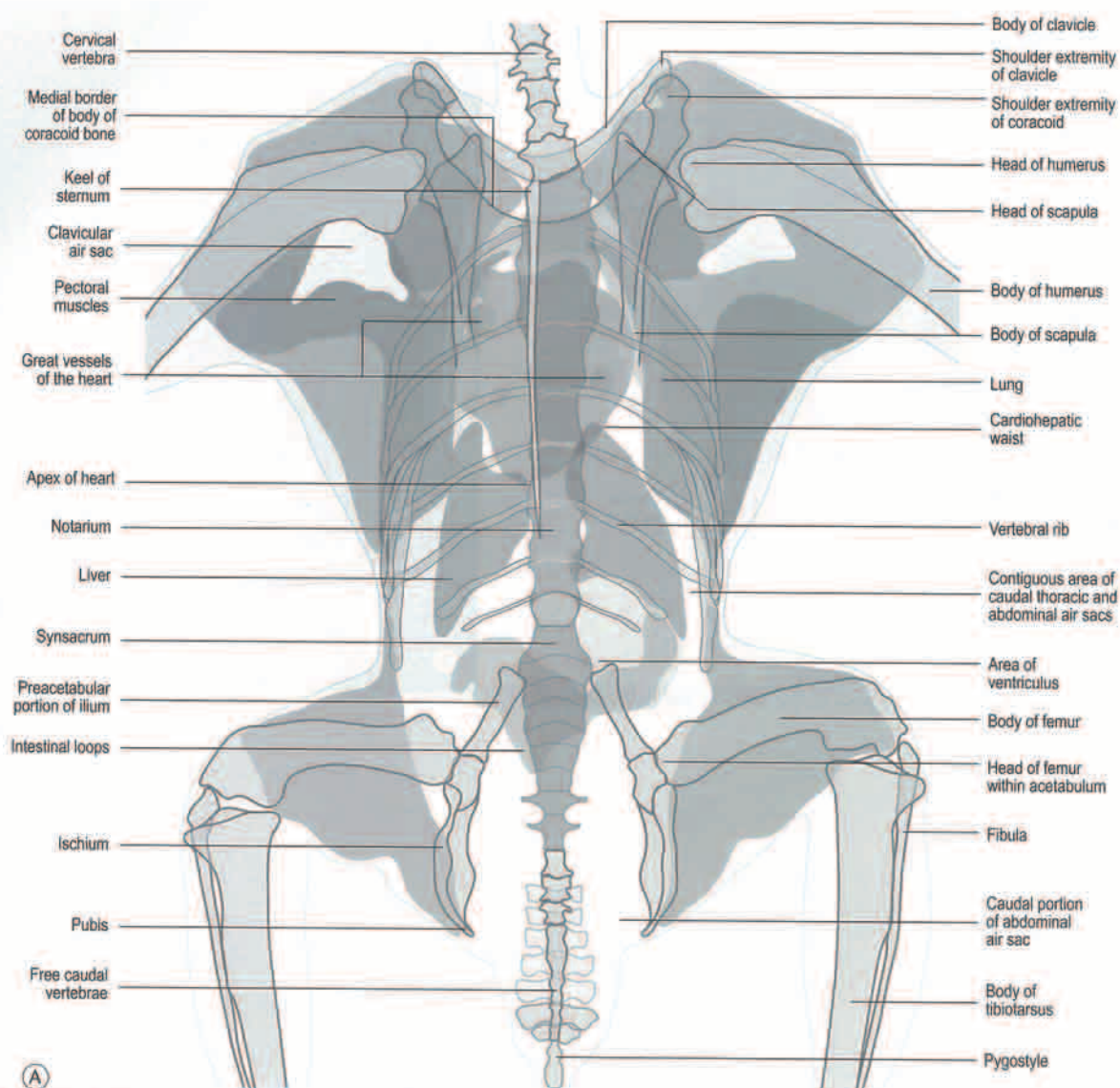


Fig. 3.51 (A and B) Ventrodorsal view of the body of the palm nut vulture.

SECTION 9 RADIOGRAPHIC SPECIES CATALOG



Fig. 3.51 (Cont'd).

SECTION 9 RADIOGRAPHIC SPECIES CATALOG

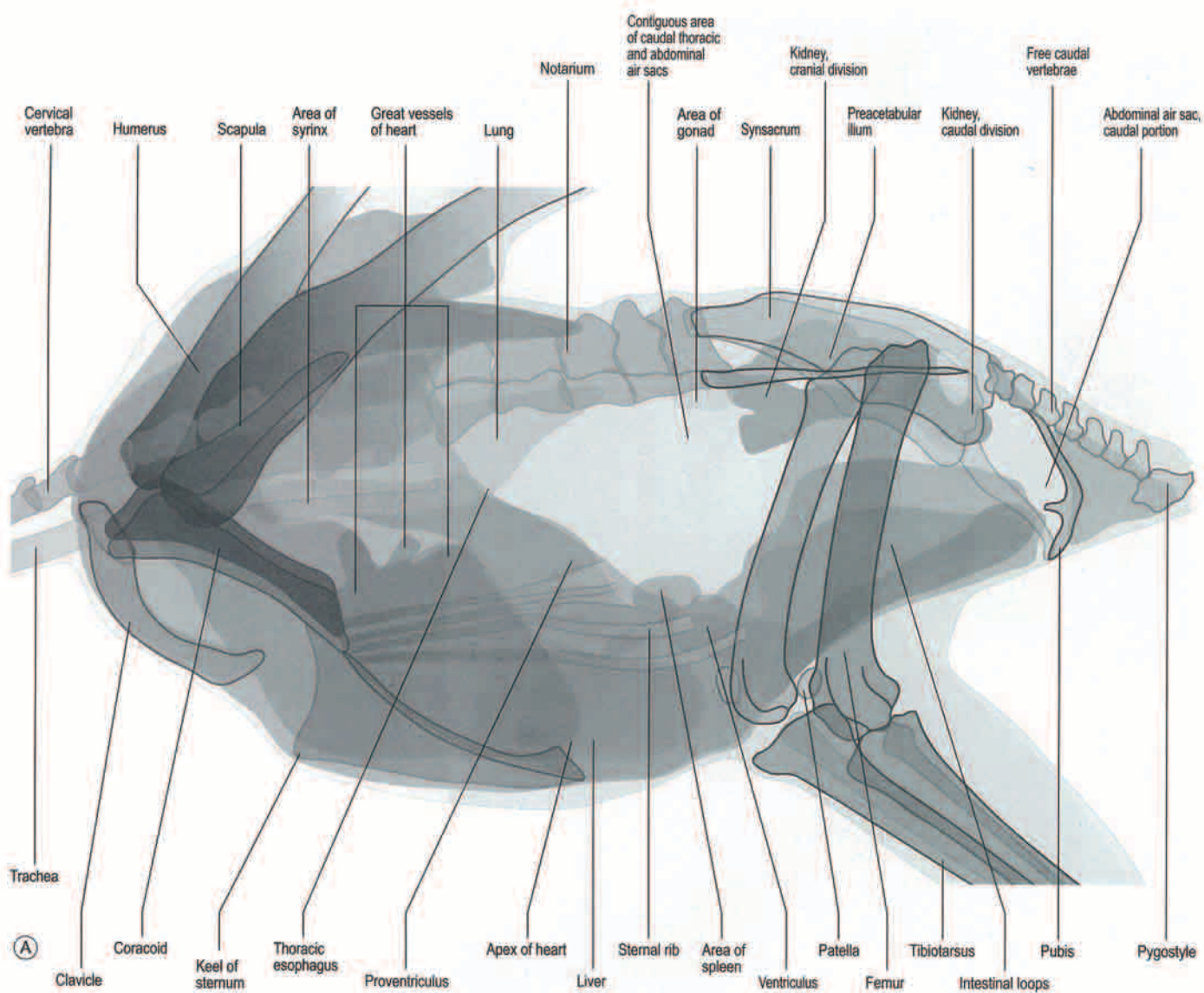


Fig. 3.52 (A and B) Lateral (Le-Rt) view of the body of the palm nut vulture.

SECTION 9 RADIOGRAPHIC SPECIES CATALOG

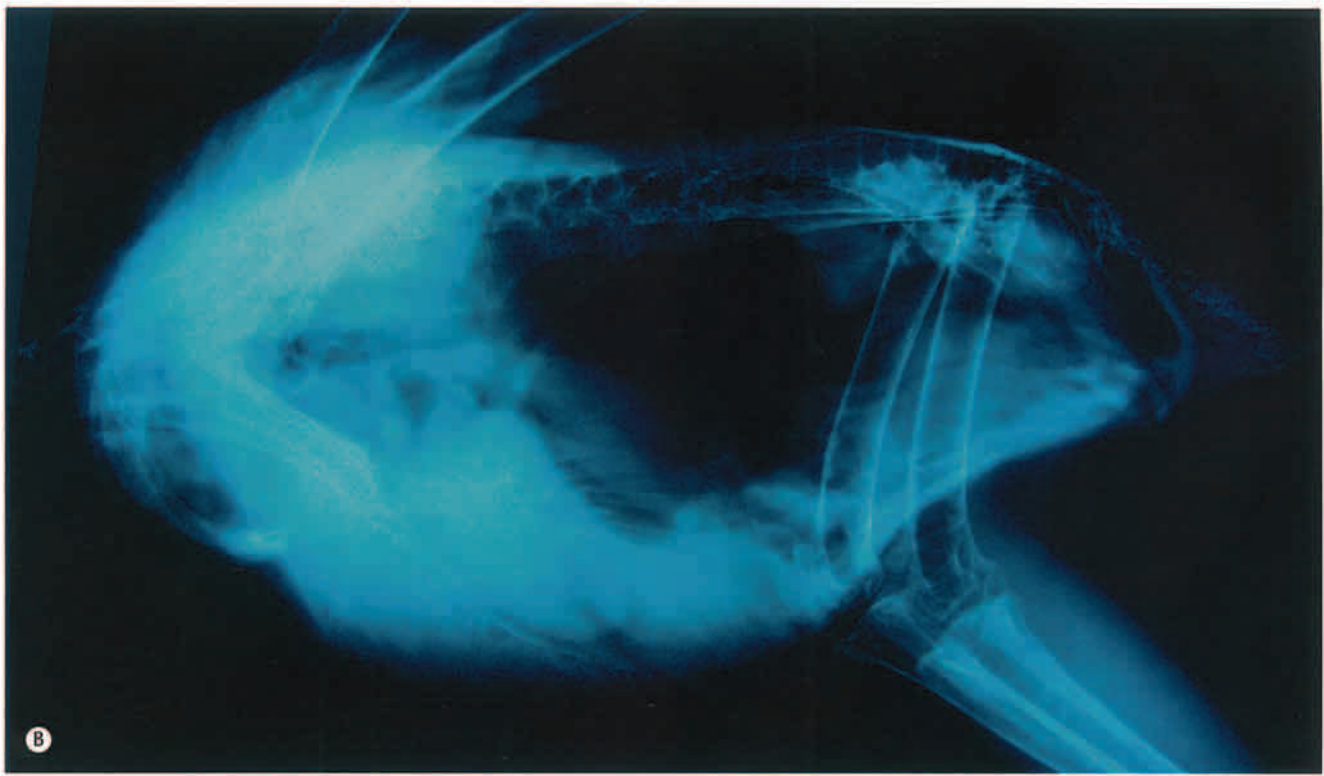


Fig. 3.52 (Cont'd).

SECTION 9 RADIOGRAPHIC SPECIES CATALOG

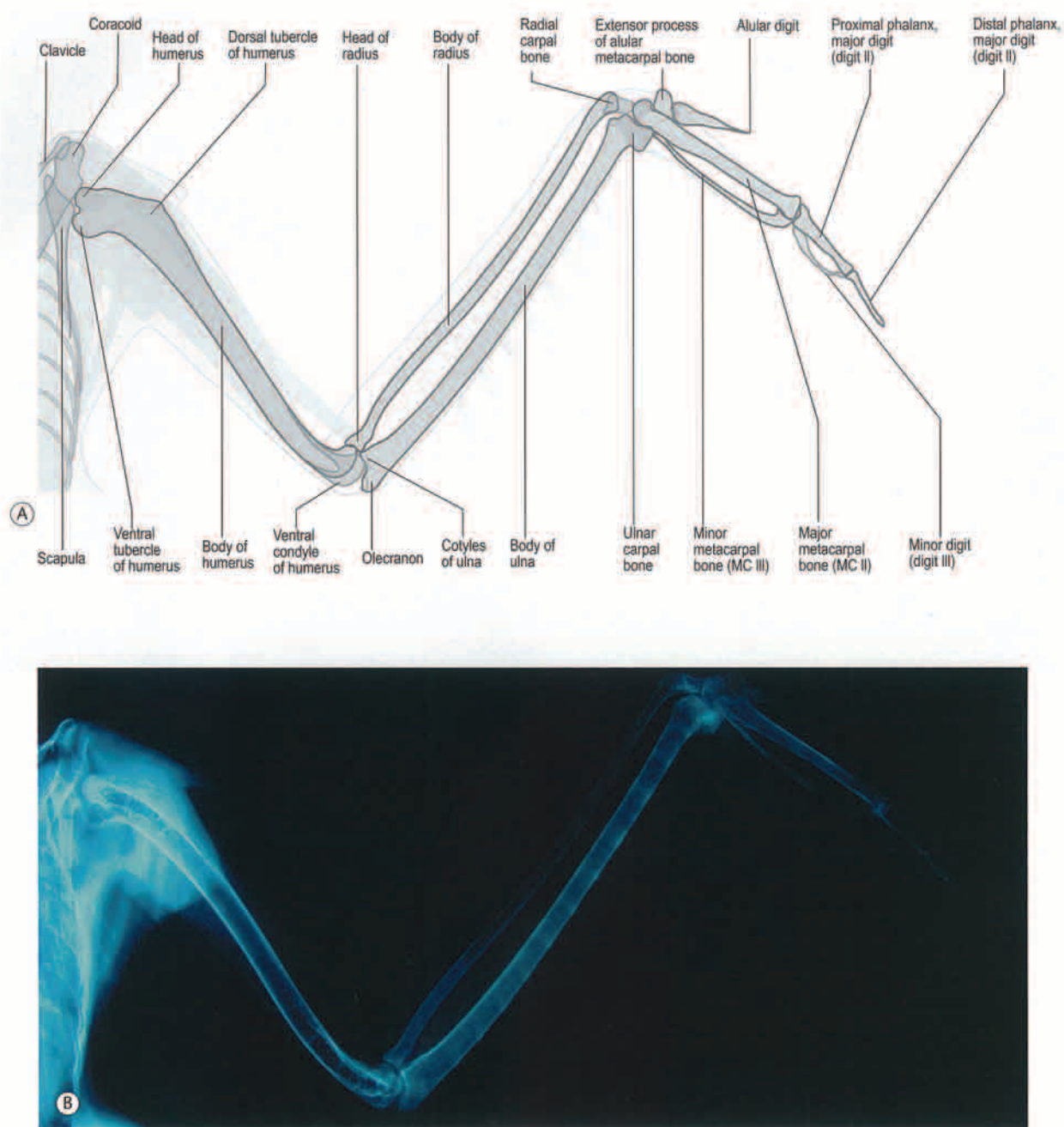


Fig. 3.53 (A and B) Ventrodorsal view of the wing of the palm nut vulture.

SECTION 9 RADIOGRAPHIC SPECIES CATALOG

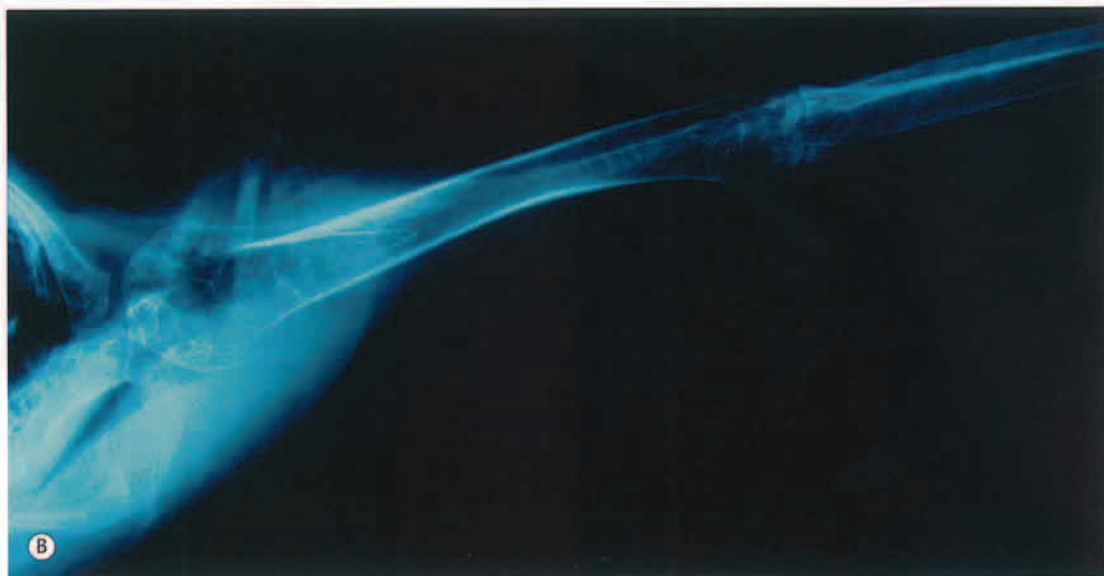
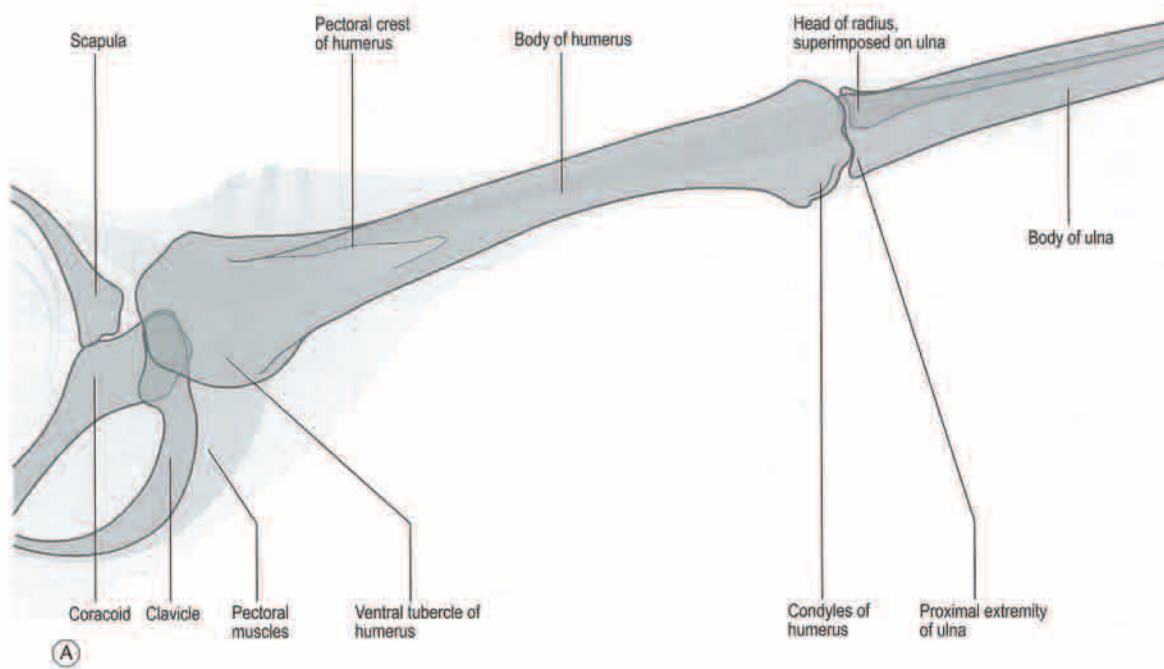


Fig. 3.54 (A and B) Craniocaudal view of the proximal wing of the palm nut vulture. Note the absence of the humeroscapular bone.

SECTION 9 RADIOGRAPHIC SPECIES CATALOG

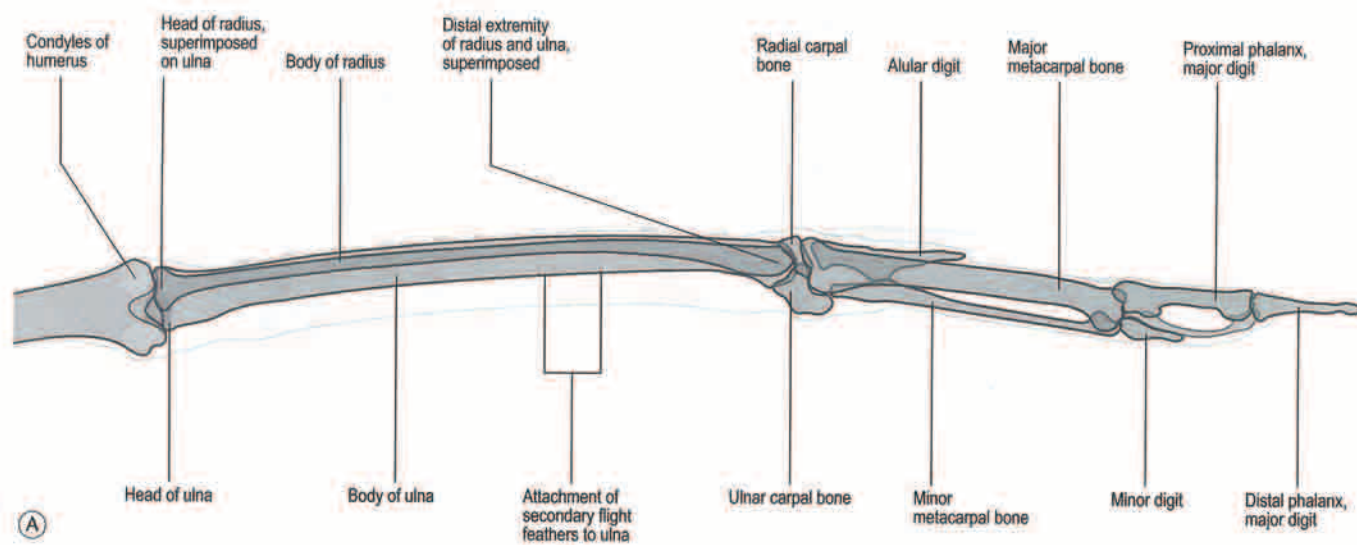


Fig. 3.55 (A and B) Craniocaudal view of the distal wing of the palm nut vulture.

SECTION 9 RADIOGRAPHIC SPECIES CATALOG

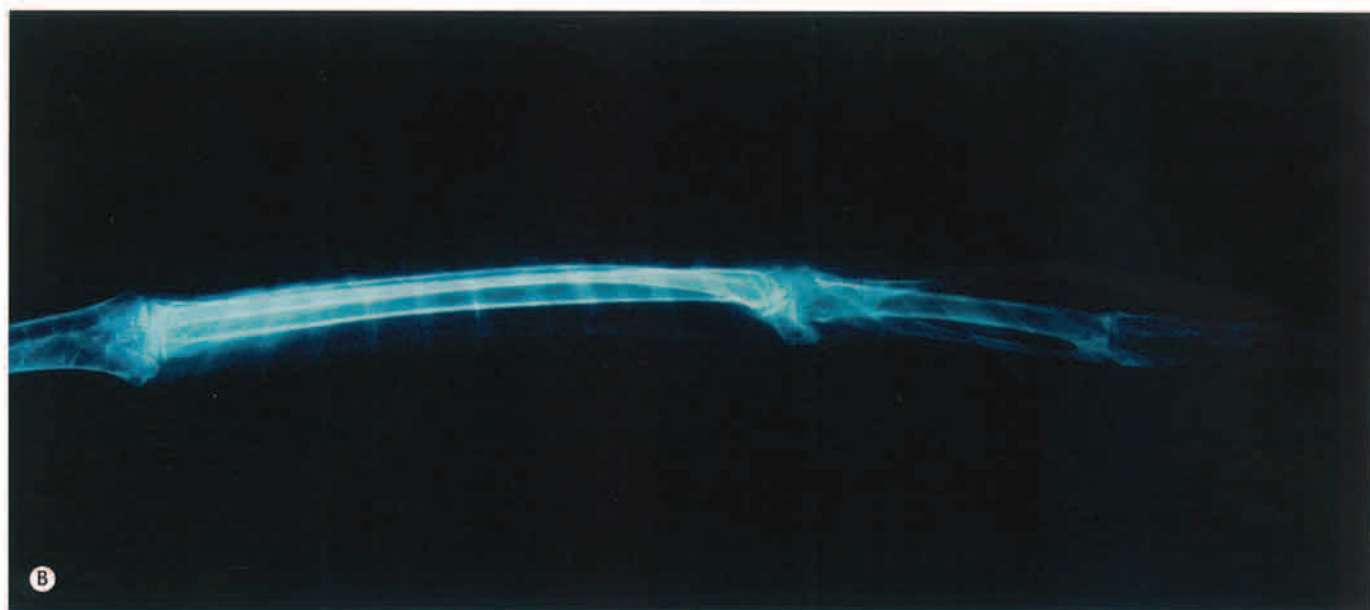


Fig. 3.55 (Cont'd).

SECTION 9 RADIOGRAPHIC SPECIES CATALOG

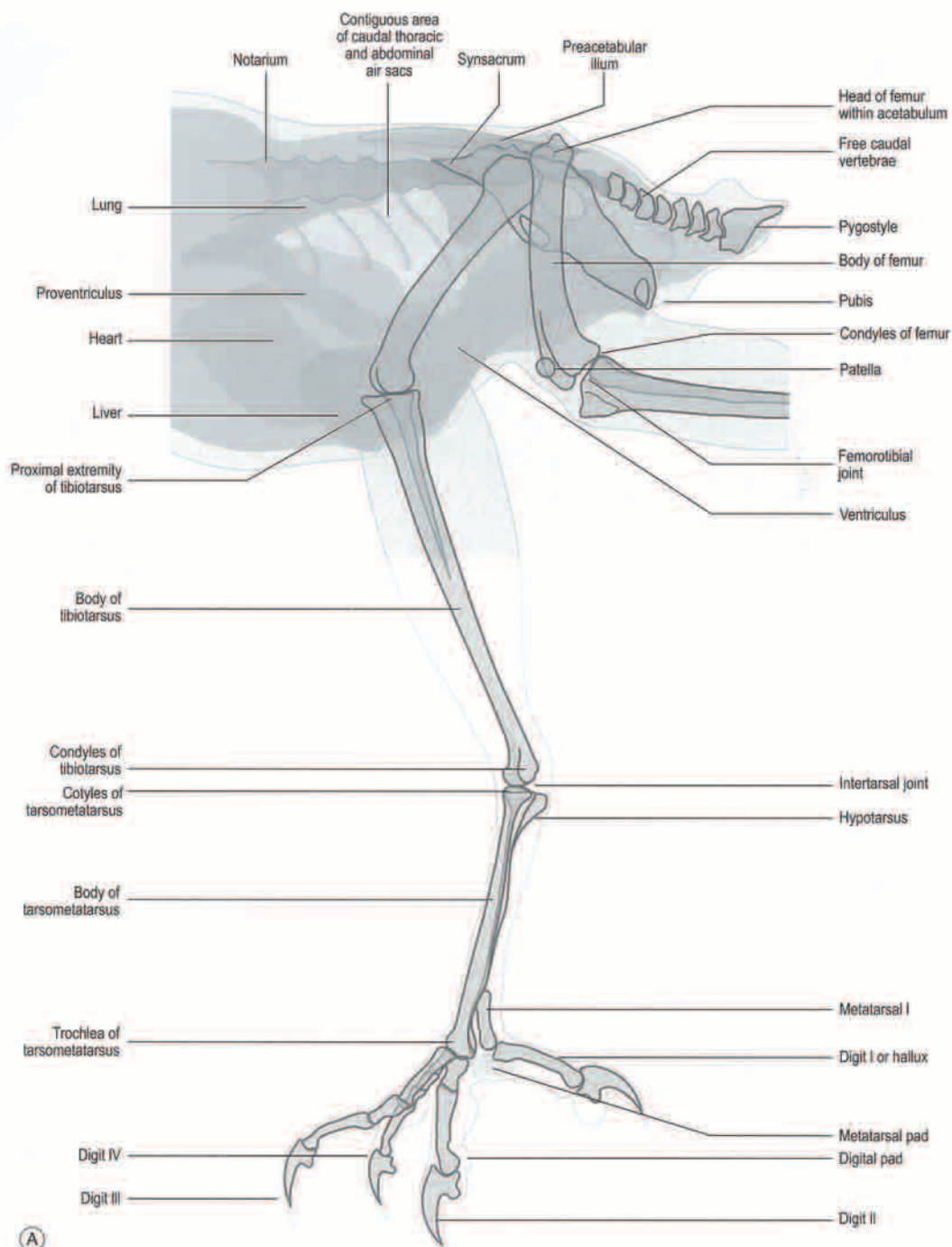


Fig. 3.56 (A and B) Mediolateral view of the pelvic limb of the palm nut vulture.

SECTION 9 RADIOGRAPHIC SPECIES CATALOG



Fig. 3.56 (Cont'd).

SECTION 9 RADIOGRAPHIC SPECIES CATALOG

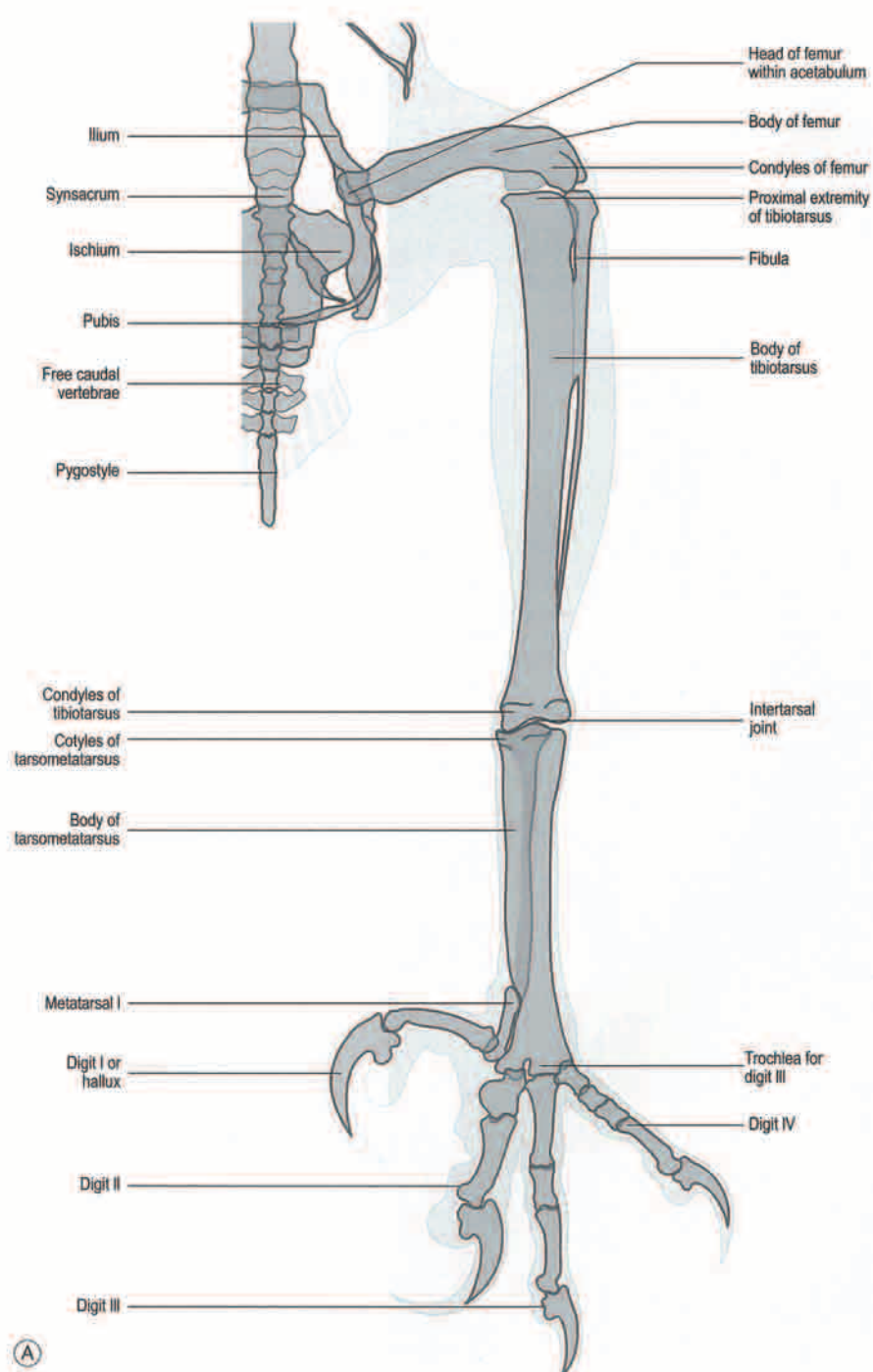


Fig. 3.57 (A and B) Craniocaudal view of the pelvic limb of the palm nut vulture.

SECTION 9 RADIOGRAPHIC SPECIES CATALOG



Fig. 3.57 (Cont'd).

SECTION 9 RADIOGRAPHIC SPECIES CATALOG

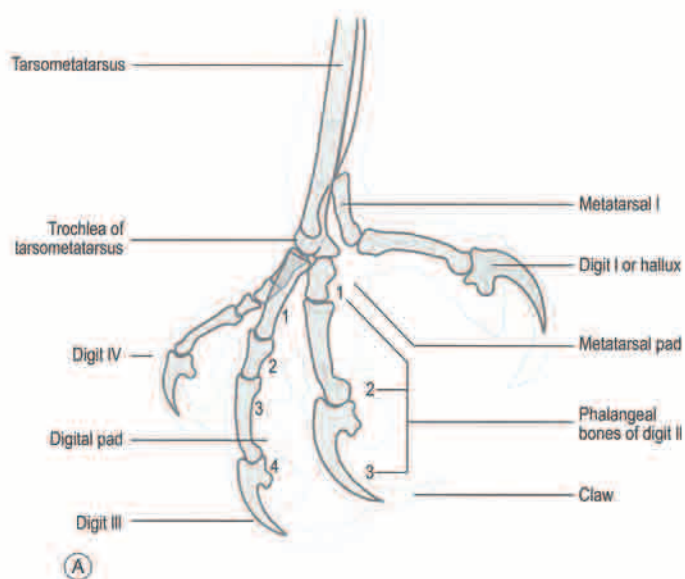


Fig. 3.58 (A and B) Mediolateral close-up of the foot of the palm nut vulture.

SECTION 9 RADIOGRAPHIC SPECIES CATALOG

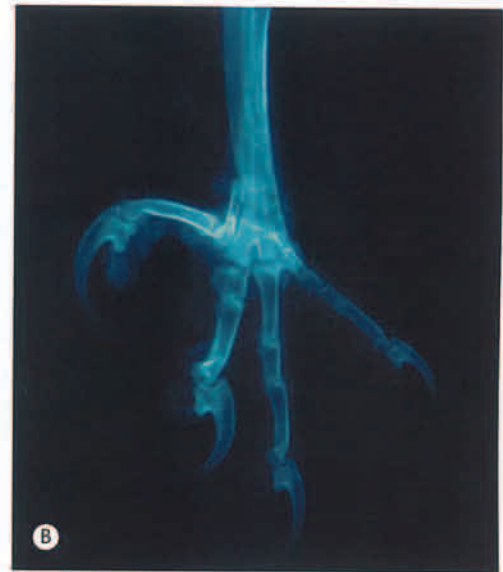
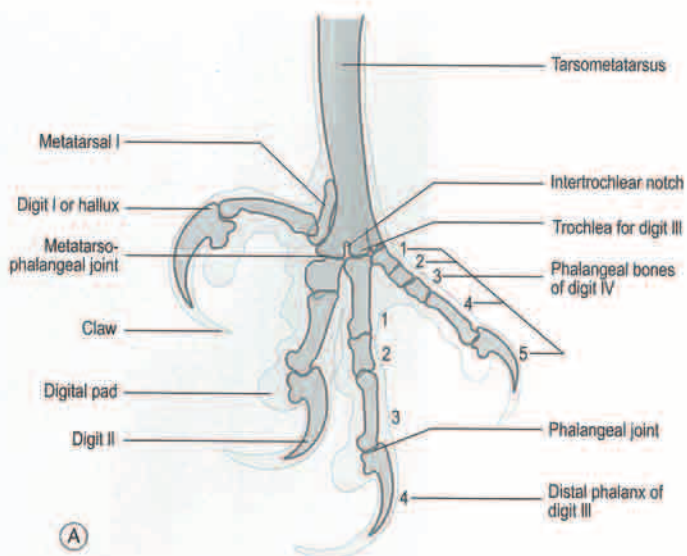


Fig. 3.59 (A and B) Craniocaudal close-up of the foot of the palm nut vulture, with digit I flexed.

SECTION 9 RADIOGRAPHIC SPECIES CATALOG

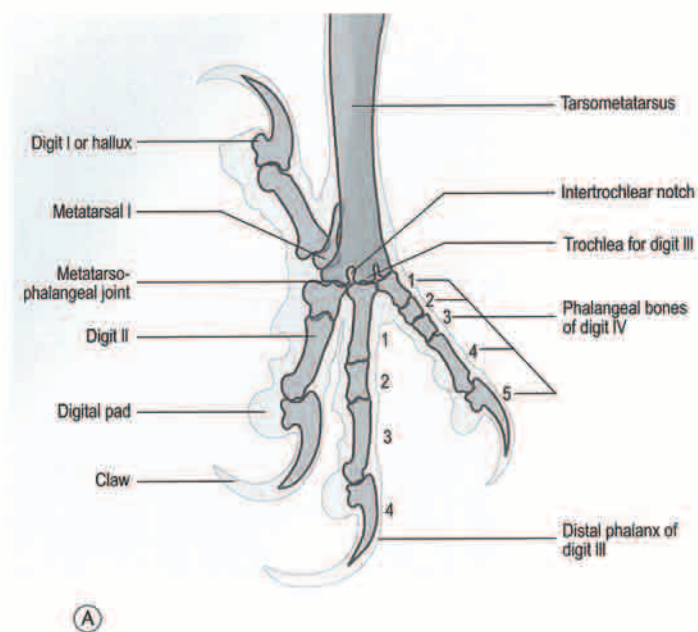


Fig. 3.60 (A and B) Craniocaudal close-up of the foot of the palm nut vulture, with digit I extended.

SECTION 9 RADIOGRAPHIC SPECIES CATALOG



Eurasian honey buzzard (*Pernis apivorus*, Linnaeus, 1758, Sweden)

The Eurasian or Western honey buzzard is a small-sized bird of prey with a body length of 52–60 cm and a wingspan of 130–150 cm. Individuals weigh between 440 and 1050 g. Honey buzzards are polymorphic with extremely variable coloration. The male of the species

generally has a gray head while the female is commonly darker with a brown head. This species is found in Europe and west Asia, from Spain, France, southeast England and east Scandinavia through west Russia and Caucasus to southwest Siberia, wintering mostly in Africa south of Sahara desert. Honey buzzards inhabit forests and woods feeding mainly on wasps and hornets, but some other insects and small mammals and birds are also taken.

SECTION 9 RADIOGRAPHIC SPECIES CATALOG

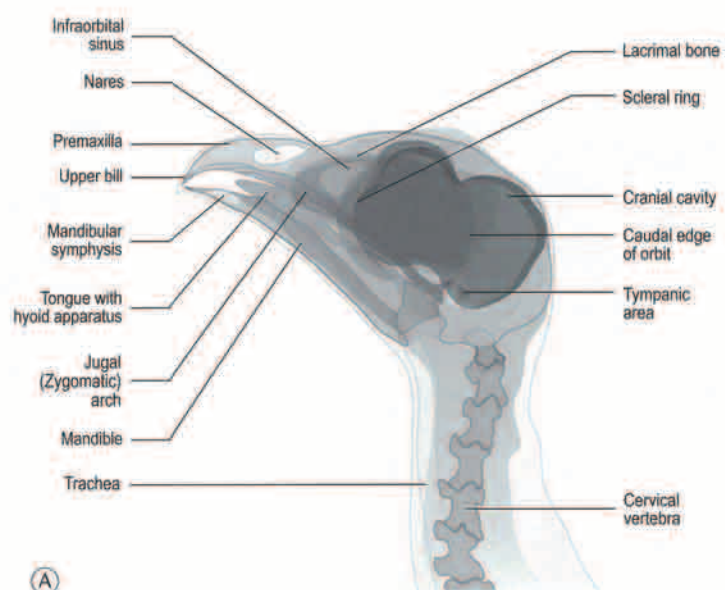


Fig. 3.61 (A and B) Lateral (Le-Rt) view of the head of the Eurasian honey buzzard.

SECTION 9 RADIOGRAPHIC SPECIES CATALOG

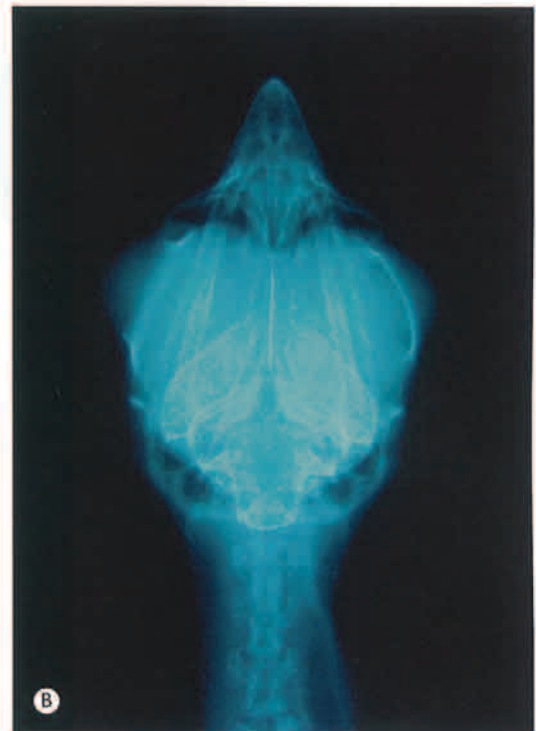
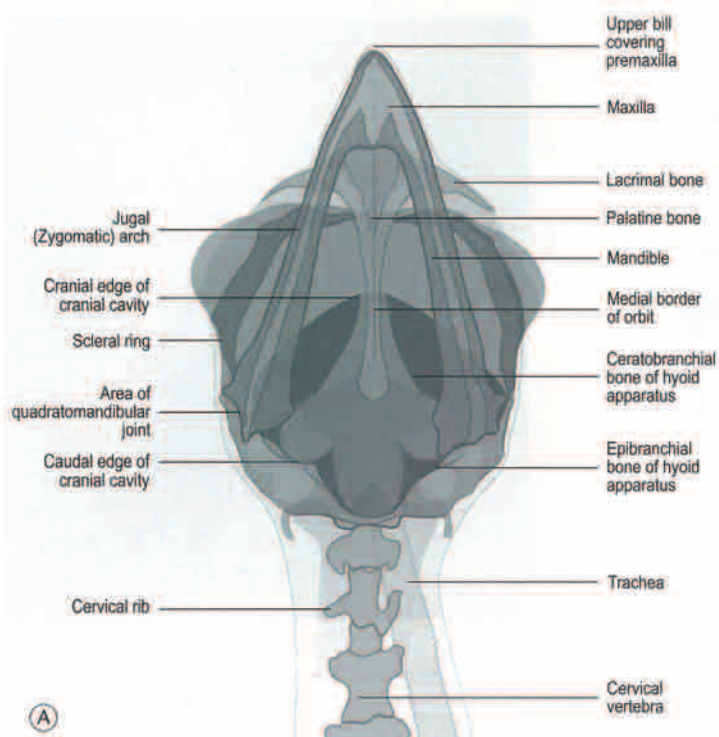


Fig. 3.62 (A and B) Ventrodorsal view of the head of the Eurasian honey buzzard.

SECTION 9 RADIOGRAPHIC SPECIES CATALOG

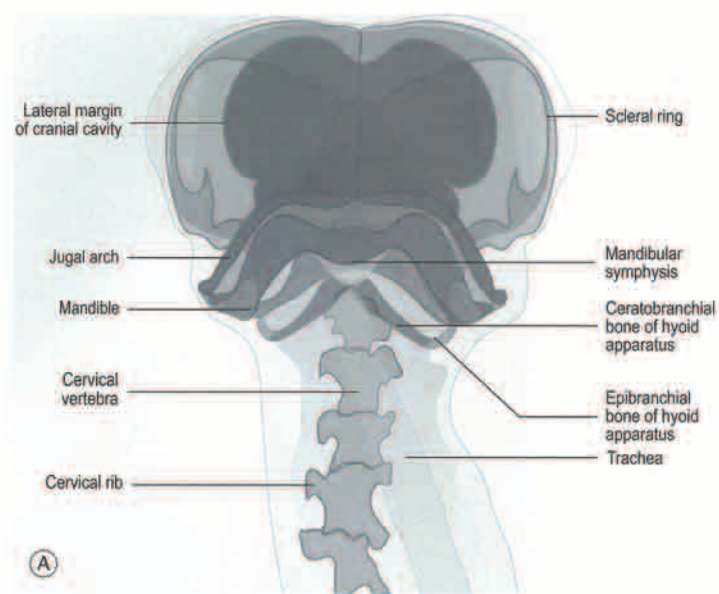


Fig. 3.63 (A and B) Rostrocaudal view of the head of the Eurasian honey buzzard.

SECTION 9 RADIOGRAPHIC SPECIES CATALOG

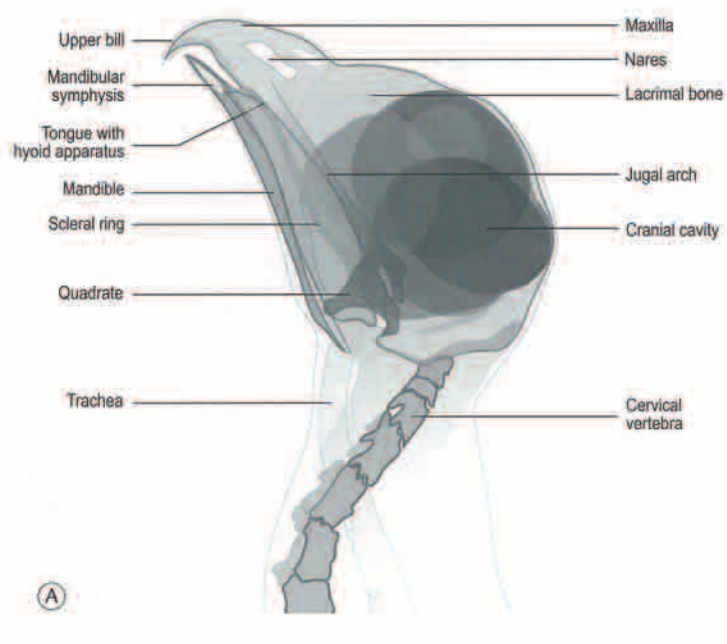


Fig. 3.64 (A and B) Oblique (LeD-RtVO) view of the head of the Eurasian honey buzzard.

SECTION 9 RADIOGRAPHIC SPECIES CATALOG

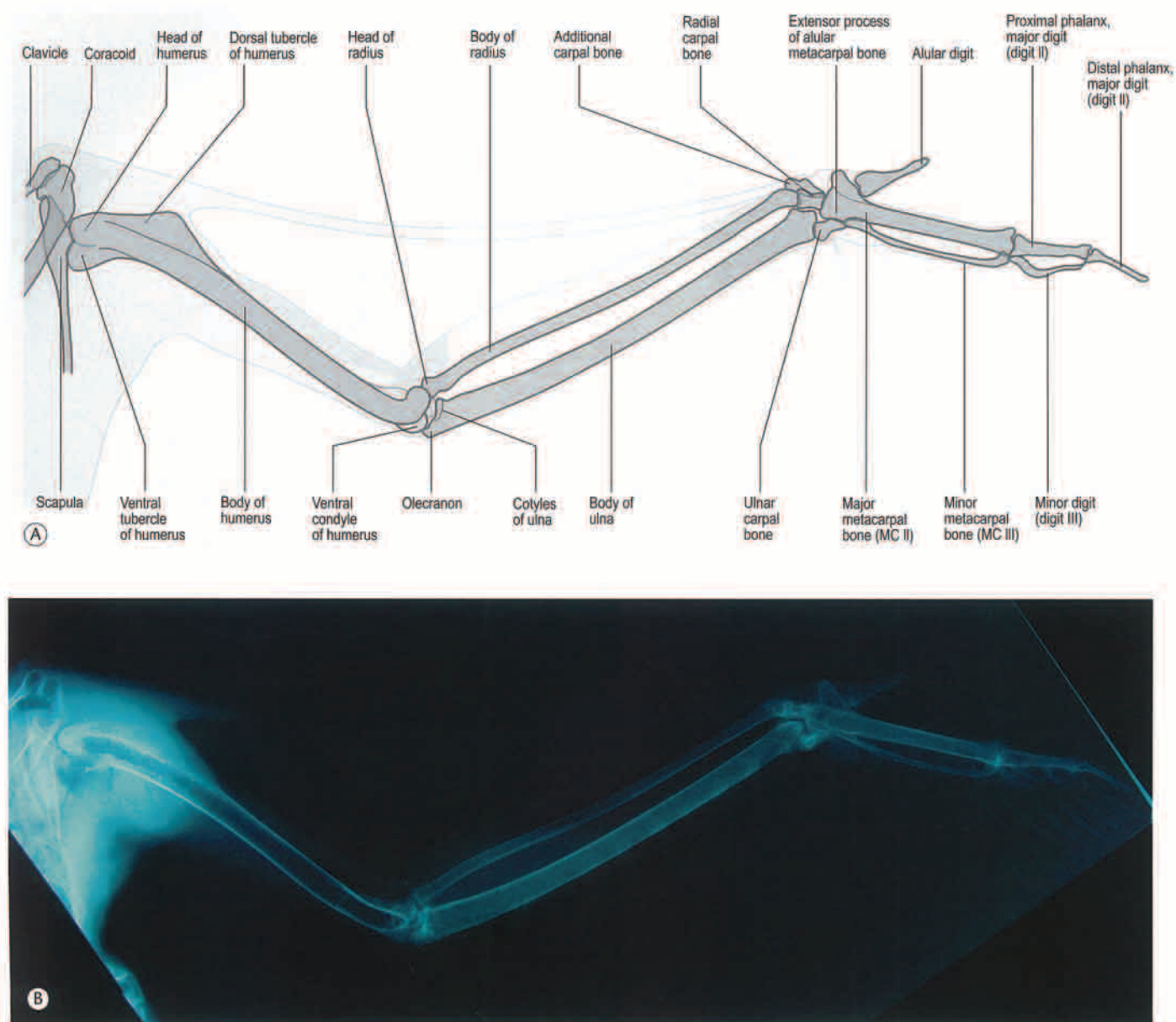


Fig. 3.65 (A and B) Ventrodorsal view of the wing of the Eurasian honey buzzard. Note the presence of the additional carpal bone.

SECTION 9 RADIOGRAPHIC SPECIES CATALOG

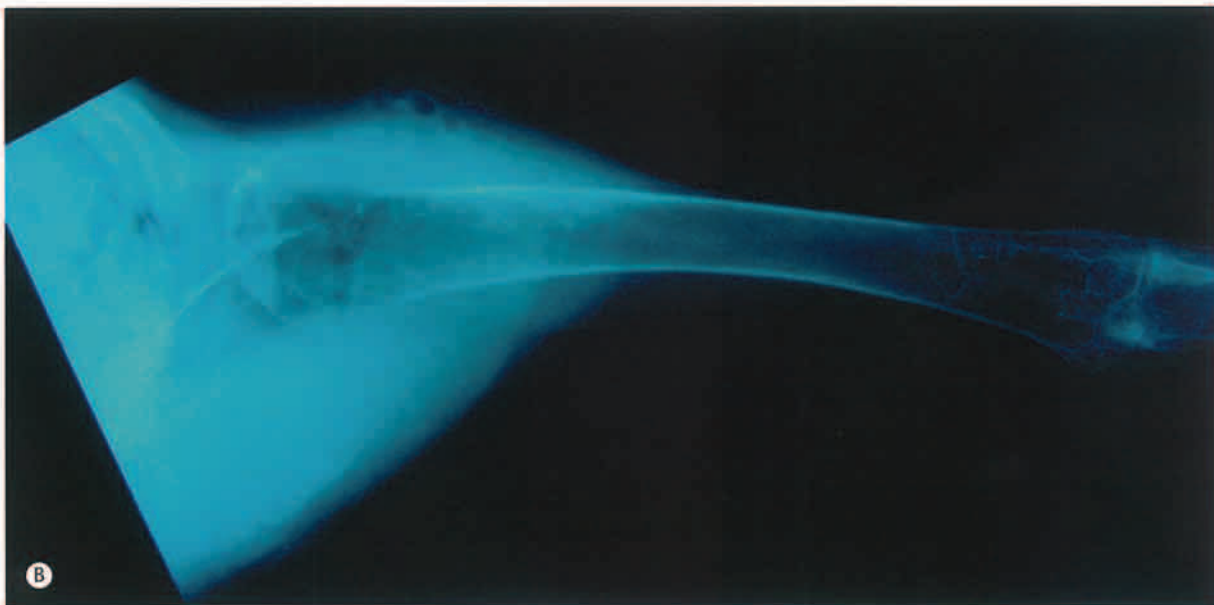
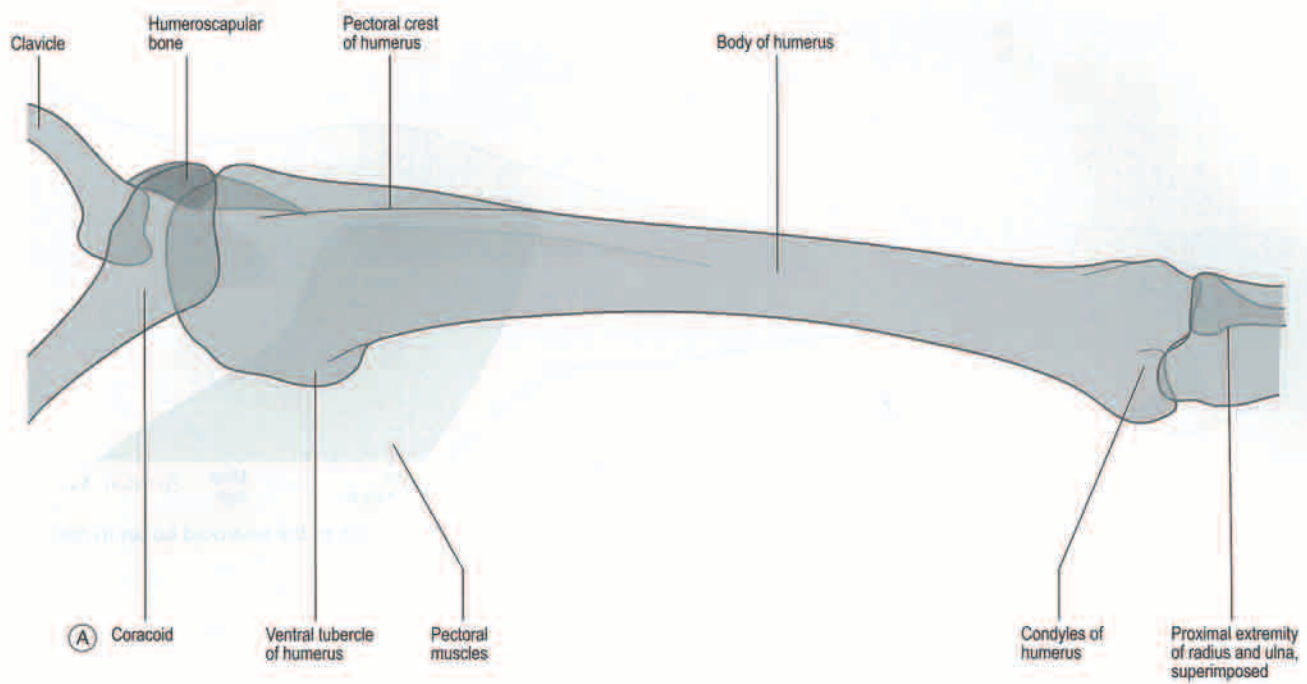


Fig. 3.66 (A and B) Craniocaudal view of the proximal wing of the Eurasian honey buzzard. Note the presence of the humeroscapular bone.

SECTION 9 RADIOGRAPHIC SPECIES CATALOG

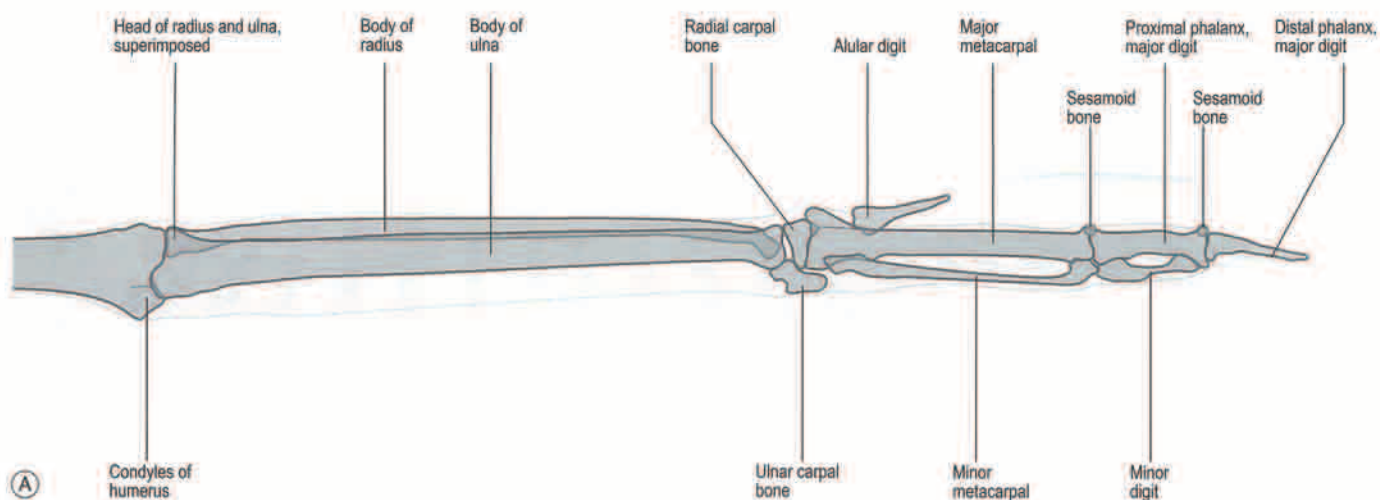


Fig. 3.67 (A and B) Craniocaudal view of the distal wing of the Eurasian honey buzzard. Note the presence of the sesamoid bones in the metacarpophalangeal joint and interphalangeal joint of the major digit.

SECTION 9 RADIOGRAPHIC SPECIES CATALOG

**Fig. 3.67** (Cont'd).

SECTION 9 RADIOGRAPHIC SPECIES CATALOG

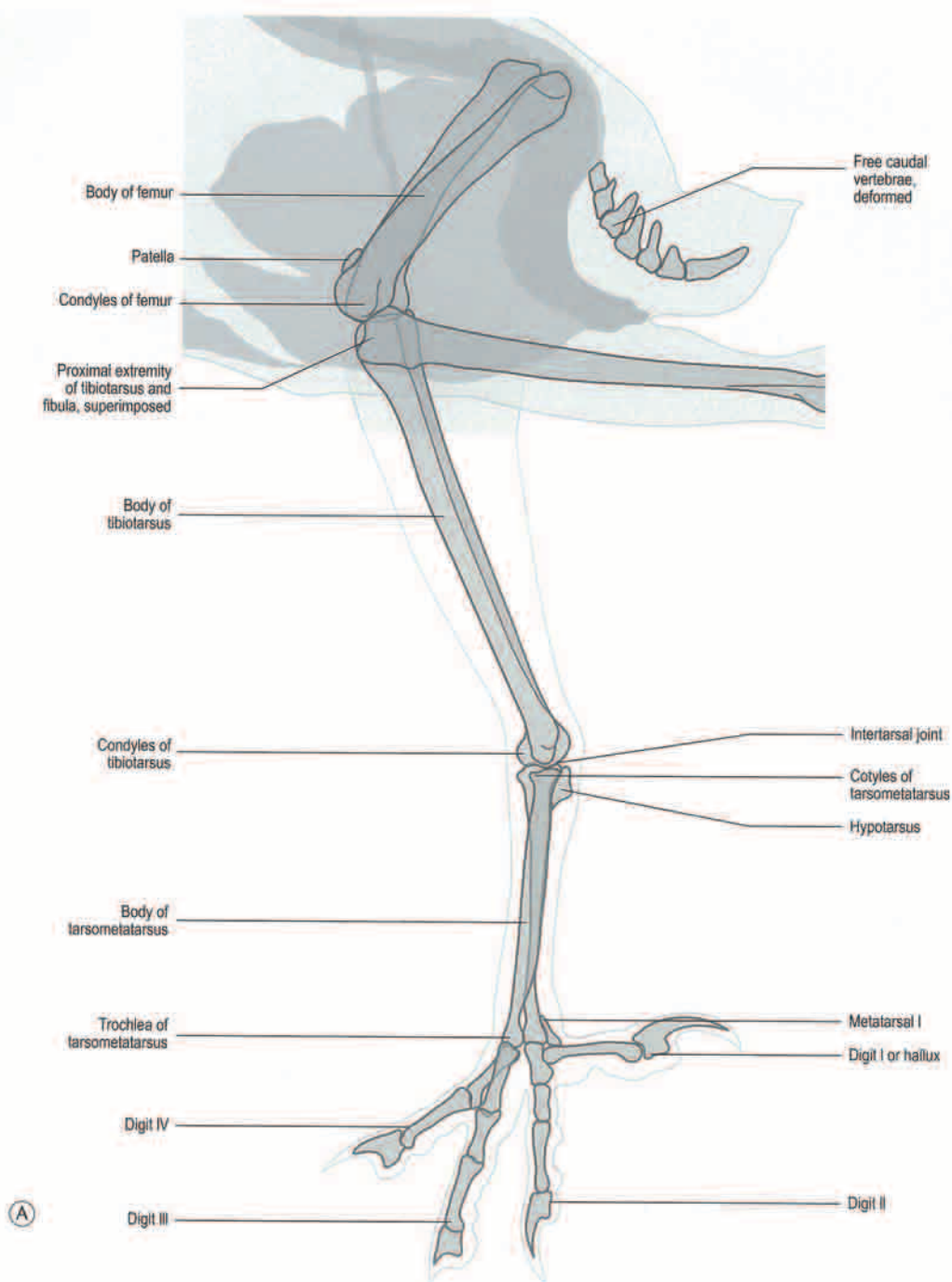


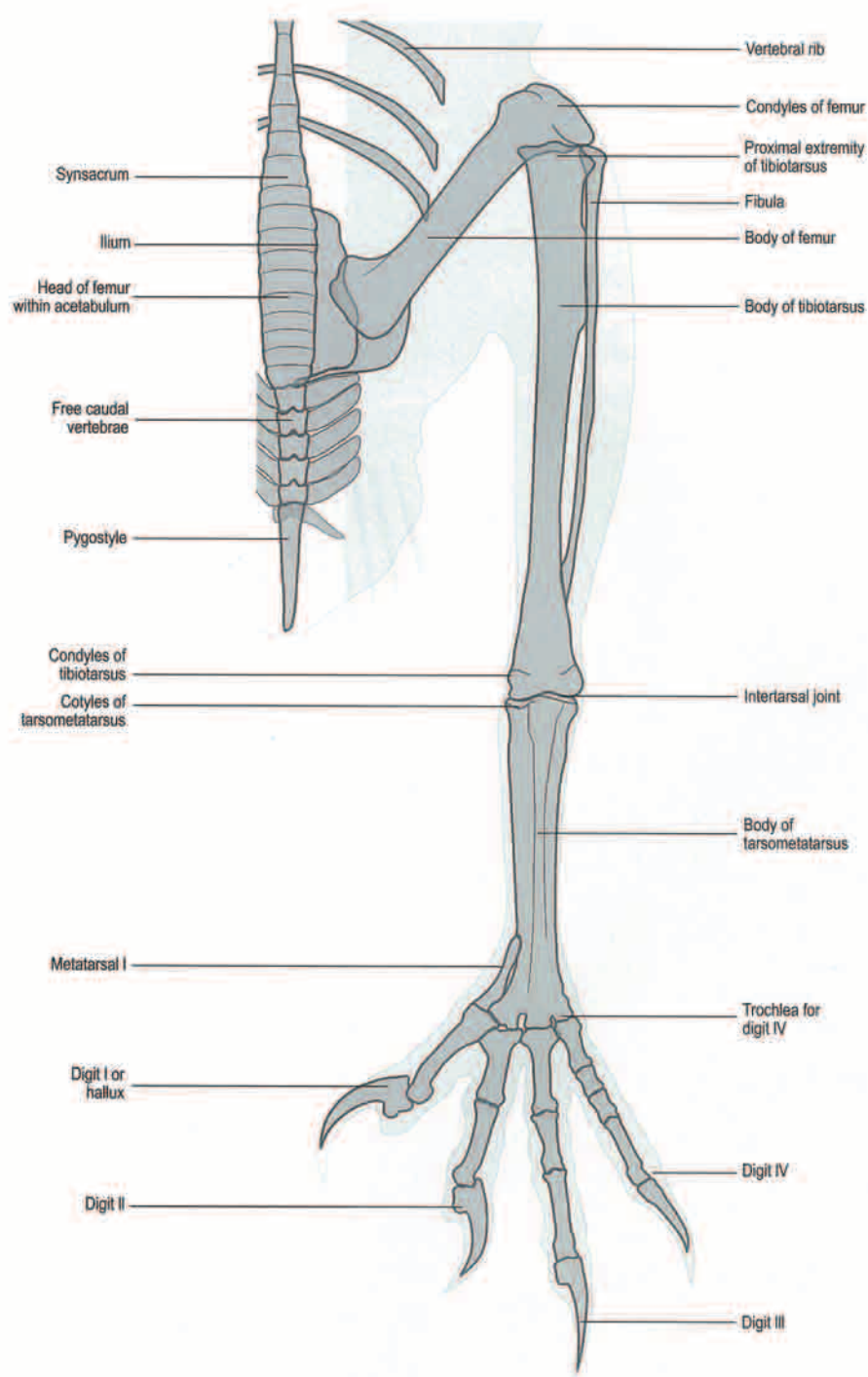
Fig. 3.68 (A and B) Mediolateral view of the pelvic limb of the Eurasian honey buzzard.

SECTION 9 RADIOGRAPHIC SPECIES CATALOG



Fig. 3.68 (Cont'd).

SECTION 9 RADIOGRAPHIC SPECIES CATALOG



(A)

Fig. 3.69 (A and B) Craniocaudal view of the pelvic limb of the Eurasian honey buzzard.



Fig. 3.69 (Cont'd).

SECTION 9 RADIOGRAPHIC SPECIES CATALOG

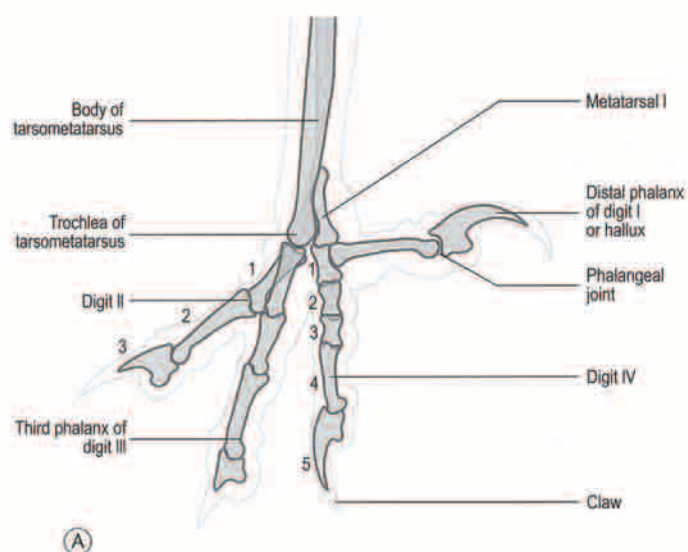


Fig. 3.70 (A and B) Mediolateral close-up of the foot of the Eurasian honey buzzard.

SECTION 9 RADIOGRAPHIC SPECIES CATALOG

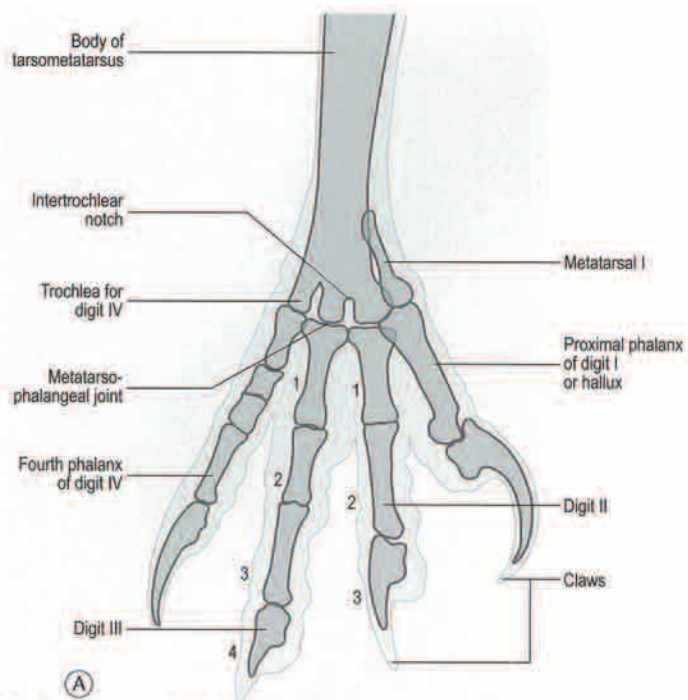


Fig. 3.71 (A and B) Craniocaudal close-up of the foot of the Eurasian honey buzzard, with digit I flexed.

SECTION 9 RADIOGRAPHIC SPECIES CATALOG

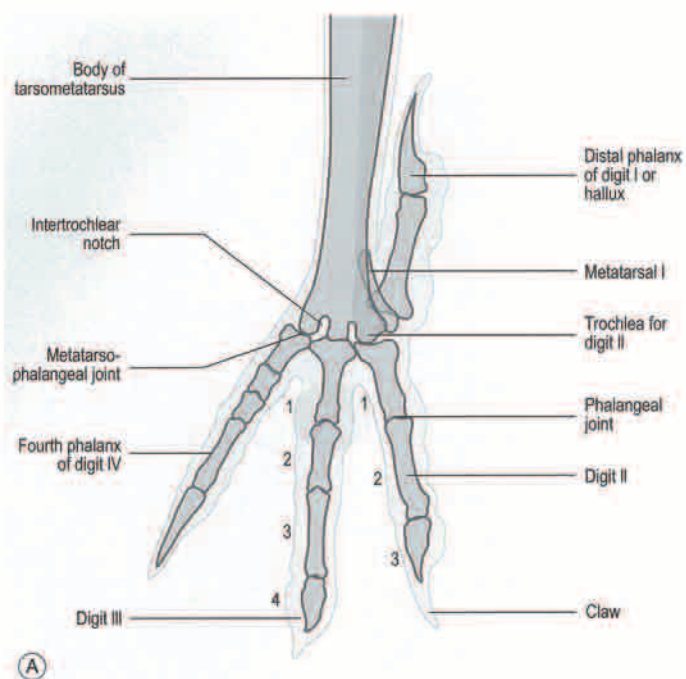


Fig. 3.72 (A and B) Craniocaudal close-up of the foot of the Eurasian honey buzzard, with digit I extended.

SECTION 9 RADIOGRAPHIC SPECIES CATALOG



Northern goshawk (*Accipiter gentilis*) (previously denominated as *Falco gentilis*, Linnaeus, 1758, Sweden)

The goshawk is a medium-sized raptor measuring 48–68.5 cm in length and with a wingspan of 96–127 cm. The body weight of males ranges between 517 and 1170 g, while females range between 820 and 1509 g. The female is significantly larger than the male. A particular external morphological characteristic of this species is the noticeable white supercilium. Eight different subspecies are currently recognized. The geographical distribution is wide including northwest Mexico, across the southwest USA to south, west and central Europe to extreme north Eurasia. Individuals of this species are normally found living at the edges of woodlands feeding on small- and medium-sized birds and mammals. Goshawks are very popular birds of prey used in Western falconry.

SECTION 9 RADIOGRAPHIC SPECIES CATALOG

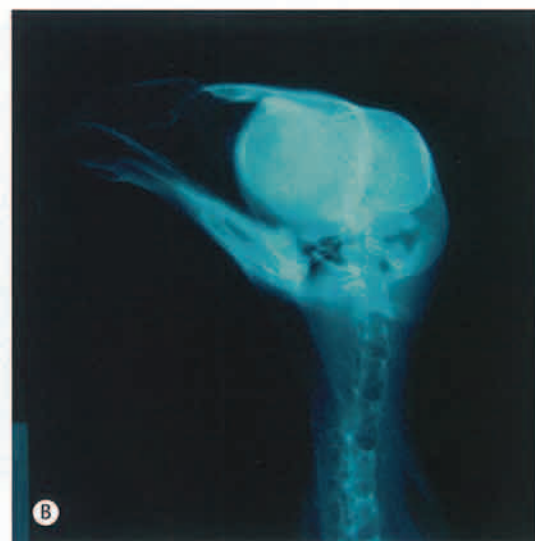
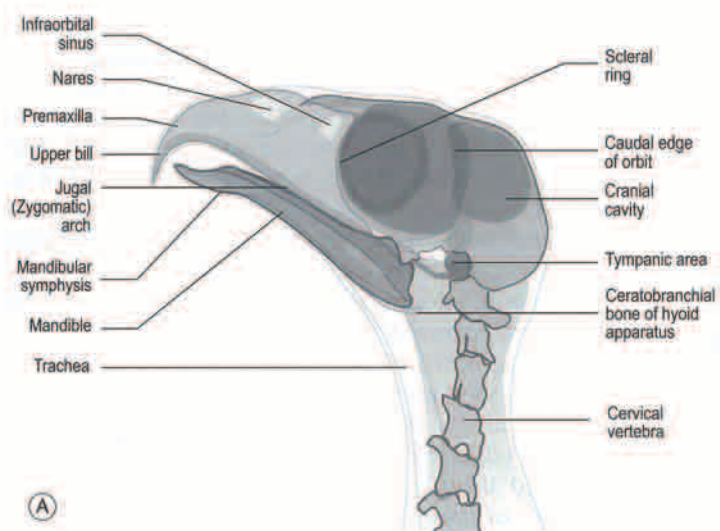


Fig. 3.73 (A and B) Lateral (Le-Rt) view of the head of the goshawk.

SECTION 9 RADIOGRAPHIC SPECIES CATALOG

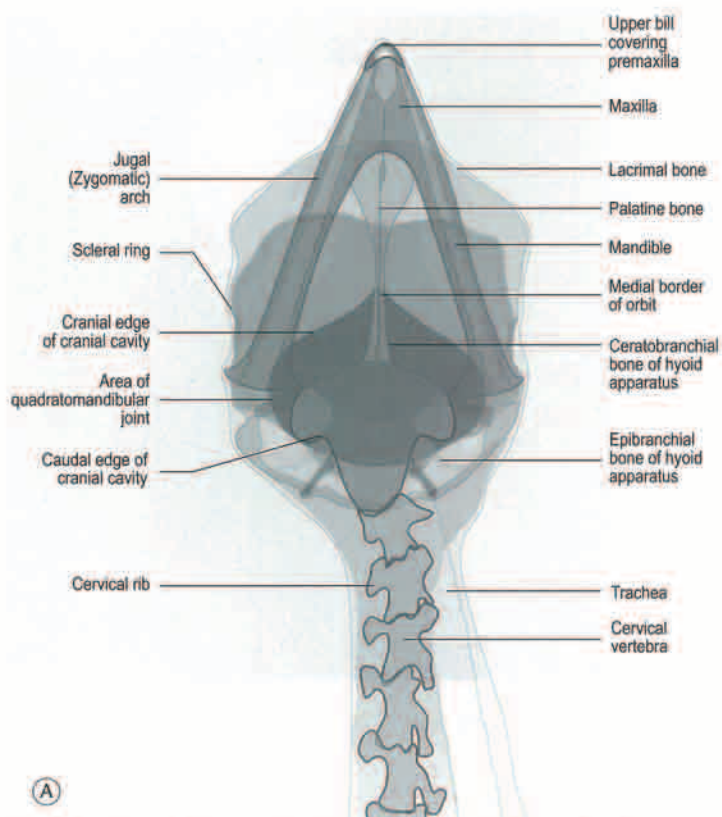


Fig. 3.74 (A and B) Ventrodorsal view of the head of the goshawk.

SECTION 9 RADIOGRAPHIC SPECIES CATALOG

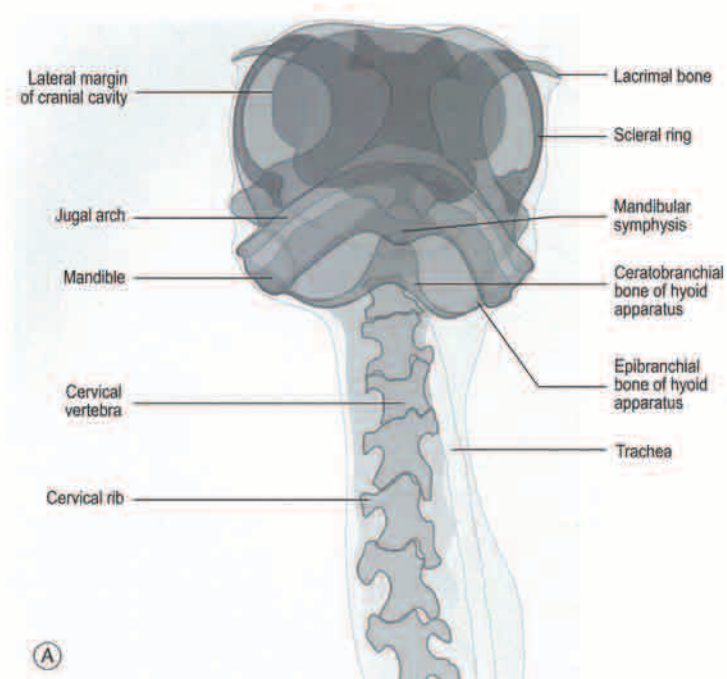


Fig. 3.75 (A and B) Rostrocaudal view of the head of the goshawk.

SECTION 9 RADIOGRAPHIC SPECIES CATALOG

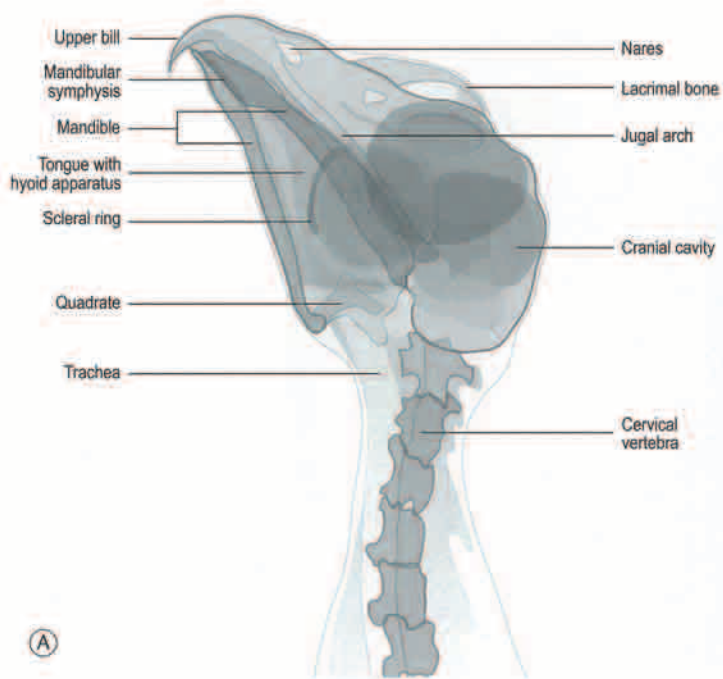


Fig. 3.76 (A and B) Oblique (LeD-RtVO) view of the head of the goshawk.

SECTION 9 RADIOGRAPHIC SPECIES CATALOG

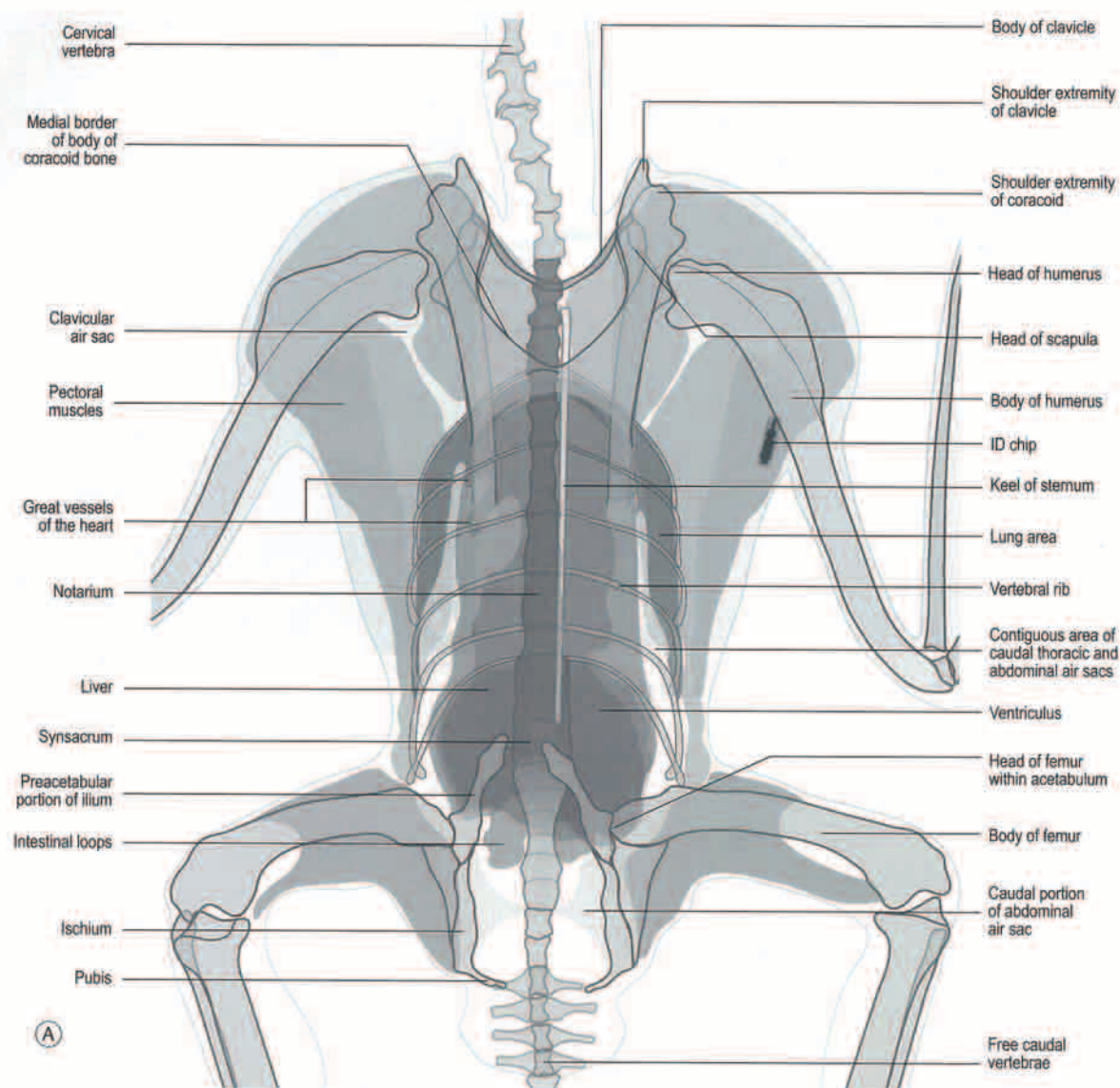


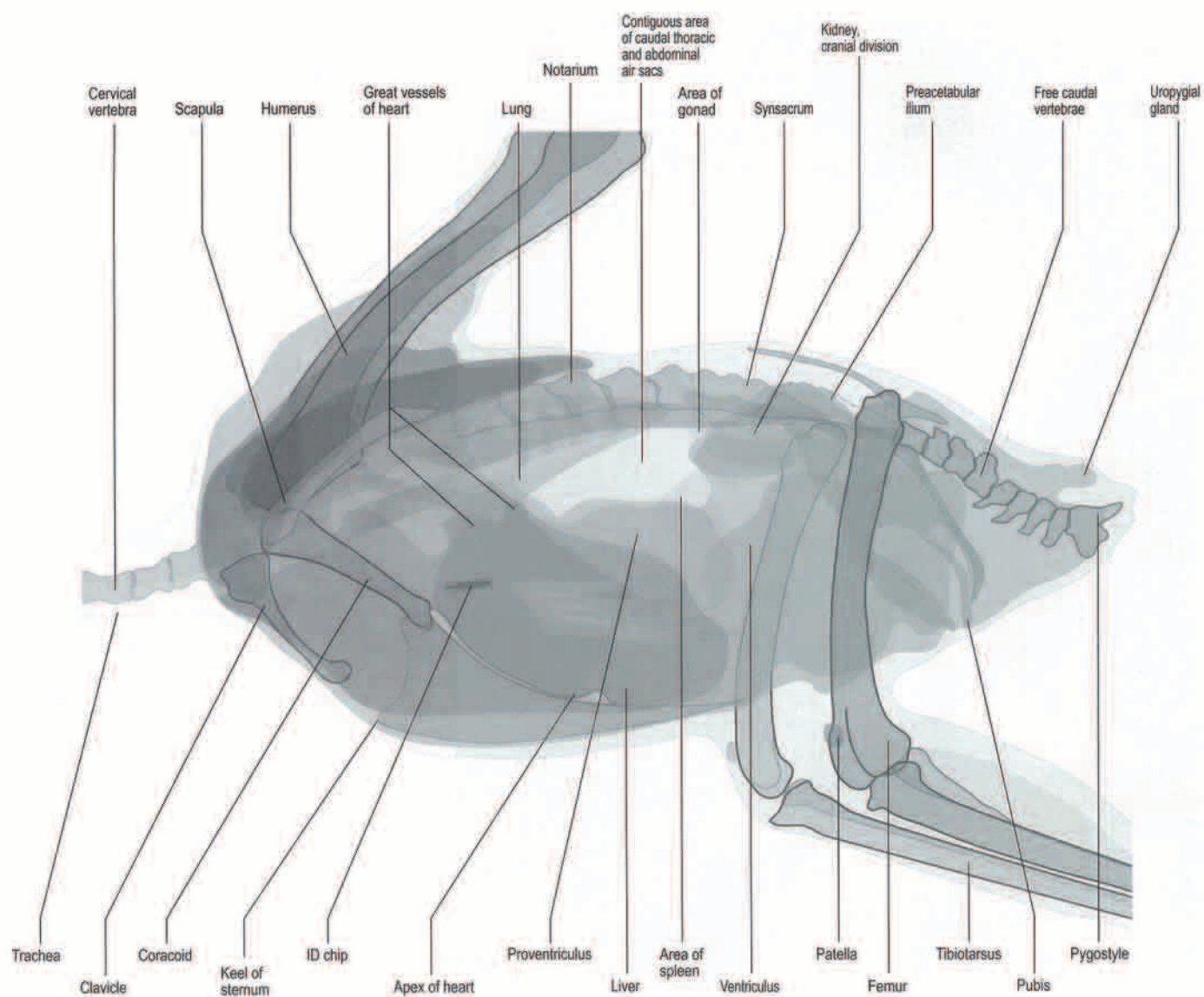
Fig. 3.77 (A and B) Ventrodorsal view of the body of the goshawk. The typical hourglass cardiohepatic waist is not pronounced in this species.

SECTION 9 RADIOGRAPHIC SPECIES CATALOG



Fig. 3.77 (Cont'd).

SECTION 9 RADIOGRAPHIC SPECIES CATALOG



(A)

Fig. 3.78 (A and B) Lateral view of the body of the goshawk.

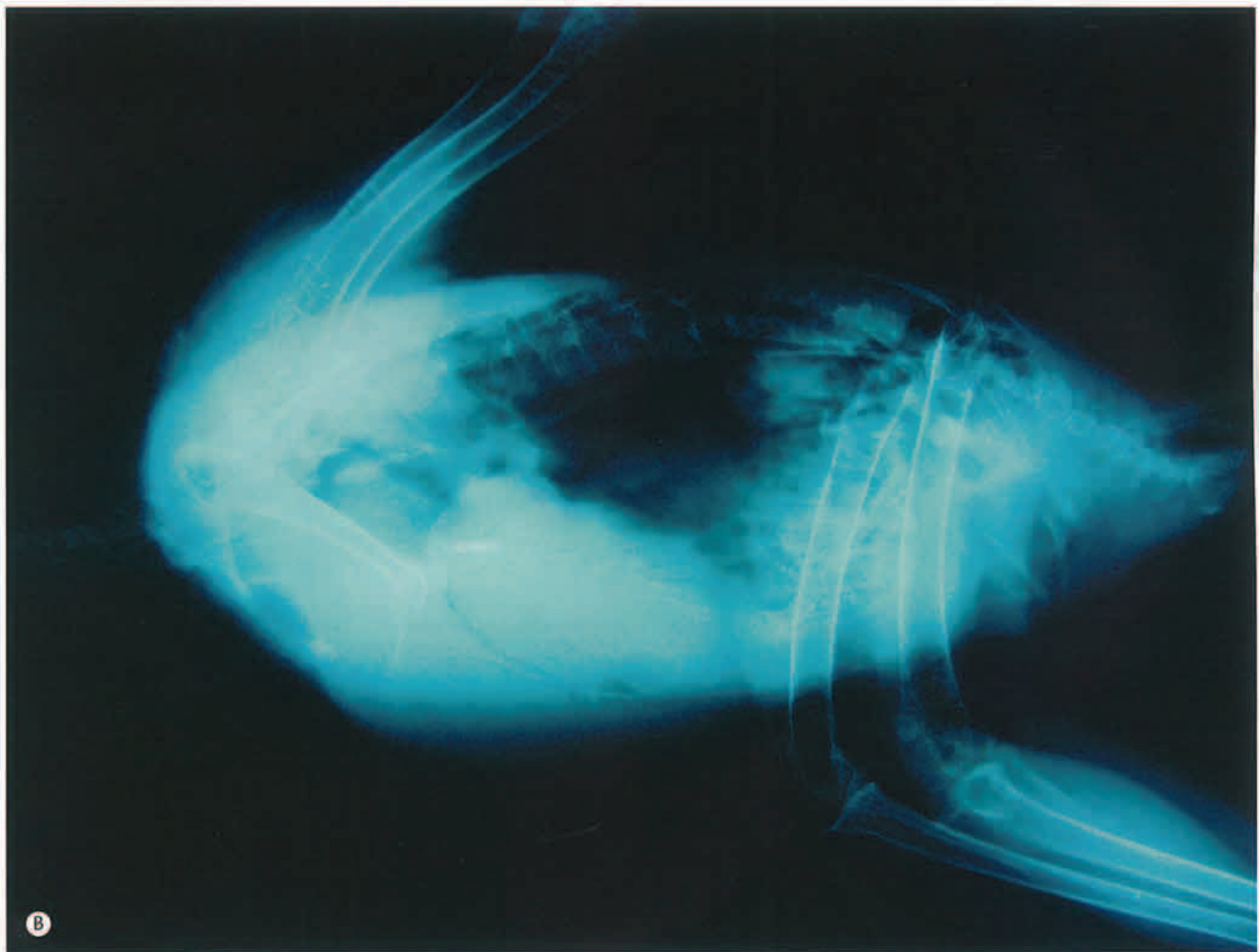


Fig. 3.78 (Cont'd).

SECTION 9 RADIOGRAPHIC SPECIES CATALOG

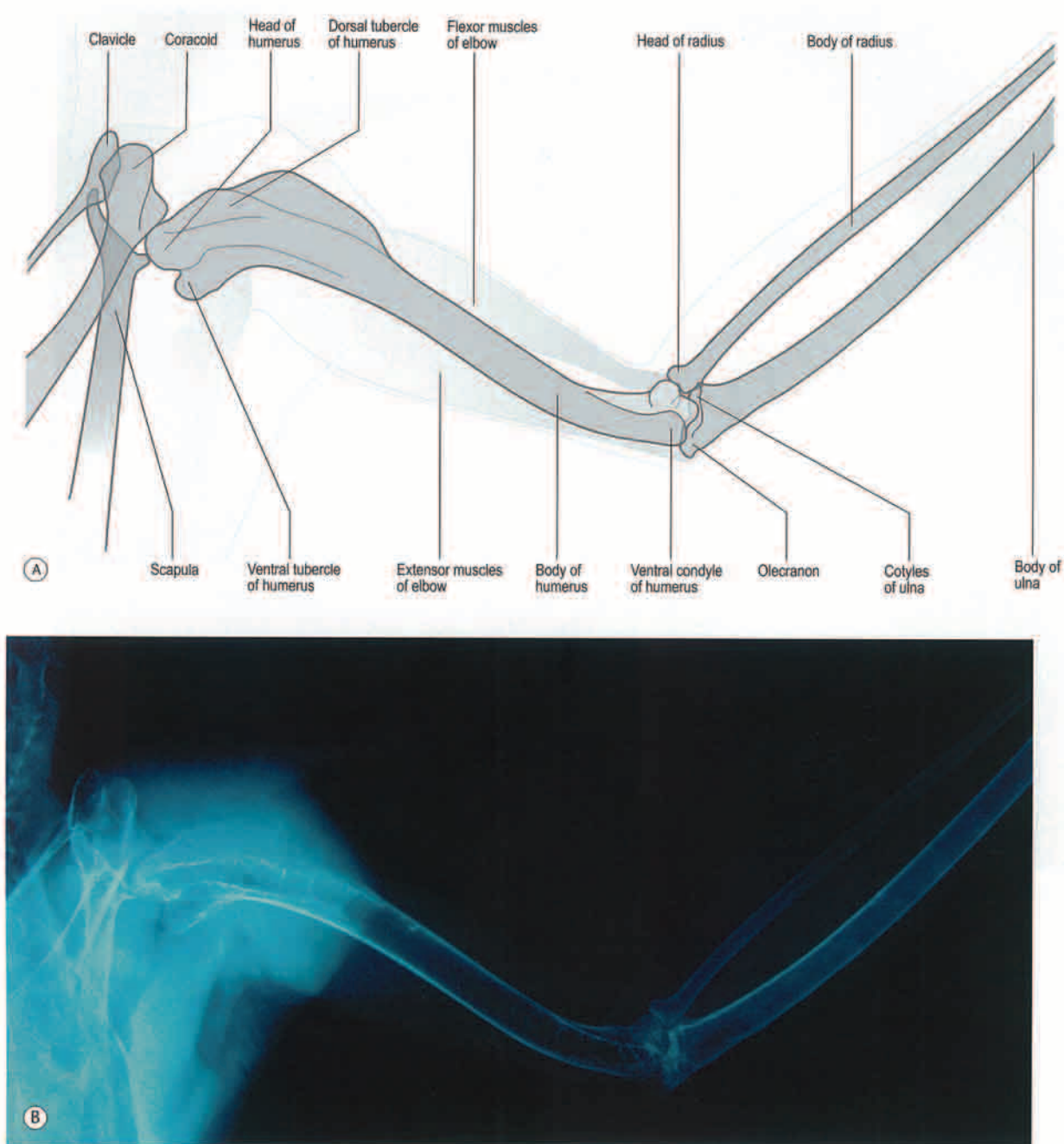


Fig. 3.79 (A and B) Ventrodorsal view of the proximal wing of the goshawk.

SECTION 9 RADIOGRAPHIC SPECIES CATALOG

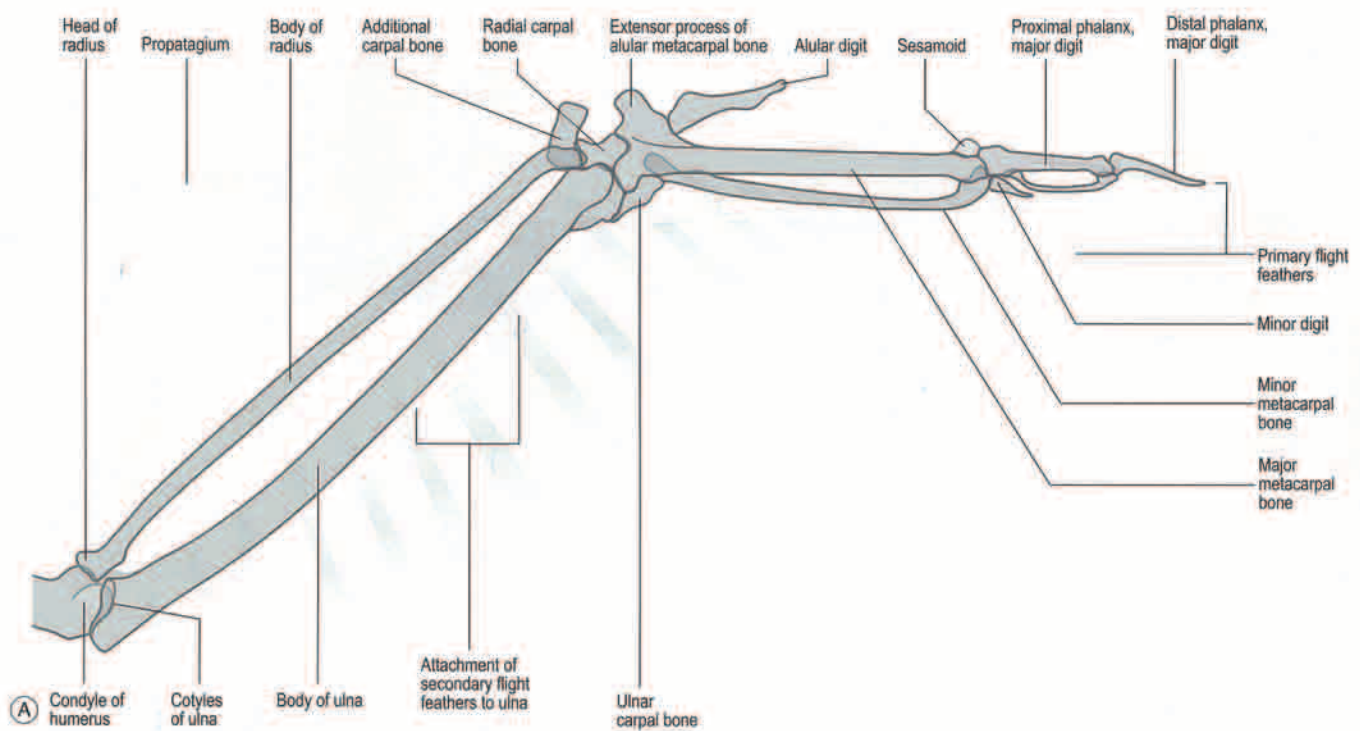


Fig. 3.80 (A and B) Ventrodorsal view of the distal wing of the goshawk. Note the presence of the additional carpal bone and the sesamoid bone in the metacarpophalangeal joint.

SECTION 9 RADIOGRAPHIC SPECIES CATALOG

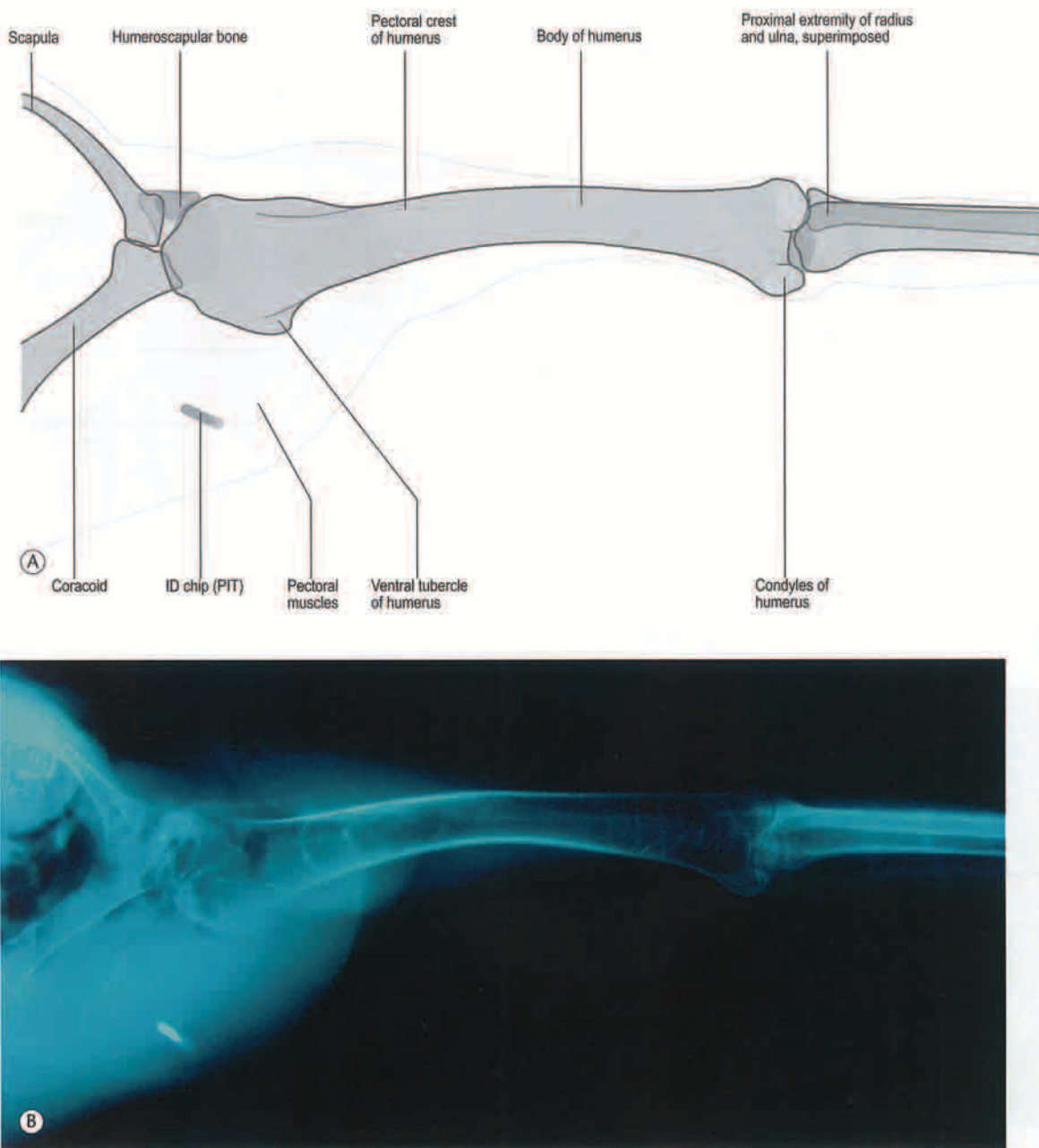


Fig. 3.81 (A and B) Craniocaudal view of the proximal wing of the goshawk. Note the presence of the humeroscapular bone.

SECTION 9 RADIOGRAPHIC SPECIES CATALOG

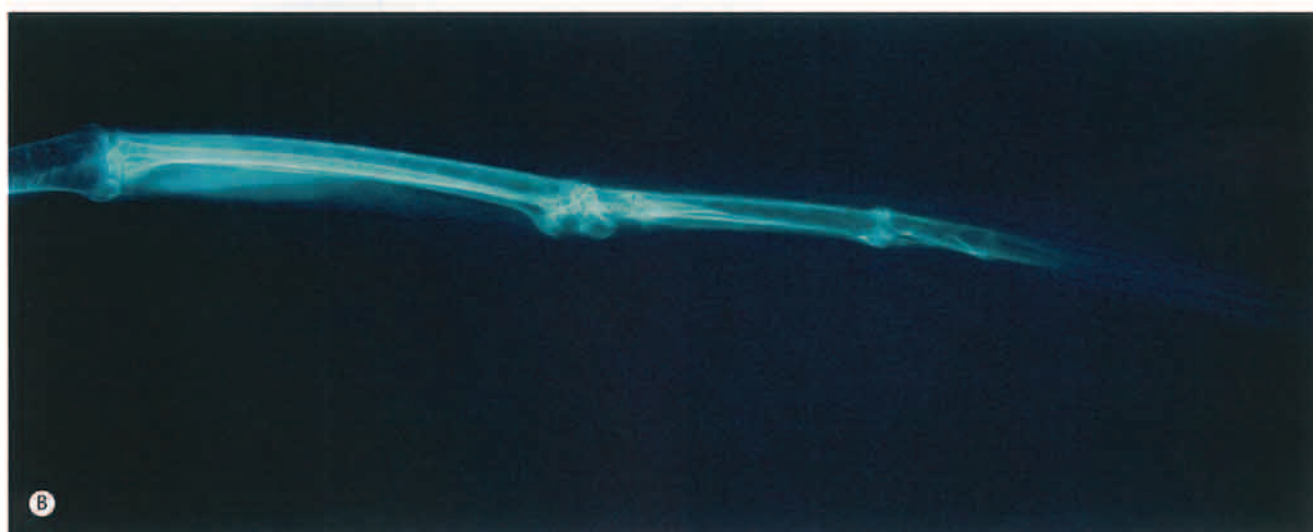
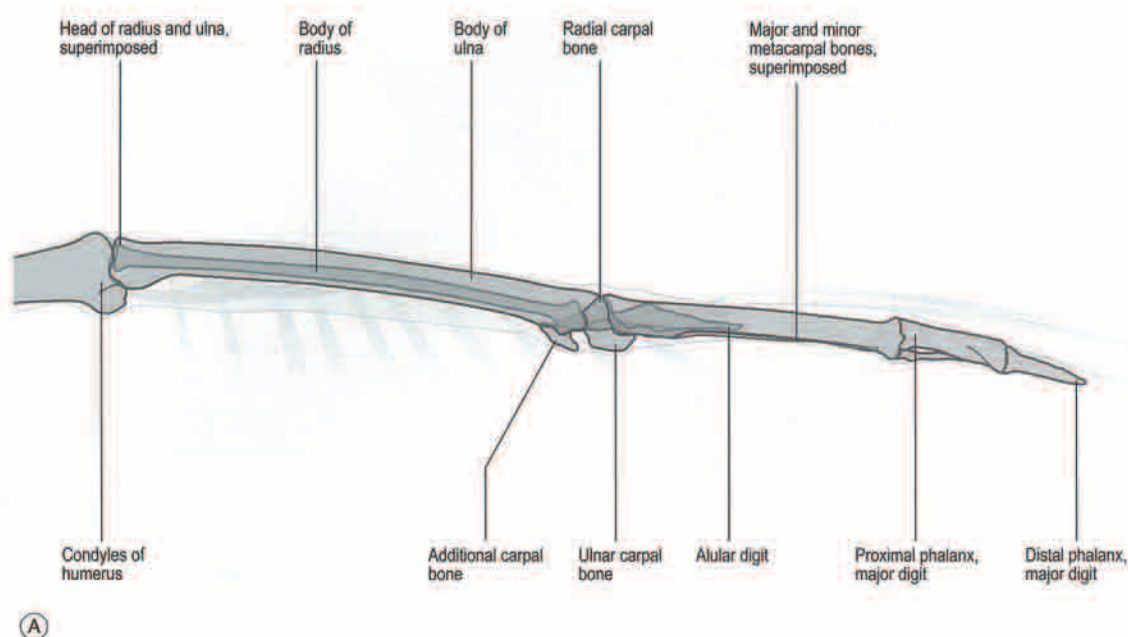


Fig. 3.82 (A and B) Craniocaudal view of the distal wing of the goshawk. Note the presence of the additional carpal bone.

SECTION 9 RADIOGRAPHIC SPECIES CATALOG

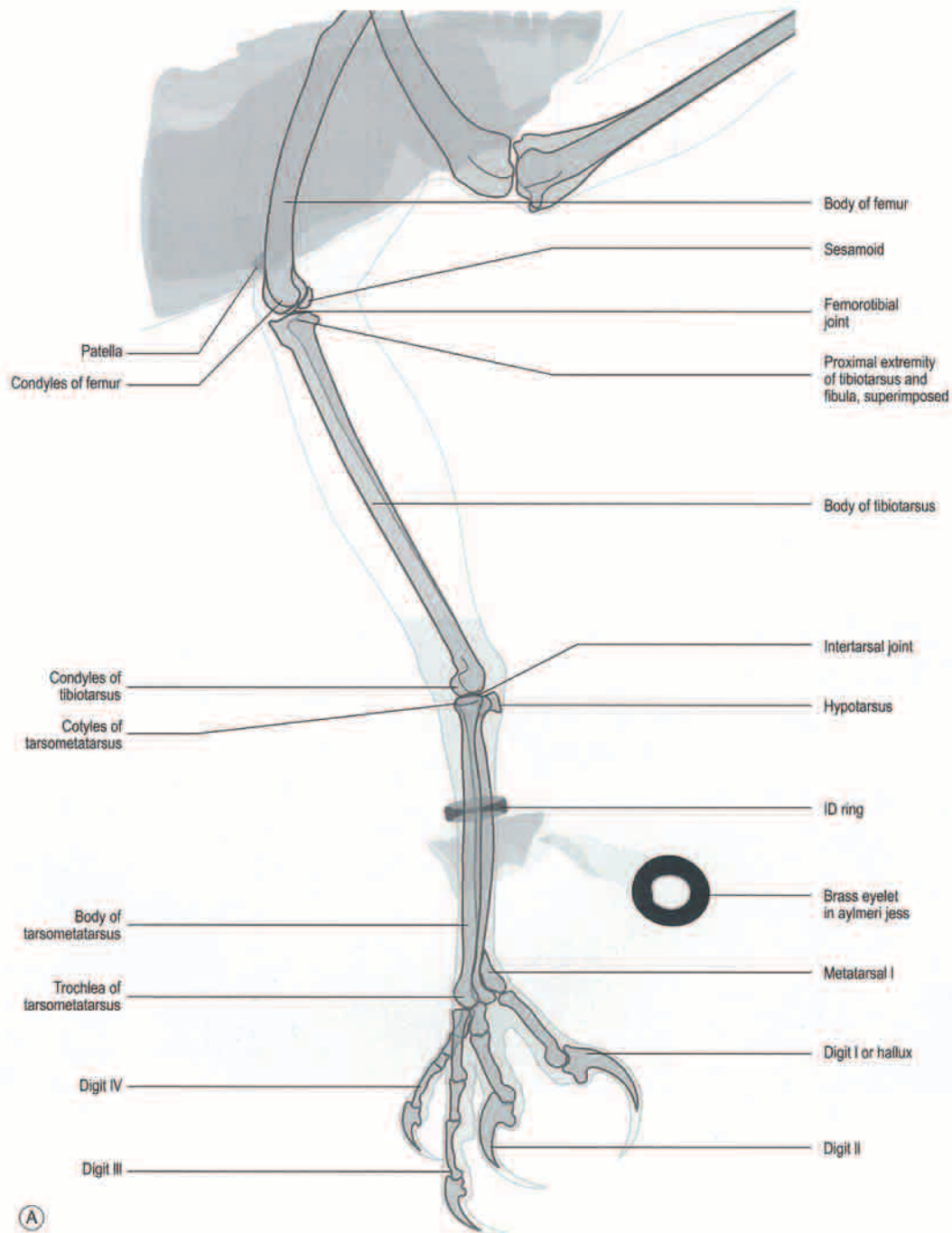


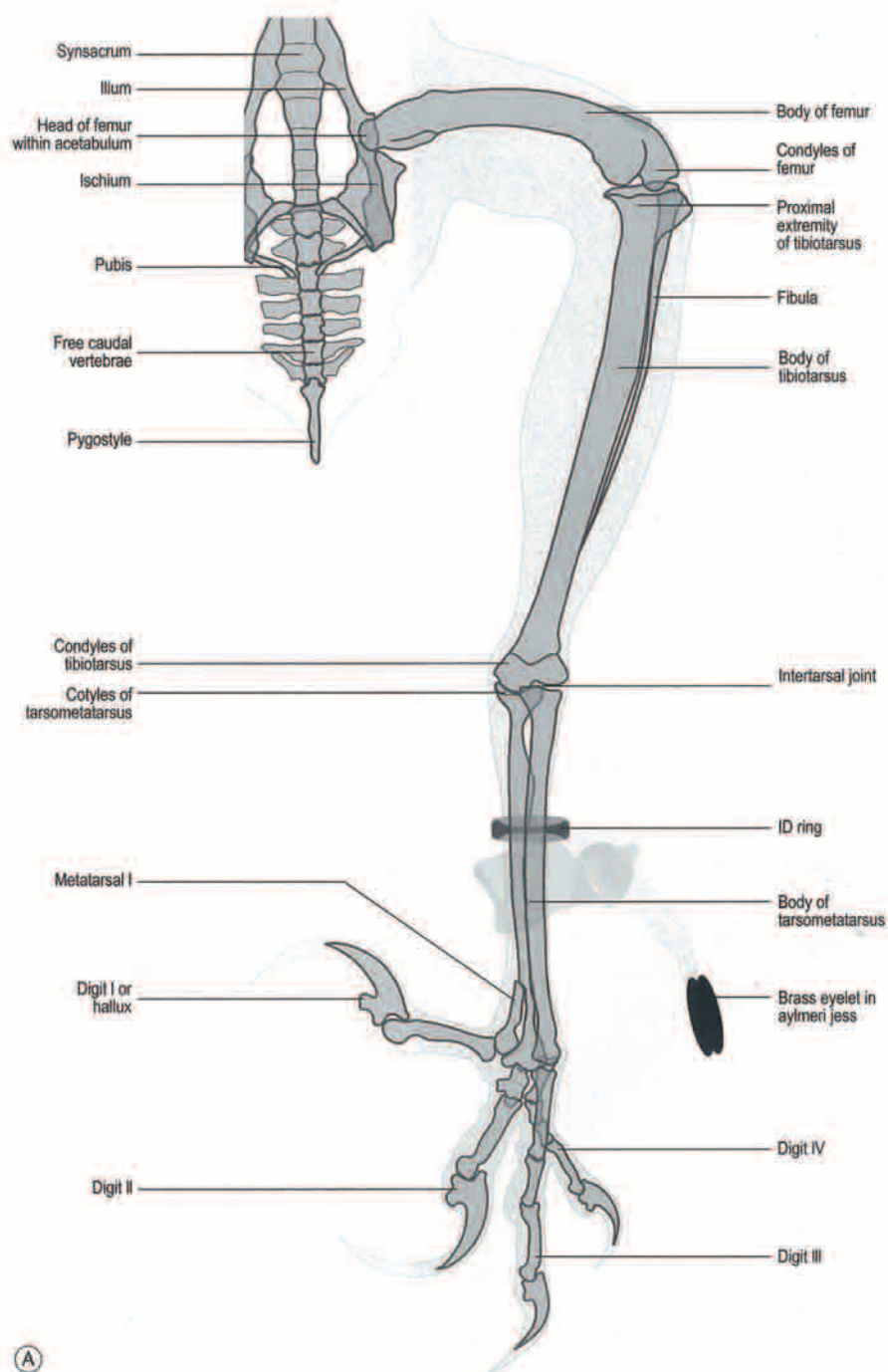
Fig. 3.83 (A and B) Mediolateral view of the pelvic limb of the goshawk. Hawks have a sesamoid in the *ansa iliofibularis*, a smaller medial hypotarsal crest than falcons, and a fused or immobile first phalangeal joint in digit II.

SECTION 9 RADIOGRAPHIC SPECIES CATALOG



Fig. 3.83 (Cont'd).

SECTION 9 RADIOGRAPHIC SPECIES CATALOG



(A)

Fig. 3.84 (A and B) Craniocaudal view of the pelvic limb of the goshawk.

SECTION 9 RADIOGRAPHIC SPECIES CATALOG

**Fig. 3.84** (Cont'd).

SECTION 9 RADIOGRAPHIC SPECIES CATALOG

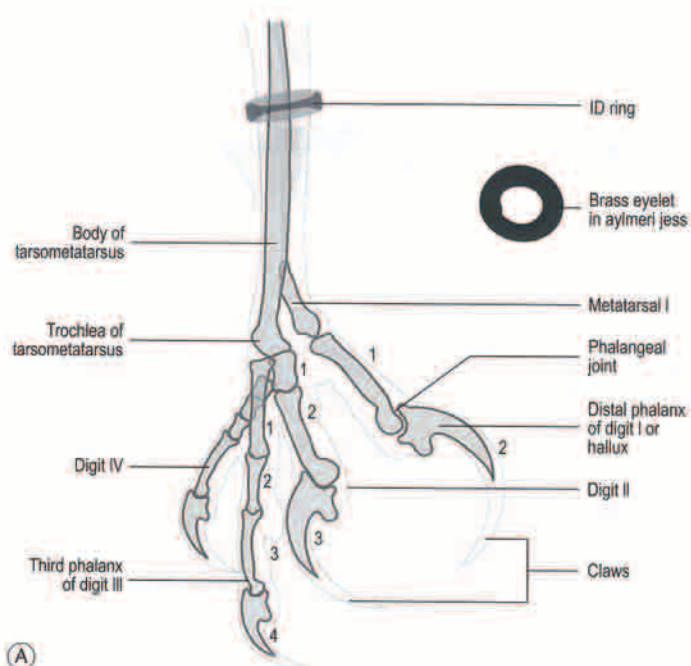


Fig. 3.85 (A and B) Mediolateral close-up of the foot of the goshawk.

SECTION 9 RADIOGRAPHIC SPECIES CATALOG

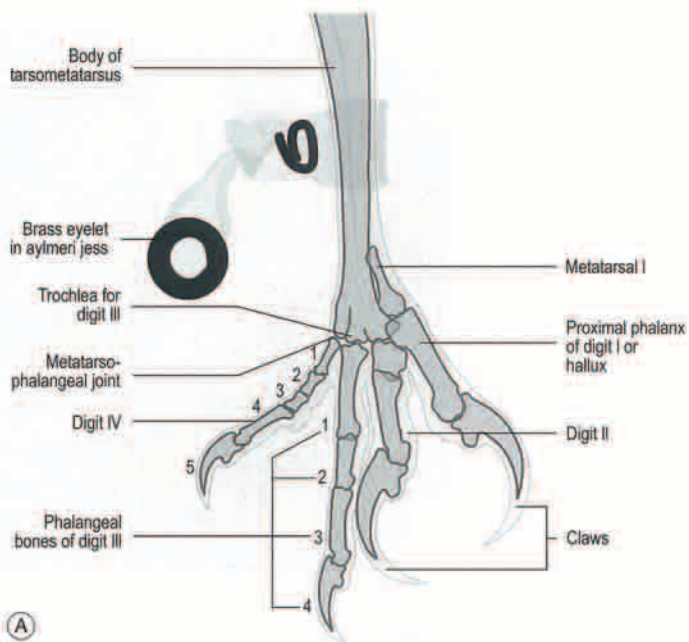


Fig. 3.86 (A and B) Craniocaudal close-up of the foot of the goshawk, with digit I flexed.

SECTION 9 RADIOGRAPHIC SPECIES CATALOG

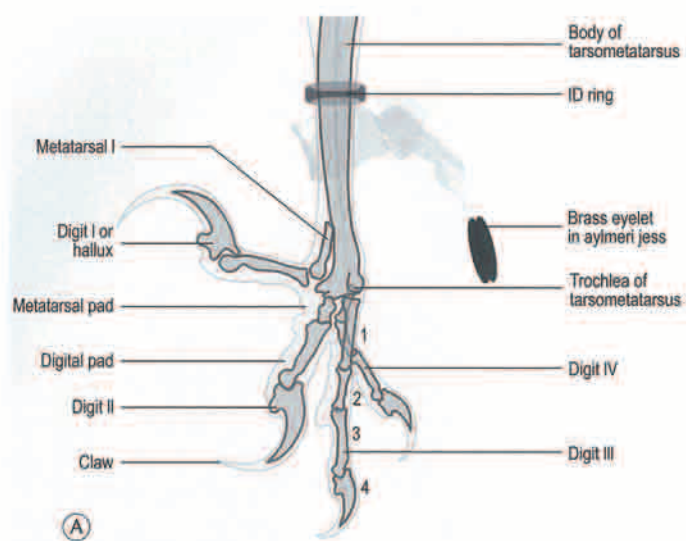


Fig. 3.87 (A and B) Craniocaudal close-up of the foot of the goshawk, with digit I extended.

SECTION 9 RADIOGRAPHIC SPECIES CATALOG

**Red kite** (*Milvus milvus*, Linnaeus, 1758, Sweden)

The red kite is a small-to-medium-sized bird of prey measuring 61–66 cm in length, with a wingspan of 175–195 cm. Individuals of this species weigh between 757 and 1221 g. Overall plumage color is red-brown with a distinct forked tail. The head is paler than the rest of the body and has pronounced white patches under primary feathers. Juveniles have paler bodies with a darker head

and less rusty colored tail. Two subspecies are recognized: *M. m. milvus* from south Sweden east to Ukraine and south through central Europe to west and central Mediterranean basin, Wales, and Caucasus, formerly Canary Islands, and *M. m. fasciicauda* from Cape Verde Island. Red kites inhabit open wooded land occurring mainly at low and medium altitude feeding on a wide variety of food items, but mainly carrion and small-to-medium-sized mammals and birds.

SECTION 9 RADIOGRAPHIC SPECIES CATALOG

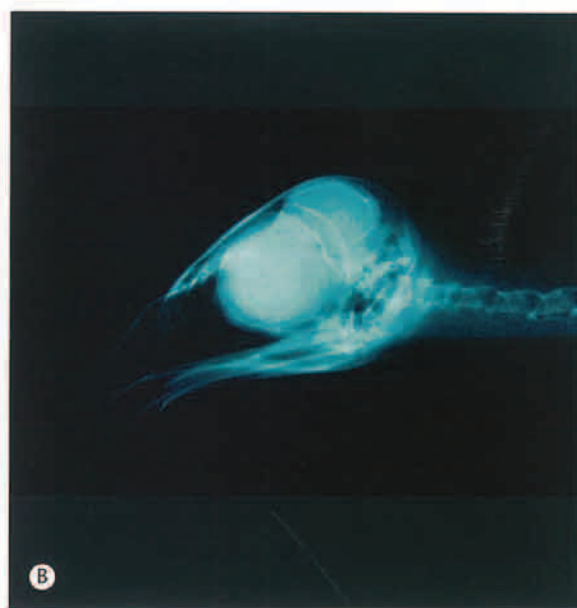
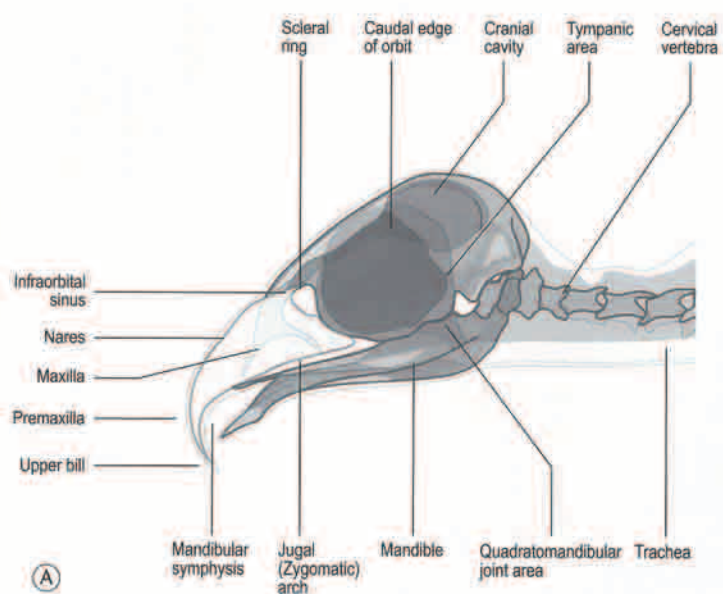


Fig. 3.88 (A and B) Lateral (Le-Rt) view of the head of the red kite.

SECTION 9 RADIOGRAPHIC SPECIES CATALOG

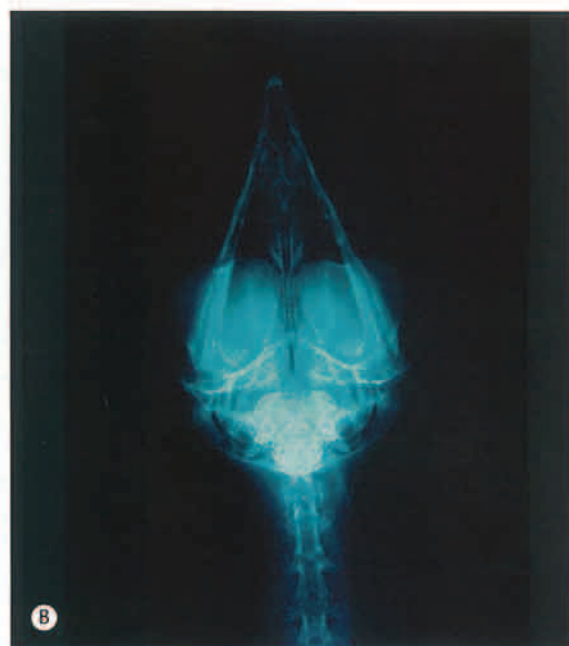
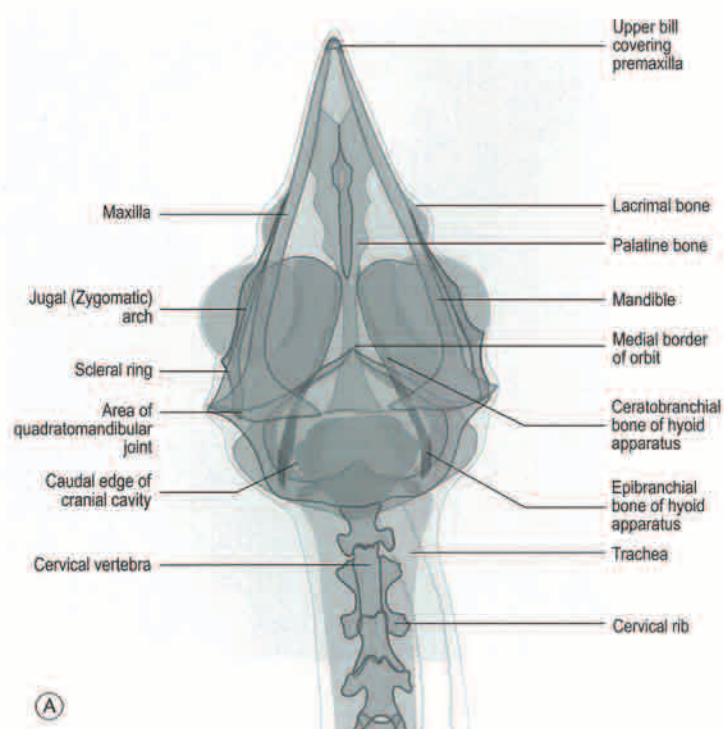


Fig. 3.89 (A and B) Ventrodorsal view of the head of the red kite.

SECTION 9 RADIOGRAPHIC SPECIES CATALOG

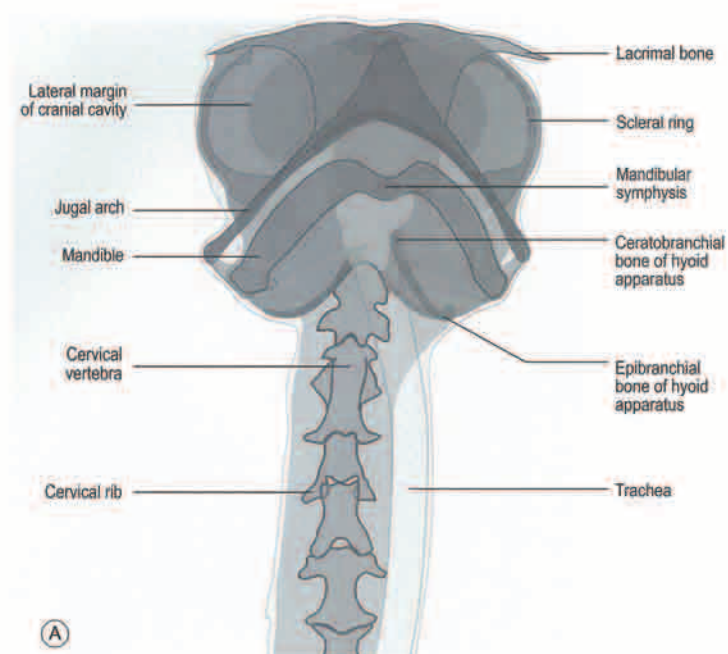


Fig. 3.90 (A and B) Rostrocaudal view of the head of the red kite.

SECTION 9 RADIOGRAPHIC SPECIES CATALOG

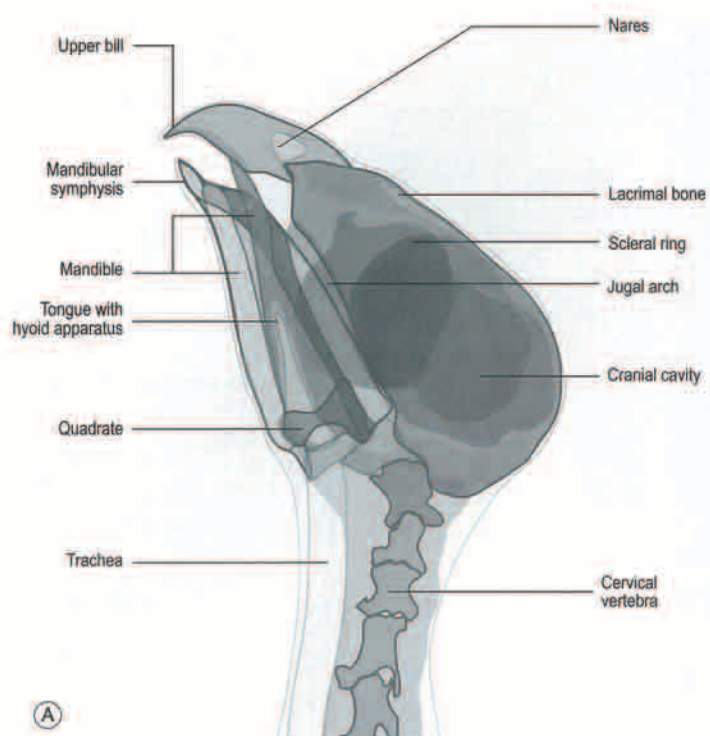
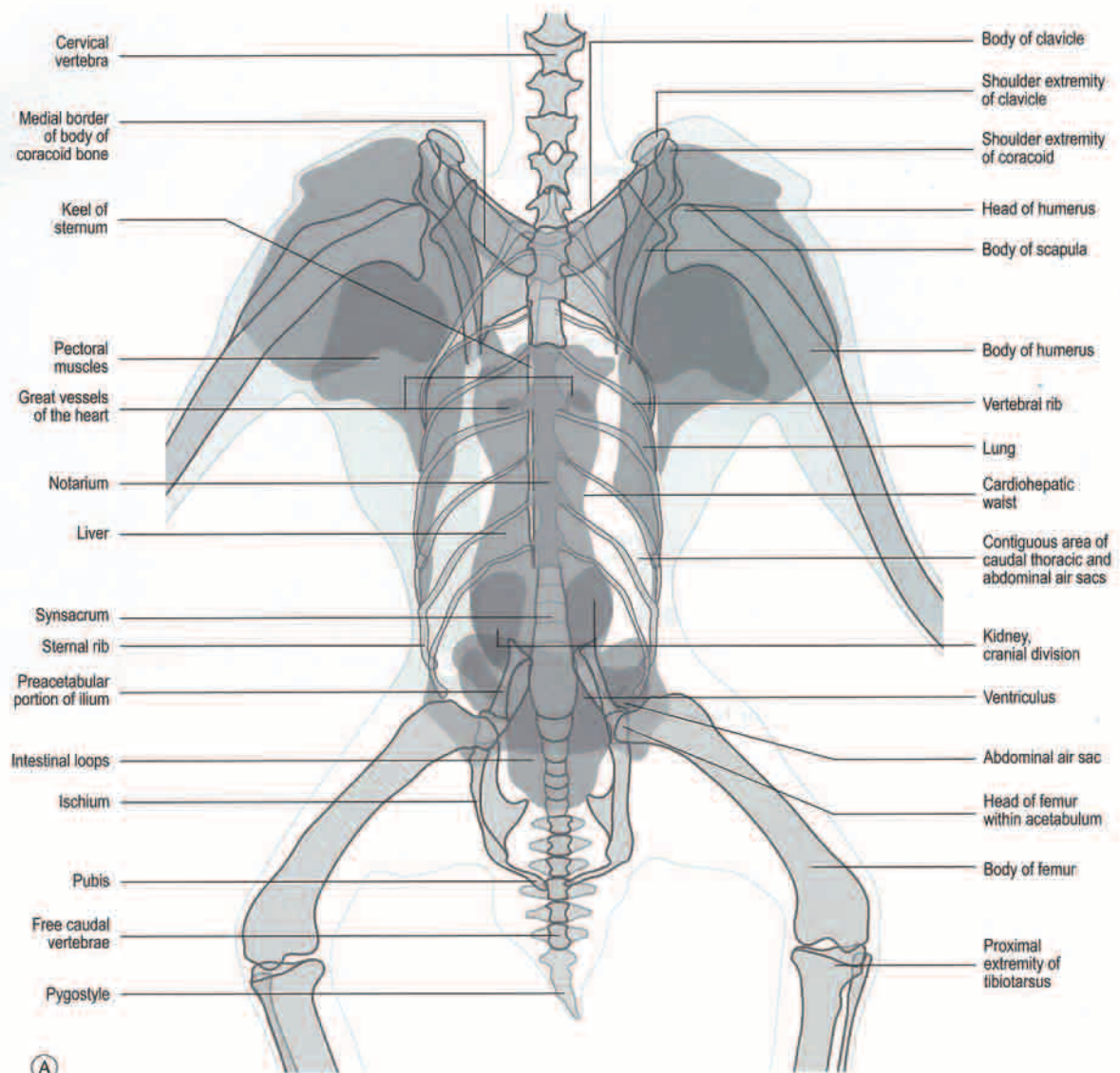


Fig. 3.91 (A and B) Oblique (LeD-RtVO) view of the head of the red kite.

SECTION 9 RADIOGRAPHIC SPECIES CATALOG



(A)

Fig. 3.92 (A and B) Ventrodorsal view of the body of the red kite.

SECTION 9 RADIOGRAPHIC SPECIES CATALOG



Fig. 3.92 (Cont'd).

SECTION 9 RADIOGRAPHIC SPECIES CATALOG

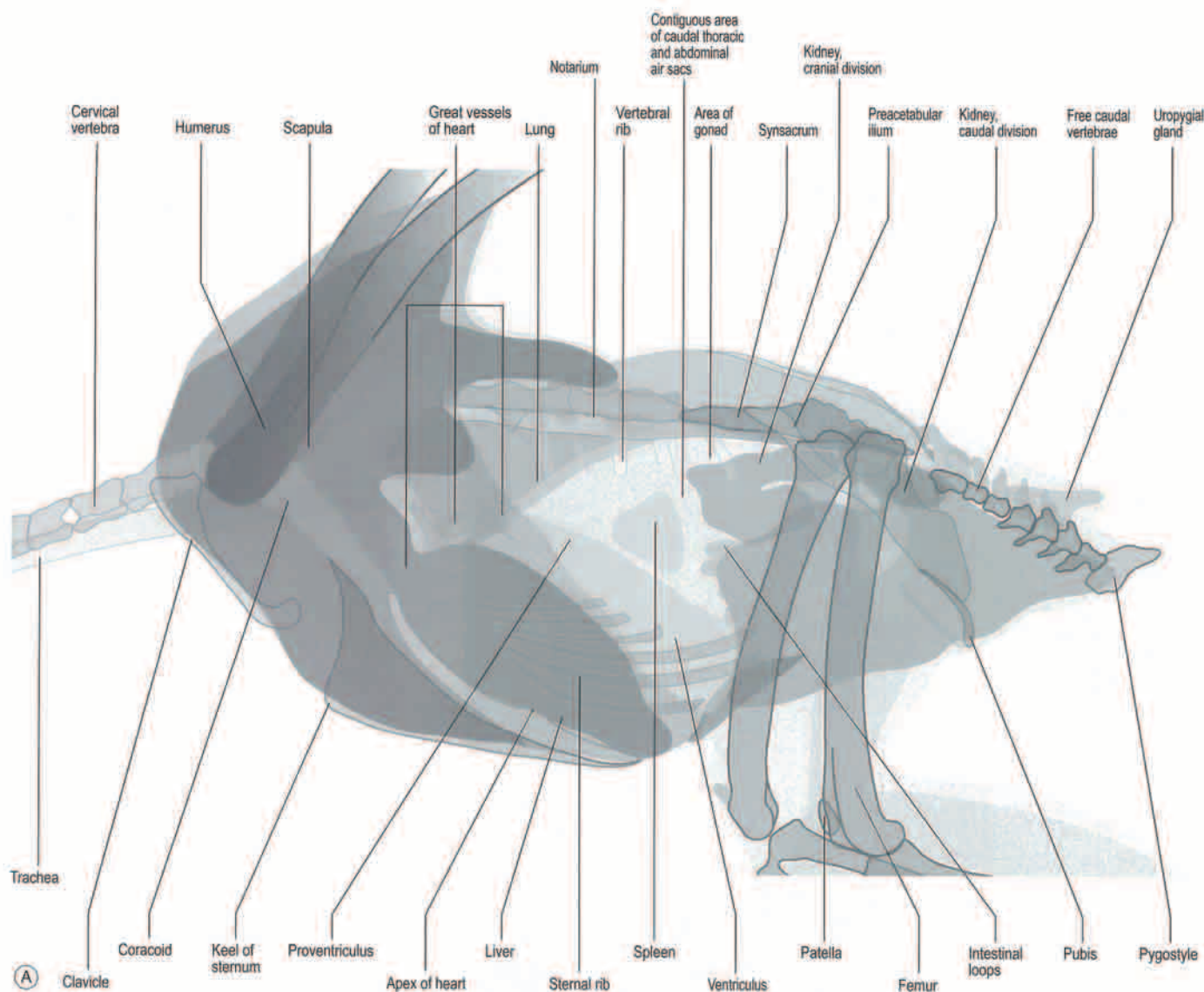


Fig. 3.93 (A and B) Lateral (Le-Rt) view of the body of the red kite.

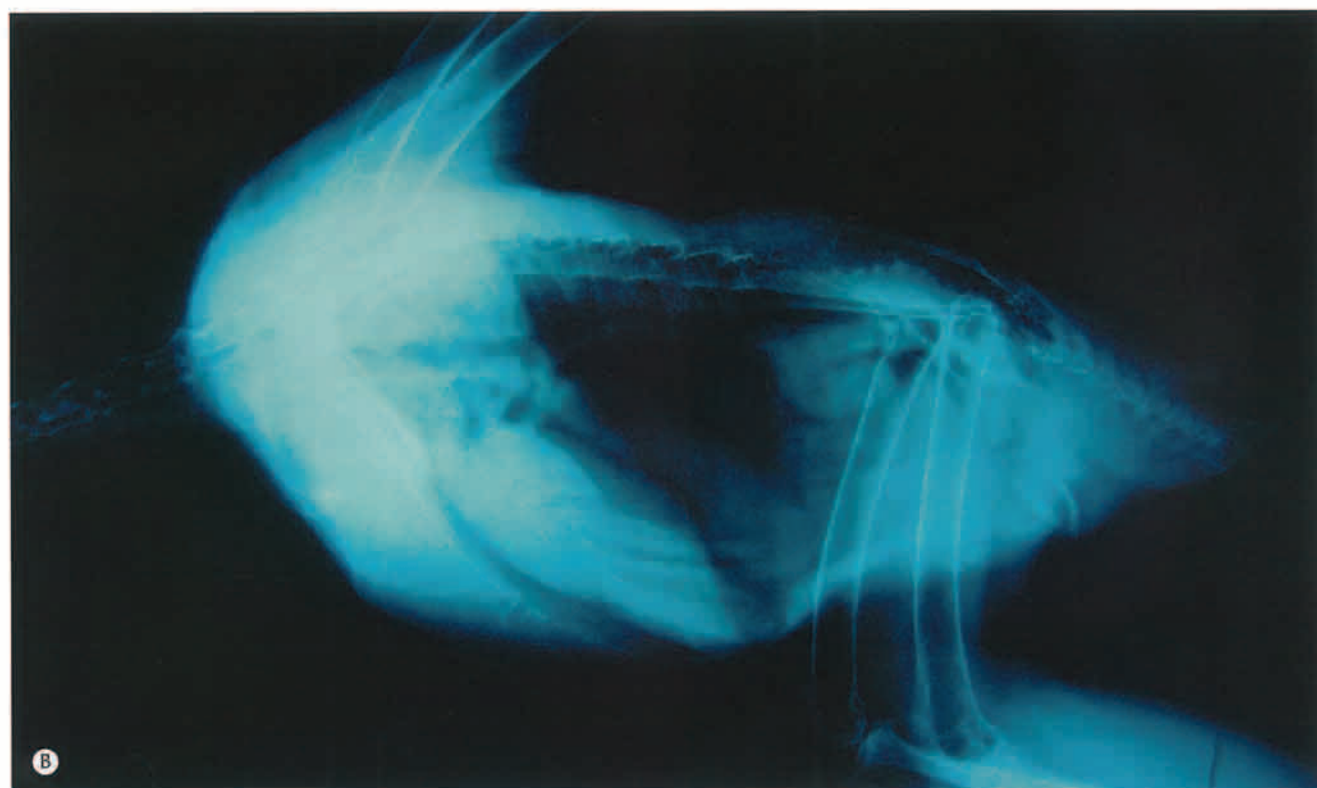


Fig. 3.93 (Cont'd).

SECTION 9 RADIOGRAPHIC SPECIES CATALOG

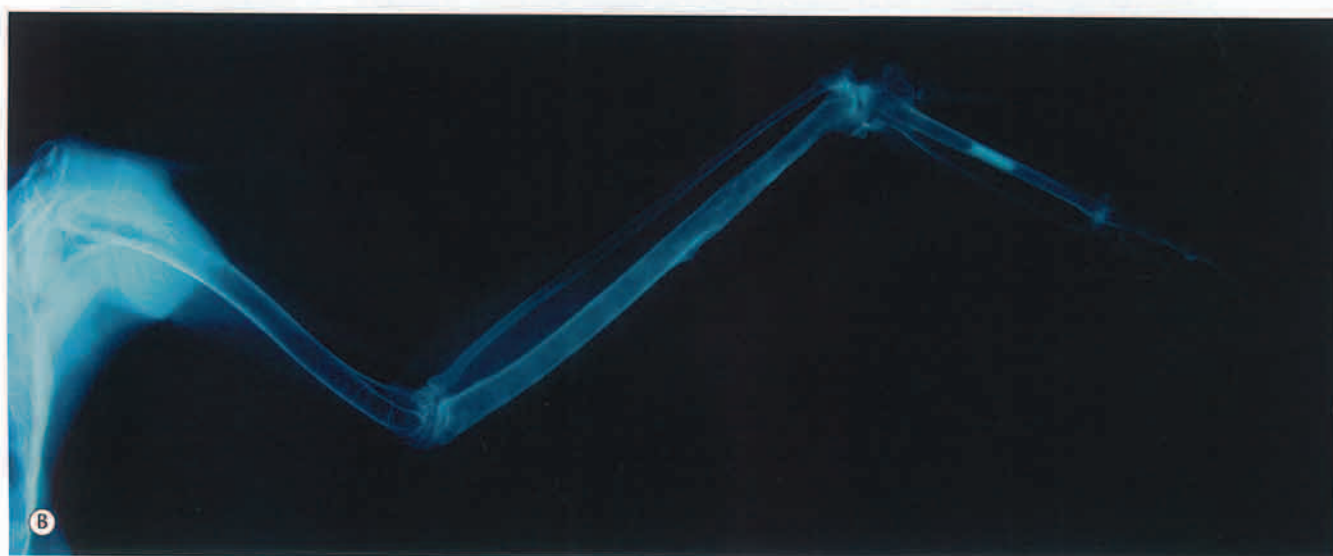
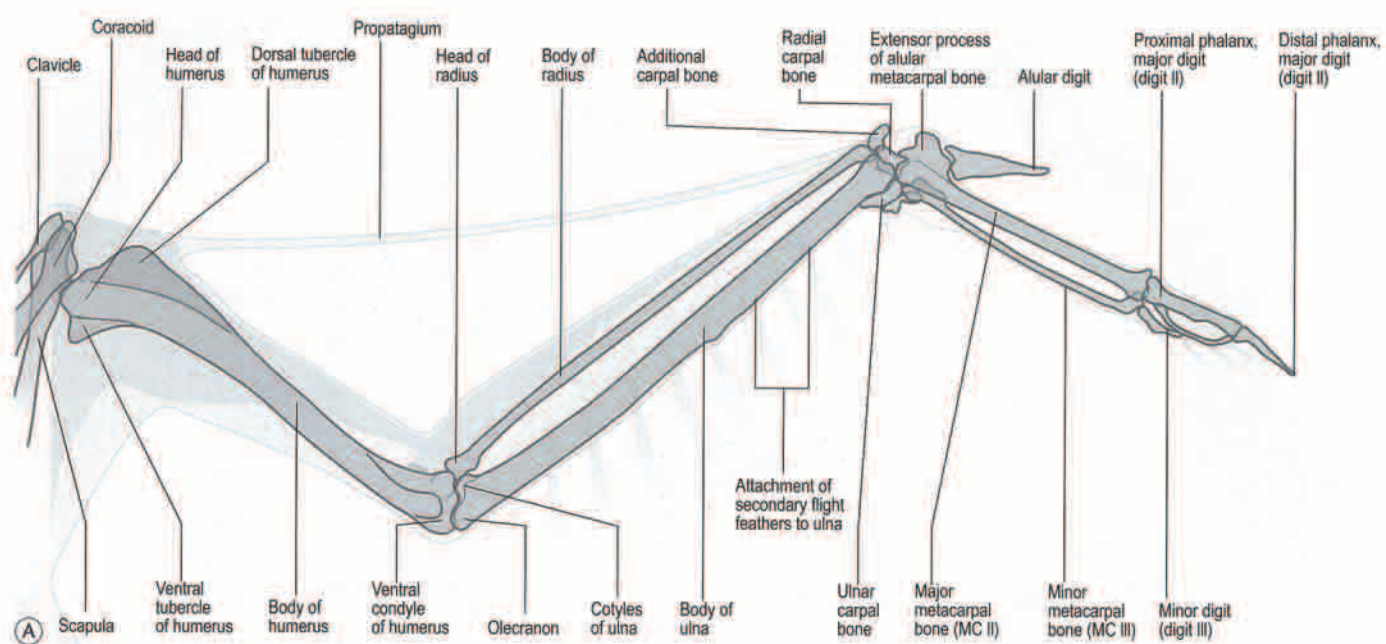


Fig. 3.94 (A and B) Ventrodorsal view of the wing of the red kite. Note the presence of the additional carpal bone.

SECTION 9 RADIOGRAPHIC SPECIES CATALOG

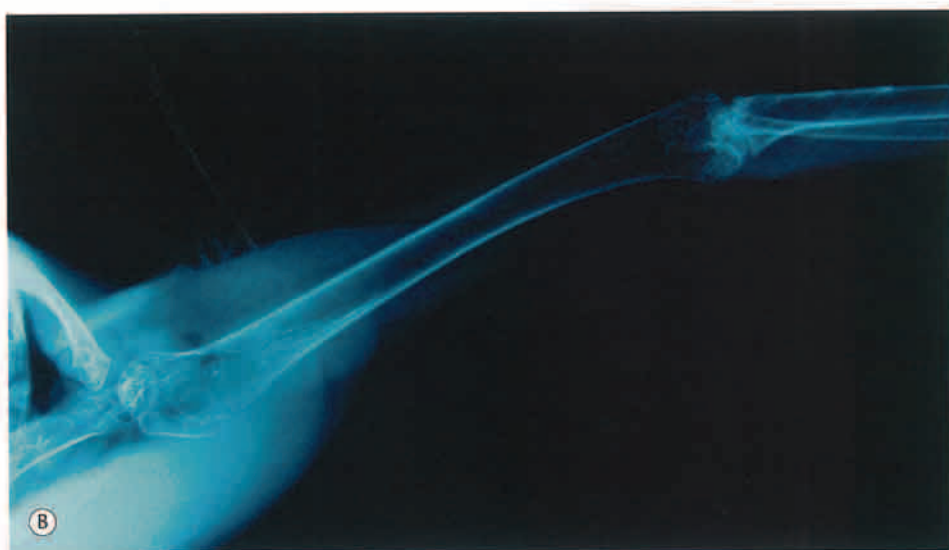
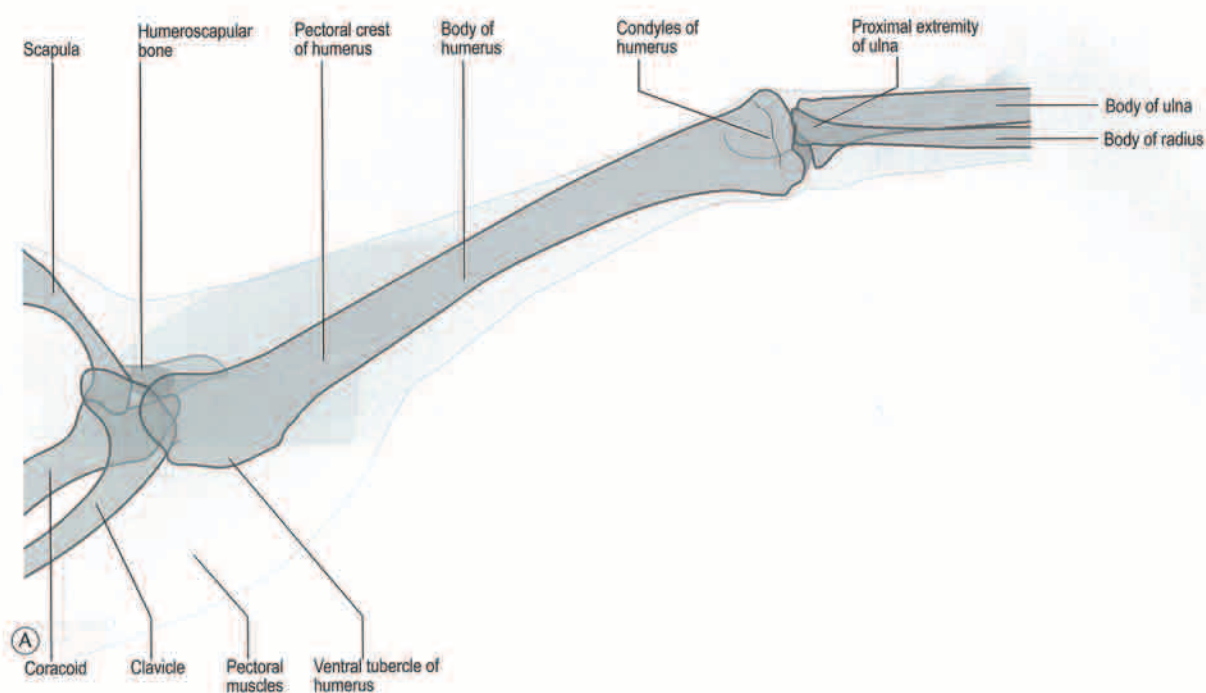


Fig. 3.95 (A and B) Craniocaudal view of the proximal wing of the red kite. Note the presence of the humeroscapular bone.

SECTION 9 RADIOGRAPHIC SPECIES CATALOG

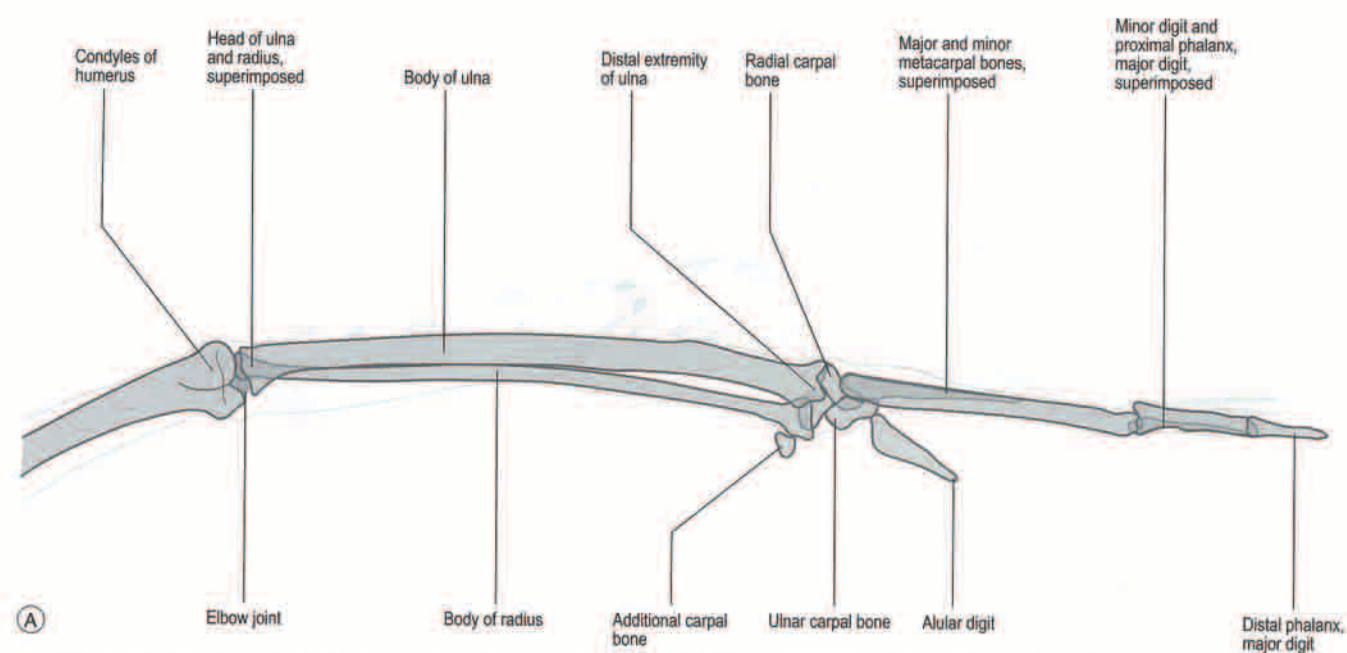


Fig. 3.96 (A and B) Craniocaudal view of the distal wing of the red kite. Note the presence of the additional carpal bone.



Fig. 3.96 (Cont'd).

SECTION 9 RADIOGRAPHIC SPECIES CATALOG

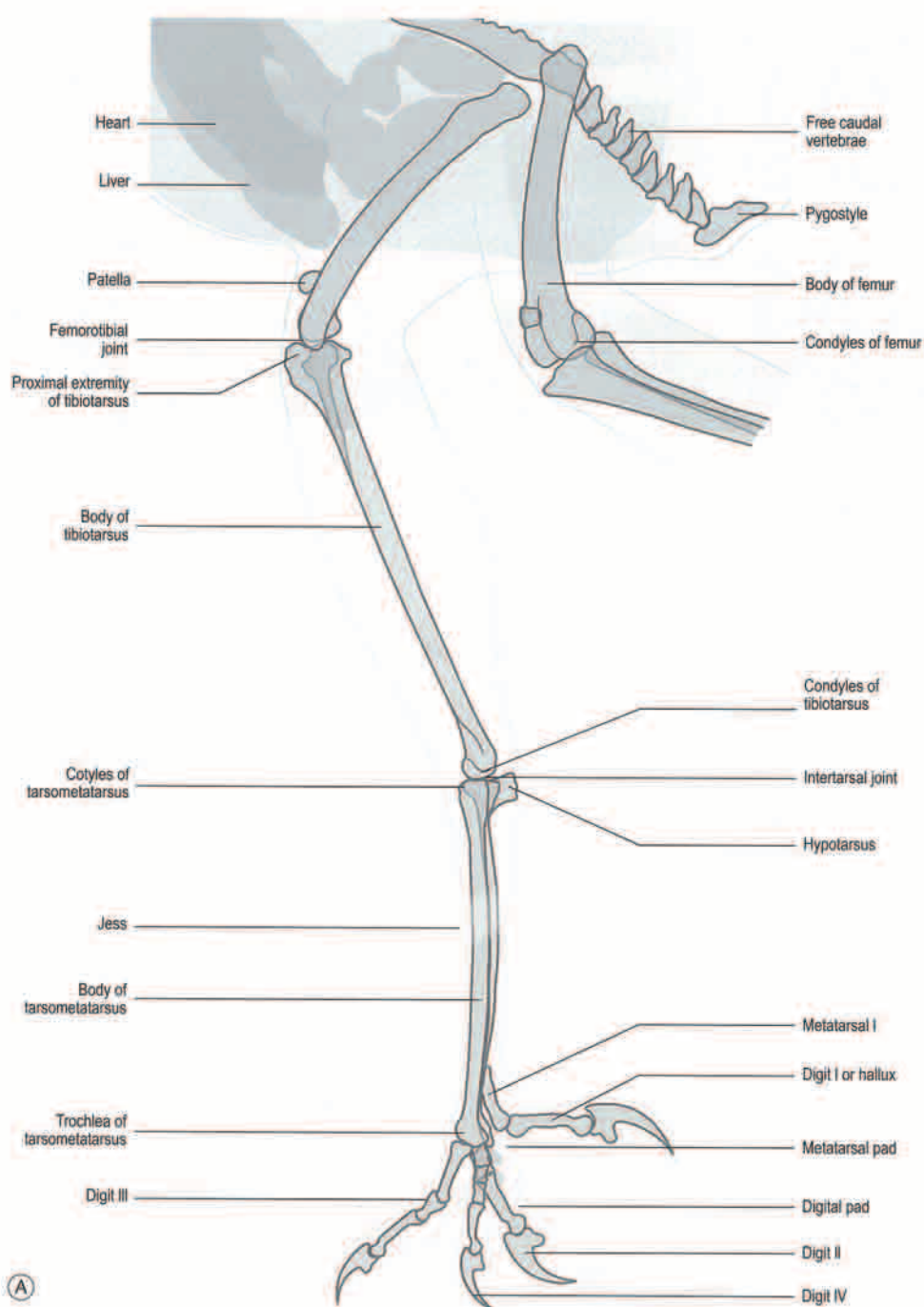


Fig. 3.97 (A and B) Mediolateral view of the pelvic limb of the red kite. Kites have small medial hypotarsal crest and a fused or immobile first phalangeal joint in digit II. In contrast to the red kite, the black kite has a radiographically evident ossified portion of tibial cartilage.

SECTION 9 RADIOGRAPHIC SPECIES CATALOG



Fig. 3.97 (Cont'd).

SECTION 9 RADIOGRAPHIC SPECIES CATALOG

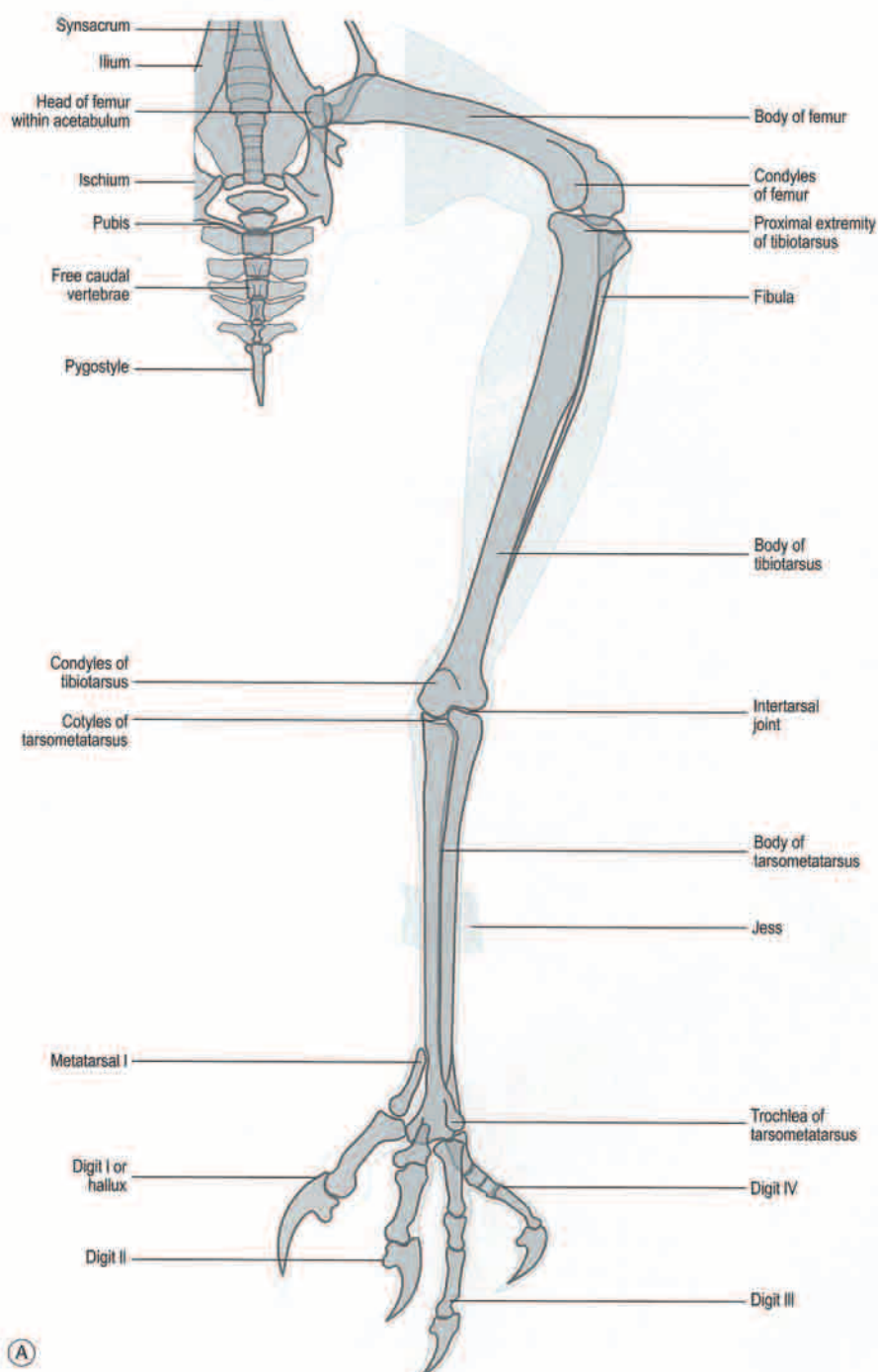


Fig. 3.98 (A and B) Craniocaudal view of the pelvic limb of the red kite.

SECTION 9 RADIOGRAPHIC SPECIES CATALOG



Fig. 3.98 (Cont'd).

SECTION 9 RADIOGRAPHIC SPECIES CATALOG

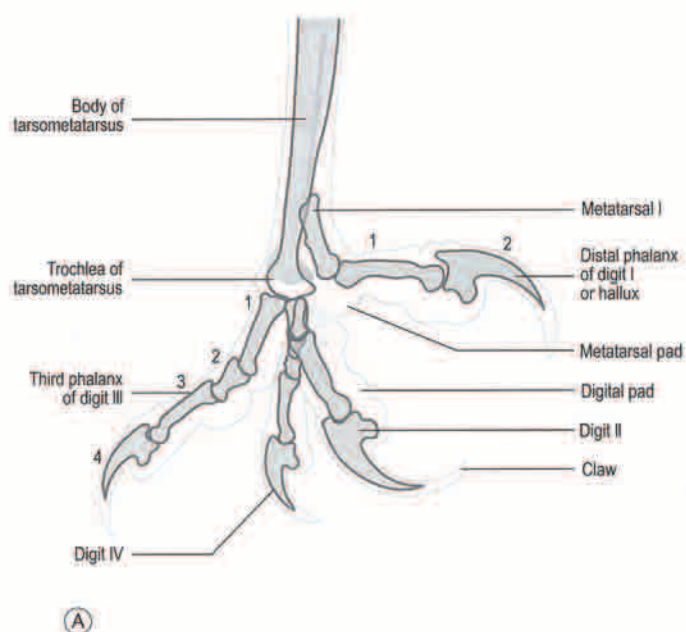


Fig. 3.99 (A and B) Mediolateral close-up view of the foot of the red kite.

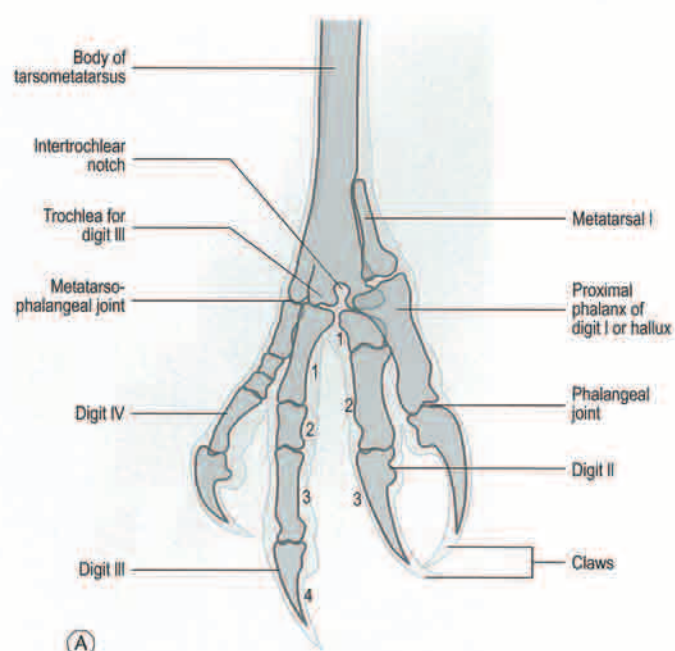


Fig. 3.100 (A and B) Craniocaudal close-up of the foot of the red kite, with digit I flexed.

SECTION 9 RADIOGRAPHIC SPECIES CATALOG

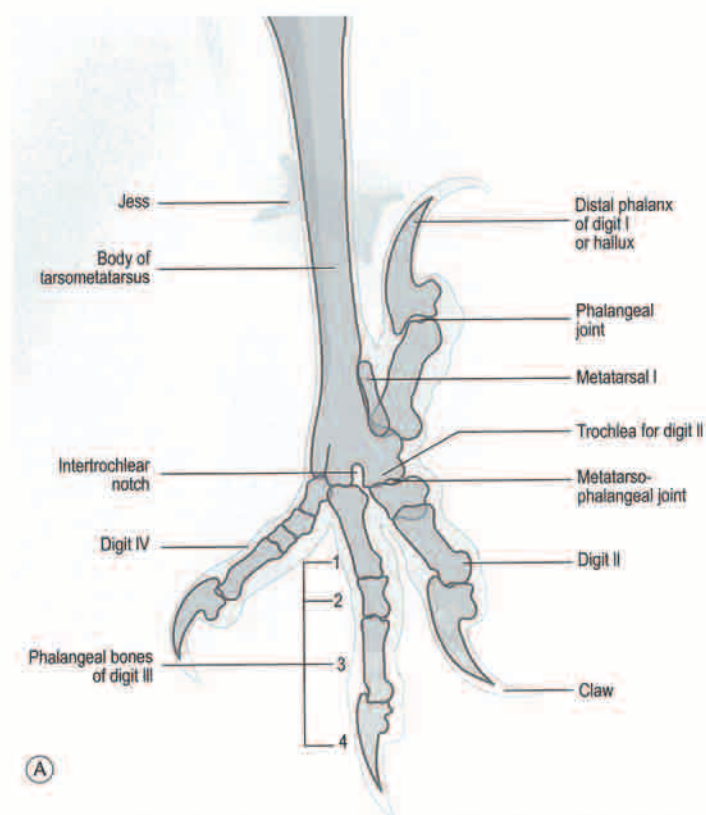


Fig. 3.101 (A and B) Craniocaudal close-up of the foot of the red kite, with digit I extended. The first phalangeal joint in digit II is fused or immobile.

SECTION 9 RADIOGRAPHIC SPECIES CATALOG

**Common barn owl** (*Tyto alba*, Scopoli, 1769, Italy)

The barn owl is a medium-sized species with a great diversity of size and plumage coloration depending on the geographical origin. Currently 46 races and at least 28 subspecies have been recognized worldwide. The subspecies found in Europe and North Africa is 29–44 cm in length and with a body weight ranging from 187 to 455 g. The barn owl has long legs and a distinct heart-shaped facial disc. It also has a white head, neck, chest and tights with a pale-brown rufous back and wings. The species is found in west and east Europe, Africa, Indian subcontinent, across South East Asia to Australia, North, Central and South America. Inhabits open woodland, farm land, rocky cliffs feeding mainly on small mammals; mice in particular.

SECTION 9 RADIOGRAPHIC SPECIES CATALOG

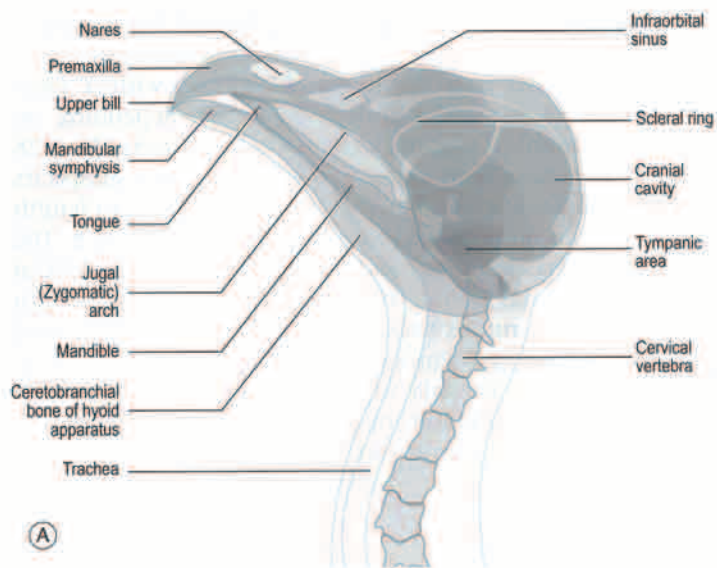


Fig. 3.102 (A and B) Lateral (Le-Rt) view of the head of the barn owl. Note the narrow, elongated head; the dished appearance of the face; the small size of the eye and the low placement of the nares.

SECTION 9 RADIOGRAPHIC SPECIES CATALOG

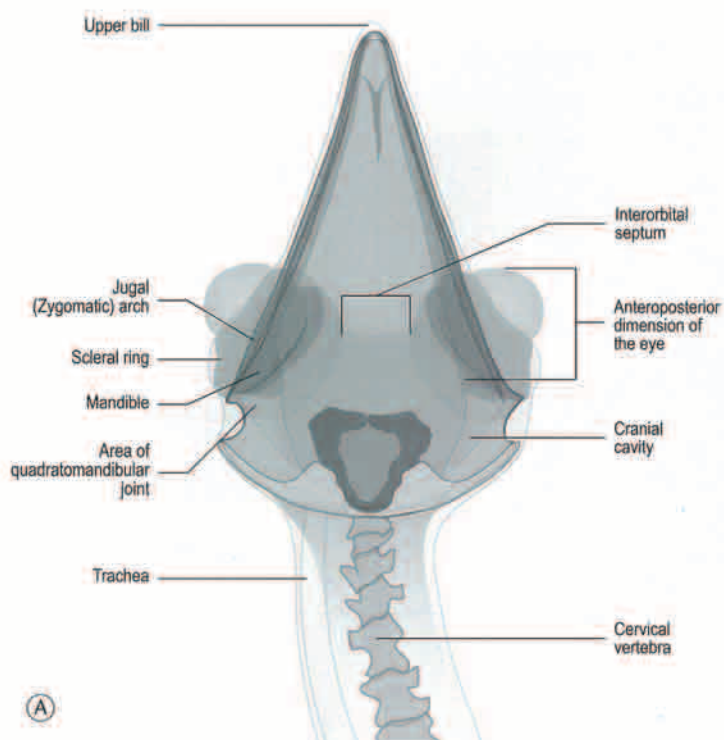


Fig. 3.103 (A and B) Ventrodorsal view of the head of the barn owl. Note the wide interorbital septum separating the eyes on the midline and the smaller scleral ring.

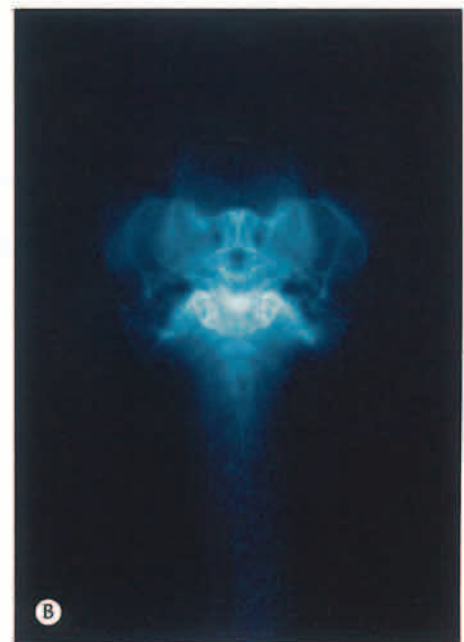
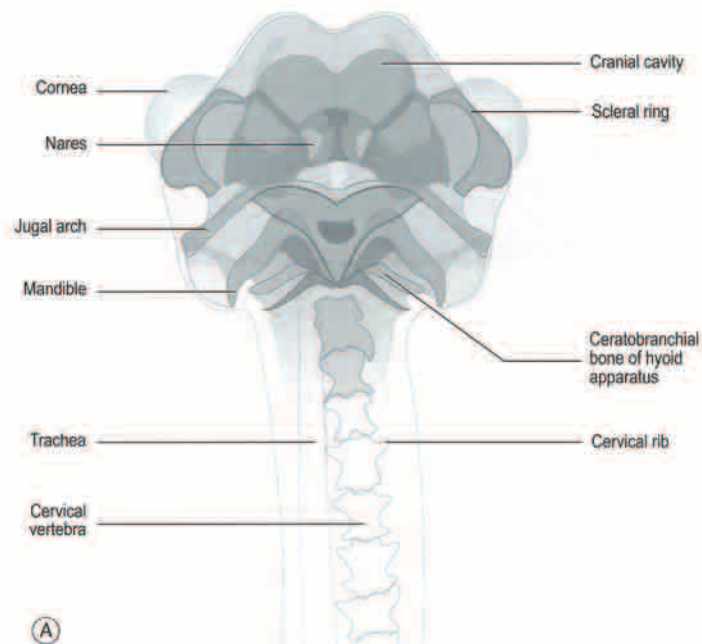
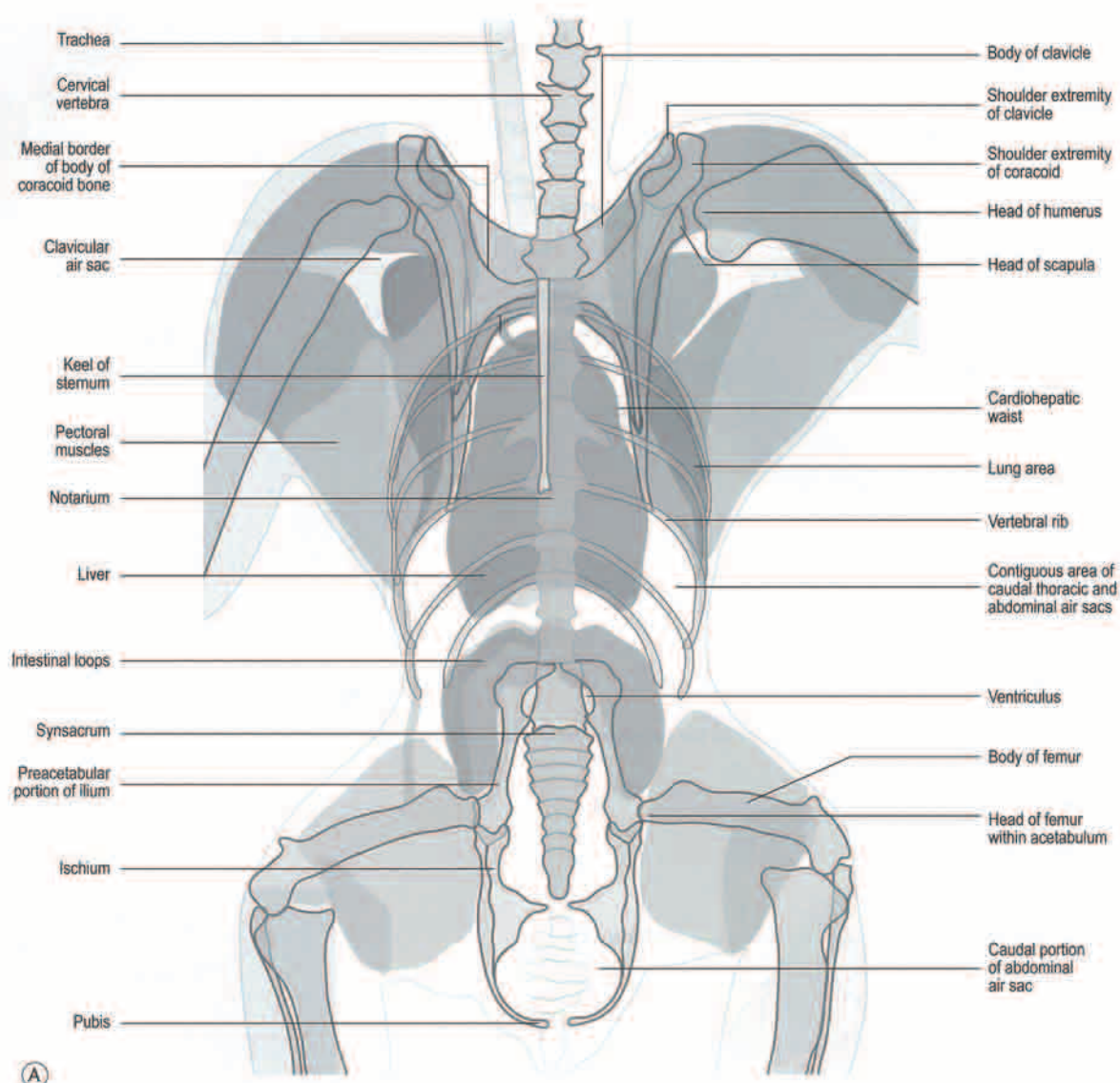


Fig. 3.104 (A and B) Rostrocaudal view of the head of the barn owl.

SECTION 9 RADIOGRAPHIC SPECIES CATALOG



(A)

Fig. 3.105 (A and B) Ventrodorsal view of the body of the barn owl. Note the absence of a prominent cardiohepatic waist.

SECTION 9 RADIOGRAPHIC SPECIES CATALOG



Fig. 3.105 (Cont'd).

SECTION 9 RADIOGRAPHIC SPECIES CATALOG

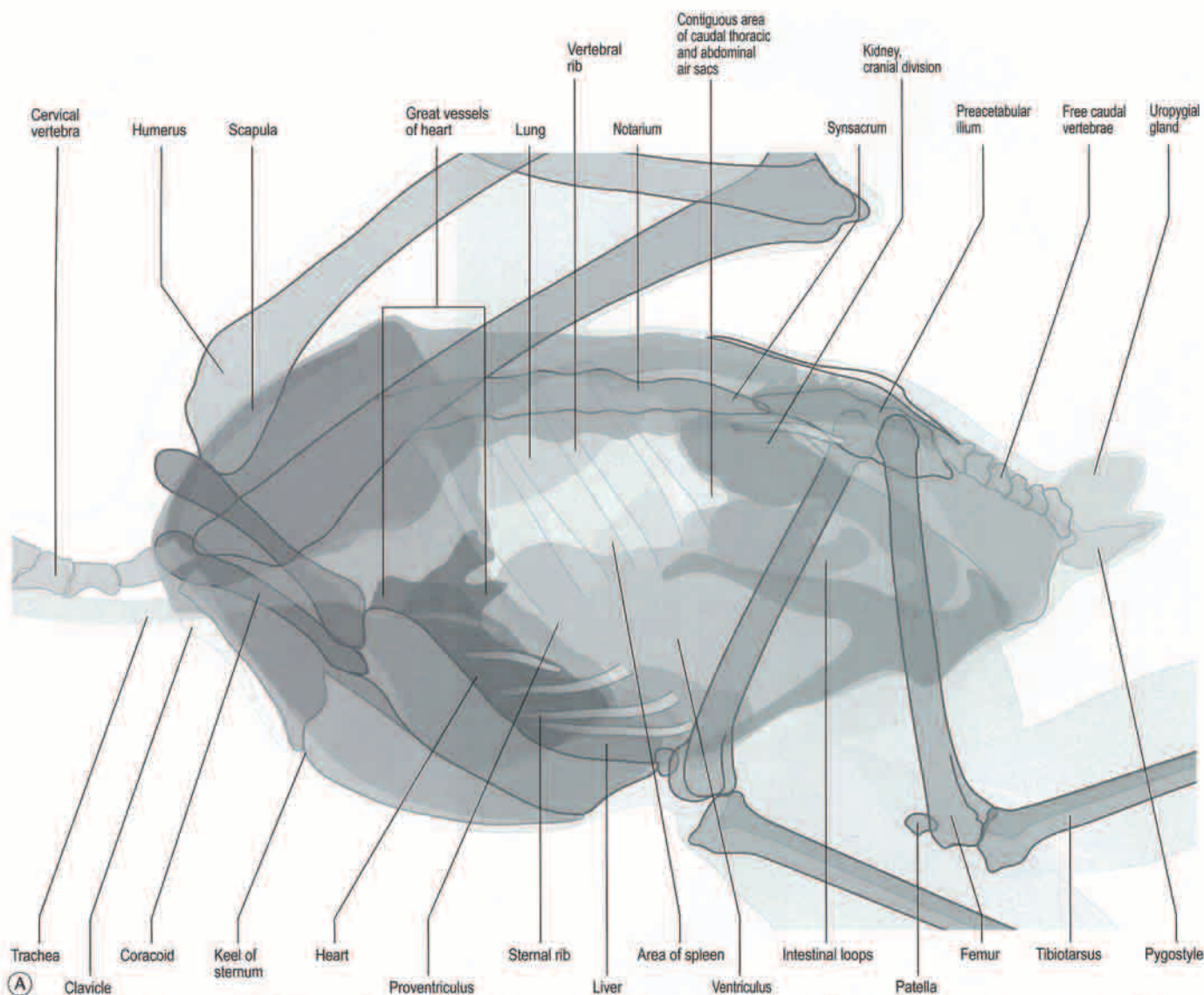


Fig. 3.106 (A and B) Lateral (Le-Rt) view of the body of the barn owl. The furcula of the clavicle is fused with the cranial ventral edge of the sternum.

SECTION 9 RADIOGRAPHIC SPECIES CATALOG

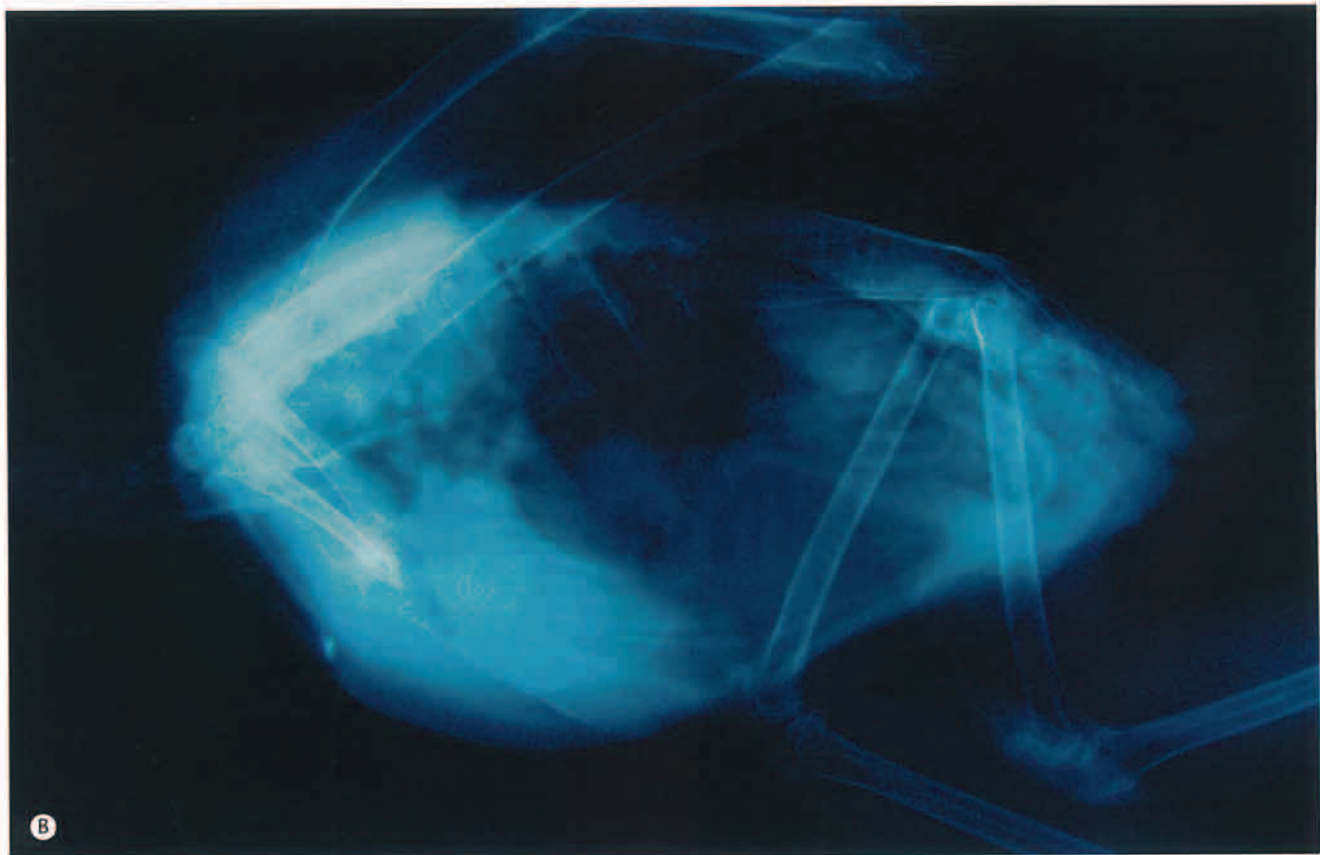


Fig. 3.106 (Cont'd).

SECTION 9 RADIOGRAPHIC SPECIES CATALOG

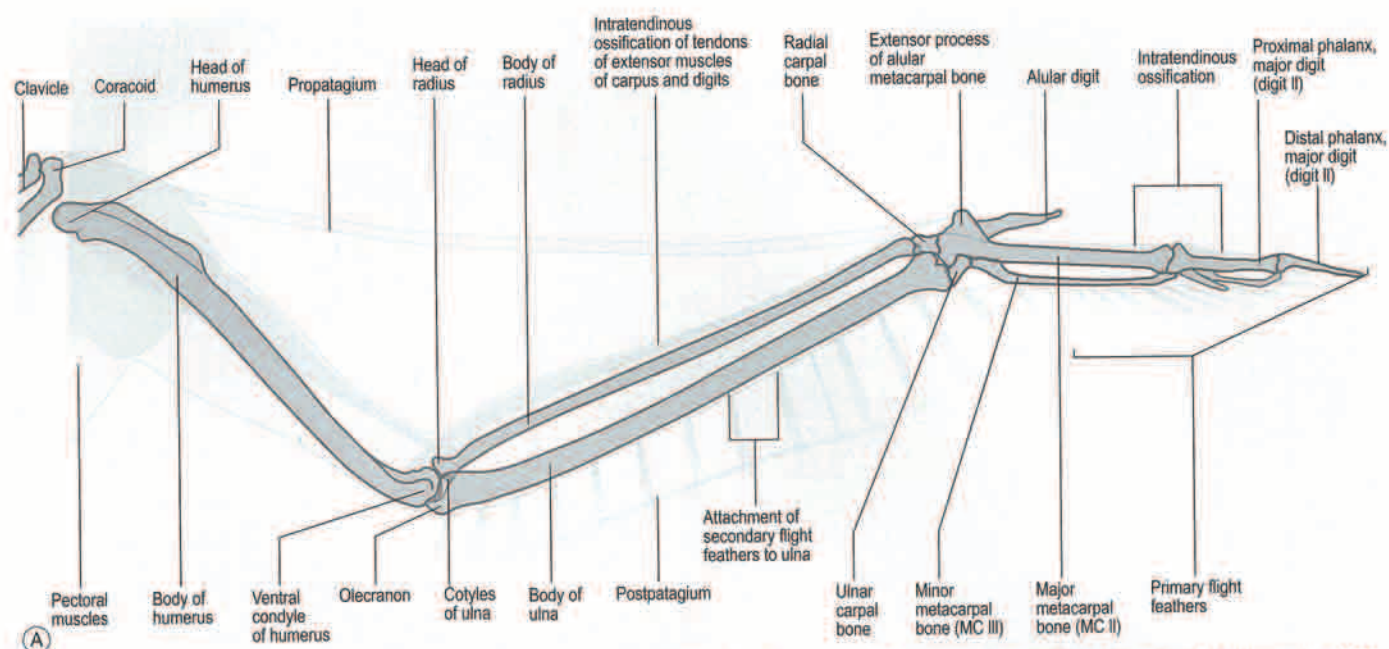


Fig. 3.107 (A and B) Ventrodorsal view of the wing of the barn owl. Note the absence of the additional carpal bone, which is present in other owl species, and the lack of ossification of the tendons of the extensor muscles of the carpus and digits. Also, barn owls do not possess the humeroscapular bone of the shoulder.

SECTION 9 RADIOGRAPHIC SPECIES CATALOG



Fig. 3.107 (Cont'd).

SECTION 9 RADIOGRAPHIC SPECIES CATALOG

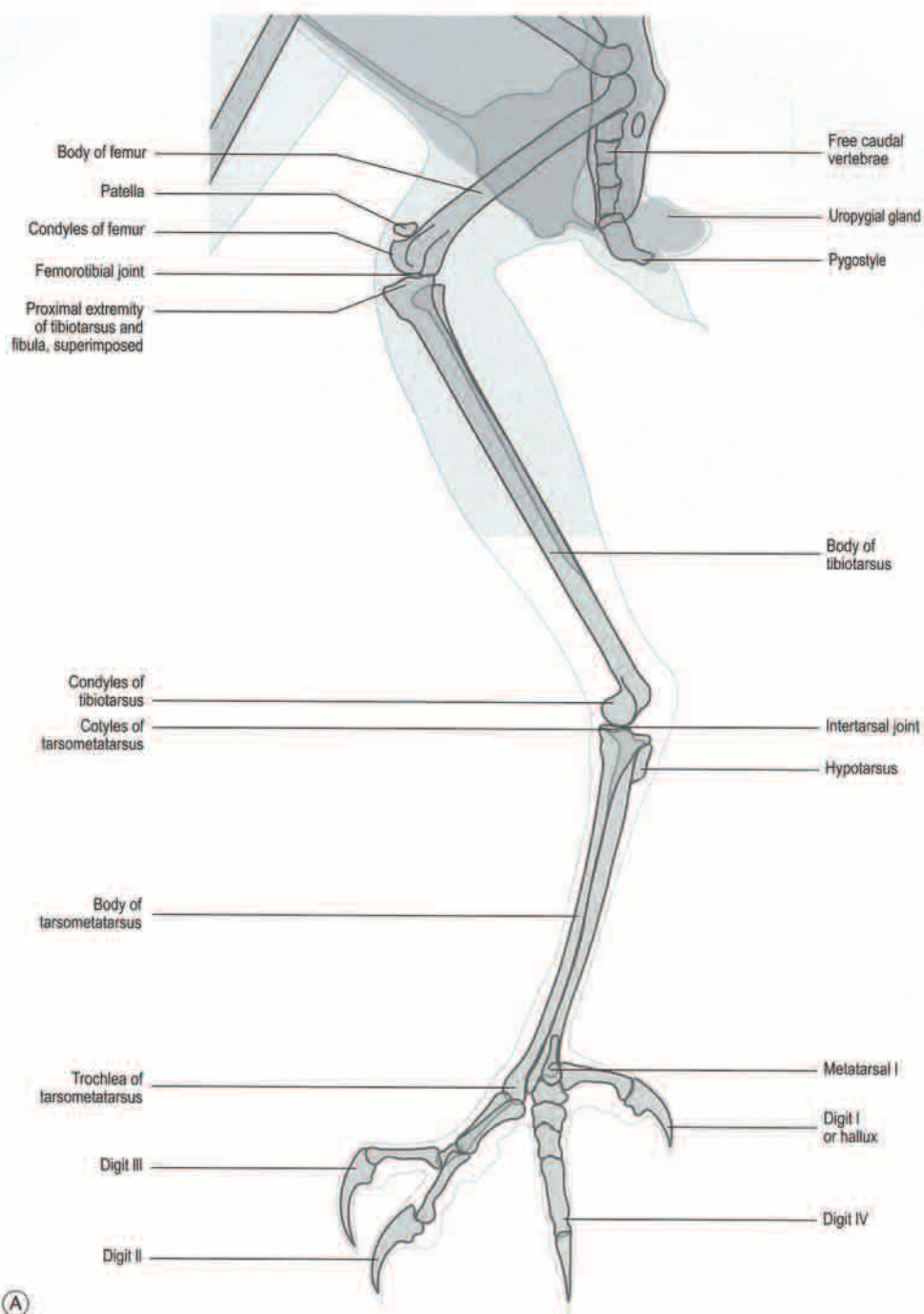


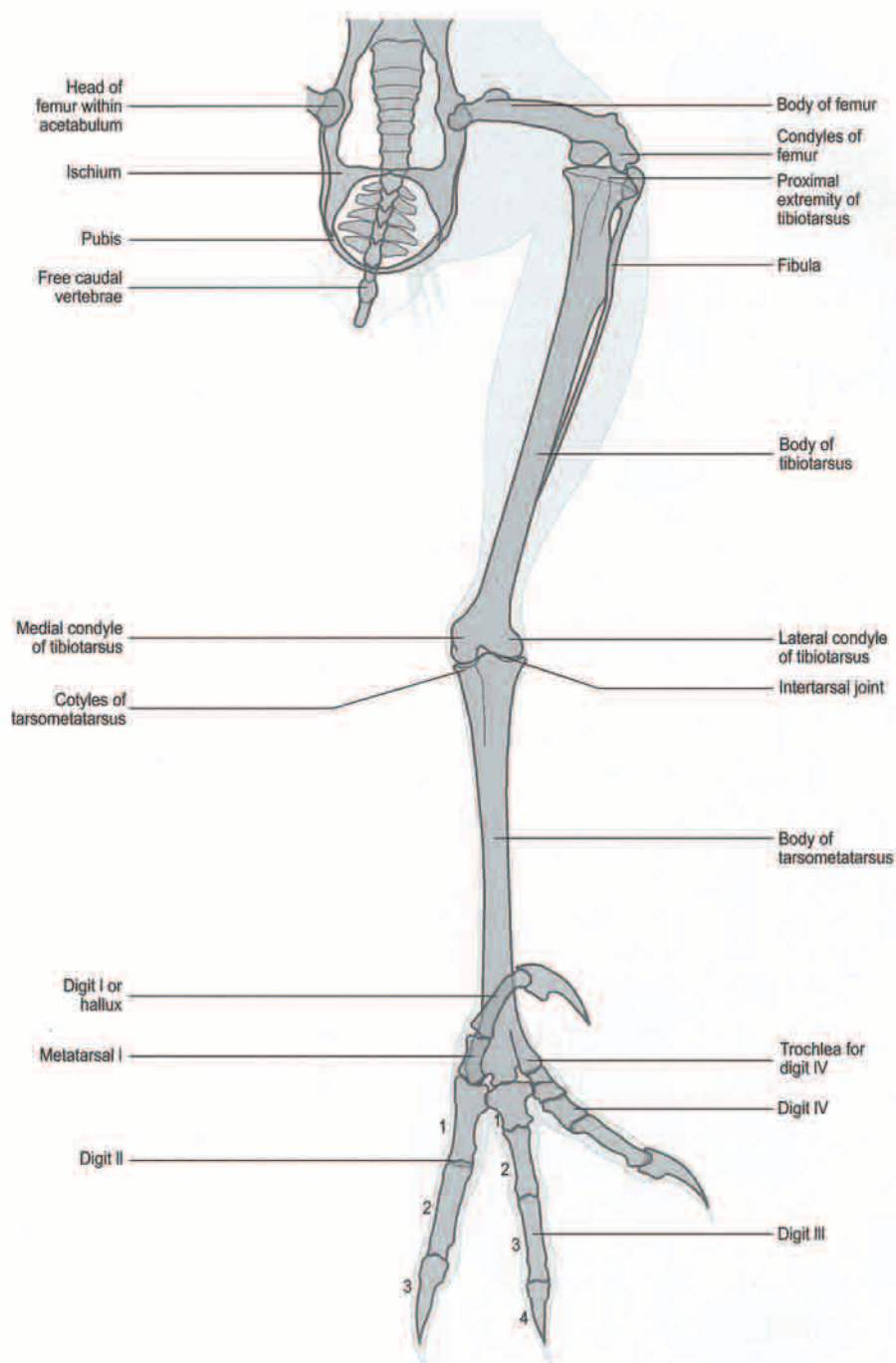
Fig. 3.108 (A and B) Mediolateral view of the pelvic limb of the barn owl. Note the well-developed uropygial gland.

SECTION 9 RADIOGRAPHIC SPECIES CATALOG



Fig. 3.108 (*Cont'd*).

SECTION 9 RADIOGRAPHIC SPECIES CATALOG



(A)

Fig. 3.109 (A and B) Craniocaudal view of the pelvic limb of the barn owl. Note the extended length of the tarsometatarsus and digit II.

SECTION 9 RADIOGRAPHIC SPECIES CATALOG



Fig. 3.109 (Cont'd).

SECTION 9 RADIOGRAPHIC SPECIES CATALOG

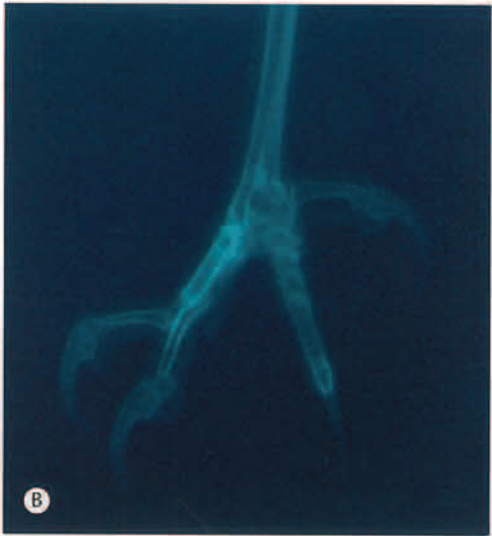
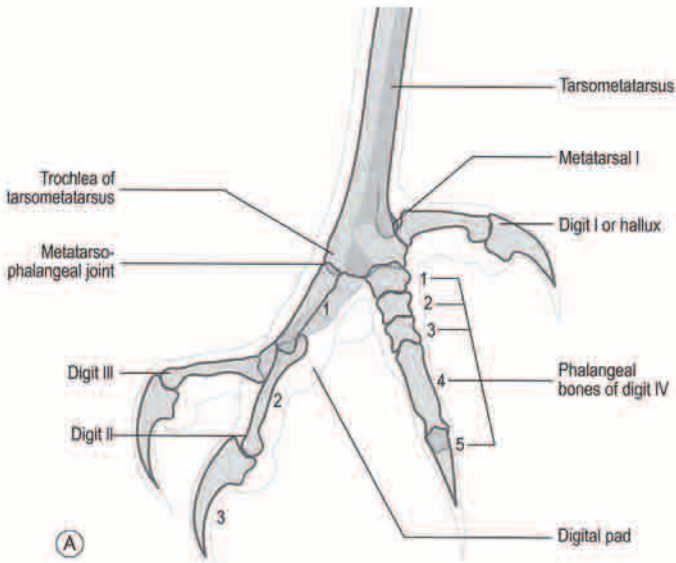


Fig. 3.110 (A and B) Mediolateral close-up of the foot of the barn owl.

SECTION 9 RADIOGRAPHIC SPECIES CATALOG

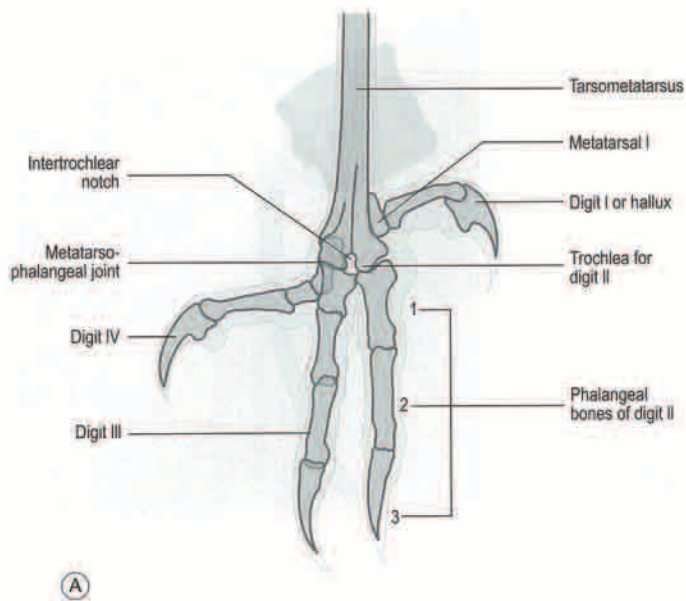


Fig. 3.111 (A and B) Craniocaudal close-up of the foot of the barn owl, with digit I flexed. Note the equal length of digit II and digit III.

SECTION 9 RADIOGRAPHIC SPECIES CATALOG

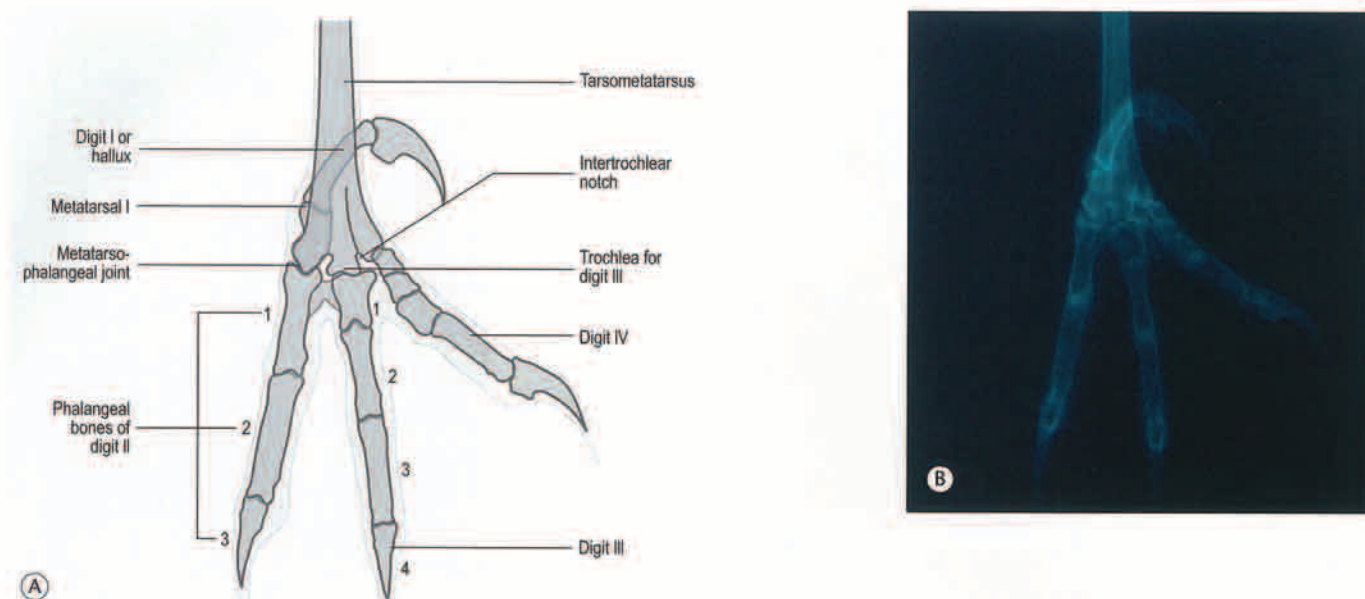


Fig. 3.112 (A and B) Craniocaudal close-up of the foot of the barn owl, with digit I extended. Note the equal length of digit II and digit III.

SECTION 9 RADIOGRAPHIC SPECIES CATALOG



Eurasian eagle owl (*Bubo bubo*, Linnaeus, 1758,
Sweden)

The Eurasian, common or great eagle owl is a large species measuring 60–75 cm in length with a wingspan of 160–188 cm. The body weight of males ranges from 1500 to 2800 g and the females from 1750 to 4200 g. This owl possesses a large barrel-shaped body, with overall dark-

brown plumage with a buffy gray-brown facial disk and prominent ear tufts. Currently, 14 subspecies have been identified. This species occurs from the Iberian Peninsula, north to Scandinavia, across Europe, south and central Asia to Korea and west China. The Eurasian eagle owls live in undisturbed woodlands, open forest, taiga, ravines and rocky cliffs feeding mainly on small-to-medium-sized mammals.

SECTION 9 RADIOGRAPHIC SPECIES CATALOG

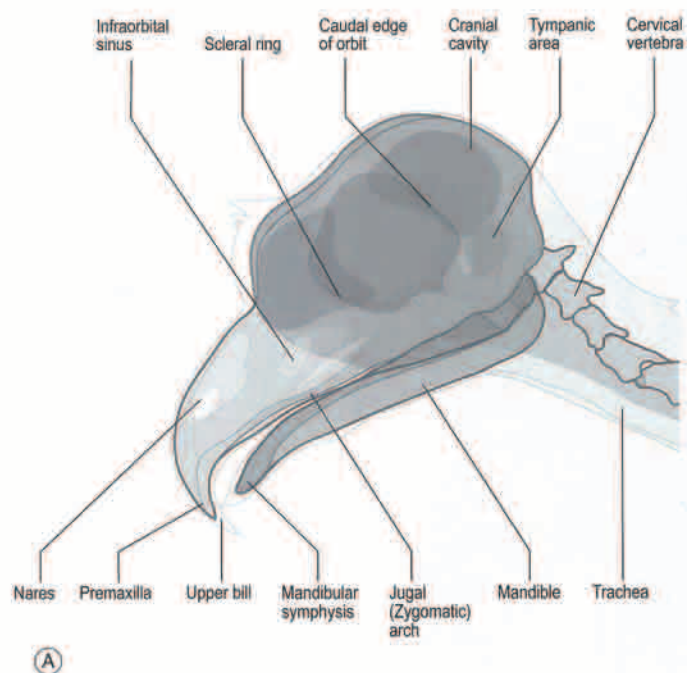


Fig. 3.113 (A and B) Lateral (Le-Rt) view of the head of the Eurasian eagle owl.

SECTION 9 RADIOGRAPHIC SPECIES CATALOG

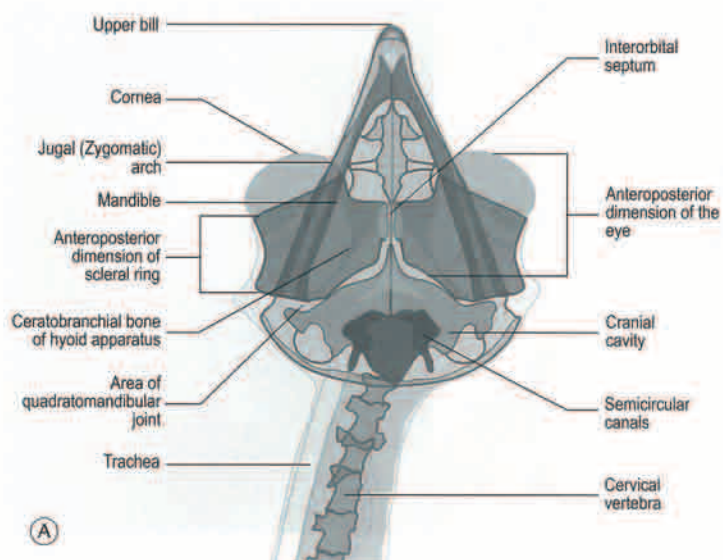


Fig. 3.114 (A and B) Ventrodorsal view of the head of the Eurasian eagle owl. Note the narrow interorbital septum.

SECTION 9 RADIOGRAPHIC SPECIES CATALOG

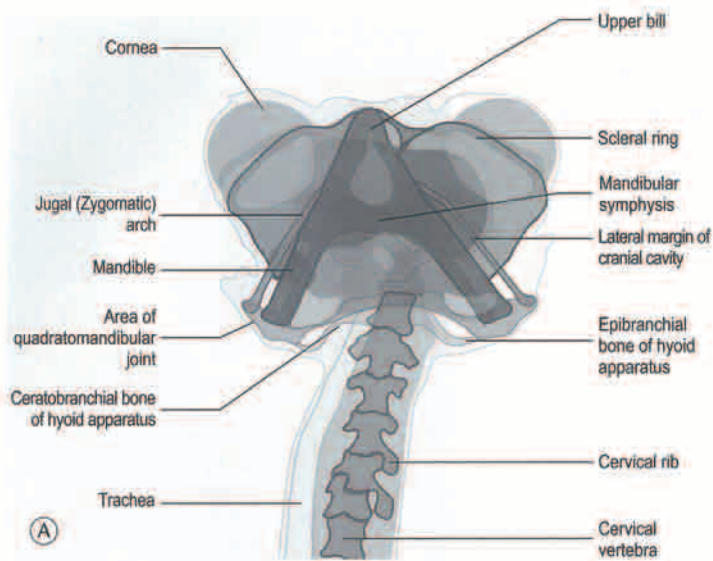


Fig. 3.115 (A and B) Rostrocaudal view of the head of the Eurasian eagle owl.

SECTION 9 RADIOGRAPHIC SPECIES CATALOG

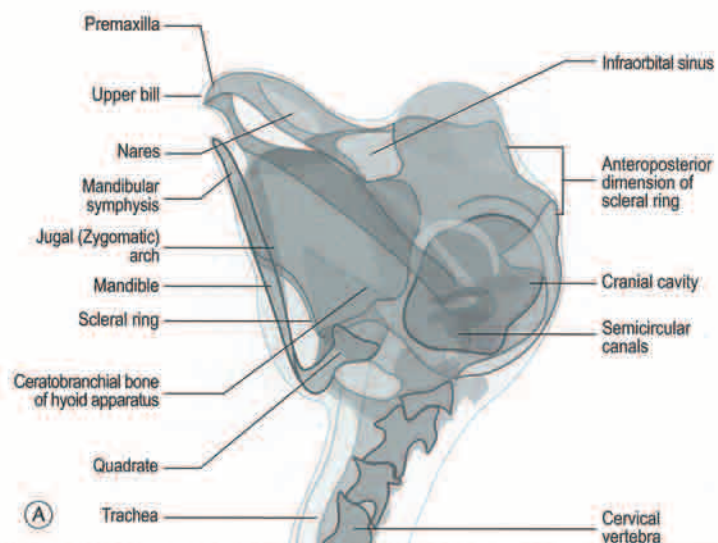
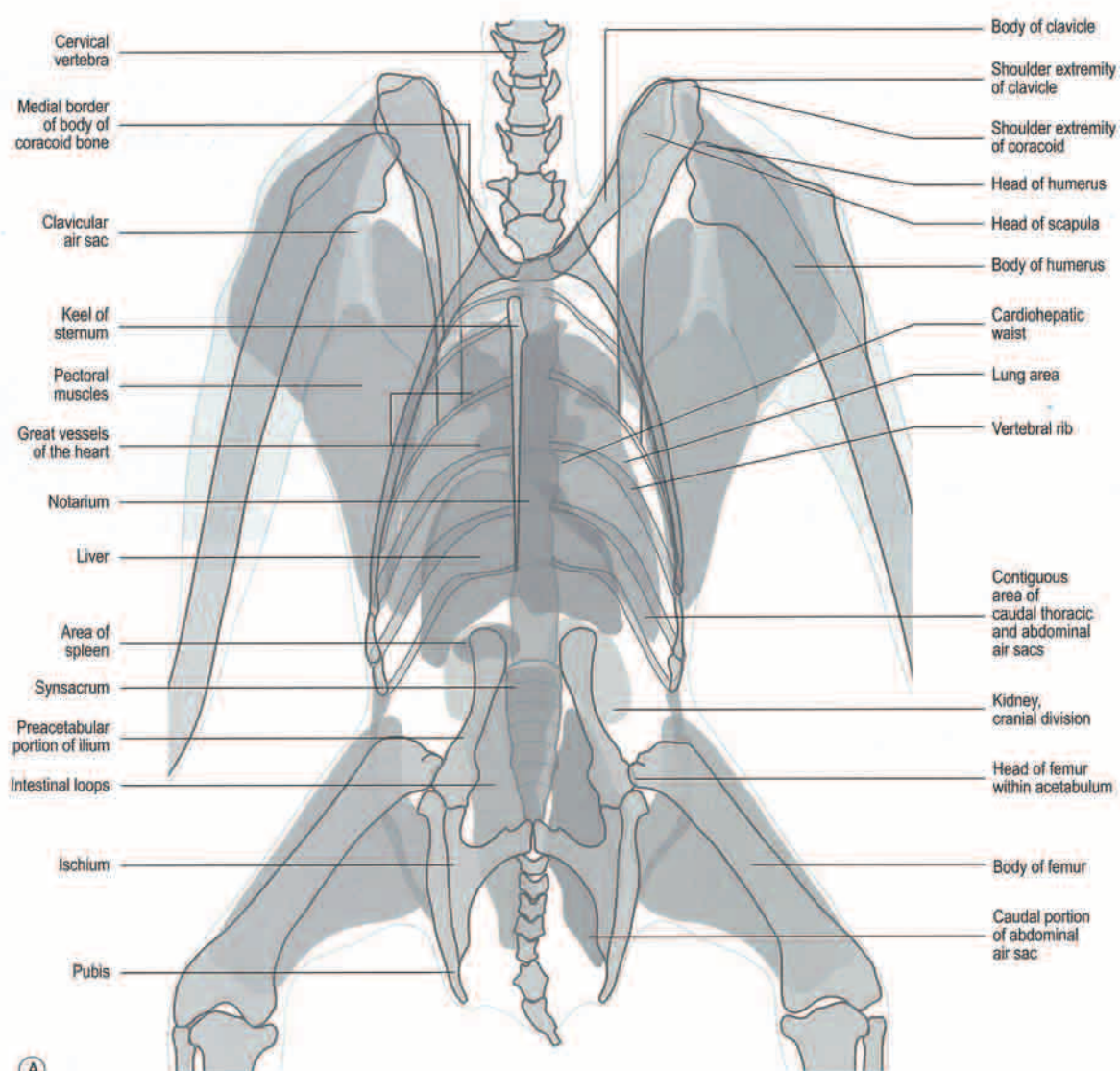


Fig. 3.116 (A and B) Oblique (LeD-RtVO) view of the head of the Eurasian eagle owl. Note the extreme depth of the anteroposterior dimensions of the scleral ossicles, which is typical of most owl eyes.

SECTION 9 RADIOGRAPHIC SPECIES CATALOG



A

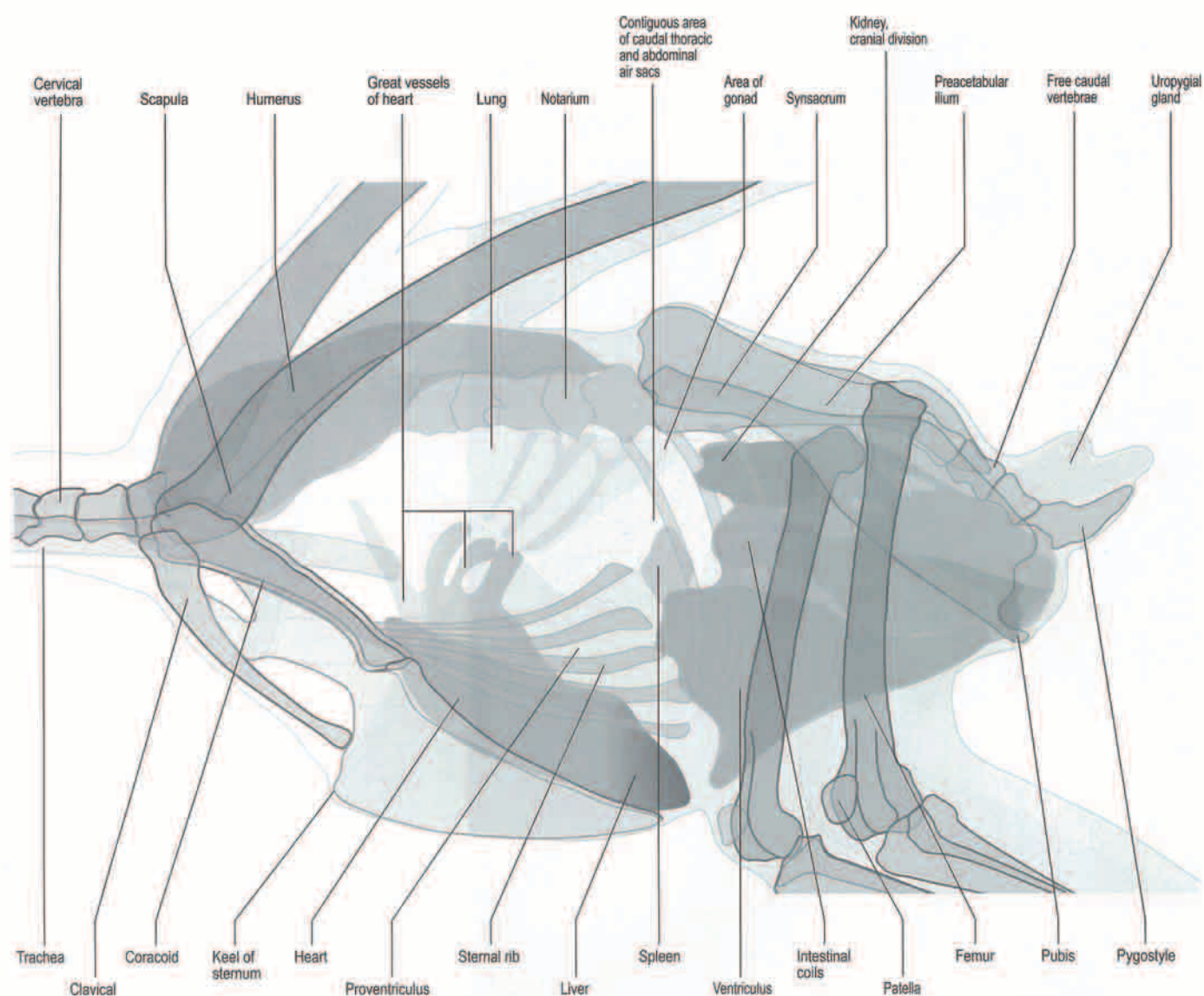
Fig. 3.117 (A and B) Ventrodorsal view of the body of the Eurasian eagle owl. The hourglass cardiohepatic waist is more prominent as compared with that of the barn owl.

SECTION 9 RADIOGRAPHIC SPECIES CATALOG



Fig. 3.117 (Cont'd).

SECTION 9 RADIOGRAPHIC SPECIES CATALOG



(A)

Fig. 3.118 (A and B) Lateral (Le-Rt) view of the body of the Eurasian eagle owl. The furcula appears fused with the cranial edge of the sternum. Note the well-developed uropygial gland.

SECTION 9 RADIOGRAPHIC SPECIES CATALOG



Fig. 3.118 (Cont'd).

SECTION 9 RADIOGRAPHIC SPECIES CATALOG

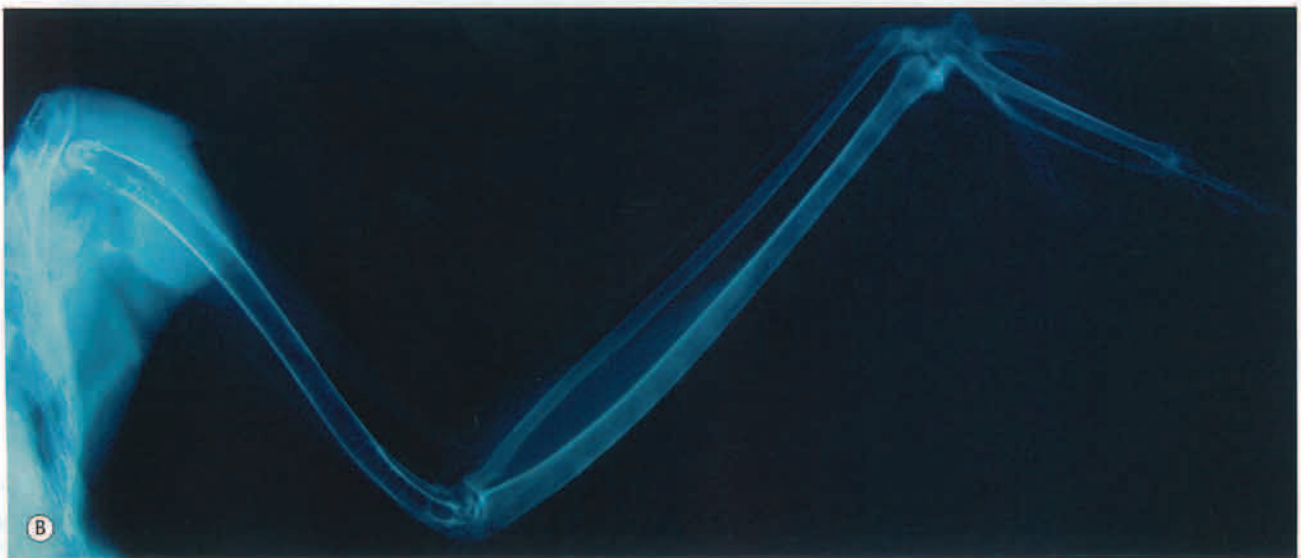
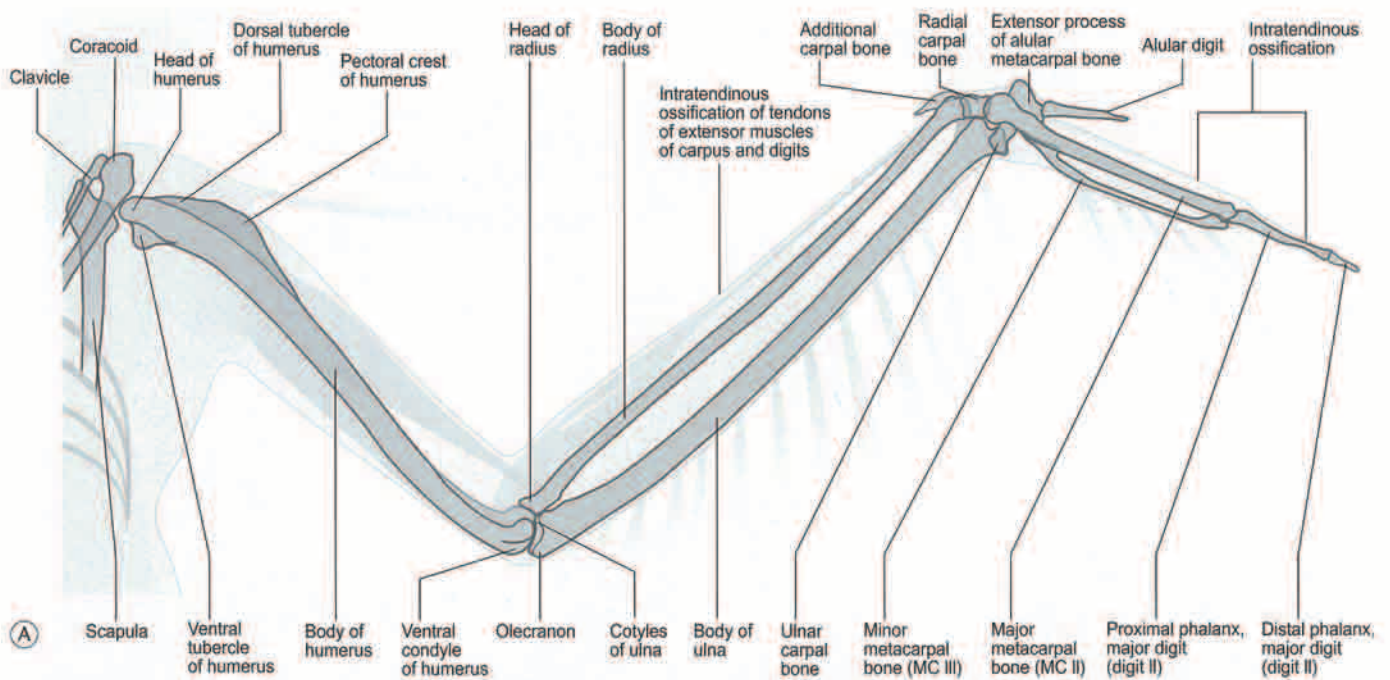


Fig. 3.119 (A and B) Ventrodorsal view of the wing of the Eurasian eagle owl. Note the presence of the additional carpal bone, which is characteristic of most species of owls except for the barn owl. Also, note the intratendinous ossification of the tendons of extensor muscles of carpus and digits.

SECTION 9 RADIOGRAPHIC SPECIES CATALOG

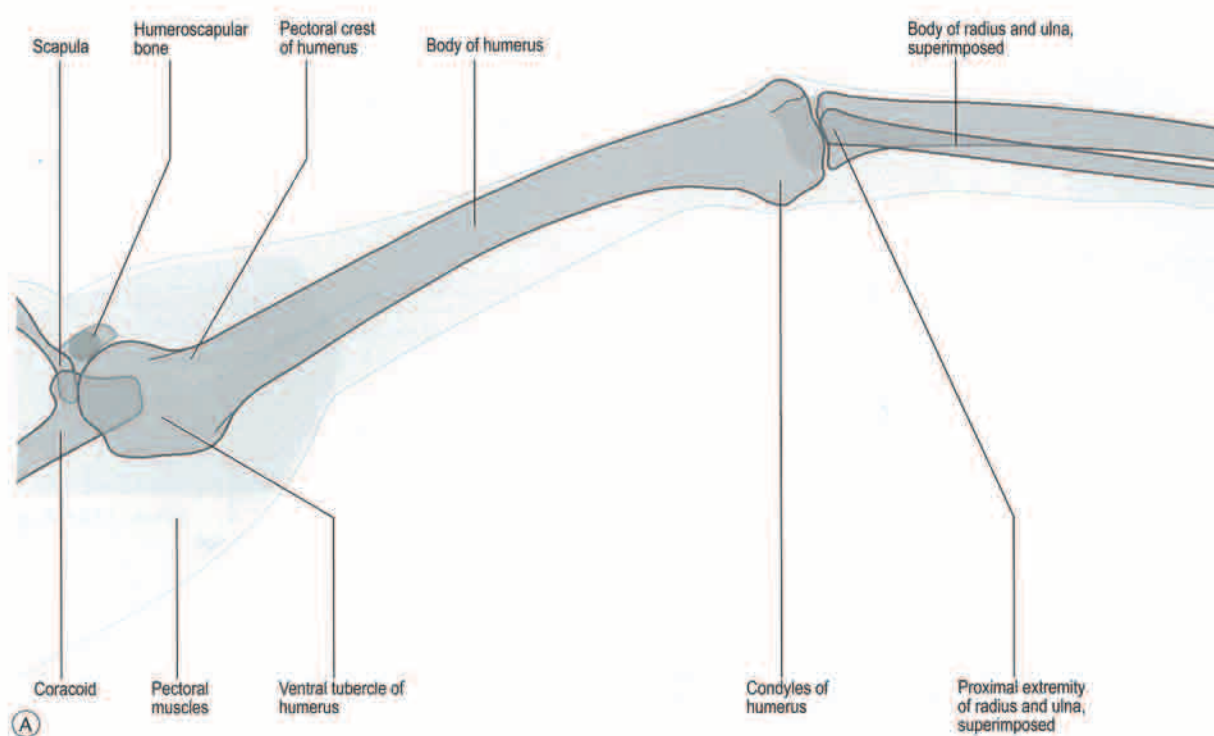
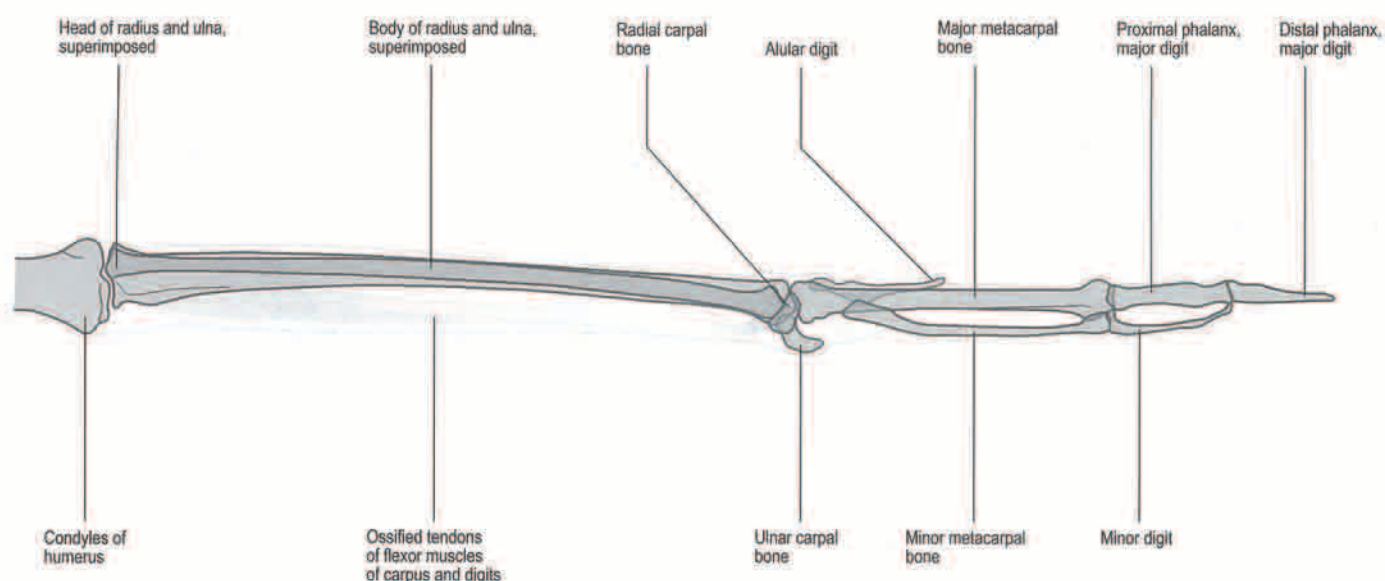


Fig. 3.120 (A and B) Craniocaudal view of the proximal wing of the Eurasian eagle owl. Note the presence of the humeroscapular bone, which is characteristic of most species of owls except for the barn owl.

SECTION 9 RADIOGRAPHIC SPECIES CATALOG



(A)

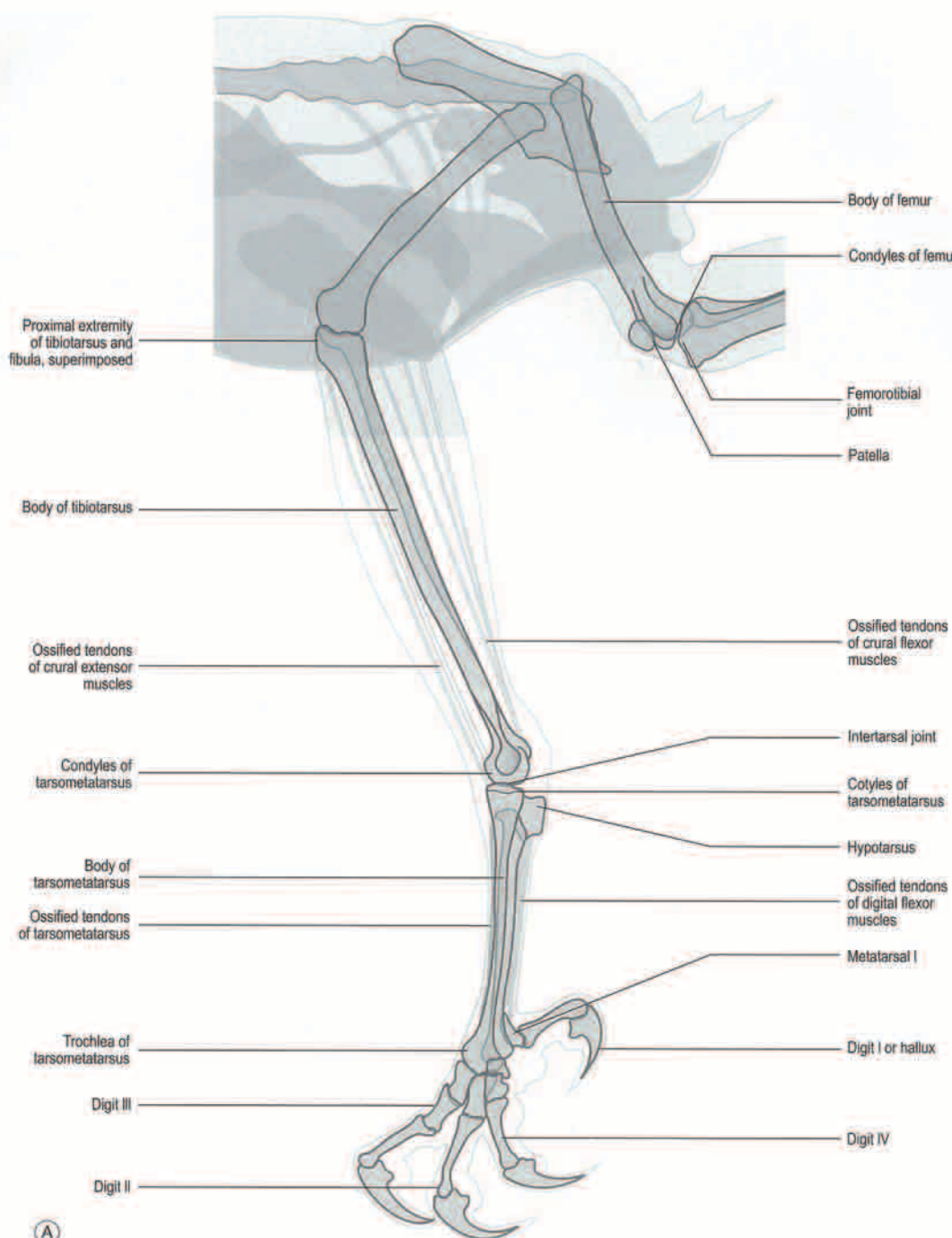
Fig. 3.121 (A and B) Craniocaudal view of the distal wing of the Eurasian eagle owl. Note the intratendinous ossification of the tendons of flexor muscles of carpus and digits.

SECTION 9 RADIOGRAPHIC SPECIES CATALOG



Fig. 3.121 (Cont'd).

SECTION 9 RADIOGRAPHIC SPECIES CATALOG



(A)

Fig. 3.122 (A and B) Mediolateral view of the pelvic limb of the Eurasian eagle owl. Note the intratendinous ossification of the tendons of the crural muscles and of the muscles of the tarsometatarsus.

SECTION 9 RADIOGRAPHIC SPECIES CATALOG



Fig. 3.122 (Cont'd).

SECTION 9 RADIOGRAPHIC SPECIES CATALOG

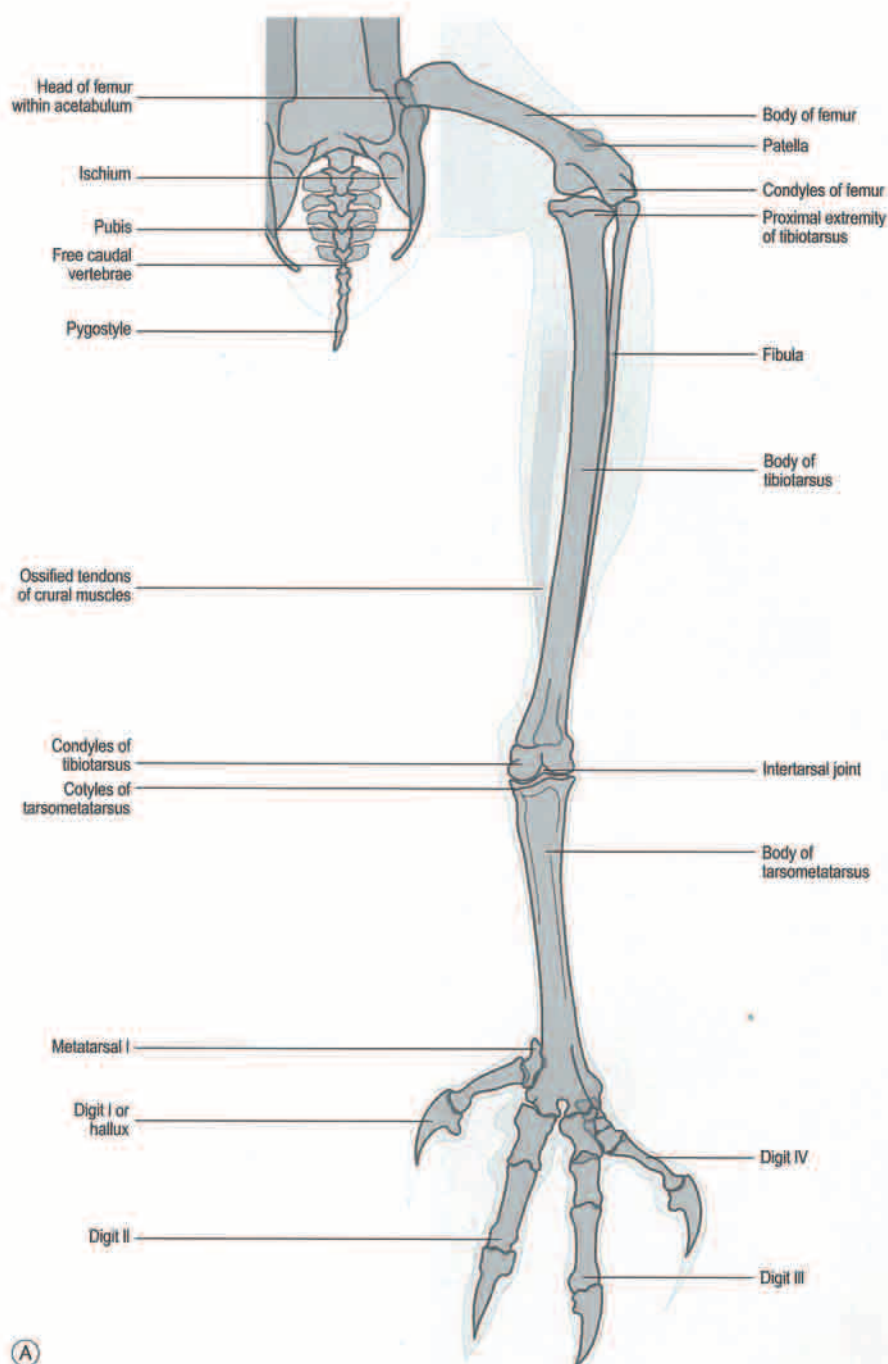


Fig. 3.123 (A and B) Craniocaudal view of the pelvic limb of the Eurasian eagle owl. Note the intratendinous ossification of the tendons of the crural muscles.

SECTION 9 RADIOGRAPHIC SPECIES CATALOG



Fig. 3.123 (Cont'd).

SECTION 9 RADIOGRAPHIC SPECIES CATALOG

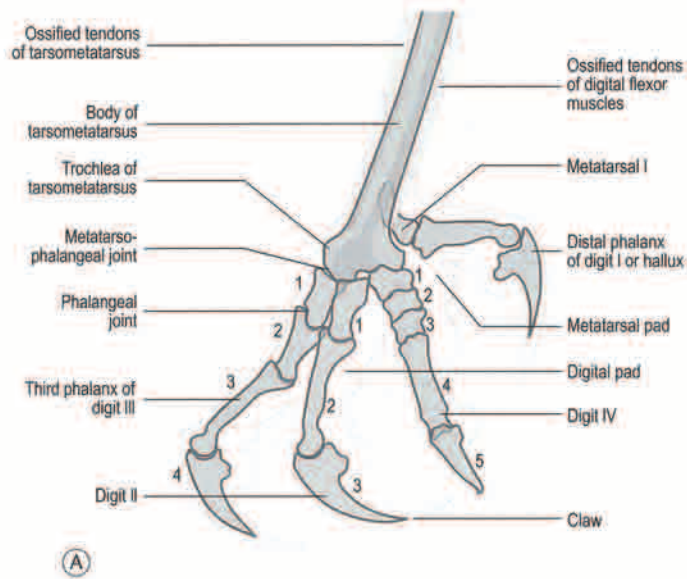


Fig. 3.124 (A and B) Medirolateral close-up of the foot of the Eurasian eagle owl. Note the intratendinous ossification of the tendons of the muscles of the tarsometatarsus.

SECTION 9 RADIOGRAPHIC SPECIES CATALOG

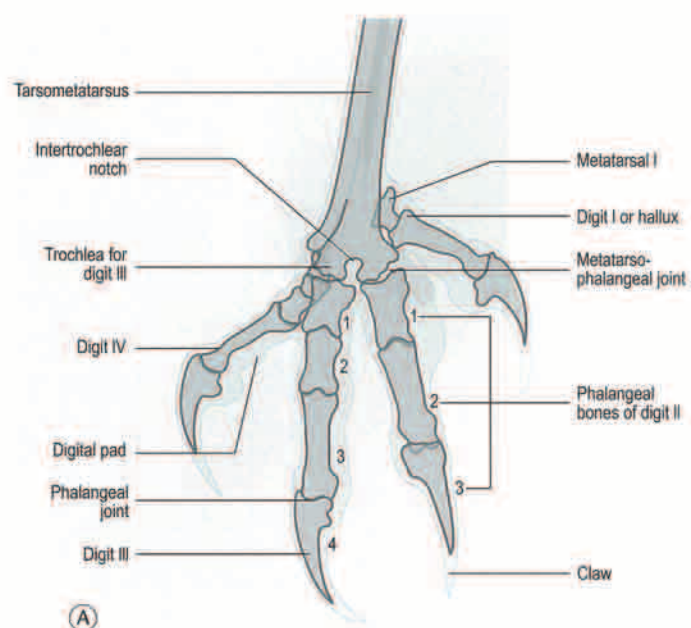


Fig. 3.125 (A and B) Craniocaudal close-up of the foot of the Eurasian eagle owl, with digit I flexed.

SECTION 9 RADIOGRAPHIC SPECIES CATALOG

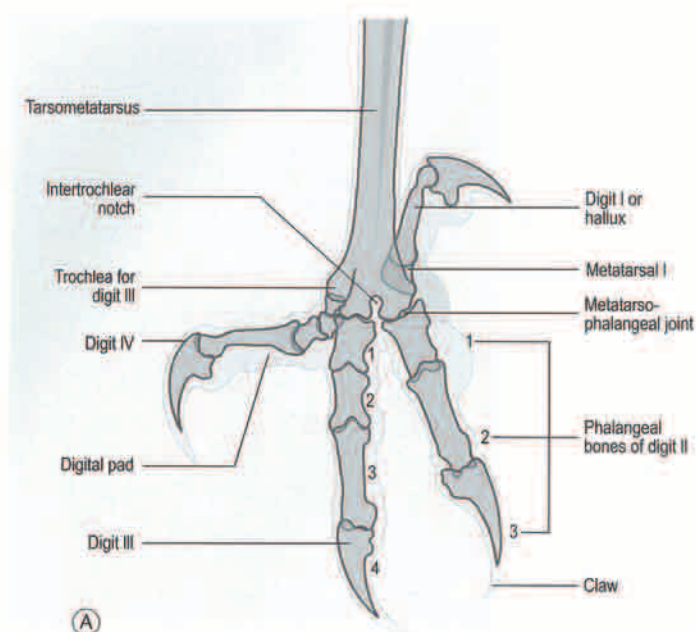


Fig. 3.126 (A and B) Craniocaudal close-up of the foot of the Eurasian eagle owl, with digit I extended.

References

- Fox N 1995 Understanding the Birds of Prey. Hancock House, Surrey, pp. 16–57
- Harcourt-Brown NH 2000 Birds of Prey: Anatomy, Radiology and Clinical Conditions of the Pelvic Limb. CD-ROM, Zoological Education Network, Lake Worth, Florida
- Harcourt-Brown NH 2001 Radiographic morphology of the pelvic limb of Falconiformes and its taxonomic implications. *Netherlands Journal of Zoology* 51(2):155–178
- King AS, McLelland J 1984 Birds: Their Structure and Function, 2nd edn. Balliere Tindall, London
- Richardson F 1972 Accessory pygostyle bone of Falconidae. *Condor* 74:350–351
- Smith SA, Smith BJ 1992 Atlas of Avian Radiographic Anatomy. WB Saunders, Philadelphia, pp. 101–160
- Zucca P, Cooper JE 2000 Osteological aspects of the falcon wing. In: Lumeij JT, Redig PT, Remple JD et al (eds) Raptor Biomedicine III. Zoological Education Network, Lake Worth, Florida, pp. 195–199

Further reading

- del Hoyo J, Elliot A, Sargatal J 1994 Handbook of the Birds of the World, vol 2. New World Vultures to Guinea-fowl. Lynx Edicions, Barcelona
- del Hoyo J, Elliot A, Sargatal J 1994 Handbook of the Birds of the World, vol 5. Barn owls to Hummingbirds. Lynx Edicions, Barcelona
- Orosz SE, Ensley PK, Haynes CJ 1992 Avian Surgical Anatomy: Thoracic and Pelvic Limbs. WB Saunders, Philadelphia
- Rubel GA, Isenbugel E, Wolvekamp P 1991 Atlas of Diagnostic Radiology of Exotic Pets. WB Saunders, Philadelphia
- Zucca P 1995 Prevalence and clinical aspects of wing pathology of European falcons. Parma University, Parma
- Zucca P 2002 Anatomy. In: Cooper JE (ed.) Birds of Prey: Health and Disease, 3rd edn. Blackwell Science, Oxford, pp. 13–27

Chapter 4

Clinical and pathological conditions

SECTION 1 Trauma-related medical conditions



Fig. 4.1 Severe soft-tissue swelling on the left foot of a saker falcon (*Falco cherrug*). Physical examination revealed an infected, penetrating wound on the plantar surface of the foot. The purulent material had caused swelling of the plantar aspect and interdigital spaces.



Fig. 4.2 Craniocaudal radiograph of the feet of a saker falcon (*Falco cherrug*) that was presented because of swollen feet and non-load bearing of the left leg. There is soft-tissue swelling of both feet and osteomyelitis of the bones of the metatarsophalangeal joint of the left foot. Note the increased joint space and erosion of articular surface of the trochlea for digits II, III and IV (arrowheads).



Fig. 4.3 Plantar surface of the feet of a saker falcon (*Falco cherrug*) with severe bilateral bumblefoot. There are large scabs on the central plantar surface, soft-tissue swelling, associated fibrosis and an underlying infection. The infection may have originated from penetrating wounds caused by the overgrown talons.



Fig. 4.4 Craniocaudal radiograph of the feet of the same bird as in Figure 4.3 showing soft-tissue swelling and marked osteolytic changes of the trochlea of the tarsometatarsus and proximal phalanges of both feet (arrowheads).

SECTION 1 TRAUMA-RELATED MEDICAL CONDITIONS



Fig. 4.5 Bilateral bumblefoot in a saker falcon (*Falco cherrug*). There is soft-tissue swelling and small penetrating wound in the caudal plantar surface of the right foot. Note the thin epithelium surrounding the scab and the loose appearance of the metatarsal pad. The plantar surface of the left foot has a large area of dry skin extending from the metatarsal pad to the digital pad of the proximal phalanges of digit IV.



Fig. 4.6 Craniocaudal radiograph of the feet of the same bird as in Figure 4.5 showing soft-tissue swelling of both feet and severe osteomyelitis of the distal tarsometatarsus and proximal phalanges of the right foot. Note the complete dissolution of the trochlea and articular surface of the proximal phalanges of digits II and III (arrowheads).



Fig. 4.7 Plantar surface of the feet of a saker falcon (*Falco cherrug*) with severe bilateral bumblefoot. There are large, thick scabs on the metatarsal pad, soft-tissue swelling, fibrosis and an underlying infection. The scabs are contaminated with dried feces and sand. Note the purulent discharge from the right foot (arrowhead). The digit II of the left foot was amputated 6 months previously. Digital function was tested before anesthesia and reflexes were absent from all digits.



Fig. 4.8 (Right) Ventrodorsal radiograph of the same bird as in Figure 4.7. There is marked soft-tissue swelling, lytic and sclerotic changes of the distal tarsometatarsus and proximal phalanges of both feet. There is hepatomegaly and possibly amyloidosis. Secondary infection that results in hepatitis and amyloidosis is a common finding in chronic bumblefoot infection. This bird was euthanized.

SECTION 1 TRAUMA-RELATED MEDICAL CONDITIONS



Fig. 4.9 Bilateral bumblefoot in a steppe eagle (*Aquila nipalensis*). The plantar surface of the feet are covered with dried feces, sand and thick scabs. There is soft-tissue swelling and an underlying infection. This bird was found in the wild with a broken wing as a result of gunshot injury several years before. It had been kept in captivity since then.

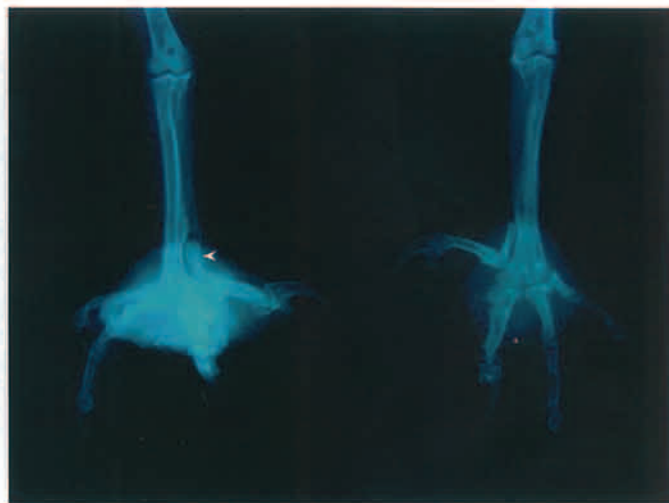


Fig. 4.10 Craniocaudal radiograph of the feet of the same bird as in Figure 4.9. There is severe soft-tissue swelling of both feet. There are periosteal changes on the distal tarsometatarsus and first metatarsal bone of the right foot (arrowhead). The condition of the bones of the metatarsophalangeal joint of the right foot is difficult to assess in this radiograph because of the radiopacity of the sand. No apparent bony changes on the left foot are evident.



Fig. 4.11 Dorsal view of the foot of a gyr falcon (*Falco rusticolus*) with subcutaneous abscess on the interdigital area between digits III and IV. The encapsulated abscess was surgically removed and no adhesion to other tissues was observed.



Fig. 4.12 Craniocaudal radiograph of the foot of the same bird as in Figure 4.11. There is soft-tissue swelling between digits III and IV without an apparent bone involvement.

SECTION 1 TRAUMA-RELATED MEDICAL CONDITIONS



Fig. 4.13 Lateral view of the foot of a Eurasian eagle owl (*Bubo bubo*) with severe lytic and sclerotic changes of all bones of the metatarsophalangeal joint and distal half of the tarsometatarsus. There is an area of osteolysis in the proximal tarsometatarsus. This is a chronic bumblefoot infection secondary to an injury (courtesy of J G de la Fuente and A L Sánchez).

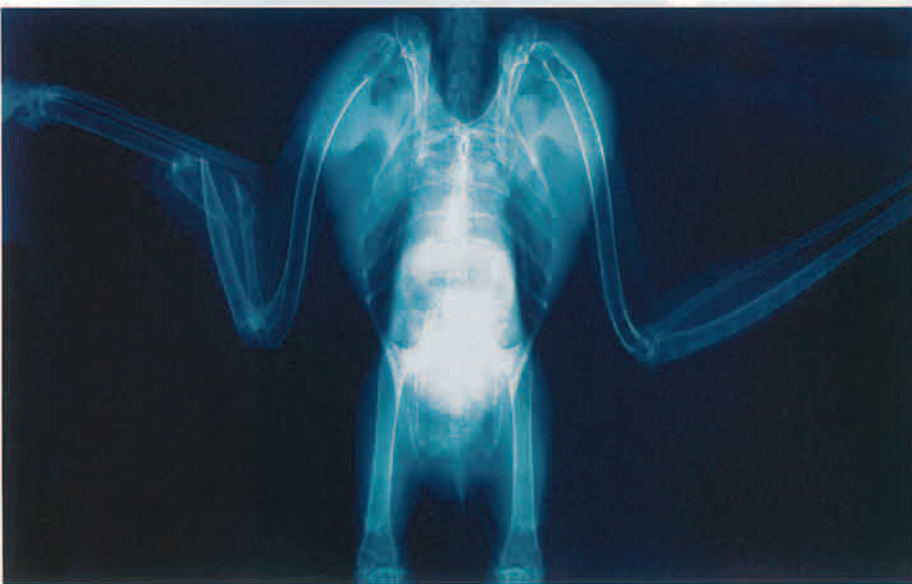


Fig. 4.14 Ventrodorsal radiograph of an adult tawny owl (*Strix aluco*) showing a high-energy comminuted fracture of the right radius and ulna. Note the less pronounced hourglass shaped cardiohepatic waist, which is characteristic of some species of owls (courtesy of J M Hatt).



Fig. 4.15 Ventrodorsal radiograph of a common kestrel (*Falco tinnunculus*) showing a high-energy comminuted fracture of the right radius and ulna, and both distal tibiotarsi. Note the soft-tissue swelling around the fracture sites on the wing.



Fig. 4.16 Ventrodorsal radiograph of an adult tawny owl (*Strix aluco*) showing high-energy fractures of both femurs and both tibiotarsi (arrowheads) (courtesy of M García-Montijano and T Álvarez).

SECTION 1 TRAUMA-RELATED MEDICAL CONDITIONS



Fig. 4.17 Ventrodorsal radiograph of a peregrine falcon (*Falco peregrinus*) showing a fracture of the right distal humerus. Incomplete ossification of the skeleton is characterized by large joint spaces in the elbow, carpal, knee and hock joints (arrowheads) and secondary ossification centers in the hock joint. The core of the immature or blood feathers appear radiodense. The gastrointestinal tract of neonates stays distended with food, making the identification of abdominal structures difficult. This bird had a sour crop as evidenced by the retained food in the crop. It did not respond to medication and it was euthanized. Mycoplasmosis was suspected based on histopathology findings (courtesy of M García-Montijano and T Álvarez).



Fig. 4.18 Saker falcon (*Falco cherrug*) with a transverse midshaft fracture of the scapula (arrowhead). This bird was presented for examination because of slightly drooped left wing. This type of fracture usually requires coaptation of the affected wing with figure-of-eight bandage for 3 weeks. Physical therapy is performed on the distal wing every 5–7 days to avoid contraction of the patagium.

SECTION 1 TRAUMA-RELATED MEDICAL CONDITIONS



Fig. 4.19 Ventrodorsal radiograph of a male gyr-peregrine hybrid falcon (*Falco rusticolus-Falco peregrinus*) showing a midshaft fracture of the right coracoid. Arrowheads indicate the fracture ends. Also, there is a healed fracture of the right rib cage and right pelvic bones.



Fig. 4.20 Ventrodorsal radiograph of a Eurasian buzzard (*Buteo buteo*) showing a comminuted fracture and dislocation of the left coracoid. Arrowheads indicate the bone fragments (courtesy of J M Hatt).

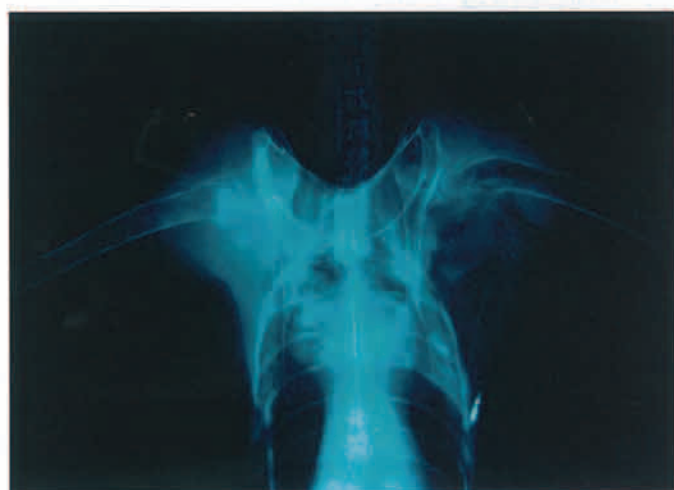


Fig. 4.21 Ventrodorsal radiograph of a gyr falcon (*Falco rusticolus*) that was presented because of drooped right wing. There is luxation of the head of the humerus from the shoulder joint and increased opacity of the soft tissues of the shoulder and pectoral muscles.

SECTION 1 TRAUMA-RELATED MEDICAL CONDITIONS



Fig. 4.22 Hepatomegaly and degenerative arthritis of the shoulder joints in a peregrine falcon (*Falco peregrinus*). There are soft-tissue swelling and lytic changes of the articular surface of the left humerus. The right humerus is also involved to a lesser degree. Note the enlarged liver shadow.



Fig. 4.23 Osteoarthritis in a lanner falcon (*Falco biarmicus*). This bird was found with the leash entangled around its left shoulder. Note the increased radiopacity of the left shoulder joint.

SECTION 1 TRAUMA-RELATED MEDICAL CONDITIONS

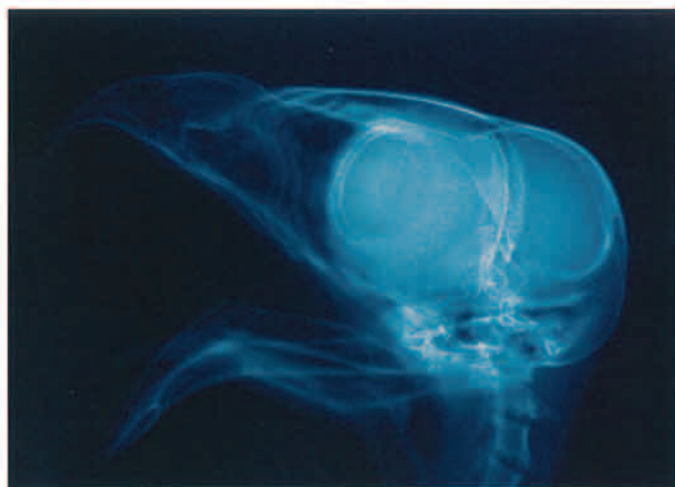


Fig. 4.24 Lateral radiograph of the head of a Eurasian buzzard (*Buteo buteo*) showing a bilateral fracture of the mandible (courtesy of J M Hatt).

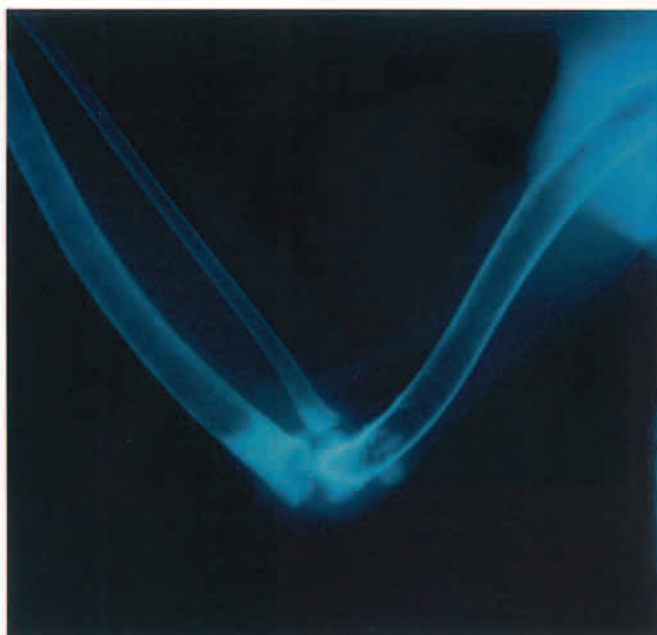


Fig. 4.25 Degenerative arthritis of the elbow joint of a saker falcon (*Falco cherrug*). There is soft-tissue swelling and degeneration of the articular surfaces of the humerus and ulna.

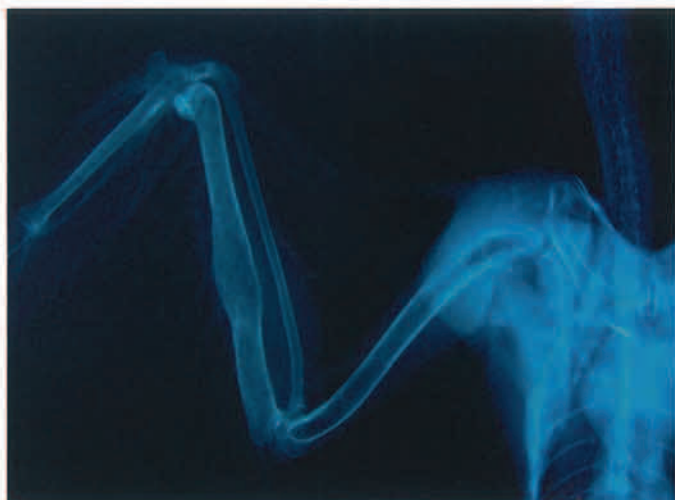


Fig. 4.26 Ventrodorsal radiograph of the wing of a saker falcon (*Falco cherrug*) showing a healed fracture of the ulna. Note the smooth periosteal new bone at the healed fracture site.



Fig. 4.27 Arthritis of distal wing in a Eurasian buzzard (*Buteo buteo*). There is intraarticular bone lysis, fracture of the distal extremity of the major metacarpal bone (black arrowhead), increased joint space and dorsal displacement of the sesamoid bone (white arrowhead) (courtesy of D Gelli).

SECTION 1 TRAUMA-RELATED MEDICAL CONDITIONS

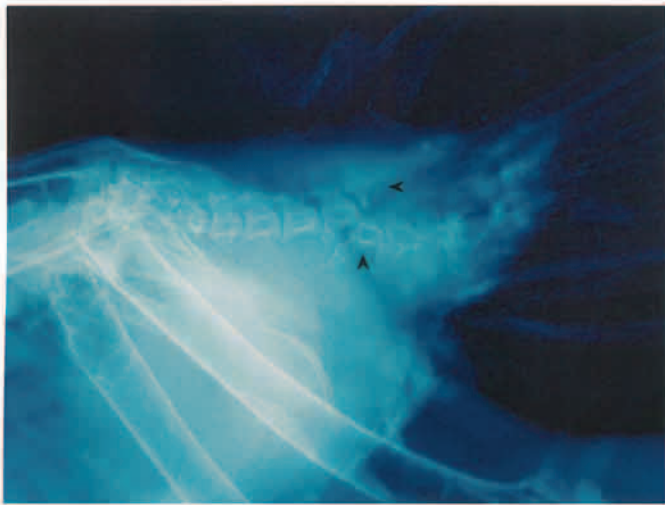


Fig. 4.28 Lateral radiograph of the free caudal vertebrae of a Eurasian buzzard (*Buteo buteo*) showing dislocation between the 5th and 6th caudal vertebrae and fracture of the 6th caudal vertebra (arrowheads). The radiopaque materials on the base of the tail are fecal urates that soiled the tail feathers (courtesy of J M Hatt).



Fig. 4.29 Craniocaudal radiograph of the left pelvic limb of a saker falcon (*Falco cherrug*) presented because of non-load bearing of the left leg. There is a transverse fracture of the femoral head (arrowhead).

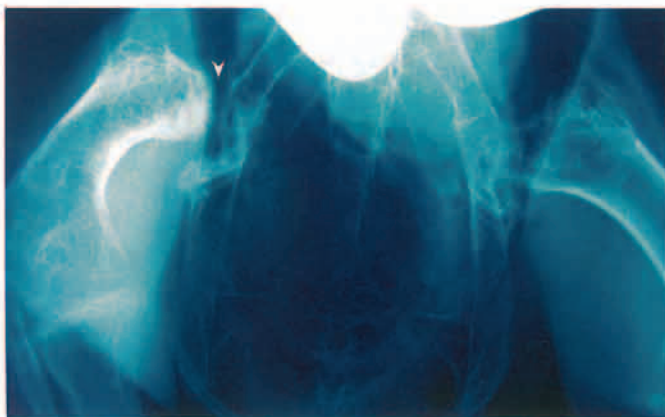


Fig. 4.30 Ventrodorsal radiograph of the pelvic girdle of a Eurasian griffon vulture (*Gyps fulvus*) showing an increased joint space between the femur and the acetabulum (arrowhead) and an increased cortical radiodensity of the proximal femur. This is due to a healed fracture of the femoral neck. Surgery was performed by removing the femoral head (courtesy of M García-Montijano).

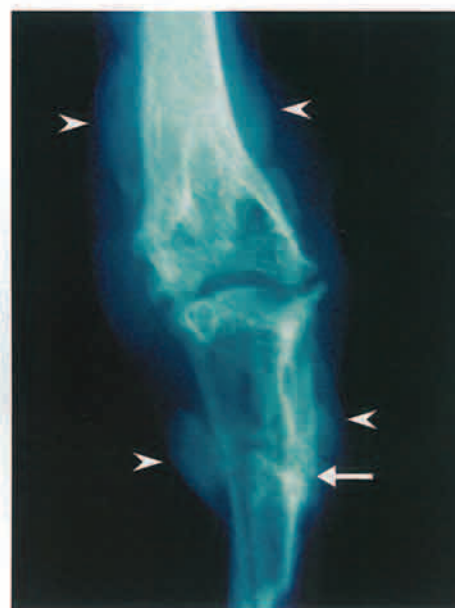


Fig. 4.31 Periostitis of the distal tibiotarsus and proximal tarsometatarsus in a gyr-peregrine hybrid falcon (*Falco rusticolus*-*Falco peregrinus*). Note the soft-tissue swelling and irregular periosteal bone (arrowheads). The fracture line in the proximal tarsometatarsus, poorly mineralized, is still evident (arrow) (courtesy of D Gelli).

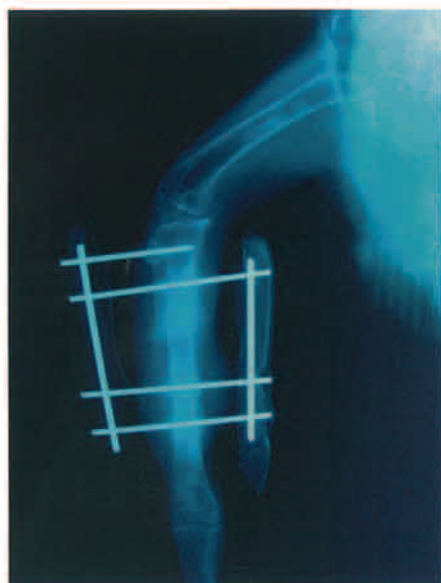


Fig. 4.32 Midshaft fracture of the tibiotarsus in a saker falcon (*Falco cherrug*) repaired using a shuttle pin and a type II external skeletal fixator (ESF). Two acrylic bars and additional metal pins within the tubing were used to maintain the fixator in position and provide extra strength. There is periosteal reaction around the fracture site, on the pin sites and on the proximal end of the fibula.



Fig. 4.33 Midshaft fracture of the tibiotarsus in a saker-peregrine hybrid falcon (*Falco cherrug-Falco peregrinus*). The fracture was repaired using an intramedullary pin external skeletal fixator (IM-ESF) tie-in technique. An IM pin was inserted in a normograde fashion from the tibial crest, positive-profile threaded pin placed distally and tie-in using a bar and clamps. There is a slight overriding of the proximal fracture end (arrow), smooth periosteal callus formation and soft-tissue swelling (arrowhead).



Fig. 4.34 Luxation and displacement of the distal phalanx of digit I (hallux) in a saker falcon (*Falco cherrug*) (arrowhead). There was no apparent damage to tendons and ligaments. The hallux was stabilized with a plaster cast and healing was completed in 3 weeks.



Fig. 4.35 Septic arthritis of the phalangeal joint of digit I (hallux) in a white-tailed eagle (*Haliaeetus albicilla*). Note the increased joint space, soft-tissue swelling and periosteal reaction on the proximal phalanx (arrowhead).

SECTION 1 TRAUMA-RELATED MEDICAL CONDITIONS



Fig. 4.36 Osteomyelitis of digit III in a peregrine falcon (*Falco peregrinus*). There is soft tissue-swelling of the entire digit (arrowheads), increased joint space and lysis of the articular surface of phalanges 1 and 2 (arrow). Caseous pus was present in the abscess. The digit was amputated along the 1st phalanx.



Fig. 4.37 Cranio-caudal radiograph of the distal limb of a saker falcon (*Falco cherrug*) showing a healed fracture of the distal third of the tarsometatarsus. Smooth periosteal new bone is present around the fracture site. The soft-tissue swelling is caused by an accompanying bumblefoot infection.



Fig. 4.38 Septic arthritis of the intertarsal joint in a saker-gyr hybrid falcon (*Falco cherrug*-*Falco rusticolus*). There is soft-tissue swelling and osteolysis of the articular surface of the distal tibiotarsus and proximal tarsometatarsus (arrowhead).



Fig. 4.39 Mediolateral radiograph of the right distal limb of a saker falcon (*Falco cherrug*) showing soft-tissue swelling around the intertarsal joint and distal tarsometatarsus (arrowheads). There is no accompanying injury on the leg. This bird was found with the leash entangled around its leg.



Fig. 4.40 (A) Ventrodorsal survey radiograph of a saker falcon (*Falco cherrug*) that was presented because of lameness of both legs. There is an increased radiopacity in the thoracosynsacral junction (arrowhead). Such abnormality is commonly related to trauma. (B) Lateral survey radiograph. There is abscess formation subsequent to trauma in the thoracosynsacral junction (arrowhead) leading to spinal luxation.



Fig. 4.41 (A) Ventrodorsal survey radiograph of a golden eagle (*Aquila chrysaetos*) showing lead fragments of different sizes embedded in the body. This bird was presented because of bilateral leg paralysis. (B) Lateral survey radiograph showing lead fragments of different sizes on the caudal thoracic vertebrae and synsacrum region. Lead pellets tend to break into smaller pieces when they strike a bone. The bird's recent meal can be observed in the ventriculus, proventriculus, thoracic esophagus and crop.

SECTION 1 TRAUMA-RELATED MEDICAL CONDITIONS

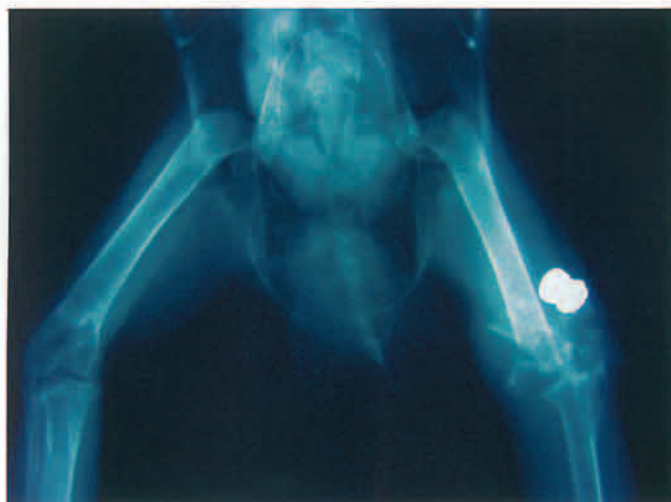


Fig. 4.42 Projectile injury in a northern long-eared owl (*Asio otus*). This is a craniocaudal radiograph of the pelvic limb showing a comminuted fracture of the distal extremity of the left femur. The femoral condyles are broken into several fragments. The large lead pellet is from an airgun rifle (courtesy of D Gelli).

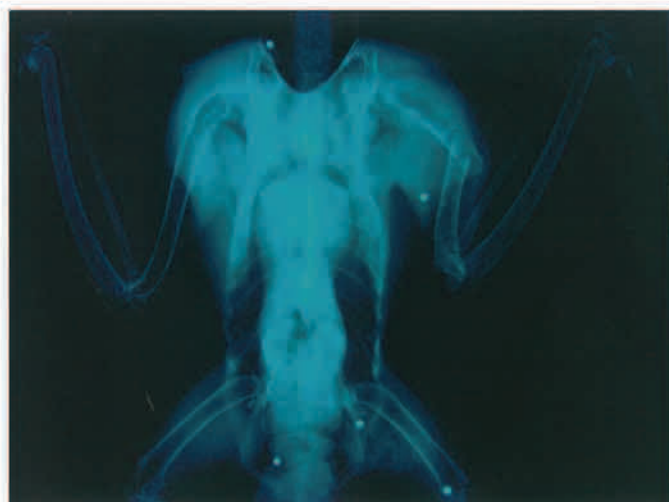


Fig. 4.43 Projectile injury in a peregrine falcon (*Falco peregrinus*). This ventrodorsal radiograph shows five shotgun pellets embedded in the body. The midshaft fracture of the left humerus was repaired using an IM-ESF tie-in technique and healing was uneventful.



Fig. 4.44 (Left) Ventrodorsal survey radiograph of a saker falcon (*Falco cherrug*) showing eight shotgun pellets embedded in the body. The bird was recently trapped by using a shotgun fired beside the bird to scare it and force it to land.

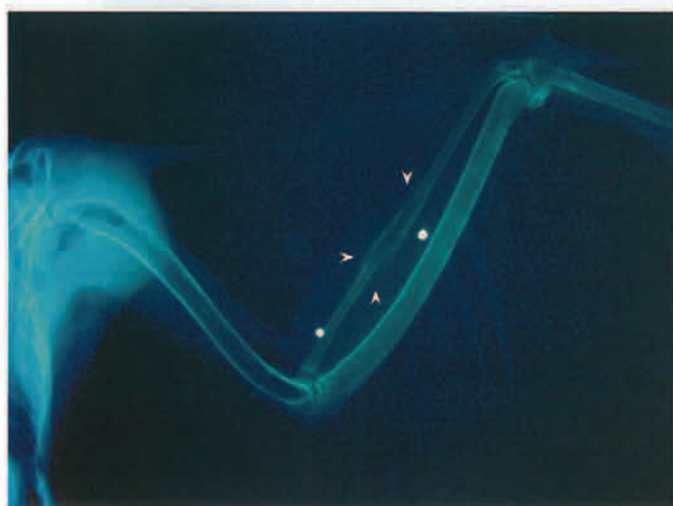


Fig. 4.45 This is a ventrodorsal radiograph of the wing of a saker falcon (*Falco cherrug*) showing two shotgun pellets and healed fractures of the radius. Note the smooth periosteal callus formation on the proximal and distal fracture sites (arrowheads). This bird was presented for an unrelated problem.

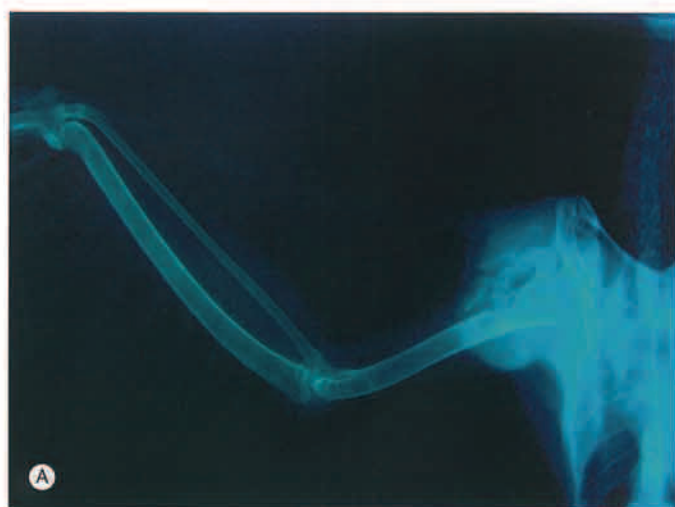


Fig. 4.46 (A) High-energy comminuted fracture of the proximal humerus in a saker-peregrine hybrid falcon (*Falco cherrug-Falco peregrinus*). (B) The fracture was repaired using an IM-ESF tie-in technique. An IM pin was inserted in retrograde fashion, two positive-profile threaded pins placed caudal to the fracture and a third pin placed in the head of the humerus. These were tied-in using a connector bar and clamps. The wing was taped against the body for several weeks. Postoperative management included physical therapy of the affected wing under anesthesia every 5 days to avoid ankylosis of the joints and contraction of the patagium. This radiograph was taken at 21 days postoperatively. (C) The ESF was removed 6 weeks after the surgery. This radiograph was taken 1 week later when the IM pin was removed. There is increased density of the medullary cavity as a result of an existing infection. Bone remodelling is not yet complete radiographically, although there is palpable, hard callus on the area. Although great efforts were made to avoid ankylosis of the joints, return to full function of the wing was not achieved.

SECTION 1 TRAUMA-RELATED MEDICAL CONDITIONS

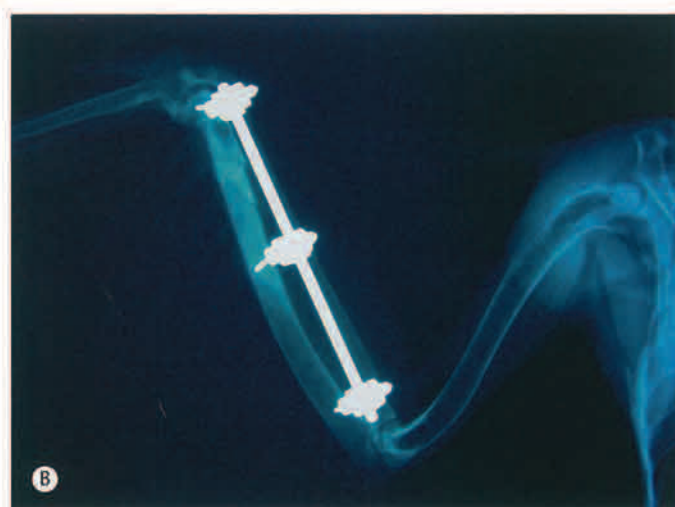


Fig. 4.47 (A) This saker falcon (*Falco cherrug*) was admitted with a closed, oblique fracture of the distal ulna (black arrowhead). In addition, there were two hairline fractures (white arrowheads) present proximally to the above fracture. (B) A type I ESF was applied to the ulna utilizing three positive-profile threaded pins placed in the proximal and distal fragments and in the proximal extremity of the ulna. The pins were tied-in using a bar and clamps. This radiograph was taken 6 days postoperatively.

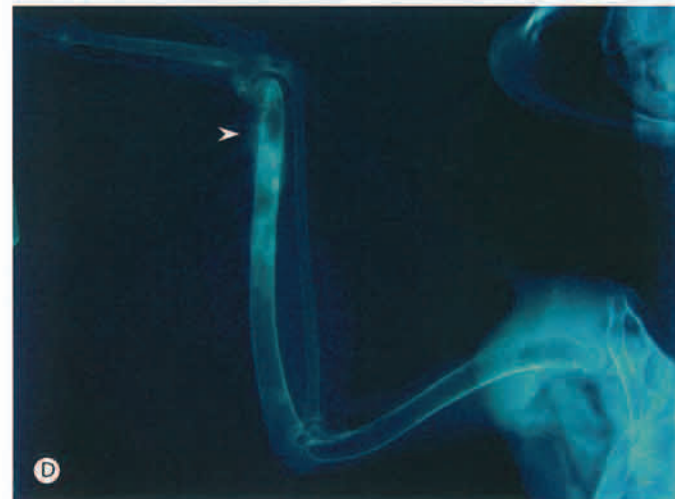


Fig. 4.47 (Cont'd) (C) The wing was coapted with a masking tape. Masking tape is lightweight compared with the conventional materials used for figure-of-eight bandaging. The bird did not show any discomfort with this technique. The tape was removed 5 days postoperatively to enable the bird to exercise its wing. (D) At 20 days postoperatively healing was complete and the fixator removed. Note the smooth periosteal callus formation around the distal fracture site (arrowhead).

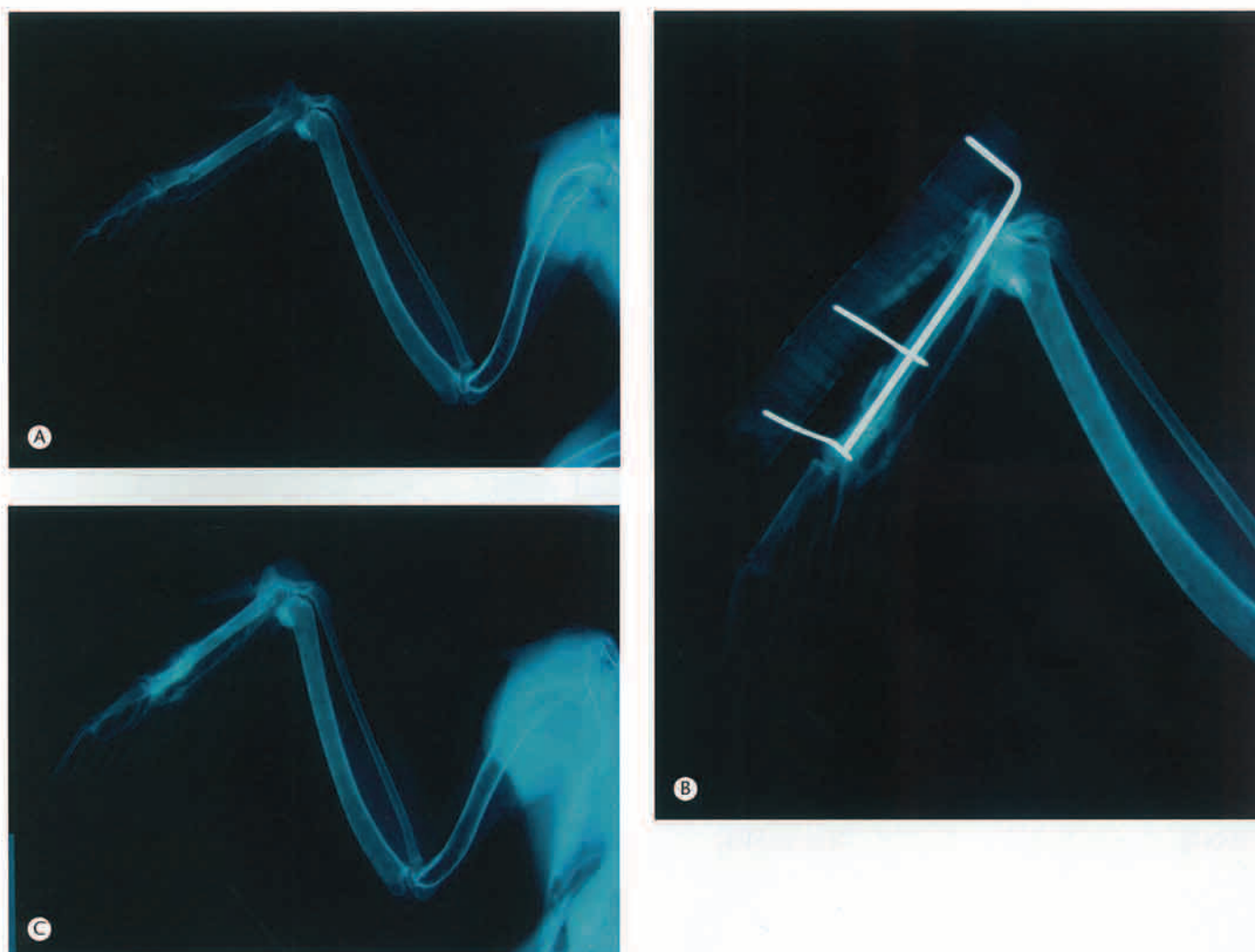


Fig. 4.48 (A) A ventrodorsal radiograph of the wing in a saker-peregrine hybrid falcon (*Falco cherrug-Falco peregrinus*) showing a low-energy fracture of the major and minor metacarpal bones incurred when the bird struck its wing against the side of an enclosure. (B) The fracture of the major metacarpal bone was repaired using an IM pin inserted in normograde fashion, two positive-profile threaded pins placed in the proximal and distal fragments and tie-in using an acrylic connector bar. The wing was coapted with a masking tape for several days. This radiograph was taken at 13 days postoperatively. Good callus formation was already evident so it was decided to remove the ESF. (C) Healing progressed normally and the IM pin was removed 20 days postoperatively.

SECTION 1 TRAUMA-RELATED MEDICAL CONDITIONS

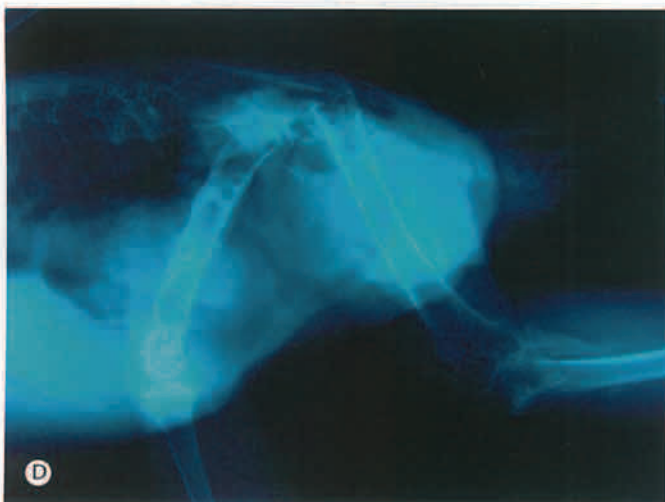
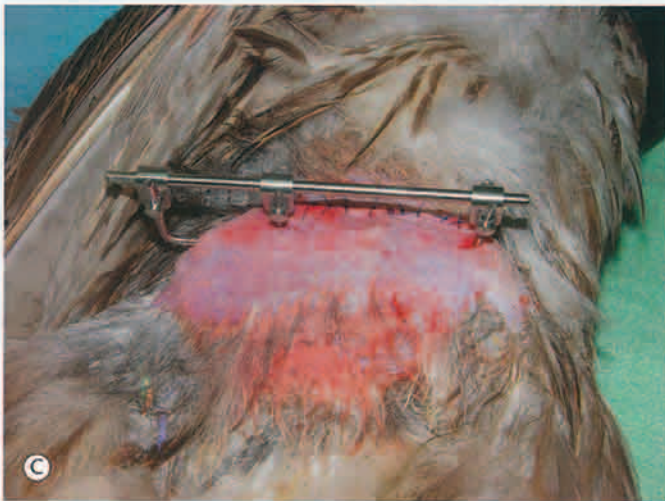
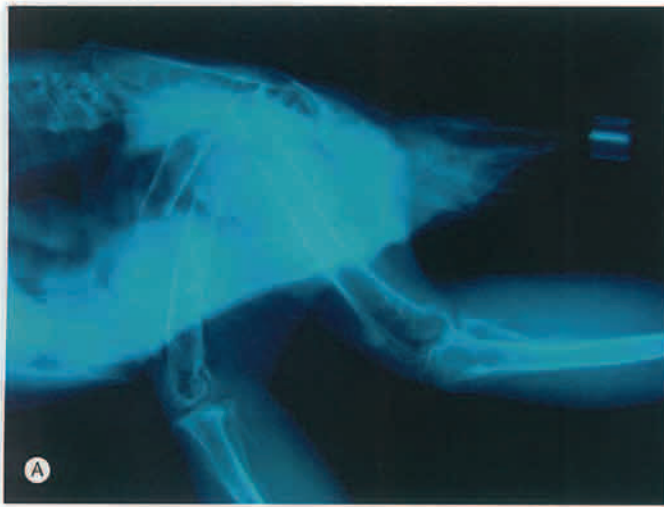


Fig. 4.49 (A) This gyr-peregrine hybrid falcon (*Falco rusticolus*-*Falco peregrinus*) was admitted with a closed, oblique, mid diaphyseal fracture of the femur accompanied by displacement of the fragments. (B) The femoral fracture was repaired using an IM-ESF technique. An IM pin was inserted in retrograde fashion, one positive-profile threaded pin placed caudal to the fracture and a second pin placed just before the condyles. These were tied-in using a bar and clamps. This radiograph was taken at 43 days postoperatively. Good callus formation was evident so it was decided to remove the ESF leaving the IM pin for another week. (C) Photograph of pin in place. (D) This radiograph was taken at 50 days postoperatively when healing was complete and after the IM pin removal. The ESF was removed a week earlier.

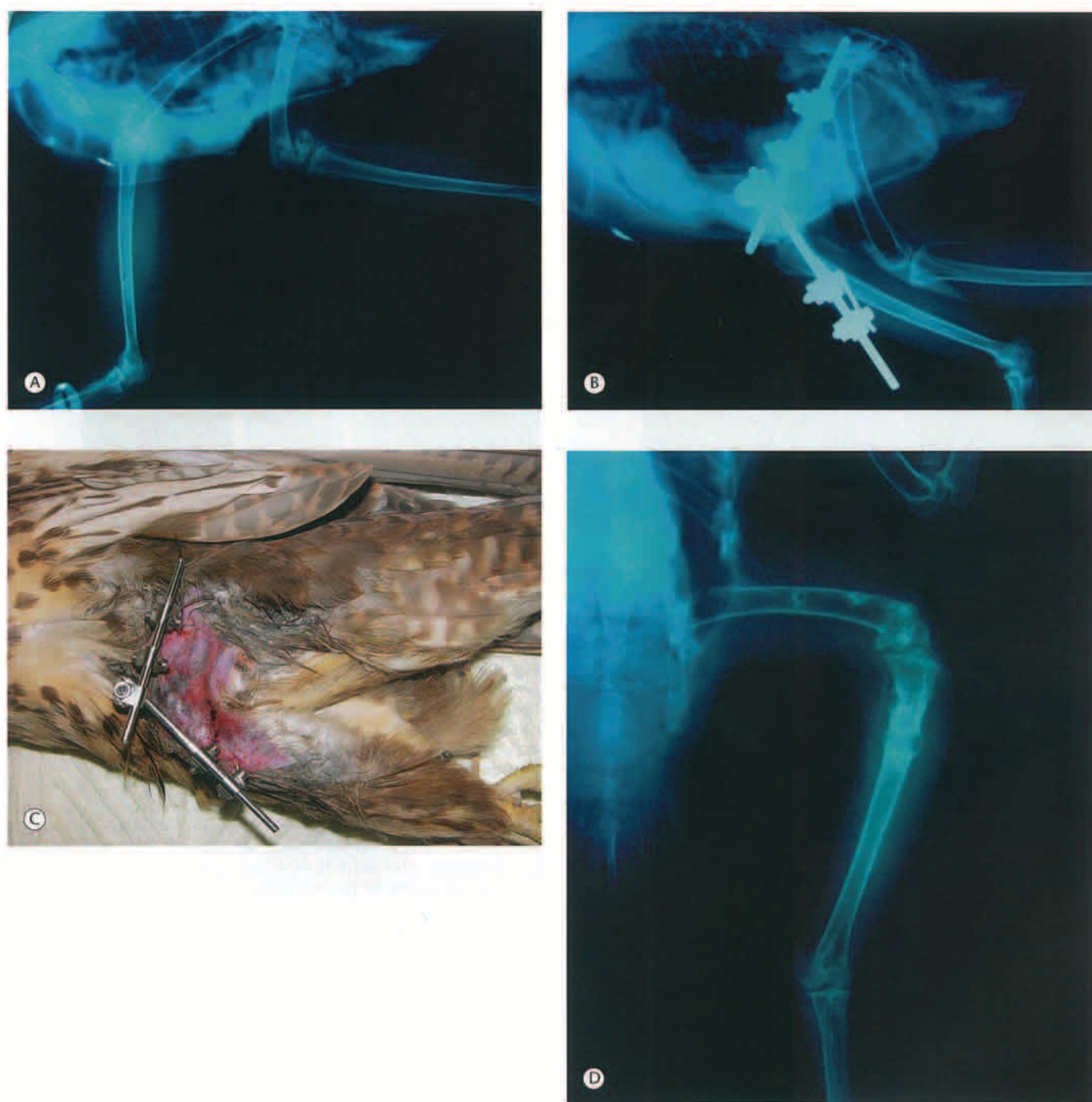


Fig. 4.50 (A) This saker falcon (*Falco cherrug*) was presented because of absence of load bearing on the left leg. This mediolateral radiograph of the left pelvic limb shows a transverse fracture of the distal femur. (B) Transarticular fixation technique for distal femoral fracture as in (A). The distal fragment was too short to stabilize with an IM-ESF. A type I transarticular fixator was applied consisting of positive-profile threaded pins, with two pins proximal to the fracture and two in the tibiotarsus. The pins were tied-in using bars and clamps with the stifle joint flexed as in a normal perching position. This radiograph was taken at 22 days postoperatively. (C) Photograph of the pin in place. (D) At 43 days postoperatively healing was complete and the fixator removed. The drawback of transarticular fixation technique is the risk of ankylosis of the joint. In this particular case, although the fracture healed uneventfully, full return to function of the leg was not attained.

SECTION 1 TRAUMA-RELATED MEDICAL CONDITIONS

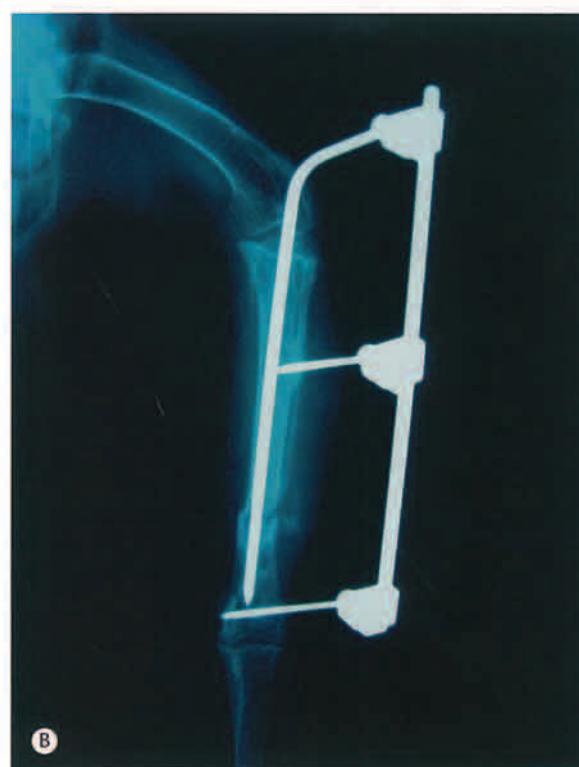


Fig. 4.51 (A) This saker-peregrine hybrid falcon (*Falco cherrug-Falco peregrinus*) was admitted with an overriding fracture of the distal tibiotarsus. This is the most common type of fracture encountered in clinical practice with captive raptors. Fractures on this bone tend to occur in newly tethered birds and during training exercises. (B) The fracture was repaired using an IM-ESF tie-in technique. An IM pin was inserted in a normograde fashion from the tibial crest, two positive-profile threaded pins placed in the proximal and distal fragments and tie-in using a bar and clamps. This radiograph was taken at 14 days postoperatively. (C) Complete union was evident at 6 weeks postoperatively after which the ESF was removed. This radiograph was taken when the IM pin was removed 1 week later.

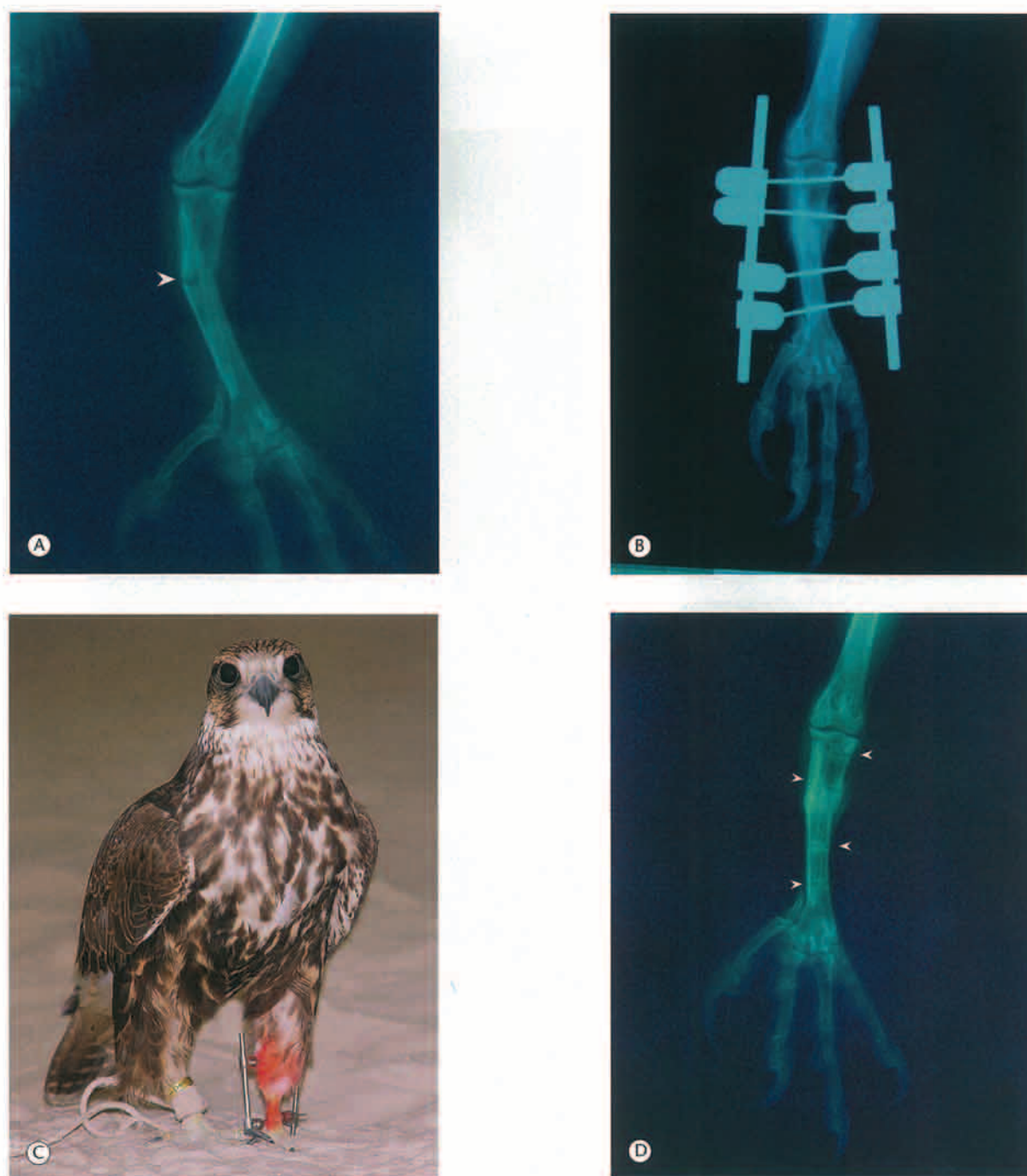


Fig. 4.52 (A) This saker falcon (*Falco cherrug*) was admitted with a transverse fracture of the tarsometatarsus (arrowhead). There is minimal soft tissue swelling around the fracture site. (B) The fracture was repaired using a type II ESF utilizing four positive-profile threaded pins placed in the proximal and distal fragments and tie-in using bars and clamps. This bird was load bearing on the affected leg 24 h postoperatively. (C) This photograph was taken 28 days postoperatively when complete union was achieved. Note that the two pins closest to the fracture were already removed. (D) At 35 days postoperatively healing was complete and the remaining pins removed. The point of insertion of the threaded pins was still evident (arrowheads). These were healed perfectly when examined 1 month later.

SECTION 2 Management-related diseases



Fig. 4.53 An adult female saker falcon (*Falco cherrug*) presented to a falcon hospital in the Middle East showing signs of emaciation and severe dehydration. Early medical attention is of paramount importance to prevent any medical disorder developing to such an extreme extent.

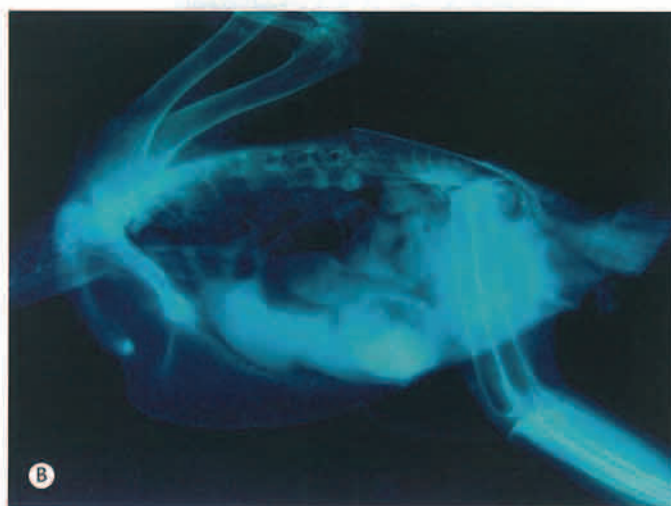


Fig. 4.54 (Right) (A) Ventrodorsal survey radiograph of the falcon in Figure 4.53. There is severe loss of muscle mass visible on the lateral side of the chest and around the wings and legs. (B) Lateral survey radiograph. Note the prominent keel bone due to loss of pectoral muscle mass. A relatively large amount of fine sand is present in the ventriculus. Blood analysis revealed that the falcon was undergoing a severe lead toxicosis after being fed on shot birds during a recent hunting trip.

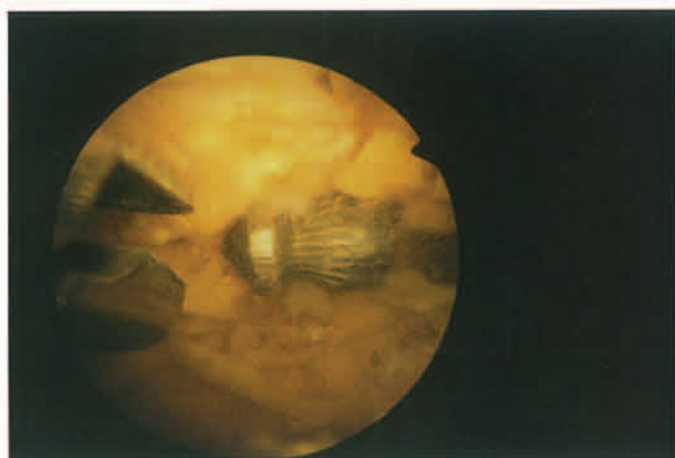


Fig. 4.55 A large lead pellet in the ventriculus of a saker falcon (*Falco cherrug*) surrounded by a large number of ingested small bones. The falconer shot a pigeon with an air rifle and gave it to the falcon assuming that the lead pellet had gone through the body. The photograph was obtained during the retrieval of the lead pellet using a long biopsy forceps clearly visible on the same image.

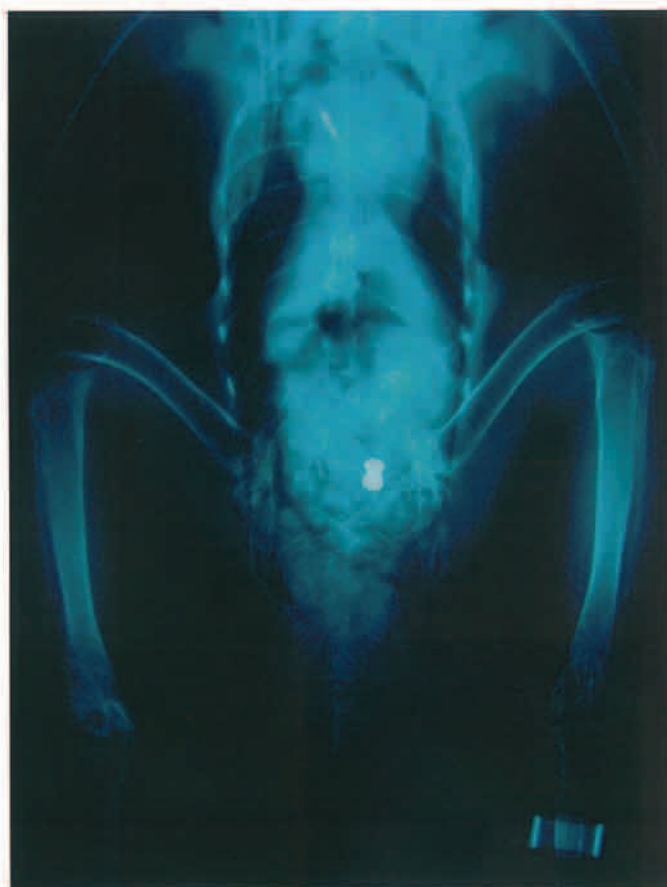


Fig. 4.56 This is a ventrodorsal survey radiograph view of the same falcon as in Figure 4.55 clearly showing the lead pellet in the ventriculus. The bones present in the ventriculus can also be observed.

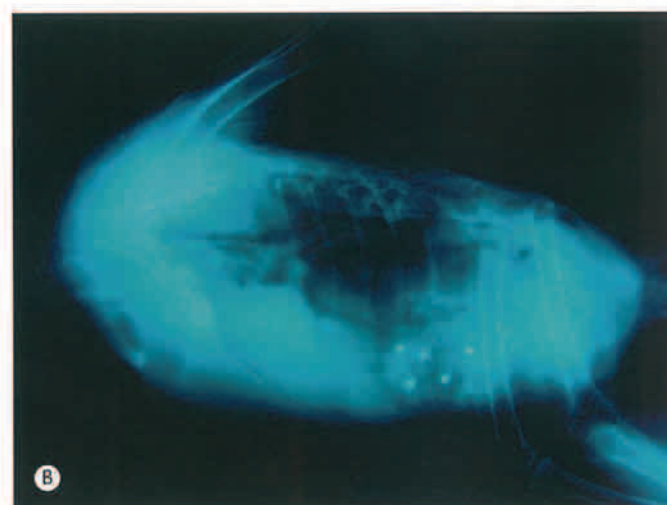
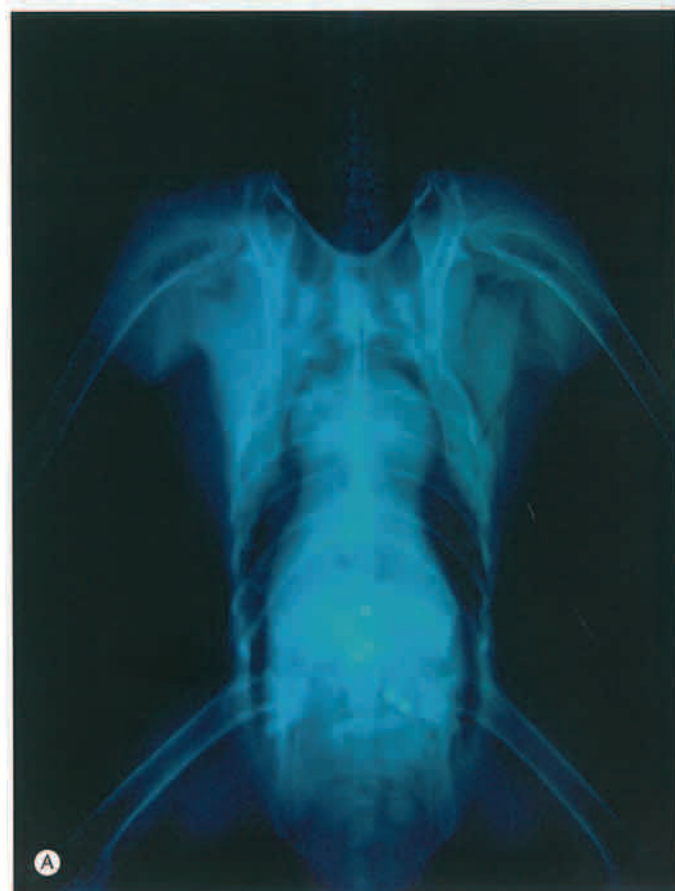


Fig. 4.57 (A) Ventrodorsal survey radiograph of a saker falcon (*Falco cherrug*) showing five lead pellets in the ventriculus together with a large quantity of bones and feathers. The falcon was fed a collared dove (*Streptopelia decaocto*) shot the previous day using a 12 bore shotgun. (B) Lateral survey radiograph. The five lead pellets can be easily observed within an exceedingly distended ventriculus filled with a large quantity of casting material in the form of bones and feathers.

SECTION 2 MANAGEMENT-RELATED DISEASES



Fig. 4.58 Ventrodorsal survey radiograph of a saker falcon (*Falco cherrug*) showing three large lead fragments in the ventriculus. These may have been full size and fully formed shotgun pellet when they were ingested, but have eroded in the ventriculus over a period of time.



Fig. 4.59 Ventrodorsal survey radiograph of a saker falcon (*Falco cherrug*) showing a large and several smaller radiodense particles within the ventriculus. Lead pellets tend to break into smaller pieces when they strike a bone of a shot prey. Repeated flushing with warm water via a gastric tube, helps remove lead particles from the ventriculus.



Fig. 4.60 An open Petri dish showing a large quantity of fine red sand retrieved from the ventriculus of a peregrine falcon (*Falco peregrinus*). The closed container shows a large quantity of coarser sand retrieved from a different falcon. Most falconers in the Middle East offer the food to falcons on their perches. However, many falcons have the tendency to take the food to the ground where it is covered with fine sand. The sand is ingested together with the food and is gradually accumulated in the ventriculus causing in some cases serious impaction.



Fig. 4.61 Lateral survey radiograph of a saker falcon (*Falco cherrug*). Note the large quantity of sand in the esophagus (e), proventriculus (p), ventriculus (v) and intestinal tract (i).



Fig. 4.62 This is a lateral survey radiograph from a different saker falcon (*Falco cherrug*) showing a large quantity of sand mainly in the ventriculus (v) and the intestinal tract (i). Small amounts of sand ingested intermittently can pass through the falcon without a major difficulty. However, the feeding on sand should be avoided. Securing the food on plastic mats (e.g. Astroturf) before offering to falcons is highly recommended. Heart (h), Liver (l), lung (lu), kidney (k) and proventriculus (p).

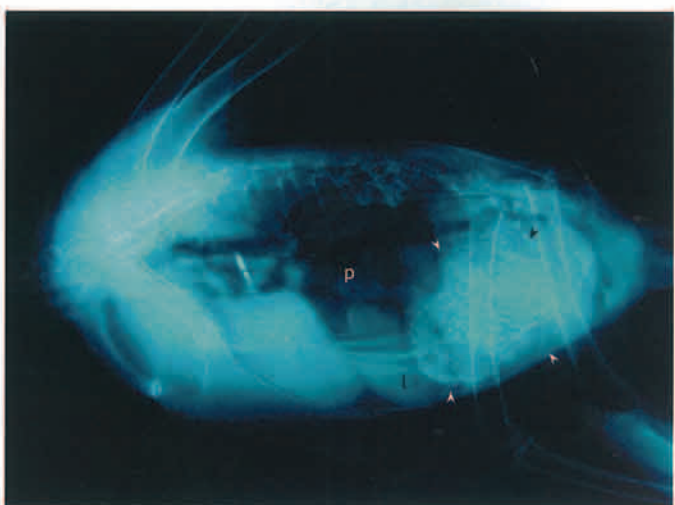


Fig. 4.63 Lateral survey radiograph of a saker falcon (*Falco cherrug*) showing a large quantity of undigested material accumulated in the ventriculus (arrowheads). Most birds of prey cast out a pellet formed by feathers, fur and bones usually the following day after a meal. Casting material should form an integral part of the diet of raptors kept in captivity. However, casting material should never be offered to weak and sick individuals as the birds may not be able to cast it out and this may lead to impaction. Proventriculus (p) and liver (l).



Fig. 4.64 (A) Ventrordorsal survey radiograph of a saker falcon (*Falco cherrug*) presented with a history of anorexia and weight loss. The radiograph shows increased radiodensity in one particular loop of the intestinal tract (arrowheads). (B) Lateral survey radiograph. A large radiodense solid object (arrows) appears to be obstructing the intestinal tract. Note the dilated intestinal loops in the rest of the intestine (arrowheads). Liver (l), proventriculus (p) and ventriculus (v). (C) Despite specific and support therapy the falcon died. The photograph shows the digestive tract of the falcon at post-mortem examination. The obstruction can be clearly seen. The offending mass was composed of dehydrated feces and sand. Cloaca (cl).



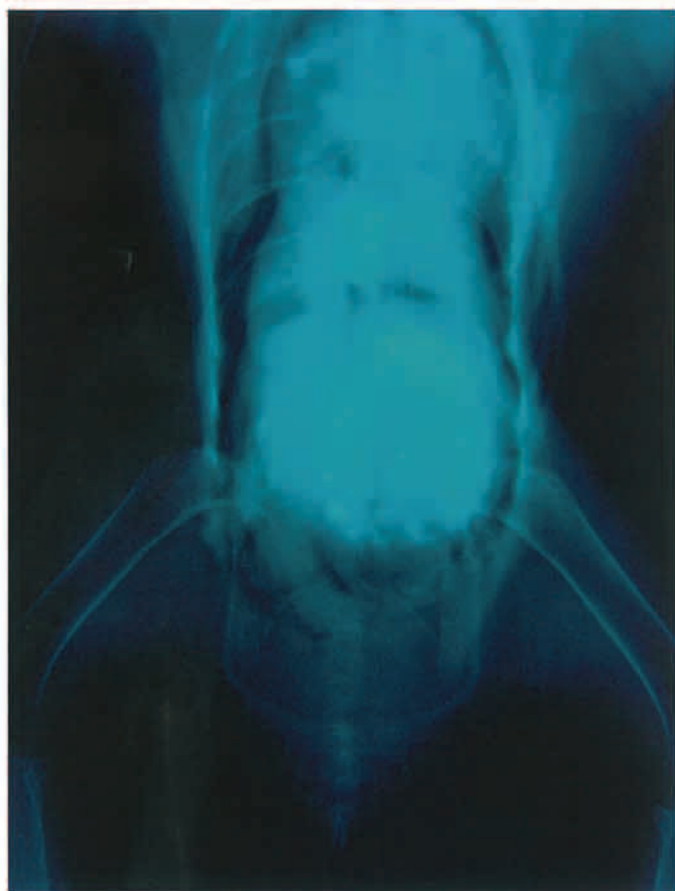


Fig. 4.65 Ventrodorsal survey radiograph of a gyr falcon (*Falco rusticolus*) showing several lead fragments surrounded by a large quantity of casting material present in the ventriculus. The falcon was in a critical condition and it died immediately after admission.



Fig. 4.66 The photograph shows a large pellet formed mostly by grass found at post-mortem examination within the ventriculus of the same falcon as in Figure 4.65. The falcon was fed everyday in the afternoon on a lawn where the grass had just been cut. Obviously, the grass used to stick to the food offered to the falcons accumulating gradually in the ventriculus. The falcon could not cast out the grass, most probably, due to the debilitating chronic disease and the lead toxicosis.

SECTION 2 MANAGEMENT-RELATED DISEASES



Fig. 4.67 (A) Ventrordorsal survey radiograph of a lappet-faced vulture (*Torgos traqueliotus*). A large radiodense object can be seen within the body. This is a satellite transmitter used for a telemetry study. The transmitter was supposed to have been implanted into the celomic cavity. However, this was wrongly implanted within the ventriculus. (B) Lateral survey radiograph. Note the presence of the transmitter within the ventriculus. The antenna of the transmitter is broken in two places. The transmitter stopped sending signals shortly after implanting it. This was retrieved surgically and the vulture made an uneventful recovery.

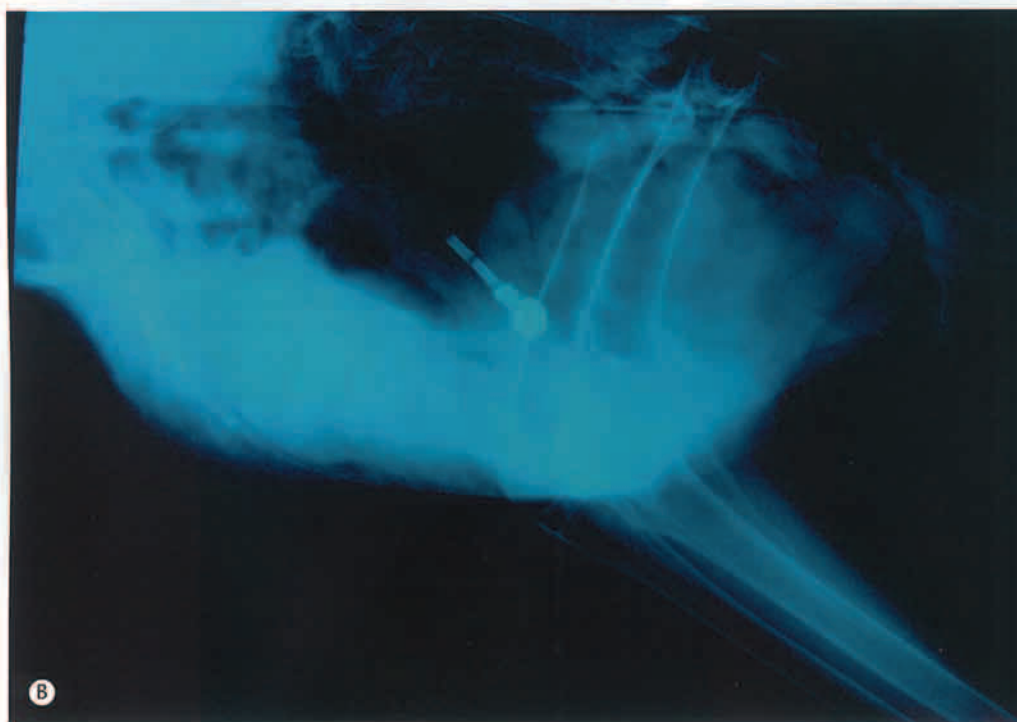
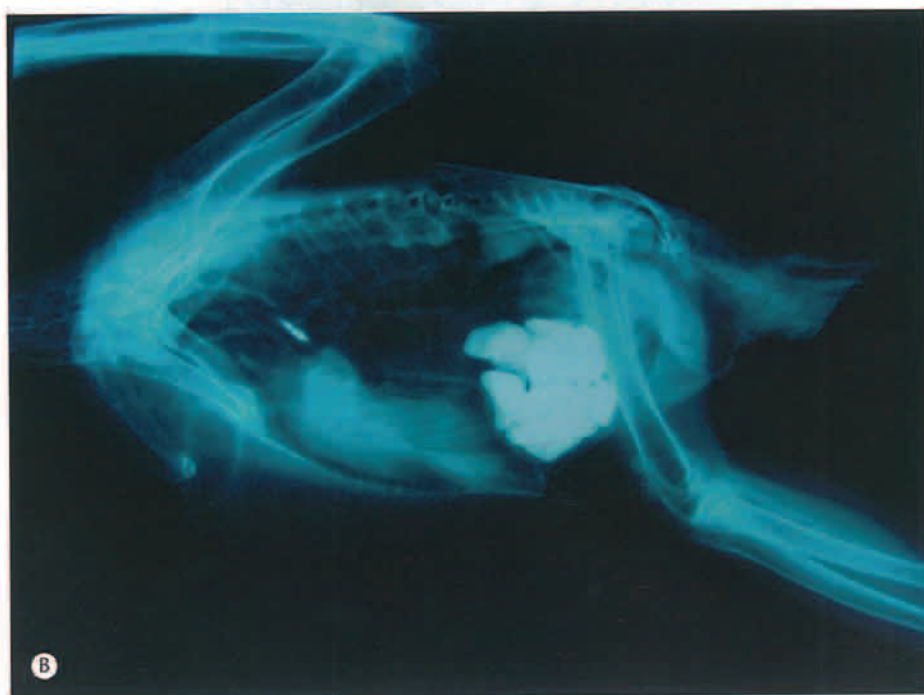




Fig. 4.68 (A) This ventrodorsal survey radiograph is of a peregrine falcon (*Falco peregrinus*) that died during the molting period after a short period of anorexia. The radiograph shows several radiodense amorphous objects within the ventriculus. (B) A lateral survey radiograph showing clearly a large number of medium-sized stones. These were used as substrate in the aviary. Note the gaseous distension of the proventriculus and intestinal loops associated with the severe impaction. In captivity falcons have the tendency of ingesting medium-sized stones and regurgitating them the following day. This is believed to help casting out undigested material during molting.



SECTION 2 MANAGEMENT-RELATED DISEASES

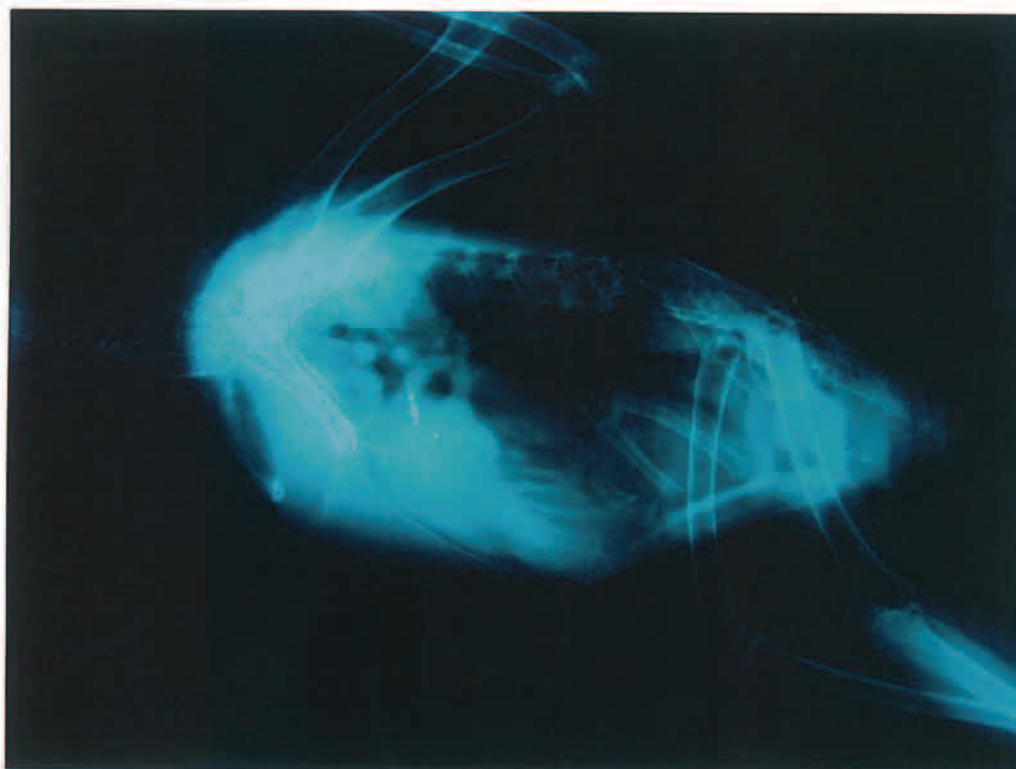


Fig. 4.69 Birds of prey in captivity often swallow entire limbs or necks of pheasants, pigeons or quails. In this lateral survey radiograph, part of the wing of a pigeon was swallowed. The ingestion of large long bones can produce impaction and in some occasions can get lodged in the esophagus leading to the death of the individual.



Fig. 4.70 A lateral survey radiograph of a short-toed snake-eagle (*Circaetus gallicus*). Note the presence of the entire limb of the prey (probably a long-legged wader) with the proximal femur occupying the thoracic inlet extending down to the caudal part of the thoracic esophagus. The tibiotalarsus occupied the proventriculus and ventriculus, and then folded at the intertarsal joint. The tarsometatarsus and the digits occupy the ventriculus, proventriculus and caudal part of the thoracic esophagus (arrowheads) (courtesy of J G de la Fuente and A L Sánchez).

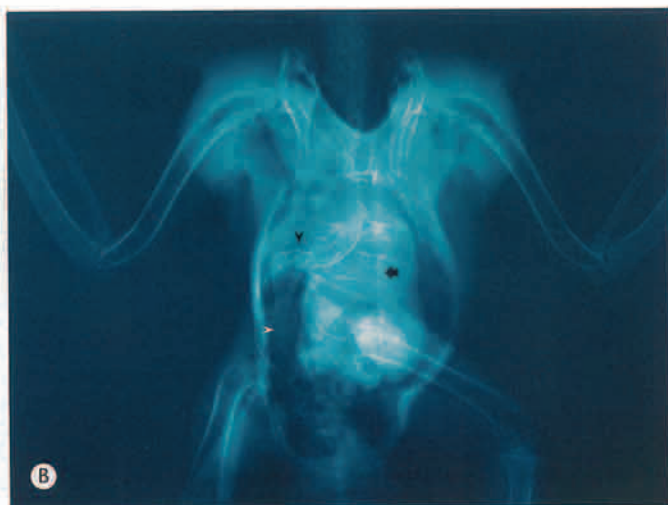


Fig. 4.71 (A) A post-mortem examination of a peregrine falcon (*Falco peregrinus*) with severe scoliosis. In cranes and other avian species, deformities of the spine are believed to be a genetic linked abnormality (courtesy of M García-Montijano and P Prieto). (B) A ventrodorsal survey radiograph. Undigested material can be observed in the ventriculus. Notarium (black arrowhead), synsacrum (white arrowhead) and keel of sternum (black arrow) (courtesy of M García-Montijano).

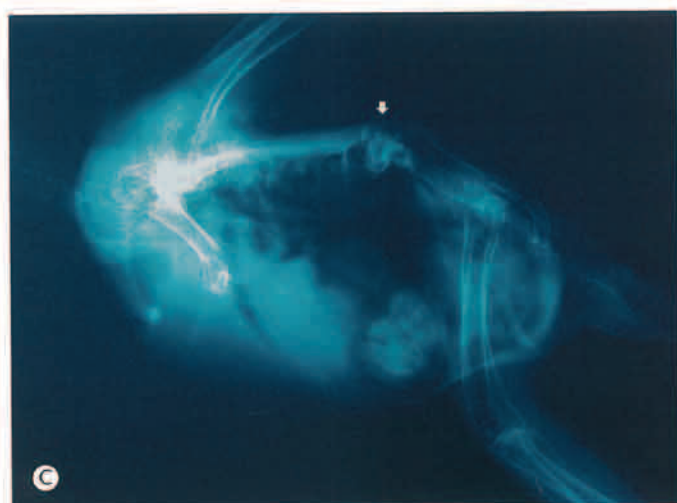


Fig. 4.71 (C) A lateral survey radiograph. Distortion of the caudal thoracic vertebrae and the synsacrum has resulted in severe deformation (arrow) (courtesy of M García-Montijano).



Fig. 4.72 (Right) Severe scoliosis of the thoracic vertebrae (dotted line) in a common barn owl (*Tyto alba*) (courtesy of J G de la Fuente and A L Sánchez).

SECTION 2 MANAGEMENT-RELATED DISEASES

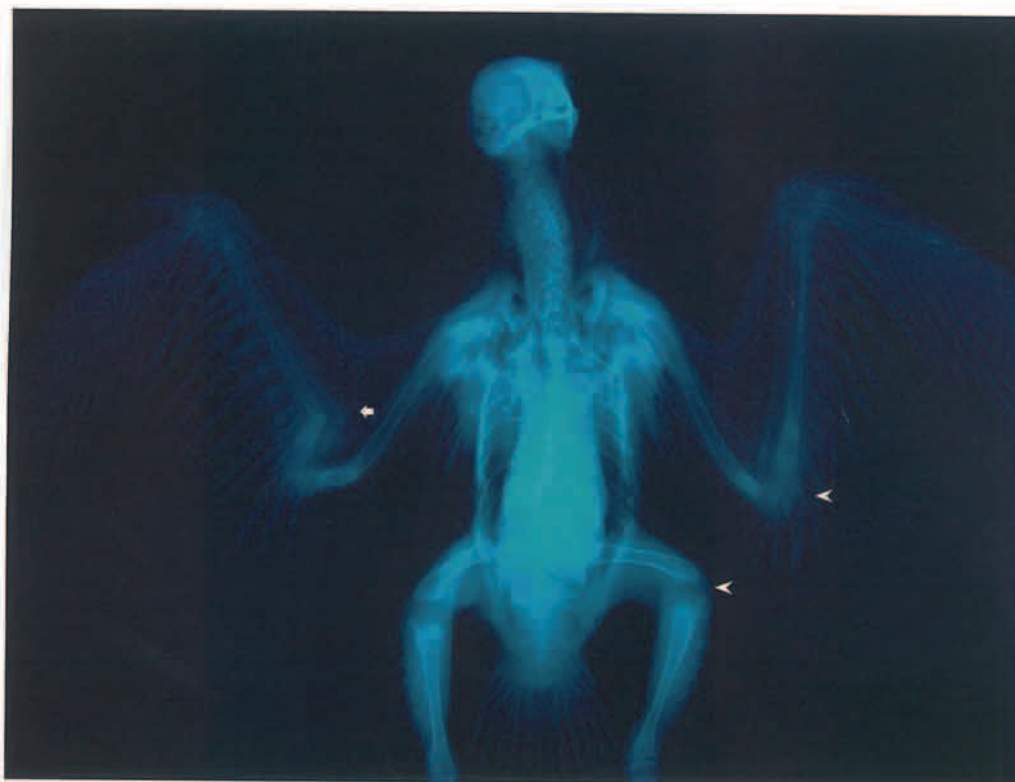


Fig. 4.73 Ventrodorsal survey radiograph of a juvenile red kite (*Milvus milvus*). There are pathological fractures on proximal right radius and ulna and bowing of both distal humeri. Note the large joint spaces (arrowheads) and secondary ossification centers in the hock joint. The core of the immature or blood feathers appear radiodense (courtesy of M García-Montijano and T Álvarez).



Fig. 4.74 Metabolic bone disease in a young bonelli's eagle (*Hieraetus fasciatus*) being reared on a meat-only diet. Bowing with pathological fractures of both ulna, radius, humeri, tibiotarsi and right femur. The overall bone density is decreased and the cortical outlines of the long bones are barely visible (courtesy of T A Bailey).

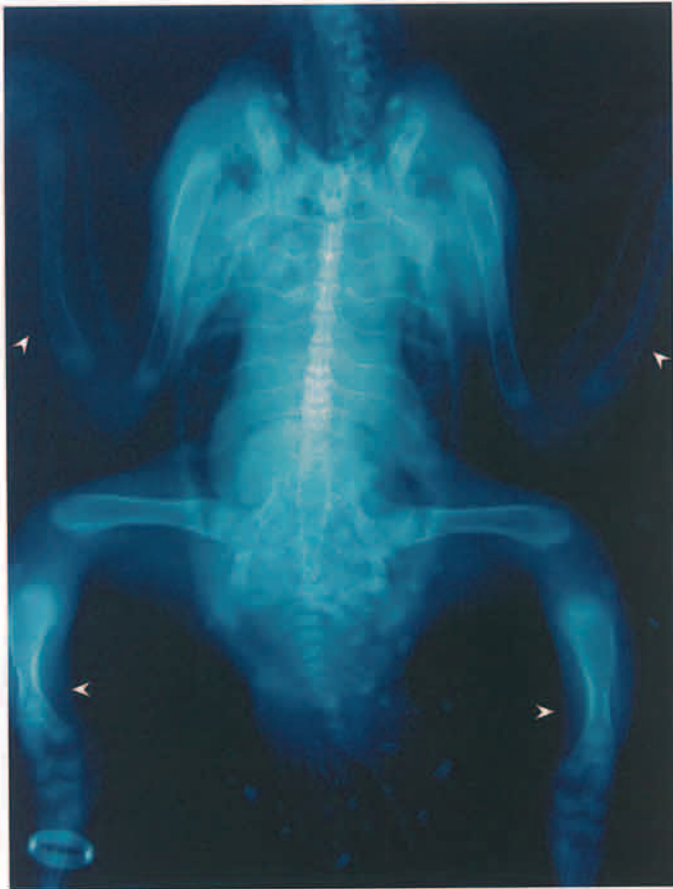


Fig. 4.75 Metabolic bone disease in a 6-week-old gyr falcon (*Falco rusticolus*). Bowing of the ribs and of both ulna and tibiotarsi (arrowheads). Note the large joint spaces and incomplete ossification of the secondary ossification centers in the hock joint, which are characteristics of an immature bird (courtesy of T A Bailey).

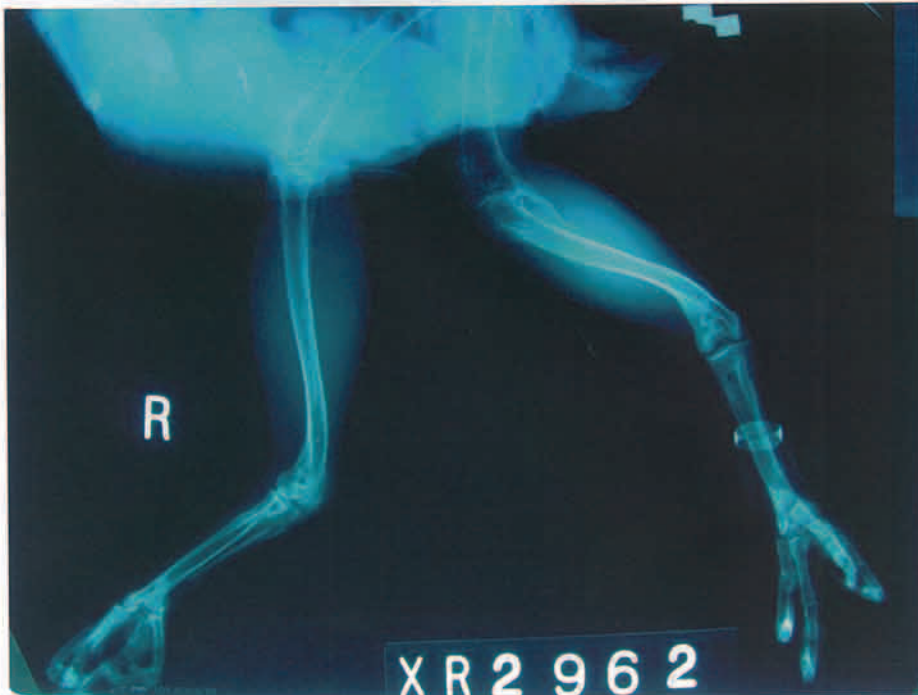


Fig. 4.76 Lateral radiograph of the pelvic limb of an adult saker falcon (*Falco cherrug*) with bowing of both distal tibiotarsi. The left tibiotarsus is shorter compared with the contralateral leg and there is rotation of the distal metaphyses. This bird suffered from metabolic osteopathy during its growth.

SECTION 3 Infectious diseases



Fig. 4.77 A saker falcon (*Falco cherrug*) displaying an exceedingly enlarged crop. Such enlargements are common after a large meal. Subsequent clinical and radiological examination revealed a single large caseous mass produced by a chronic infection with the protozoan parasite *Trichomonas gallinae*. The infection is commonly acquired after feeding on pigeons (*Columba livia*) and collared doves (*Streptopelia decaocto*) commonly used as food items across the Middle East.

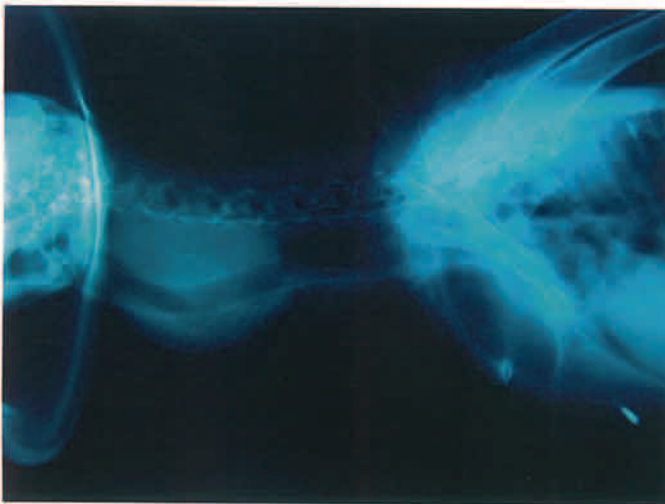


Fig. 4.78 Lateral survey radiograph of a saker falcon (*Falco cherrug*) showing a large radiodense mass on the neck.



Fig. 4.79 Ventrodorsal view of a similar case as in Figure 4.78. After clinical examination it was confirmed that the mass observed was a large caseous trichomonosis growth within the crop.



Fig. 4.80 Lateral photograph of the head of an anesthetized saker falcon (*Falco cherrug*) showing multiple periorbital swellings. This was an unusual case of a chronic infection with *Trichomonas gallinae* within the periorbital diverticulae of the infraorbital sinus. Such infections are acquired through the oropharyngeal cavity and spread across the sinus through the choana.

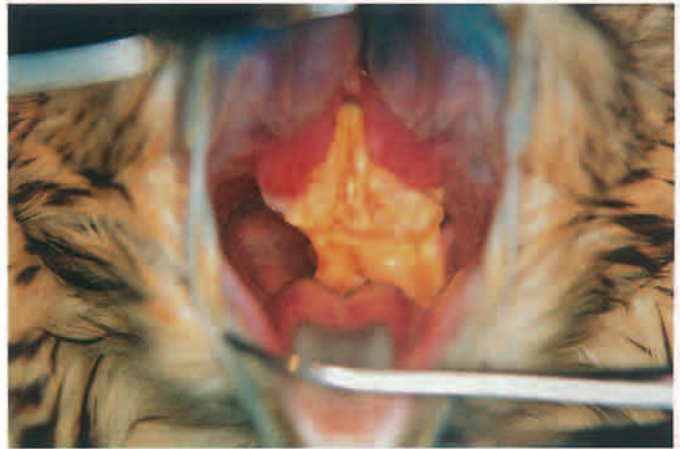
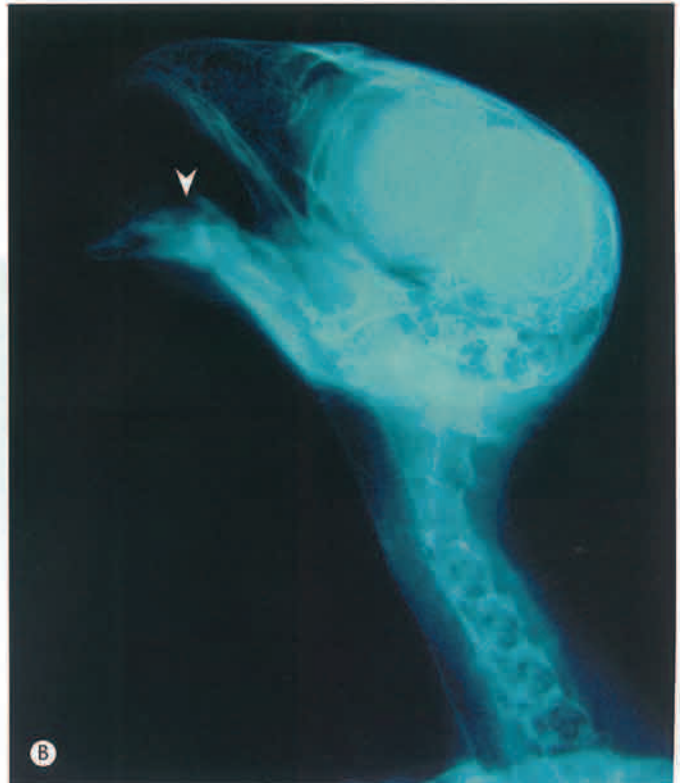


Fig. 4.81 A large caseous mass produced by *Trichomonas gallinae* obstructing the choana and infundibular cleft, on the dorsal aspect of the oropharynx in a saker falcon (*Falco cherrug*). This type of infection is more typical of trichomonosis in birds of prey.



Fig. 4.82 (A) A saker falcon (*Falco cherrug*) with severe necrosis of the proximal portion of the lower mandible caused by a trichomonosis infection. (B) Lateral radiograph of the head showing osteolysis of the cranial portion of the mandible (arrowhead).



SECTION 3 INFECTIOUS DISEASES

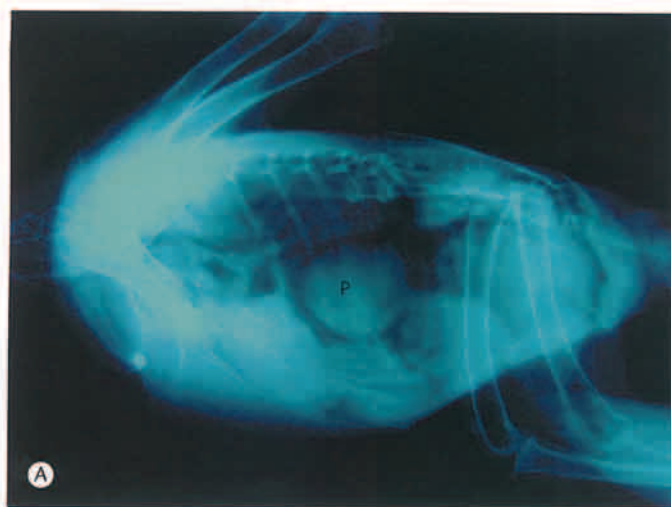


Fig. 4.83 (A) Lateral survey radiograph of a saker falcon (*Falco cherrug*) showing a severely enlarged proventriculus (p). The falcon was presented severely ill with a history of reduced appetite and vomiting. The falcon failed to respond to therapy and died soon after admission. (B) A photograph of the post-mortem examination of the saker falcon (*Falco cherrug*). The examination revealed an enlarged proventriculus containing numerous dark encapsulated parasitic forms protruding through its surface. The parasite is currently undergoing different morphological studies in order to identify the species.

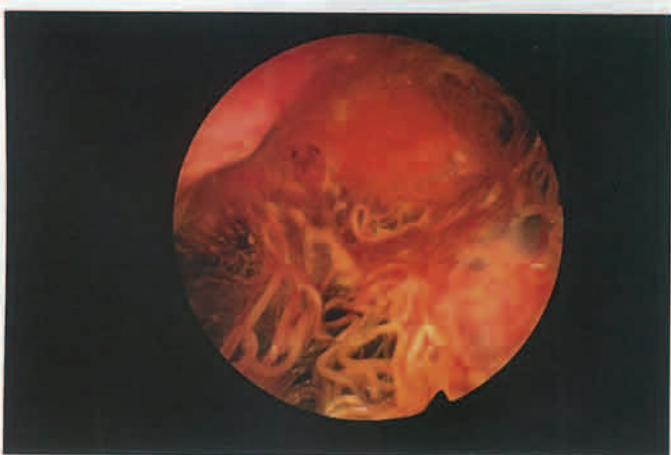
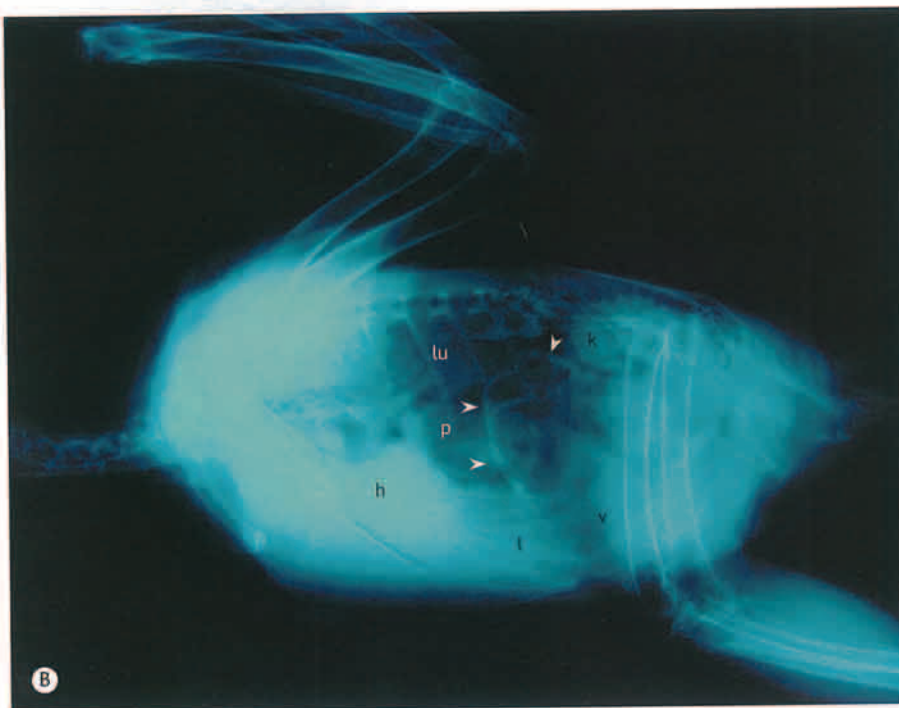


Fig. 4.84 An endoscopic view of the celomic cavity of a gyr-saker hybrid falcon (*Falco rusticolus-Falco cherrug*) showing numerous adult filarial worms associated with diffused and focal thickening of the air sac walls. This parasite is very common throughout the Middle East. Taxonomical studies have identified it as *Serratospiculum seurati*.



Fig. 4.85 (A) Ventrordorsal survey radiograph of a saker falcon (*Falco cherrug*) displaying moderate bilateral diffused radiopacities affecting the caudal thoracic and abdominal air sacs. (B) Lateral survey radiograph showing thickening of the caudal thoracic and abdominal air sac walls (arrowheads). Airsacculitis in birds of prey is very often associated with bacterial and fungal infections. However, this finding can also be observed with some severe infections with *Serratospiculum seurati* filarial worms. Heart (h), liver (l), lung (lu), kidney (k), proventriculus (p) and ventriculus (v).



SECTION 3 INFECTIOUS DISEASES

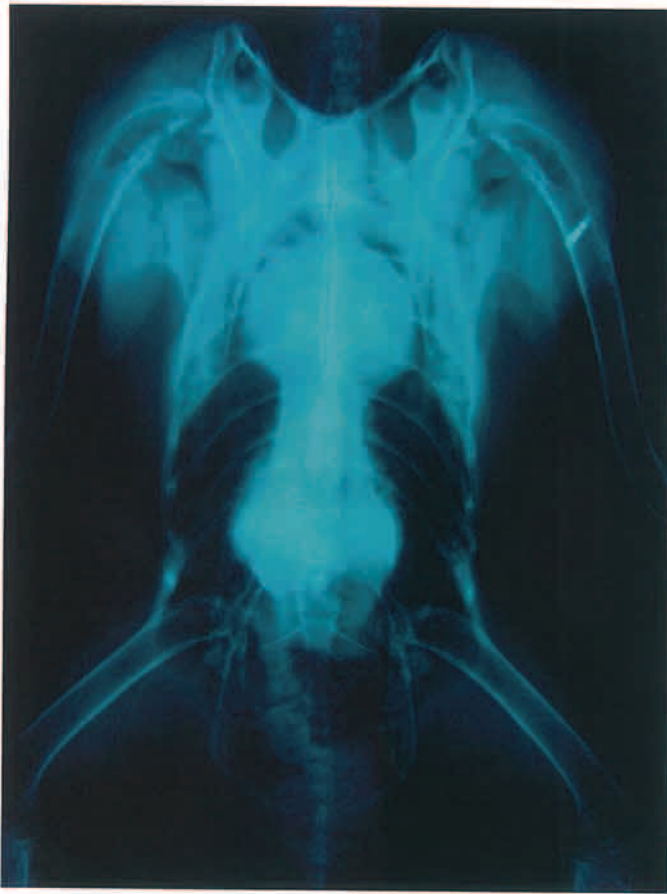


Fig. 4.86 Ventrodorsal survey radiograph of a saker falcon (*Falco cherrug*) showing mild diffused airsacculitis around the ventriculus and liver shadows. This pathological condition is commonly known as 'sun-burst' effect and has been increasingly observed in Saudi Arabia in hunting falcons undergoing severe parasitic infections with *Serratospiculum seurati*.

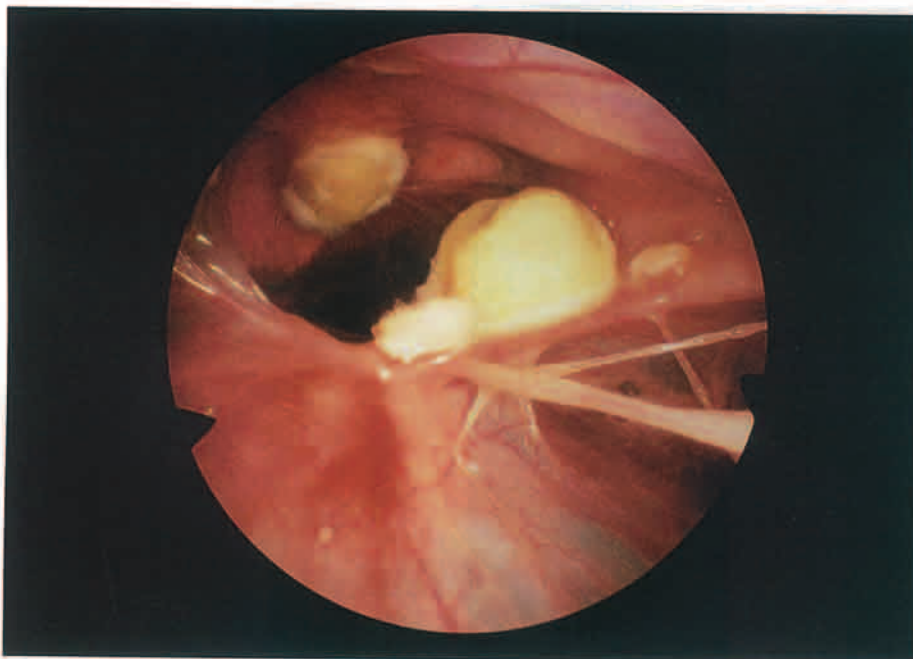


Fig. 4.87 Fungal plaques attached to the walls of the *ostium pulmonare* of the abdominal air sac. Larger fungal growths in such anatomical sites can produce mechanical obstruction of the airway leading to air trapping within the abdominal air sacs.

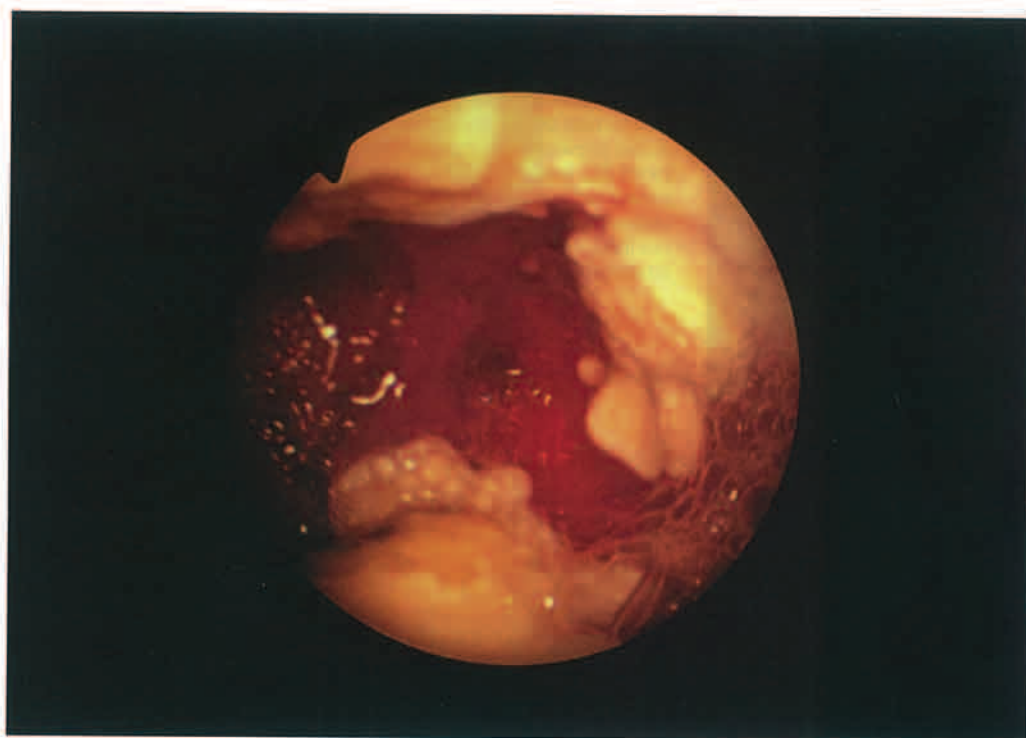


Fig. 4.88 Endoscopy view of the caudal thoracic air sac of a gyr-peregrine hybrid falcon (*Falco rusticolus*-*Falco peregrinus*) showing extensive and diffused aspergillosis.

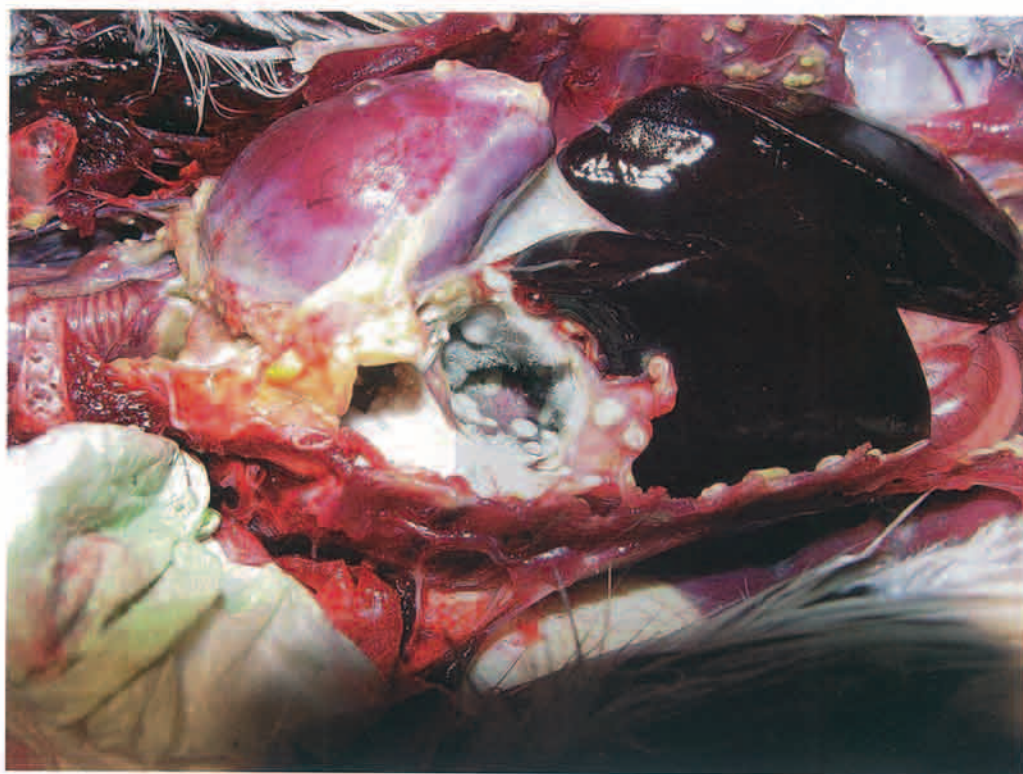


Fig. 4.89 Post-mortem examination of a gyr falcon (*Falco rusticolus*) that died of a severe aspergillosis infection. Note the extensive fungal growth covering the cranial and caudal thoracic air sacs. In the Middle East, a significant number of newly imported gyr falcons and gyr falcon hybrids succumb to aspergillosis due to the prevalent high temperatures and high humidity at the beginning of the training season (August–September) coupled with intensive exercising practices.

SECTION 3 INFECTIOUS DISEASES



Fig. 4.90 (A) Ventrrodorsal survey radiograph of a saker falcon (*Falco cherrug*) presented with a history of reduced flight performance and dyspnea. The radiograph shows severe air trapping of the caudal thoracic and abdominal air sac field probably due to mechanical obstruction of the *ostia pulmonare*. A medium-sized radiodense mass is also present in the central area of the celomic cavity (arrowhead). Heart (h), liver (l), ventriculus (v) and intestinal loops (i). (B) Lateral survey radiograph. Extensive air trapping of the caudal thoracic and abdominal air sac field (arrowheads). The organs are displaced cranially. Heart (h), liver (l), proventriculus (p), ventriculus (v) and intestinal loops (i).

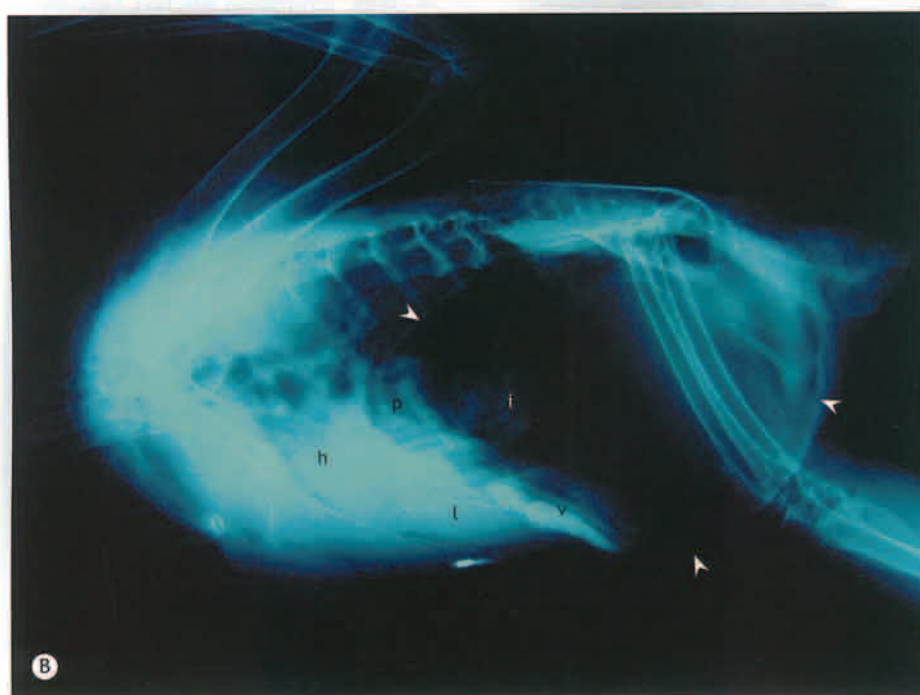




Fig. 4.91 Ventrodorsal survey radiograph of a saker falcon (*Falco cherrug*) with generalized, non-homogeneous, increased radiopacities throughout the celomic cavity. The heart, lungs, and liver cannot be differentiated. The ventriculus (v) appears to contain some casting material. A large rounded focal radiodense mass can also be clearly seen in the caudal thoracic air sac (arrowhead). This is probably a large encapsulated aspergilloma.

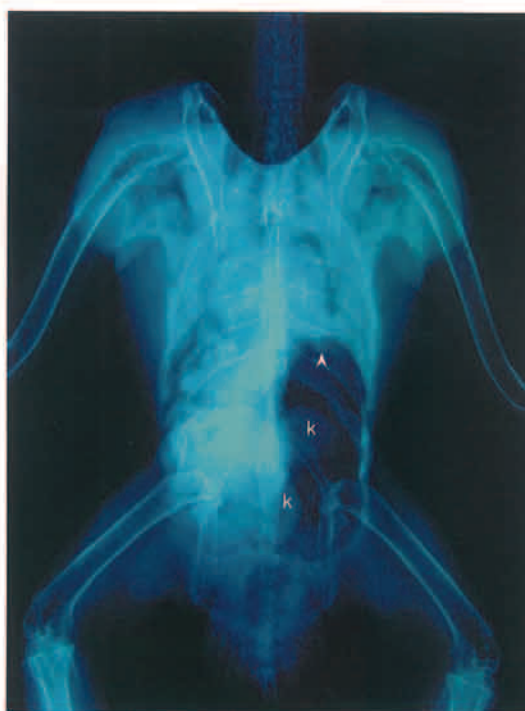


Fig. 4.92 Unilateral generalized non-homogeneous increased radiopacity affecting mainly the caudal thoracic and the abdominal air sacs. Air trapping is evident in the left caudal thoracic and abdominal air sac field. A smaller focal radiodense area can also be observed at the cranial thoracic air sac near the apex of the heart on the left side (arrowhead). Kidneys (k).



Fig. 4.93 (Right) Ventrodorsal survey radiograph of a peregrine falcon (*Falco peregrinus*) with advanced aspergillosis that was presented because of severe dyspnea, poor flight performance, reduced appetite, and light green urates. A generalized, nonhomogenous, increased radiopacity is present in the lung fields and thoracic air sacs, and air trapping is present in the abdominal air sacs. The heart, lungs, liver, and other organs cannot be differentiated, and there is a loss of air space in both clavicular air sacs (black arrowheads). A medium-sized round radiodense mass can be clearly seen in the midline of the celomic cavity (white arrowhead).

SECTION 3 INFECTIOUS DISEASES

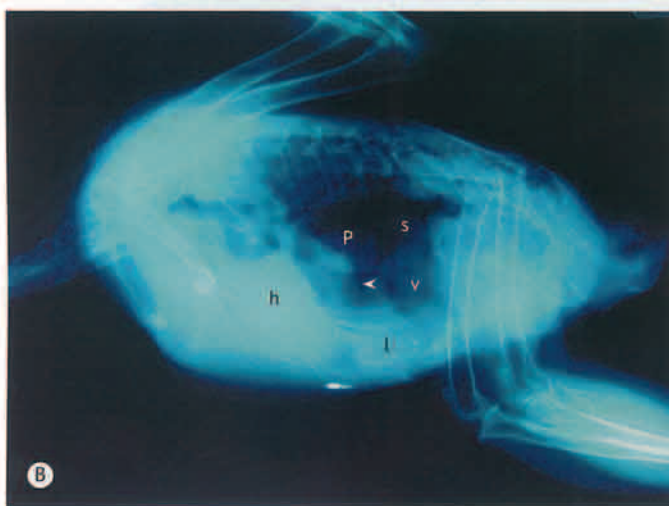
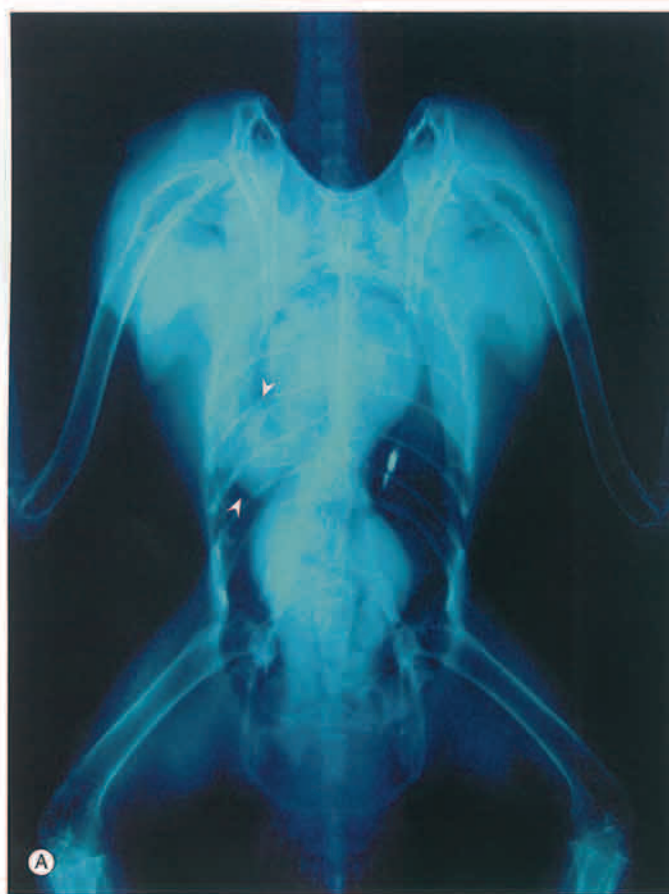


Fig. 4.94 (A) A single large radiodense mass (arrowheads) can be observed between the heart and the liver in this ventrodorsal survey radiograph of a saker falcon (*Falco cherrug*). A passive induced transponder (PIT) can be observed on the opposite side. (B) A lateral survey radiograph. The large radiodense mass (arrowhead) can be observed between the dorsal aspect of the heart (h) and the liver (l) obstructing partially the proventriculus (p). Ventriculus (v) and spleen (s). (C) Photograph of the post-mortem examination. The bird died shortly after the survey radiographs were obtained. On further examination the mass was found to be an encapsulated aspergilloma. The presence of a single large aspergilloma is not uncommon in birds of prey. Resolution of such cases commonly involves surgical excision of the mass after a period of specific antifungal therapy.

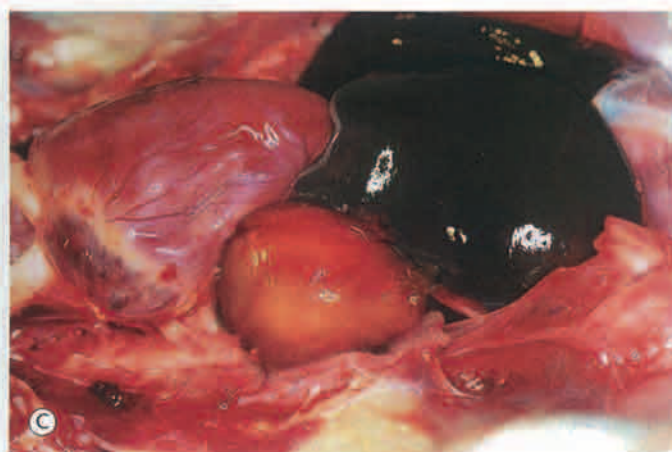




Fig. 4.95 Ventrodorsal survey radiograph of a peregrine falcon (*Falco peregrinus*) with unilateral diffuse radiopacity of the cranial thoracic air sac. Endoscopy examination revealed a large caseous mass occupying the space of the air sac. Such masses are very commonly the result of bacterial or fungal infections.



Fig. 4.96 Ventrodorsal survey radiograph of a saker falcon (*Falco cherrug*) with diffuse and focal radiopacities affecting the cranial thoracic and caudal thoracic air sacs (white arrowheads). There is a loss of air space in both clavicular air sacs (black arrowheads).

SECTION 3 INFECTIOUS DISEASES

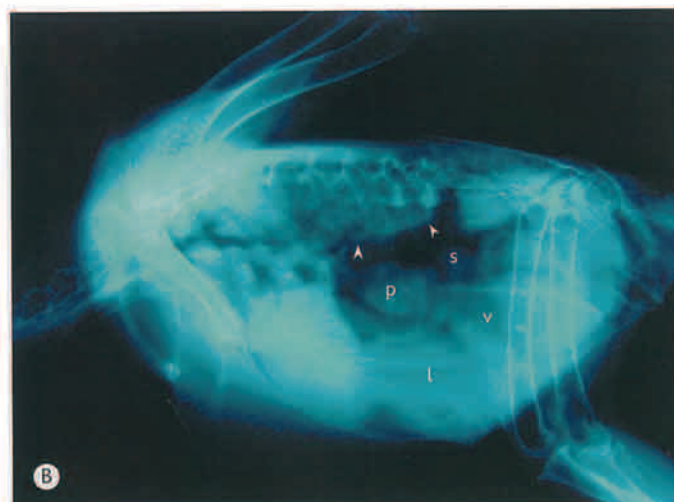


Fig. 4.97 (A) Ventrodorsal survey radiograph of a saker falcon (*Falco cherrug*) peppered with bilateral radiopacities spread throughout the lung area. (B) Lateral survey radiograph. Note the increased radiopacity of the lung field (arrowheads). The falcon was affected with severe pneumonia of bacterial origin. The liver (l) shadow appears enlarged displacing the ventriculus (v) caudodorsally. Spleen (s) and proventriculus (p).

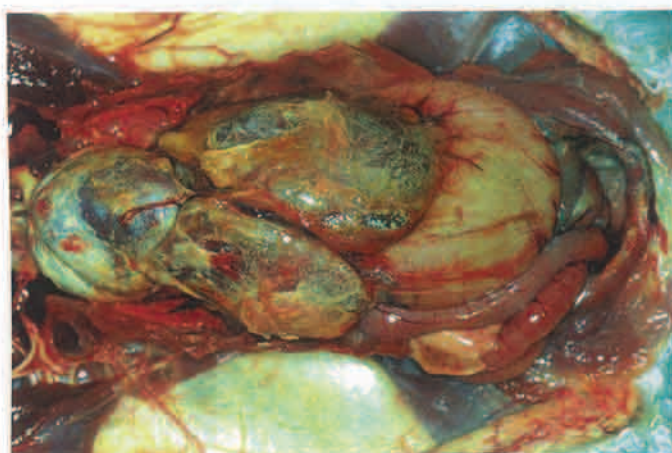
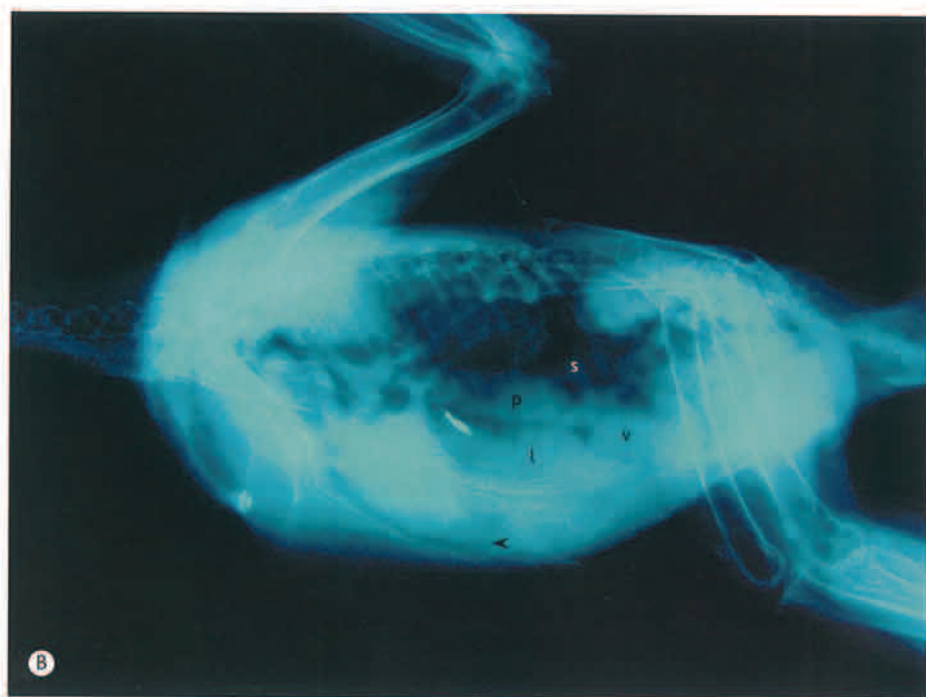


Fig. 4.98 A post-mortem examination of a saker falcon (*Falco cherrug*). Uric acid deposits were observed covering the pericardial sac and the liver typical of visceral gout. The liver was severely enlarged. Histopathology examination of this organ revealed severe amyloid deposits in the Disse space affecting most of the parenchyma of the organ resulting in dysfunction.



Fig. 4.99 (A) Ventrordorsal survey radiograph of a saker falcon (*Falco cherrug*) showing a severely enlarged liver. (B) Lateral survey radiograph. The enlarged liver (l) has displaced the proventriculus (p) and spleen (s) dorsally and the ventriculus (v) caudodorsally. The heart shadow also appears to be elongated (arrowhead).



SECTION 3 INFECTIOUS DISEASES

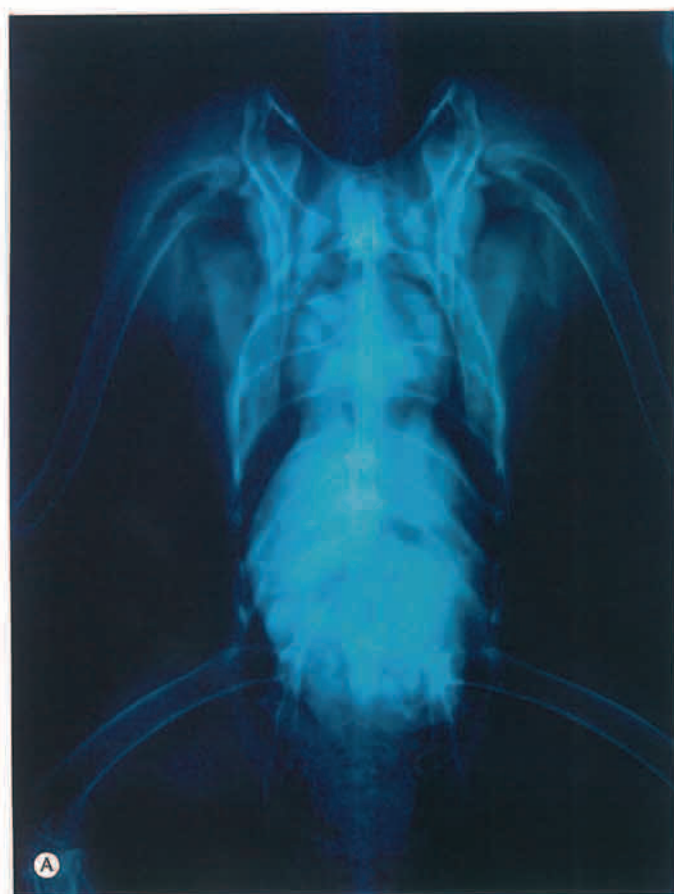


Fig. 4.100 (A) Ventrrodorsal survey radiograph of a peregrine falcon (*Falco peregrinus*) showing an enlarged liver. A follow-up biopsy revealed severe amyloid deposits in the liver. (B) Lateral survey radiograph. Arrowheads indicate the caudal margin of the severely enlarged liver. Note the caudal displacement of the ventriculus (v), which is distended and contains a large amount of undigested material.

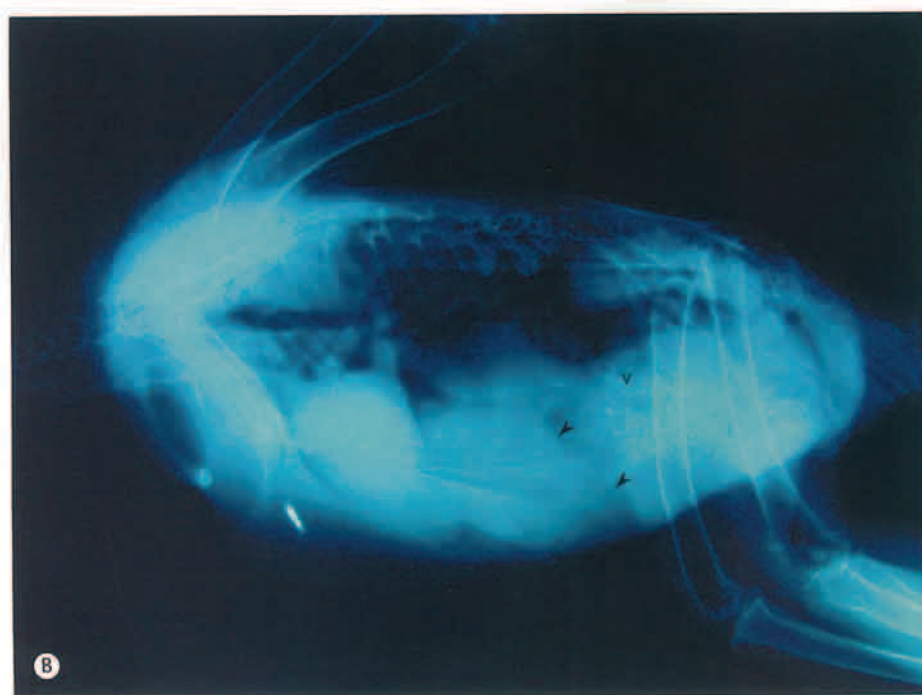




Fig. 4.101 A saker falcon (*Falco cherrug*) affected by the viscerotropic form of Newcastle disease. This form is characterized by reduced to total absence of appetite, regurgitation, vomiting of partially digested blood, mucoid-hemorrhagic diarrhea, constant distress vocalization and sudden death.



Fig. 4.102 (A) Ventrodorsal survey radiograph of a saker falcon (*Falco cherrug*). Note the gaseous distention and thickening of the walls of the ventriculus (black arrowheads) and the intestinal loops (white arrowheads). (B) Lateral survey radiograph. Note the gaseous distention and thickening of the walls of the ventriculus (white arrowheads) and the intestinal loops (black arrowheads). Ventriculitis and occasionally, enteritis are characteristic radiological findings observed in more than 60% of falcons affected with the viscerotropic form of Newcastle disease.

SECTION 3 INFECTIOUS DISEASES

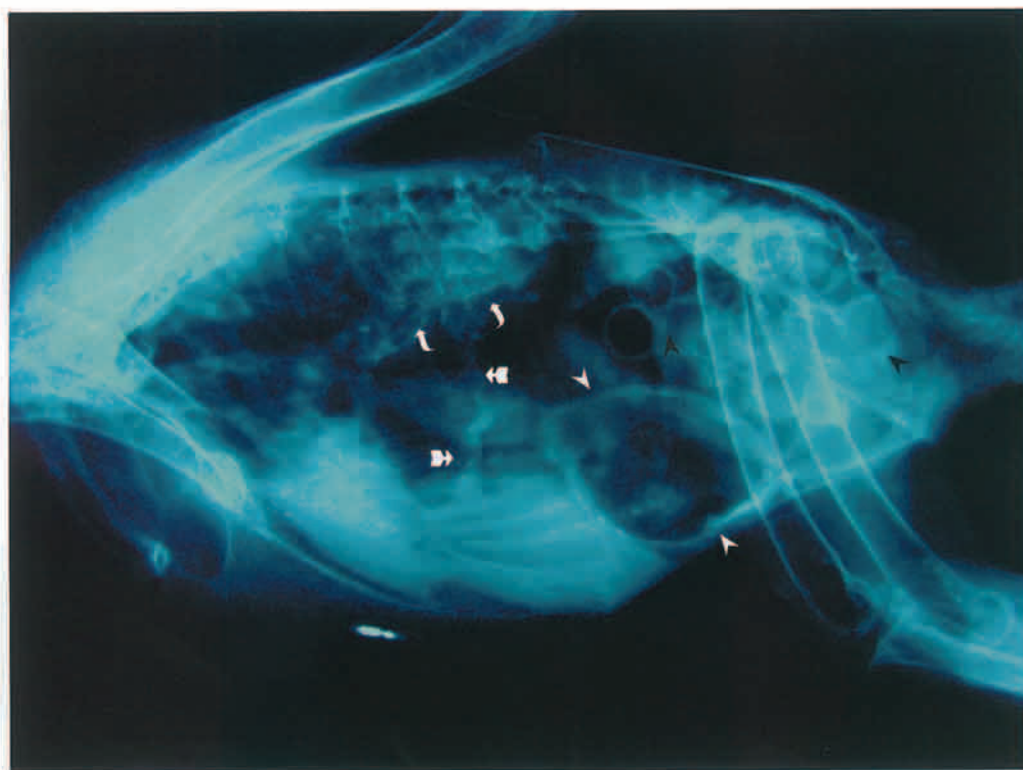


Fig. 4.103 Lateral survey radiograph of a saker falcon (*Falco cherrug*) affected with the viscerotropic form of Newcastle disease. The ventriculus (white arrowheads) and the intestinal tract (black arrowheads) are severely distended. In addition, the falcon was affected by airsacculitis and pneumonia. Note the increased parabronchial density (curve arrows) and the thickened air sac wall (thick arrows).

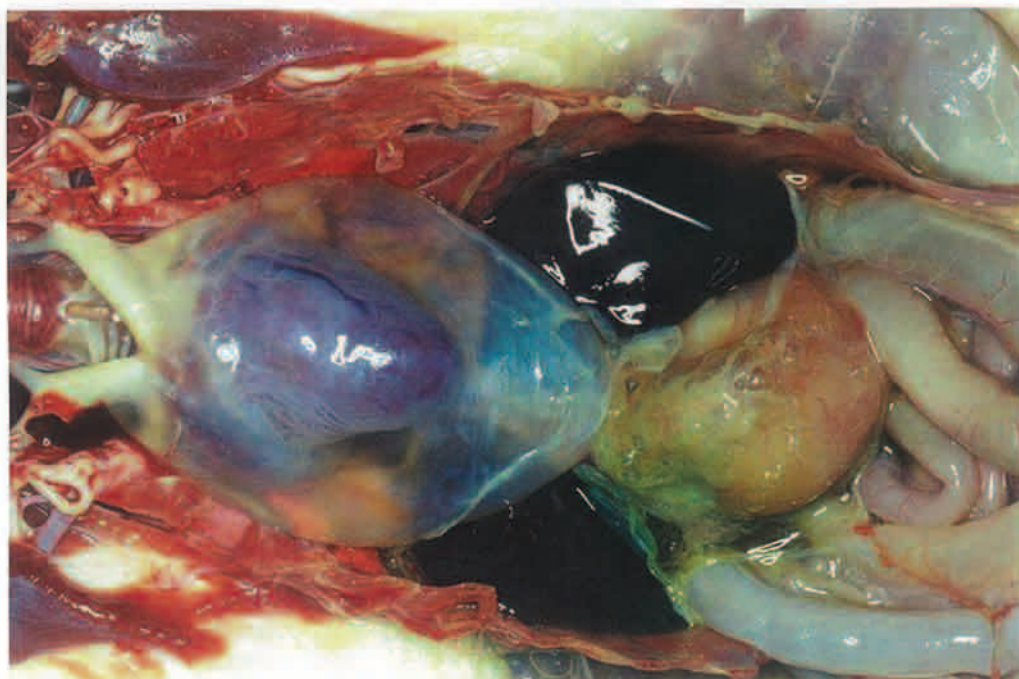
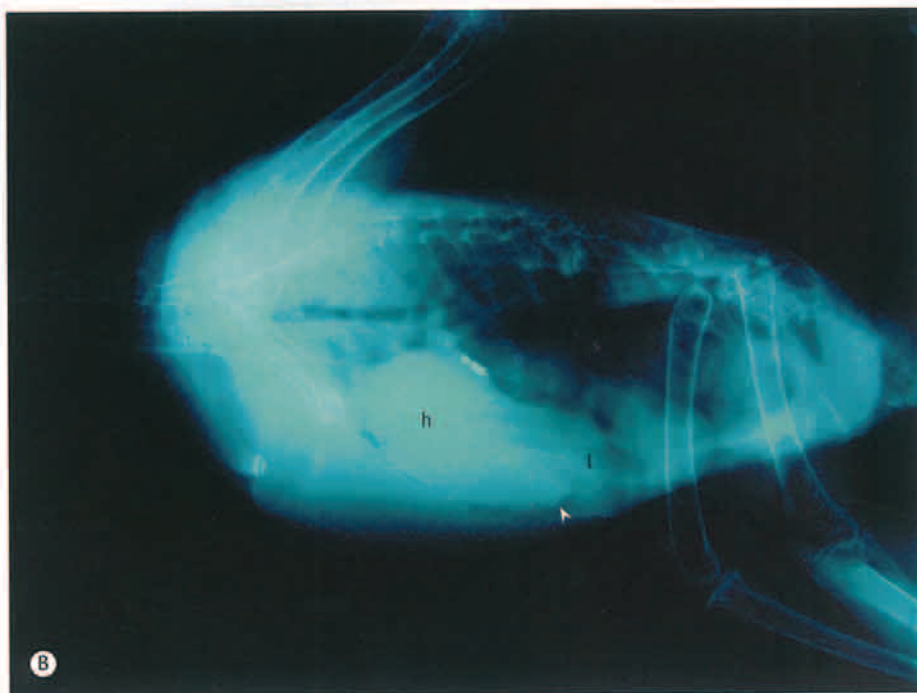


Fig. 4.104 Post-mortem examination of a peregrine falcon (*Falco peregrinus*) showing a severely distended pericardial sac. This was the result of a chronic liver disorder.



Fig. 4.105 (A) Ventrodorsal survey radiograph of a gyr falcon (*Falco rusticolus*) showing an enlarged heart shadow. (B) Lateral survey radiograph. Note the severely enlarged heart (h) shadow. The arrowhead indicates the heart apex. Cardiomegaly is very often the result of septicemias of bacterial origin. The radiopaque object between the heart and proventriculus (p) shadow is a passive induce transponder (PIT) identification chip. Liver (l), ventriculus (v) and spleen (s).



SECTION 3 INFECTIOUS DISEASES



Fig. 4.106 (A) Ventrodorsal survey radiograph of a saker falcon (*Falco cherrug*). A large rounded radiodense mass (arrowheads) can be observed within the celomic cavity close to the midline. (B) Lateral survey radiograph. The radiodense mass is an exceedingly enlarged spleen (arrowheads) clearly seen on the dorsal aspect of the ventriculus. Massive spleen enlargement could be due to bacterial (tuberculosis, chlamydophylosis) or viral diseases, or lymphoma.





Fig. 4.107 (A) Ventrordorsal survey radiograph of a gyr-saker hybrid falcon (*Falco rusticolus*-*Falco cherrug*) showing severe gaseous distension of the intestinal loops (arrowheads). The falcon was presented with a history of reduced appetite, chronic vomiting and progressive weight loss. The characteristic hourglass cardiohepatic waist is lost. (B) Lateral survey radiograph. Note the thickening of the wall of the ventriculus (black arrowheads) and intestinal loops (white arrowheads). This case of severe gastroenteritis was the result of a bacterial infection. The heart (h) and liver (l) shadows are displaced cranially.



SECTION 3 INFECTIOUS DISEASES



Fig. 4.108 Ventrodorsal survey radiograph of a saker falcon (*Falco cherrug*) showing gaseous distention of the ventriculus (black arrowheads) and cloaca (white arrowheads). A large and several smaller radiodense particles (open arrowhead) are observed within the ventriculus. These are lead particles originated from ingesting shot prey. The kidney (k) shadow appears enlarged.

SECTION 4 Degenerative diseases



Fig. 4.109 (A) Ventrodorsal survey radiograph of a gyr-saker hybrid falcon (*Falco rusticolus-Falco cherrug*). The radiograph shows a moderately enlarged liver. This was an incidental finding since the radiograph was obtained due to the compound fracture of the right humerus. The falcon was euthanized at the request of the owner. Histopathology confirmed the diagnosis of severe amyloidosis. (B) Photograph of the post-mortem examination. The liver is enlarged and dark green-brown in color. Amyloidosis is a metabolic disease characterized by mild to extensive deposition of an amorphous eosinophilic extra cellular material in several organs and tissues but mainly the liver, spleen and kidneys. In common with other avian species, AA-amyloid may be involved in this disease in falcons. In the Middle East, secondary amyloidosis has been associated with chronic inflammatory conditions such as bumblefoot.

SECTION 4 DEGENERATIVE DISEASES

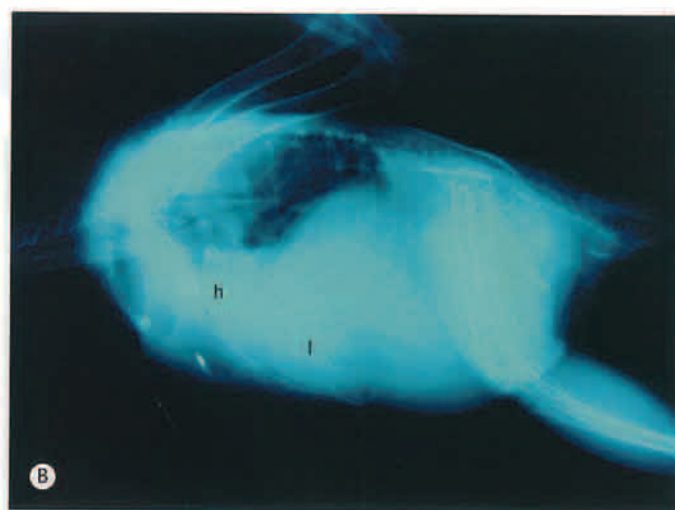
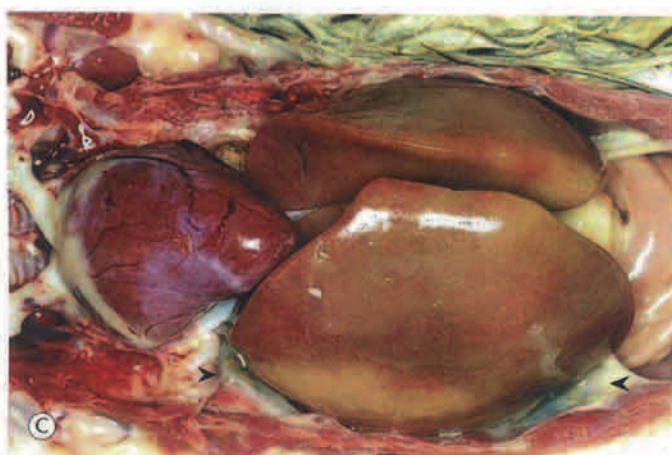


Fig. 4.110 (A) Ventrodorsal survey radiograph of a saker falcon (*Falco cherrug*) showing extensive diffuse radiopacity across the hepatic and peritoneal celomic cavities. On the radiograph it is not possible to differentiate the cardiohepatic waist or the gastrointestinal tract. The bird was suffering from ascites associated with severe amyloidosis affecting mainly the liver. Ascites is the accumulation of serous fluids in one or various celomic cavities. Heart (h) and liver (l). (B) Lateral survey radiograph. Ascites associated with severe liver congestion is the result of increased portal venous hydrostatic pressure and decreased portal venous colloid osmotic pressure. The falcon had a history of passing metallic-green urates, severe dyspnea and decreased appetite. The normal air sac triangle above the proventriculus is obliterated and the heart (h) and liver (l) are being displaced cranially. (C) Post-mortem examination. The liver is severely enlarged and with a yellow-green color. On sectioning, the liver was hard in consistency and had a waxy appearance typical of amyloidosis. Note the presence of serous fluids on the lateral aspect of the liver (arrowheads).



SECTION 5 Neoplastic diseases



Fig. 4.111 A large lipoma near the carpal joint of a saker falcon (*Falco cherrug*). This type of neoplasia is rare in raptors. The growth was successfully removed using standard surgical procedures.



Fig. 4.112 Bursitis or 'blaine' in a saker falcon (*Falco cherrug*) presenting as a swelling about the elbow joint. Serous-sanguinolent material is usually present in mild cases. However, in advanced cases purulent or caseous material may be present. This particular case was caused by constant rubbing of the elbow on the wall of an enclosure. Also note the droopy appearance of the wing.

SECTION 5 NEOPLASTIC DISEASES

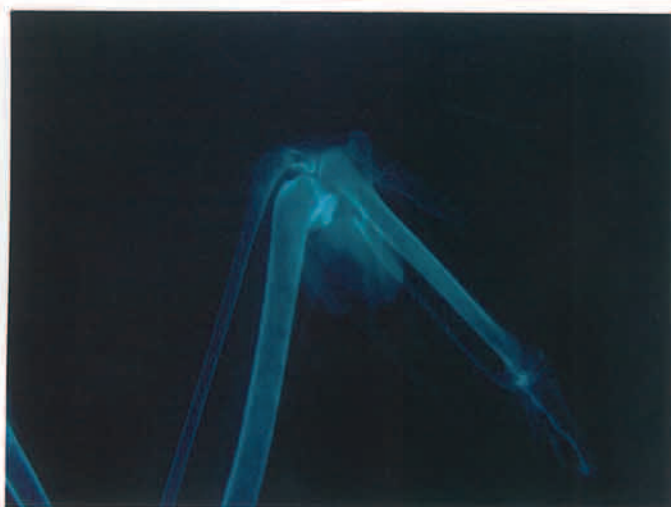


Fig. 4.113 Ventrodorsal radiograph of the distal wing of a falcon with mild carpal bursitis or 'blaine' showing soft tissue swelling of the carpus. Blaine is caused by trauma when a tethered falcon or hawk inflame the carpal tendon sheaths by knocking the carpus against the ground as they attempt to fly from their perch. No changes on the bone structures are evident in this radiograph. An aspirate should be collected for cytology, bacteriology and sensitivity tests. Treatment should include corrective husbandry, joint irrigation and appropriate antibiotic treatment. In chronic cases surgical intervention may be needed.

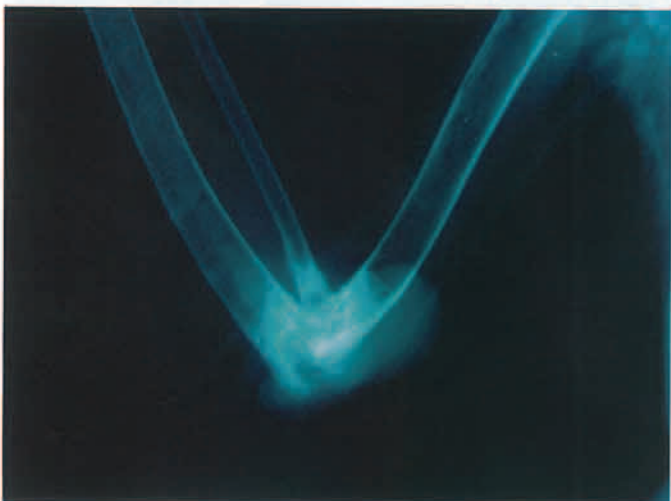


Fig. 4.114 Ventrodorsal radiograph of the elbow joint showing peri-articular soft-tissue swelling and lysis of the articular surfaces of the bones of the elbow joint.



Fig. 4.115 Craniocaudal radiograph of the elbow joint showing peri-articular soft-tissue swelling on the dorsal aspect of the joint and lysis of the articular surfaces of the bones of the elbow joint.

Chapter 5

Common diagnostic mistakes



Fig. 5.1 Misaligned ventrodorsal survey radiograph of a saker falcon (*Falco cherrug*). Note the position of the keel bone (black arrowhead) to the right of the median plane and the asymmetrical position of the wings and the pelvic limbs. In this radiograph, evaluation of the internal organs could result in a misdiagnosis. In addition, misalignment of the thoracic girdle could lead to a misinterpretation of a fracture of the clavicle (white arrowhead).



Fig. 5.2 Ventrodorsal radiograph of an egg-bound common kestrel (*Falco tinnunculus*) with what appears to be an abnormally sized egg. This bird laid the egg the following day without any difficulty. Members of the Falconidae lay large eggs. For instance, a 100 g kestrel can normally lay eggs weighing 15 g (courtesy of M Garcia-Montijano).



Fig. 5.3 (A) Ventrordorsal survey radiograph of a gyr-saker hybrid falcon (*Falco rusticolus-Falco cherrug*) with an apparent hepatomegaly (arrowheads). (B) Lateral survey radiograph showing a distended ventriculus full with a recent meal (arrowheads). The ventriculus is displacing the liver (l) cranially resulting in an enlarged liver shadow as seen in the ventrodorsal view. Falcons and other raptorial species should be fasted for a minimum of 12 h, but ideally 24 h before radiographic examination. In addition, raptors should be allowed to cast out any undigested material (pellet) composed of bones, fur and feathers from the previous meal.

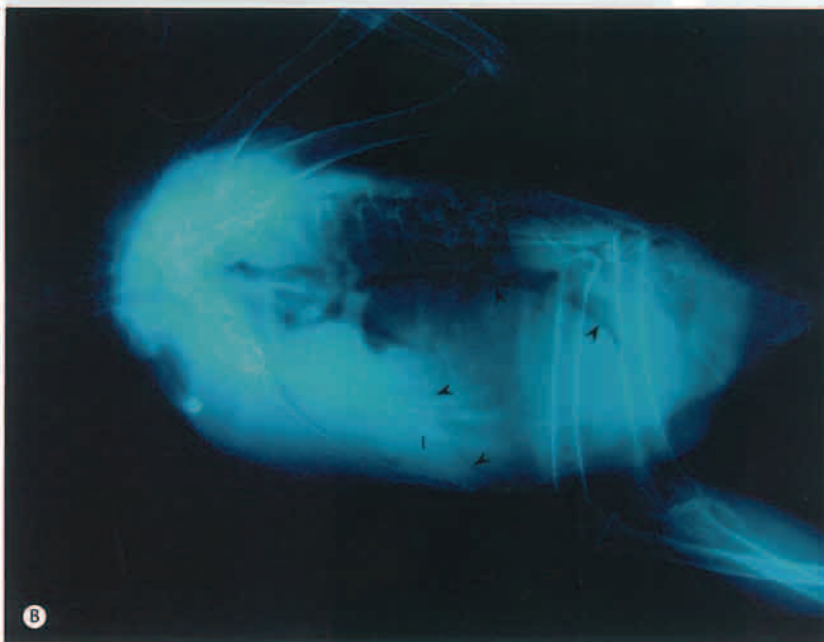
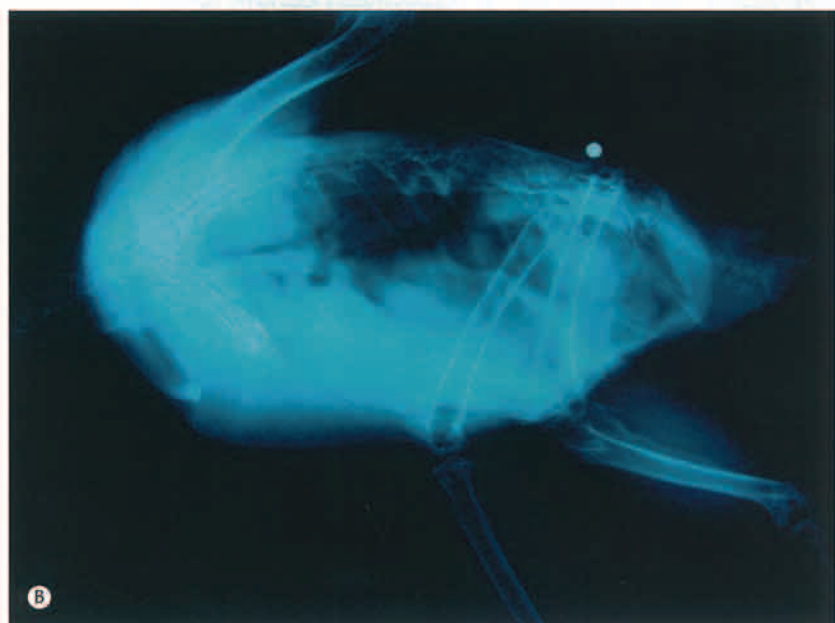




Fig. 5.4 (A) A shotgun lead pellet that appears to be within the gastrointestinal tract or the peritoneal cavity of a saker falcon (*Falco cherrug*). (B) Lateral survey radiograph showing the shotgun pellet lodged on the dorsal synsacrum region. Obtaining both ventrodorsal and lateral radiographs of the whole body is mandatory in order to avoid any misinterpretation of findings.



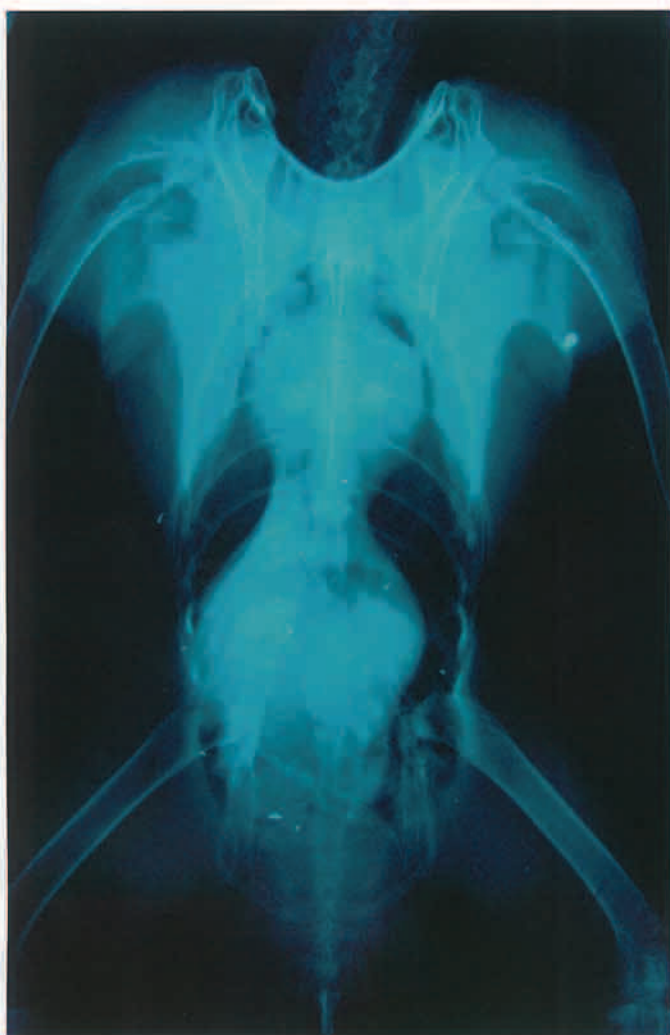


Fig. 5.5 Artifacts within the radiographic cassette. The radiopaque objects in this radiograph are actually lead paint flakes that chipped off from the sides of an old cassette. The lateral radiograph of this bird taken using a different cassette did not show these radiopaque materials. The radiopaque object in the left axilla is a passive inducer transponder (PIT) identification chip.

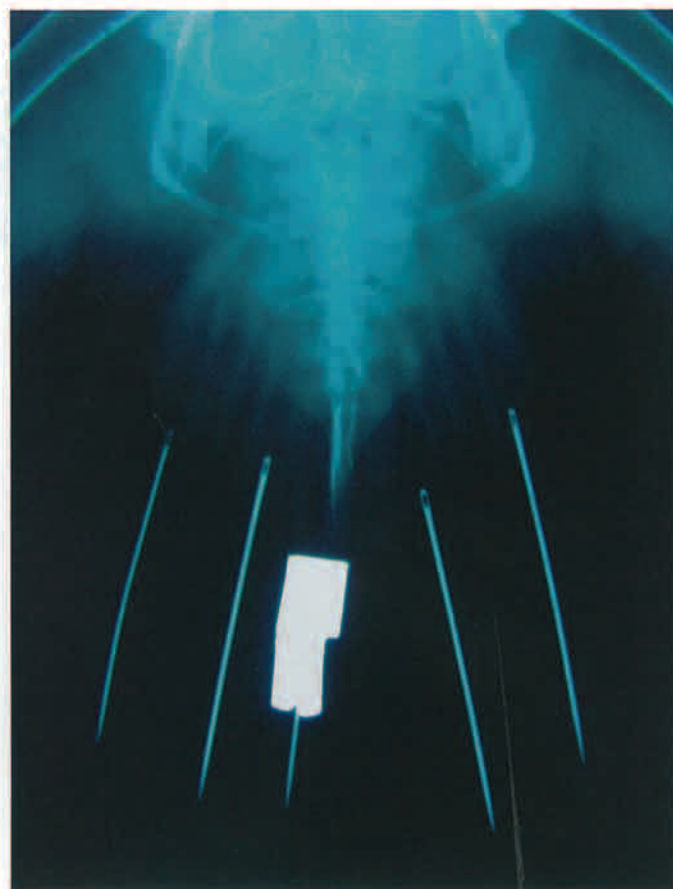


Fig. 5.6 Five stitching needles used to repair or imp the broken tail feathers. The large radiopaque object overlapping the middle needle is a custom made tail mount where a telemetry radio transmitter is attached during training or hunting.

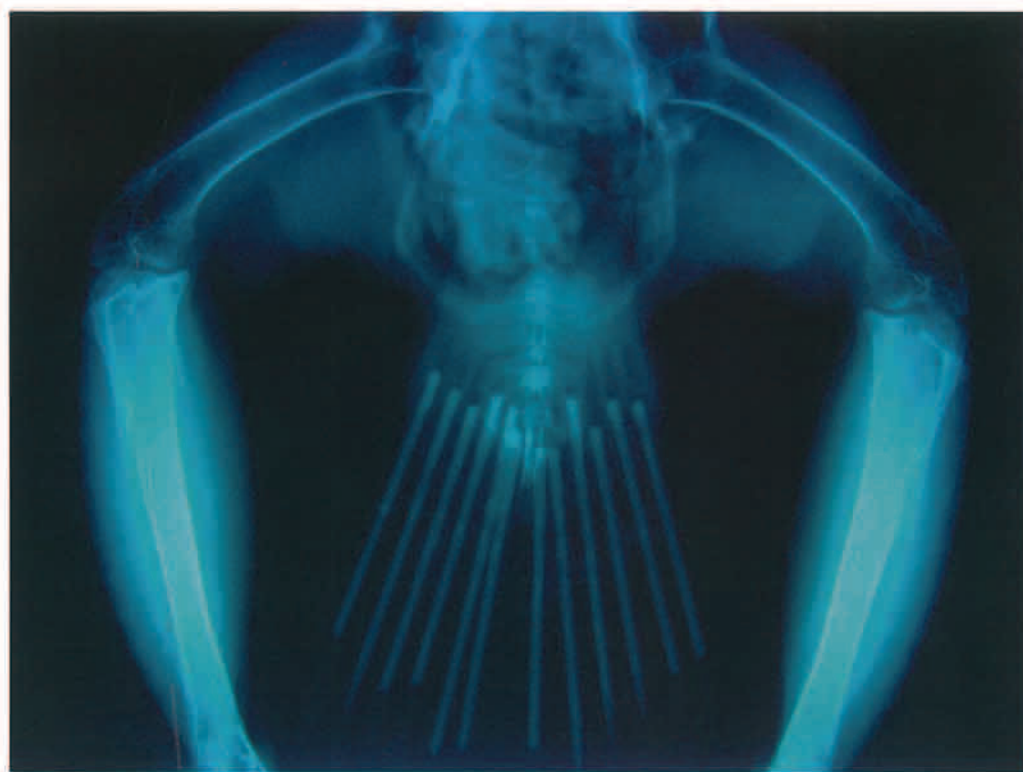


Fig. 5.7 All 12 tail feathers that were damaged beyond repair were cut near the base and replaced with a new set of feathers. Metallic knitting pins were used as splints to attach the new feathers to the old feather shafts and calamus.

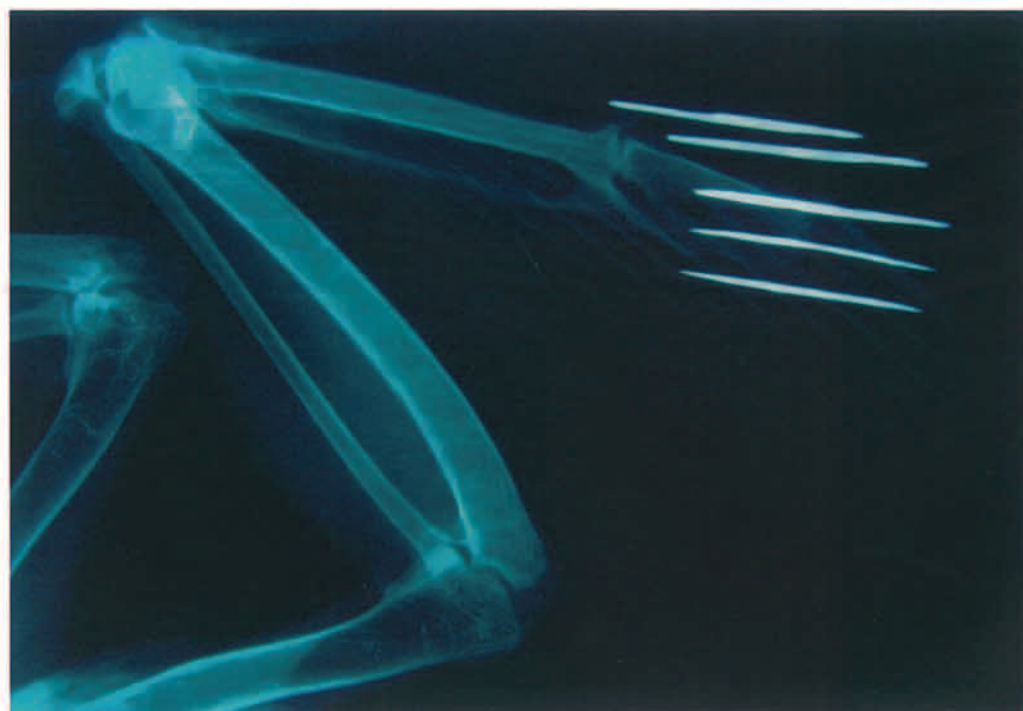


Fig. 5.8 This is a lateral survey radiograph of a falcon wing showing five metallic imping needles used to repair the broken distal third of the primary feathers. The needles are commonly manufactured from hair pin fasteners and glued in place using cyanoacrylate glue.



Fig. 5.9 (A) Ventrodorsal survey radiograph of a saker falcon (*Falco cherrug*) showing a severely distended ventriculus with a recent meal (arrowheads). This bird was fed four hours prior to examination. Some food is still in the crop as evidenced by the soft-tissue radiopacity in the caudal neck region (arrows). Similar soft-tissue opacities in the neck region could be observed in cases of trichomonosis and candidiasis infections. (B) Lateral survey radiograph. Fragments of bones and other food items are present in the severely distended ventriculus (arrowheads) and proventriculus. Also, note the increased radiopacity in the caudal neck region (arrow). The condition of the spleen, intestines and abdominal airsacs cannot be assessed in this radiograph.



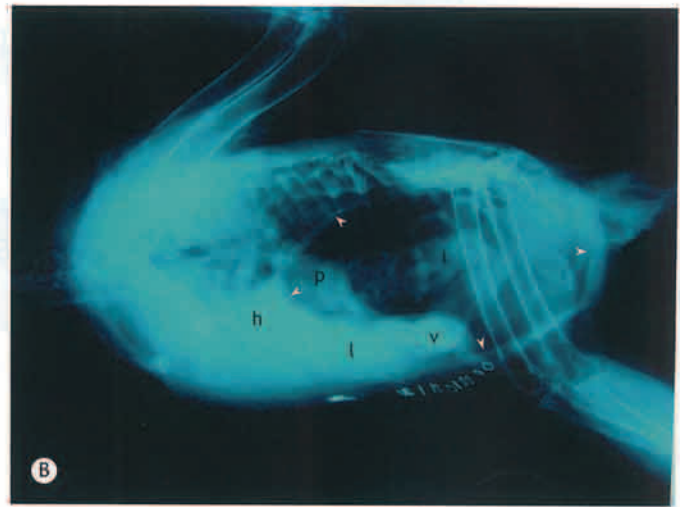
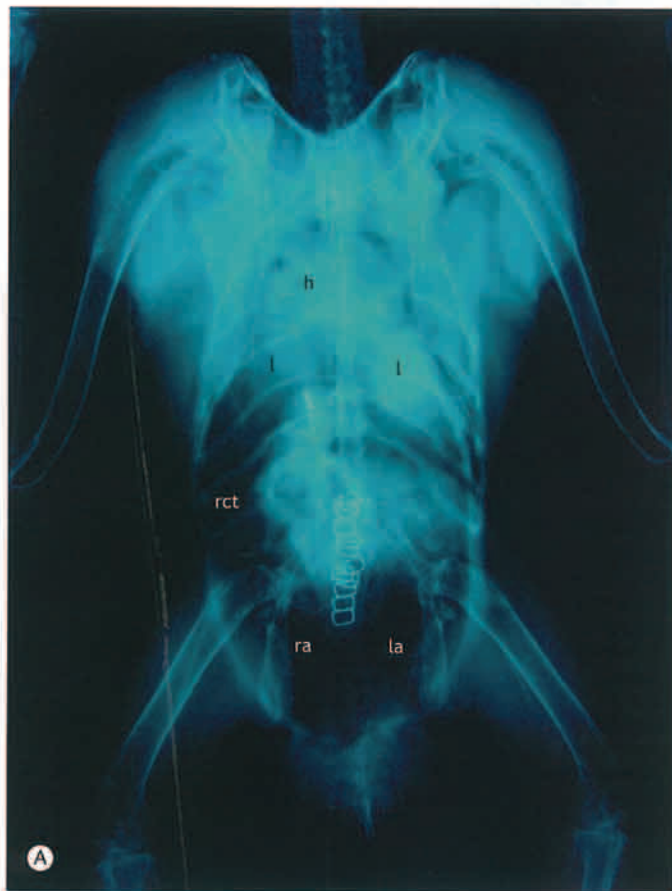


Fig. 5.10 (A) Ventrodorsal survey radiograph of a saker falcon (*Falco cherrug*) presented for examination with dyspnea, poor flight performance, reduced appetite and green urates. Extensive air trapping is evident in the right caudal thoracic (rct), right abdominal (ra) and left abdominal (la) air sac fields. The organs are displaced cranially toward the left celomic cavity. Note the surgical staples used to close the abdominal skin incision made during an exploratory coeloscopy examination. Heart (h) and liver (l). (B) Lateral survey radiograph. Note the cranial displacement of the organs and the extensive air trapping of the caudal thoracic and abdominal air sacs (arrowheads). The radiopaque object cranial to the staples is a PIT identification chip. Liver (l), heart (h), proventriculus (p), ventriculus (v) and intestines (i).

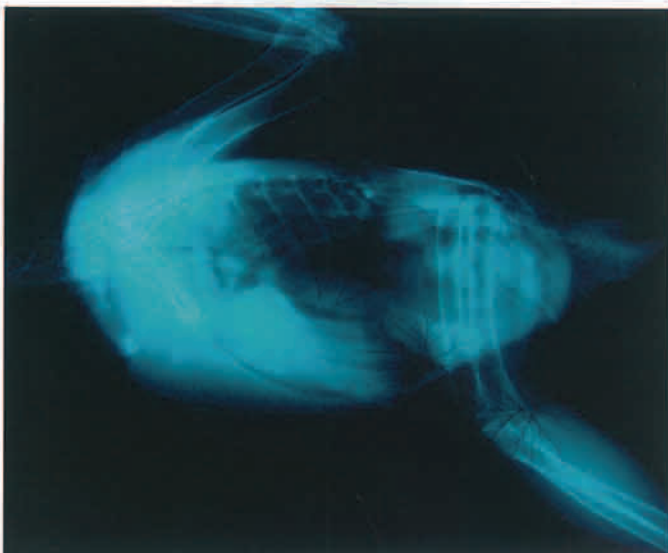


Fig. 5.11 Lateral survey radiograph with different spider-web patterns due to exposure to static electricity.

Chapter 6

Advanced clinical anatomy imaging

Paolo Zucca, Roberto Pozzi-Mucelli, Donatella Gelli, Mauro Delogu

SECTION 1 The importance of advanced diagnostic imaging in veterinary medicine

Every enough advanced technology is not distinguishable from magic

Third Clark's Law, Murphy's Law (Block 1988)

Radiology has become an essential diagnostic tool in veterinary medicine since its discovery in 1895. An early and accurate diagnosis very frequently requires the support of radiology. Since the early 50s, when veterinarians began to introduce diagnostic radiography in their daily practice (Burk & Ackerman 1996, Schnelle 1945), several advanced diagnostic imaging techniques have been developed and used in veterinary clinical practice. In the 60s, the sonar technology, developed for military purposes, was applied to diagnostic imaging with the production of the first ultrasound apparatus. This diagnostic technique is nowadays widely used in the daily veterinary patient management and care. During the past 30 years, several diagnostic

imaging tools, each exploiting different physical phenomena and allowing physiologic and clinical interpretation, have been developed (Higgins et al 1997). These include digital radiology (DR), computed tomography (CT scan), magnetic resonance imaging (MRI), and nuclear medicine (including single photon emission computed tomography [SPECT] and positron emission tomography [PET]). As mentioned previously, veterinary radiology plays a central role in the medical care and management of animals, and DR, ultrasound, CT scan and MRI are increasingly being used on a regular basis by veterinarians in several countries. However, due to the high costs related to the purchase and maintenance of units such as those for CT scan and MRI, only few veterinary centers are equipped. As a consequence, animal patients are commonly examined in human hospitals or medical centers.



Fig. 6.1 Tawny owl (*Strix aluco*), adult, CT scan, 3D surface representation, frontal view. Please note the almost complete protrusion of the left eye due to trauma.

SECTION 2 Material and methods

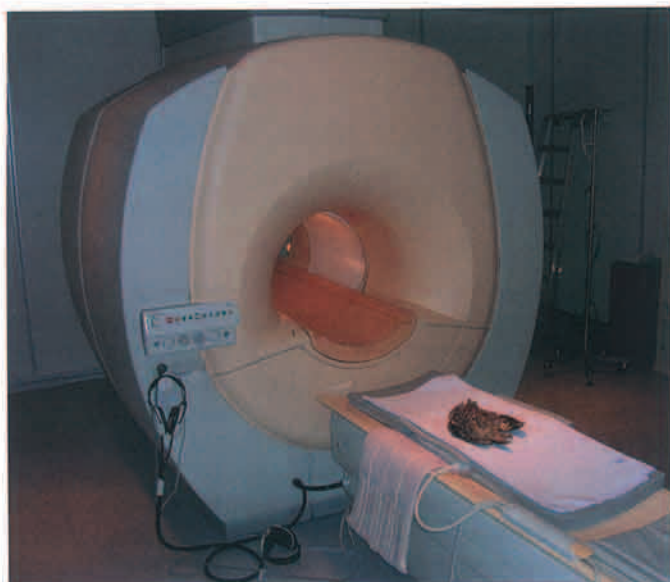


Fig. 6.2 Tawny owl (*Strix aluco*), adult, died in a raptor rescue and rehabilitation center due to traumatic injuries, before to be positioned inside the MRI 1.5 Tesla room (Cattinara University Hospital, Trieste, Italy).

A critical point in digital imaging and telemedicine in veterinary medicine is related to the background knowledge (see also Talbot 1991, Smith & Williams 2000) that is required to manage and to refer a DR, a CT or a MRI scan. It is technically impossible to move directly from the use of classic radiography to the new advanced diagnostic imaging tools without acquiring a basic knowledge of image manipulation, in the broadest meaning of the term. The aim of this Chapter and the related interactive DVD enclosed with this book is to be learning tools for those who want to acquire a basic knowledge of veterinary digital imaging in the field of avian medicine. The content of the Chapter and the DVD are strictly related, but different. In this Chapter, after a brief description of the Digital Imaging and Communications in Medicine (DICOM) standard and its use in veterinary imaging, we focus on the advanced diagnostic imaging techniques and their use in the avian patient.

The interactive DVD has different contents, but basically includes the same philosophy. Commonly, digital images when published, especially if related to medical topics, are always protected and readers can simply observe them from a 'locked' perspective. This is not the best way to learn the use of a new tool. We decided to create a pedagogic 'open source' DVD to allow interested colleagues to practice with veterinary digital imaging on their own home computer. We used two species of raptors as models, one

nocturnal, a tawny owl (*Strix aluco*) and one diurnal, a lanner falcon (*Falco biarmicus*). Both birds had suffered traumatic injuries and have died in a raptor rehabilitation center. The tawny owl suffered a traumatic injury with lesions on the left side of the body (eye, wing and foot, see pictures and captions), while the lanner falcon died of an abscess of traumatic origin close to the crop and the lower jaw. Both specimens were frozen for several weeks. For each bird in the same position, full body CT and MRI scans were performed. A MRI study of the tawny owl head was also obtained. CT scans were conducted using a spiral CT unit (Philips AV1, Philips, Eindhoven, The Netherlands). Three mm thick slices, with 5 mm table increments were acquired (pitch 1.4) and images were reconstructed every 3 mm. MRI scans were conducted using a 1.5 T unit (Intera, Philips, Eindhoven, The Netherlands), slice thickness 2.00 mm, interslice gap 0.2 mm, using spin echo and gradient echo sequences. These images were digitally stored and then processed with a DICOM imaging program (Stack View package for CT/MR images) on an independent workstation (EasyVision Release 5.2 system of Philips Medical Systems, Philips, Eindhoven, The Netherlands) to produce different transverse slices and 3D models of the two raptors species. Figure 6.7C and Figure 6.8 have been produced using a freeware DICOM program (*MRicro*, see below).

The complete sets of DICOM images are stored in different folders on the DVD. The DVD also contains a freeware program, *MRicro*, kindly provided by Professor Chris Rorden from the University of Nottingham (UK), that allows seeing and modifying the different format on which the digital images can be stored. The program contains several features that allows examining a DICOM set of images along the different planes of the space, axial, coronal, sagittal and furthermore allows users to render 3D images starting from a set of DICOM images. For further details please refer to the DVD index, the related video tutorial and help files enclosed within the DVD. The animal models used for ultrasonography were a Eurasian buzzard (*Buteo buteo*) and three tawny owls (*Strix aluco*), all adults and recovered from a local raptor center. Ultrasound studies, captions and videos were made using a new generation hand-held echography unit (My Lab 30, ESAOTE, Genoa, Italy). This is a miniaturized ultrasound machine equipped with instrumentation for standard echography and provided with new software for tissue Doppler and contrast echocardiography. Furthermore, the unit is equipped with several I/O devices, such as, a RW/DVD and a USB port for a quick transfer of diagnostic data.

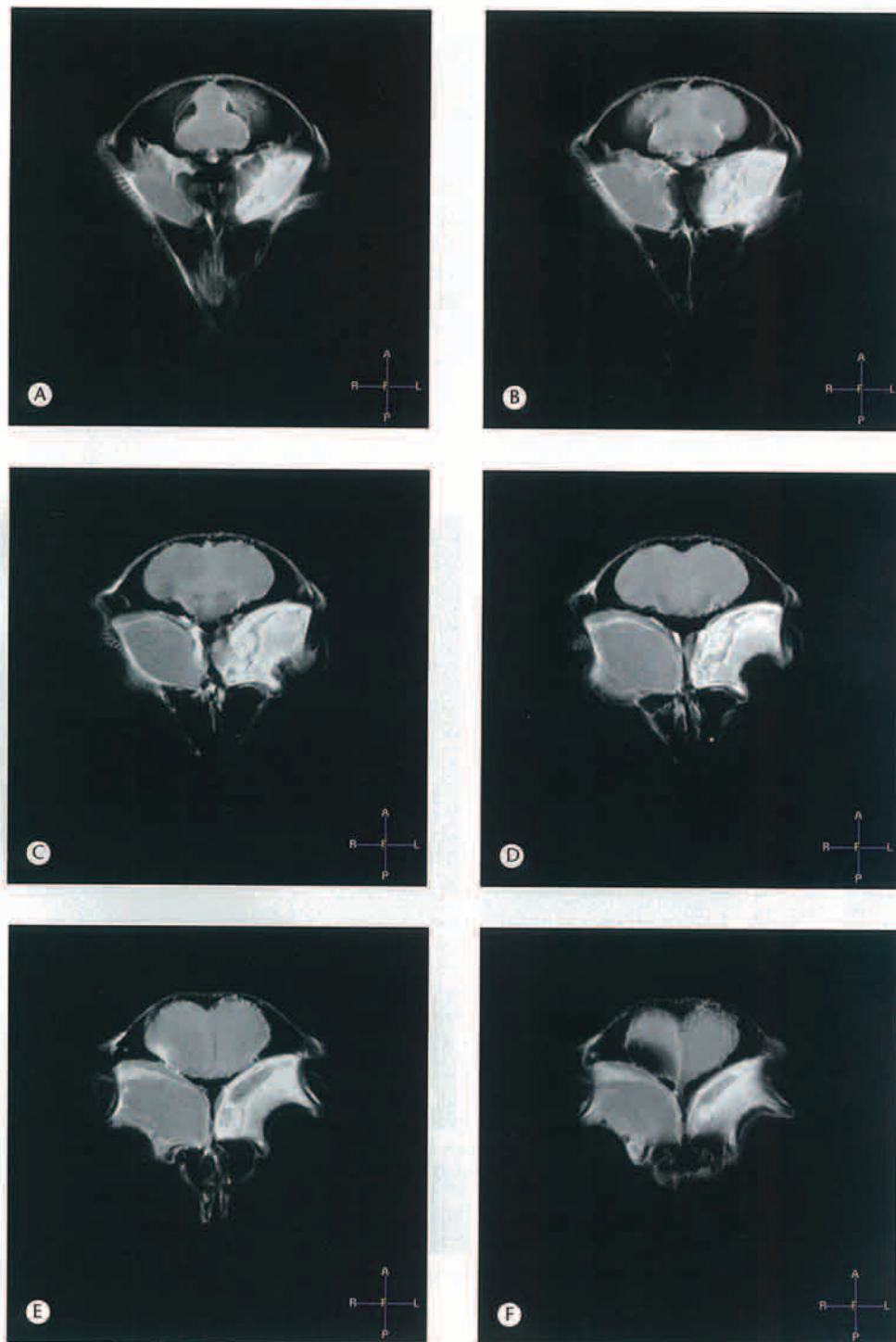


Fig. 6.3 (A–F) Tawny owl (*Strix aluco*), adult, MRI scan, axial sections of the head, DICOM images saved as TIFF. The traumatic injuries to the left side of the head involved the eye and also the brain (see also Figs 6.5 & 6.7).

SECTION 3 THE DIGITAL IMAGING AND COMMUNICATIONS IN MEDICINE STANDARD (DICOM)

SECTION 3 The Digital Imaging and Communications in Medicine standard (DICOM)

The DICOM Standards Committee (<http://medical.nema.org/>) exists to create and maintain international standards for the communication of biomedical, diagnostic and therapeutic information in those medical disciplines that use digital images and associated data. One of the DICOM standards defines a file format for the distribution of images and people refer to images files that are compliant with part 10 of the DICOM standard as DICOM format file (NEMA PS 3-10 and Version 4.0 Strategic Document 2004). DICOM images will become a

standard also for veterinary medicine and, in a non-distant future, you will be able to view or refer an animal for ultrasound, CT or MRI saved with this format. You need to know how to view these images and how to get from them additional information.

The DVD of the book contains free software (*MRicro*) that allows opening and viewing every DICOM file and gives the opportunity to create 3D reconstructions of CT and MR data sets, similar to Figures 6.1, 6.4 and 6.6–6.8.

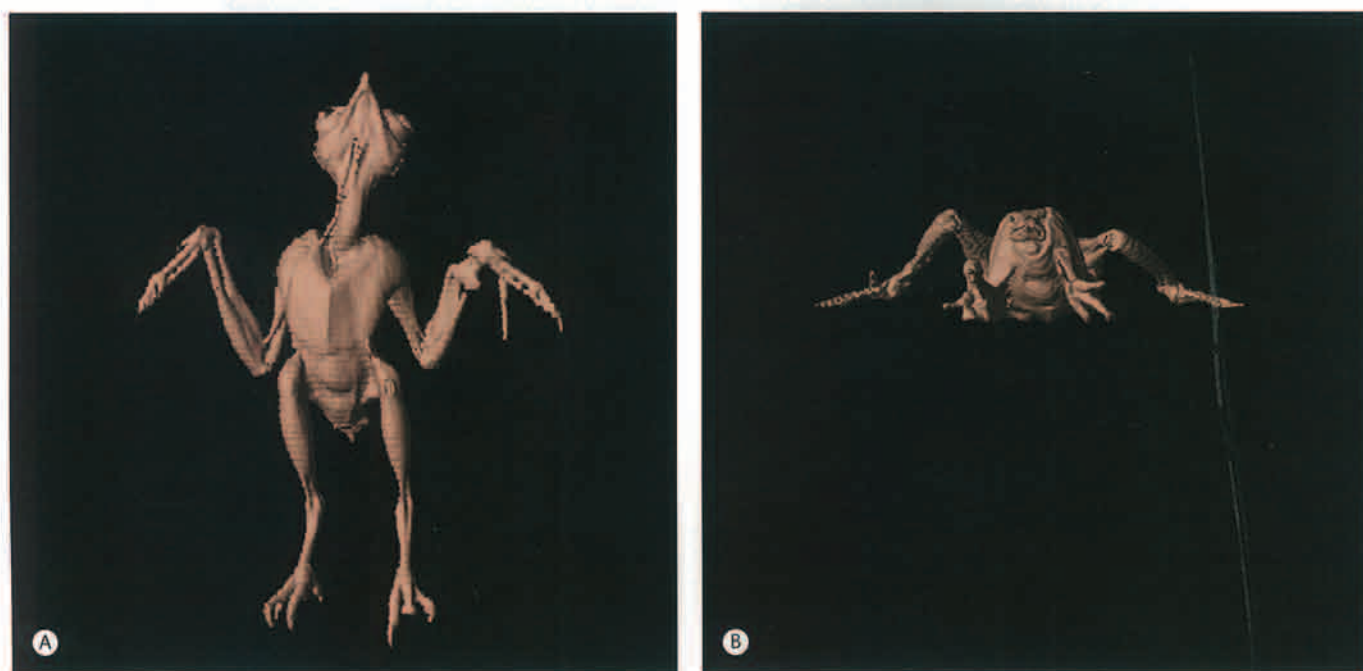


Fig. 6.4 Tawny owl (*Strix aluco*), adult: CT scan, 3D surface representation of the six different views of the body, respectively (A) ventral, (B) caudal. It is possible to observe several lesions to the left side of the body (eye, wing and talon).

SECTION 3 THE DIGITAL IMAGING AND COMMUNICATIONS IN MEDICINE STANDARD (DICOM)



Fig. 6.4 (Cont'd) Tawny owl (*Strix aluco*), adult: (C) frontal, (D) right lateral, (E) left lateral, (F) dorsal. It is possible to observe several lesions to the left side of the body (eye, wing and talon).

SECTION 4 Advanced diagnostic imaging techniques

Ultrasound for the avian patient

The use of ultrasonography in birds has been limited due to the anatomical features of this Class. The centralization of internal organs inside the celomic cavities, surrounded dorsally by bones and ventrally and laterally by the anechogenic air sacs, makes echography a diagnostic technique not easy to perform in the avian patient. However, several acoustic windows allow access to the internal organs. The liver is the abdominal organ that allows the easiest ultrasound investigation. Through the liver, several organs, such as the proventriculus, ventriculus and spleen can be visualized. The cloaca with its fecal content and urates can also be easily investigated with ultrasound. The reproductive tract can be best examined during the breeding season, although in larger birds some structures, such as the oviduct, can be visualized under normal conditions. The kidneys can also be examined in the larger avian patient, although the presence of the vertebral column and the pelvic bones do not allow the use of a sufficiently wide acoustic window and often limit the visualization of these organs. In birds, the kidneys are usually detected when pathological conditions cause their enlargement. With regards to echocardiography, the thoracic anatomy only allows a transhepatic approach, although filling the crop with water is possible to create a

virtual window and to obtain good ultrasound thoracic images. The four chambers of the avian heart can be investigated only in a long axis view, as the presence of the ribs does not allow a short axis projection. Ocular ultrasonography is a valuable diagnostic tool in human and veterinary medicine because it allows the evaluation of the internal structures of the eye and of the retrobulbar soft tissues, which may be obscured from direct visualization by several diseases that cause ocular enlargement and opacity. Several studies have been performed to improve the use of ultrasound in birds (Carrani et al 2003, Krautwald-Junghanns & Enders 1994, Krautwald-Junghanns et al 1995, Pees et al 2003). This imaging technique is now considered a useful diagnostic tool. Echocardiography should be considered an integral part of the clinical examination of 'athletic patients' such as hunting falcons. Furthermore, introducing ultrasound examination of birds in the daily practice could allow detection of other alterations in different organs (e.g. spleen enlargement in *Chlamydophila* infection, proventricular dilatation in avian gastric yeast infection, cloacal pathologies) for which an early diagnosis could be important. However, more studies are needed to create a standard set of reference avian echographic values and to relate them to clinical and laboratory findings.

SECTION 4 ADVANCED DIAGNOSTIC IMAGING TECHNIQUES

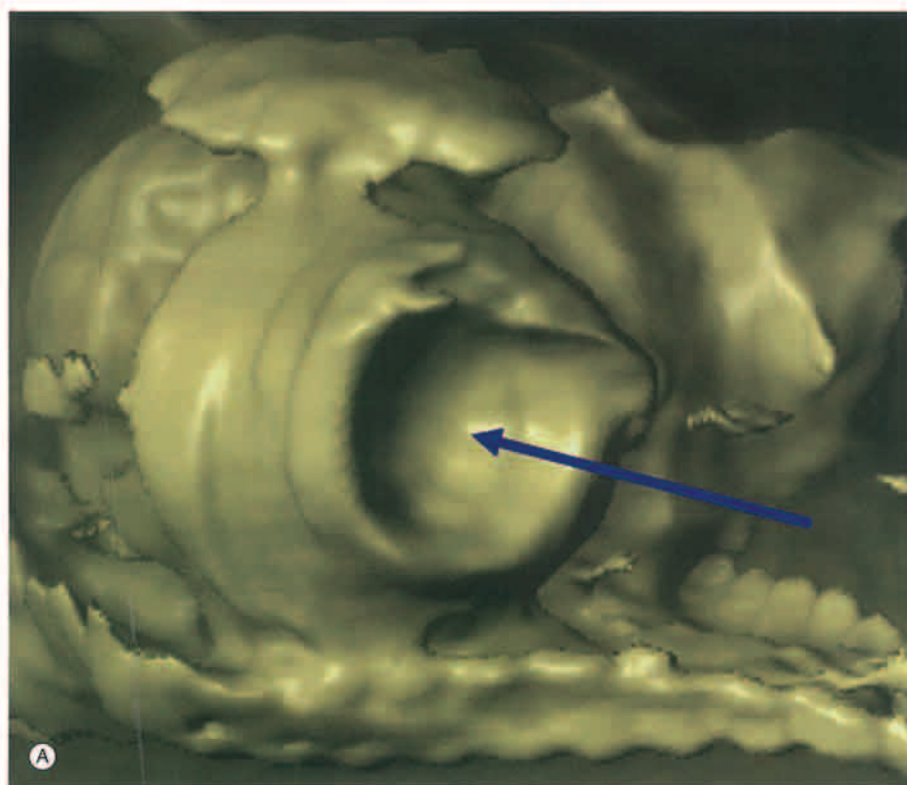
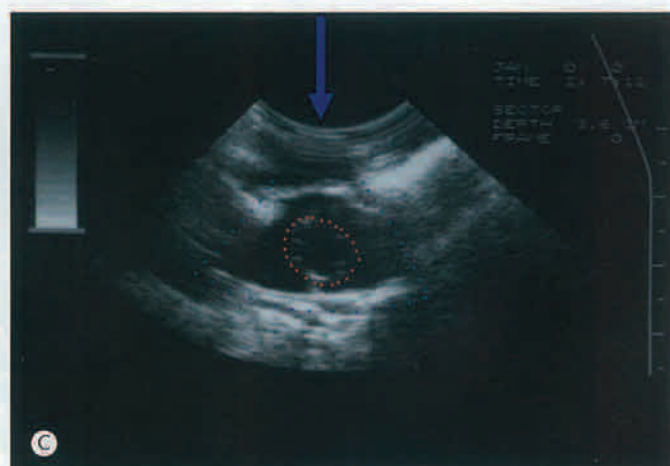


Fig. 6.5 Tawny owl (*Strix aluco*), adult: (A) CT scan, 3D surface representation of the head, detail, right lateral view – the blue arrow shows the window used for the ultrasound study of the eyes in different tawny owls. See (B) and (C) below. (B) ultrasound study of the eye, traumatic detachment of the retina; (C) ultrasound study of the right eye, posterior luxation of the lens.



SECTION 4 ADVANCED DIAGNOSTIC IMAGING TECHNIQUES

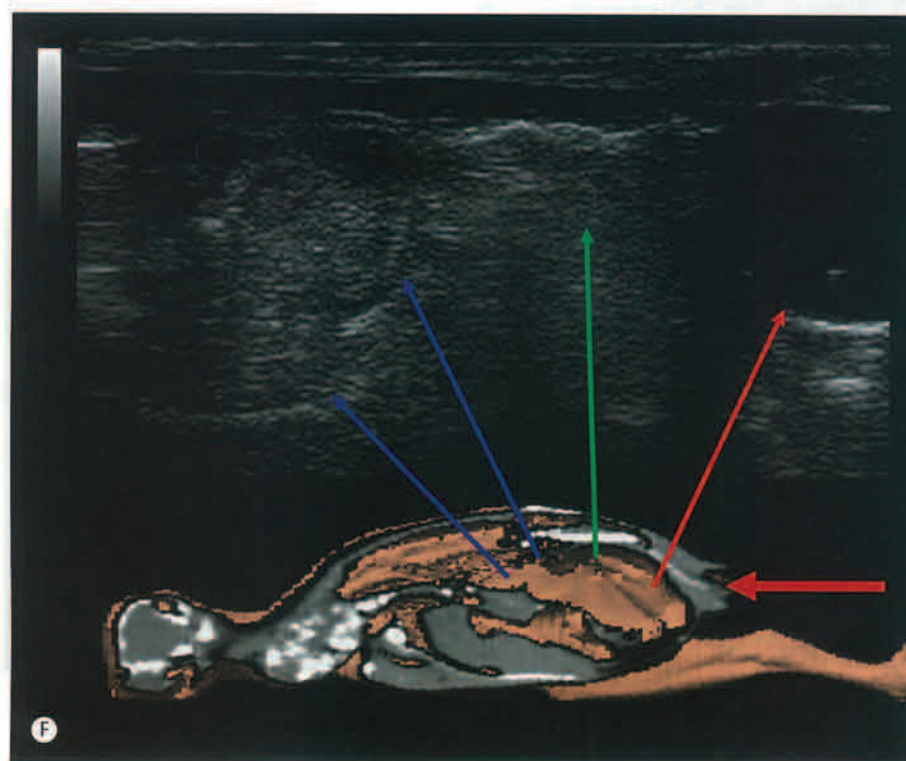
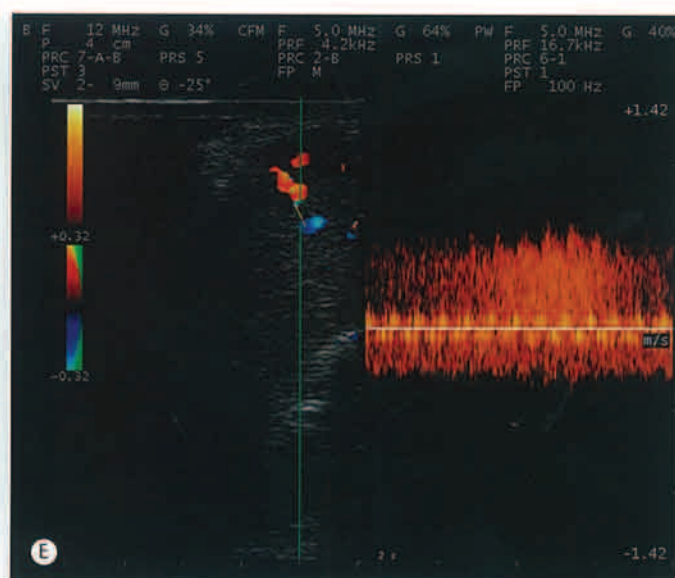
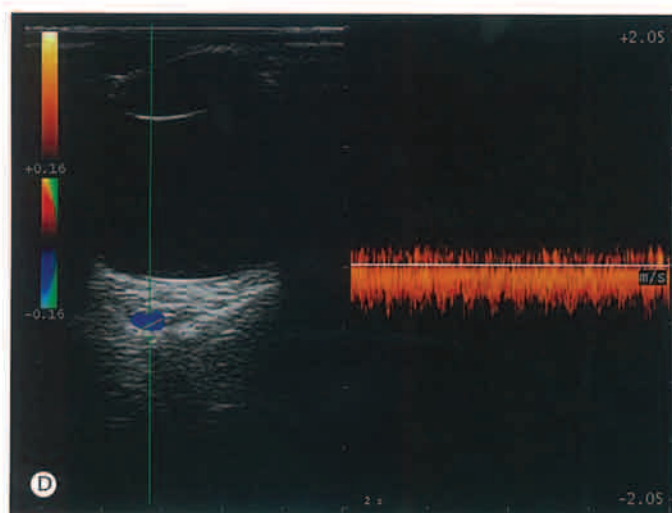


Fig. 6.5 (Cont'd) Eurasian buzzard (*Buteo buteo*), adult: (D) ultrasound study of the left eye, eco-Doppler of a vessel under the retina. (E) eco-Doppler of an hepatic vessel; (F) long axis examination of the stomachs (blue arrows), intestine (green arrow) and cloaca (orange arrow).

SECTION 4 ADVANCED DIAGNOSTIC IMAGING TECHNIQUES

Computed tomography for the avian patient

Although CT cannot yet be defined as a routine diagnostic tool in veterinary medicine, the number of veterinary practices using CT scan for the diagnosis of diseases in pets is increasing fast all over the world. With regards to birds, there are only a handful of papers referring specifically to these species (Bartels et al 2000, Garland et al 2002, Gumperberger & Henninger 2001, Gumperberger & Korbel 2001, Krautwald-Junghanns et al 1998a, 1998b, Orosz & Toal 1992, Romvari et al 2004, Silverman 1993).

One of the main problems performing a correct CT scan in birds with a small body size is related to the adequate choice of a scanning protocol that takes into consideration the needs for coverage and resolution. The section thickness is another parameter that has to be evaluated before the start of the examination. 3D CT scan with volume/surface representation has a great potential for increasing anatomical knowledge of avian species. The quality of the 3D reconstructions is also related to the section thickness. The smaller the slice thickness and the slice gap are the better is the image resolution in the 3D reconstruction, expanding the imaging possibility of this diagnostic tool in avian medicine.



Fig. 6.6 Lanner falcon (*Falco biarmicus*), adult: (A) CT scan, 3D surface representation of the full body, cranial view; (B) details of the right wing; (C) caudal view, please note the angle of the wing's joints.



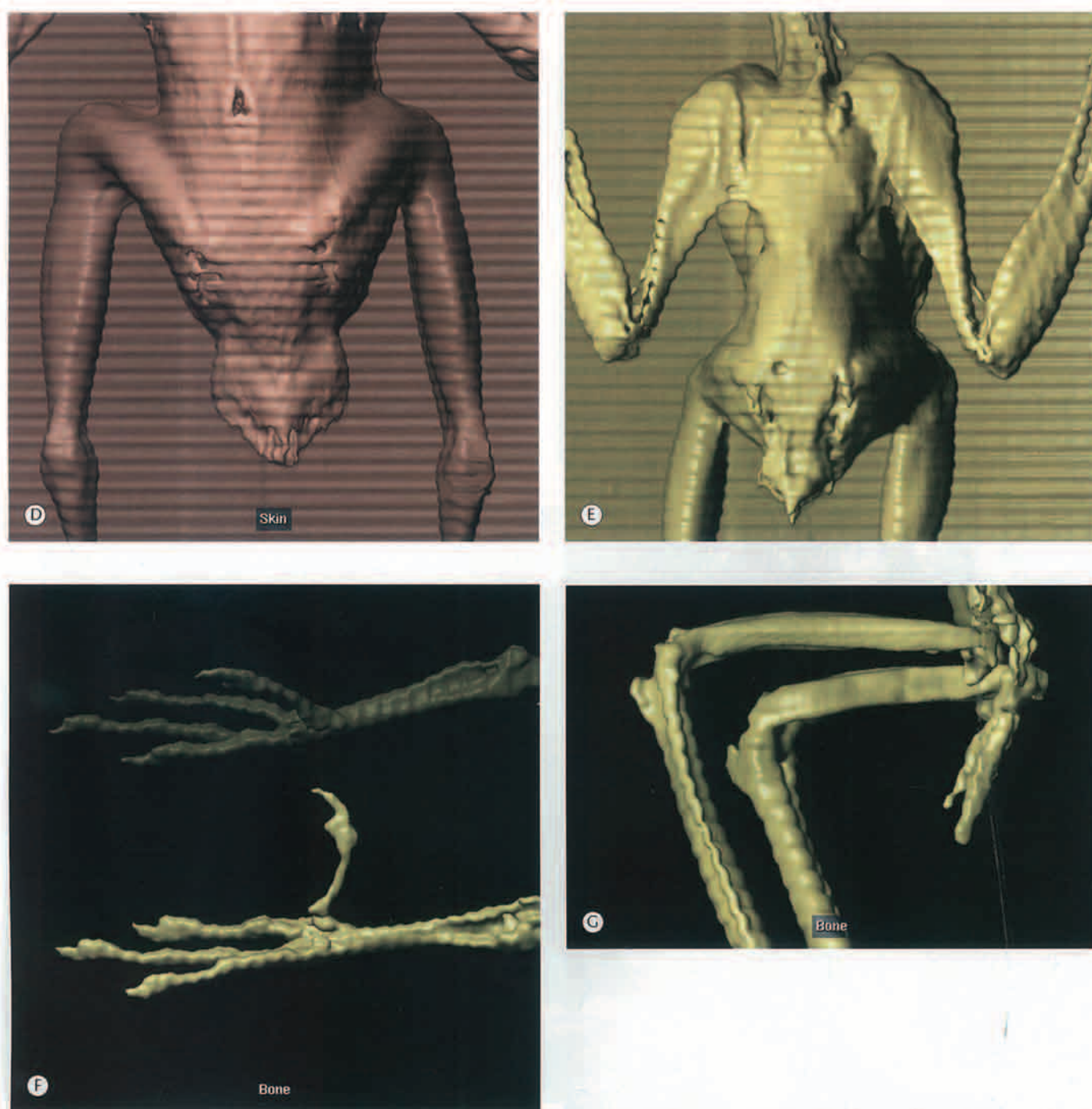


Fig. 6.6 (Cont'd) Lanner falcon (*Falco biarmicus*), adult: (D) dorsal view, magnification of the synsacrum and the femoral area. Tawny owl (*Strix aluco*), adult: (E) CT scan, 3D surface representation of the body, dorsal view, magnification of the synsacrum and the femoral area. Lanner falcon (*Falco biarmicus*), adult: (F) CT scan, 3D surface representation of the legs, bone layer, dorsal right lateral view; (G) it is possible to see the bone layer, synsacrum, femurs and tibiotarsus (partially), left dorsolateral view.

SECTION 4 ADVANCED DIAGNOSTIC IMAGING TECHNIQUES

Magnetic resonance imaging for the avian patient

MRI is not commonly used in avian medicine and there are very few references available (Fleming et al 2003, Romvari et al 2004). However, several MRI studies have been performed on different avian species in order to study neuroanatomy and functions and neuronal plasticity of the avian brain (Tindemans et al 2003, Van der Linden et al 1998, 2004, Verhoye et al 1998). The main problem with MRI use in avian patient is to establish common scanning protocols for this Class. Learning to position the

bird properly and choosing the correct imaging sequences and scanning planes are essential for a successful MRI scanning. Furthermore, each system or organ requires a different protocol. Veterinary spine or brain MRI scanning protocols are already available for pet species such as dogs and cats, but not for avian patients. However, MRI has the same great potential in increasing the anatomical and diagnostic investigations in avian species, as mentioned for CT scan and its actual limit is simply related to the high costs involved in the purchase and maintenance of the equipment.

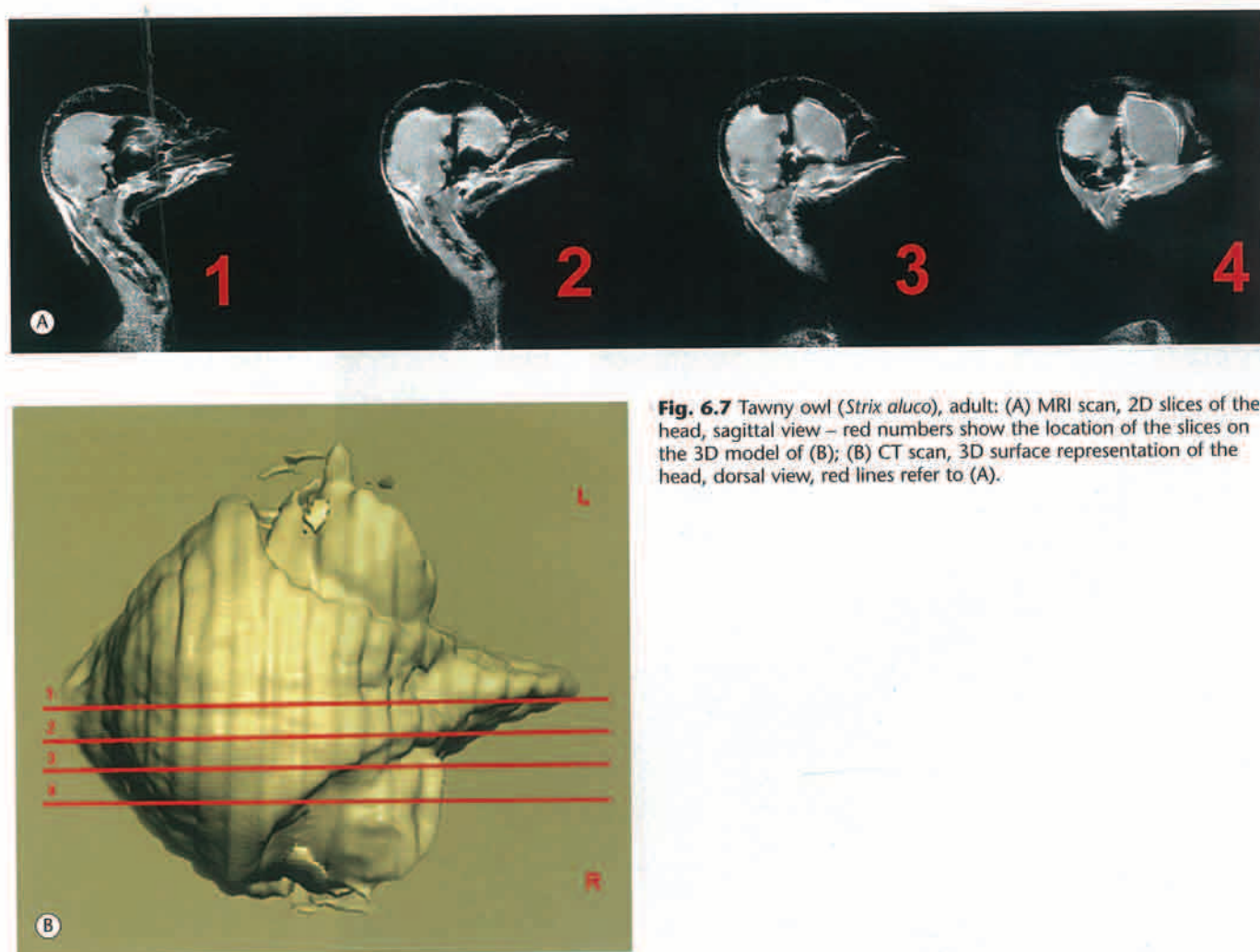


Fig. 6.7 Tawny owl (*Strix aluco*), adult: (A) MRI scan, 2D slices of the head, sagittal view – red numbers show the location of the slices on the 3D model of (B); (B) CT scan, 3D surface representation of the head, dorsal view, red lines refer to (A).

SECTION 4 ADVANCED DIAGNOSTIC IMAGING TECHNIQUES

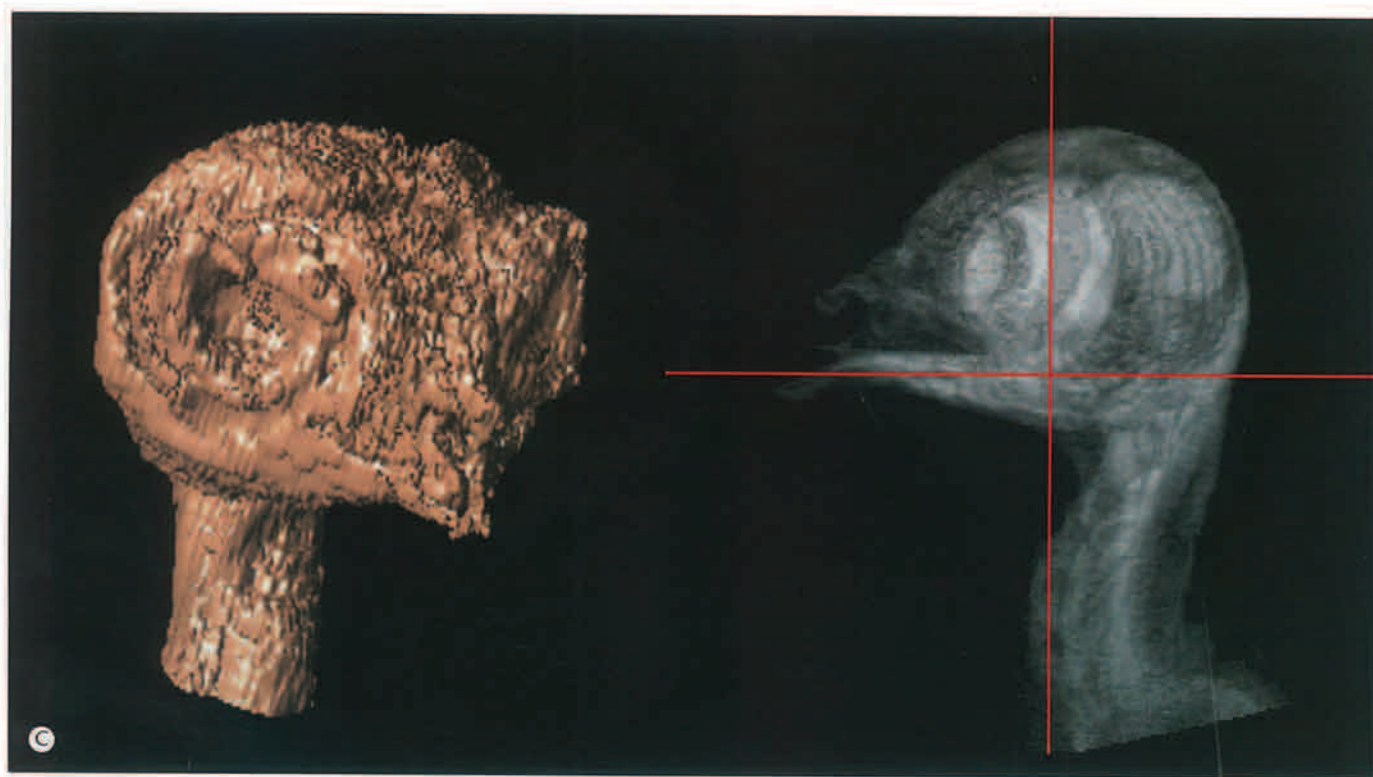


Fig. 6.7 (Cont'd) Tawny owl (*Strix aluco*), adult: (C) MRI scan, 3D representation of the head: 'surface' mode on the left and 'image' mode on the right. Please note the difference with a similar 3D surface representation obtained from the same specimen but from the CT scan examination as in Figures 6.1, 6.5A and 6.7B.

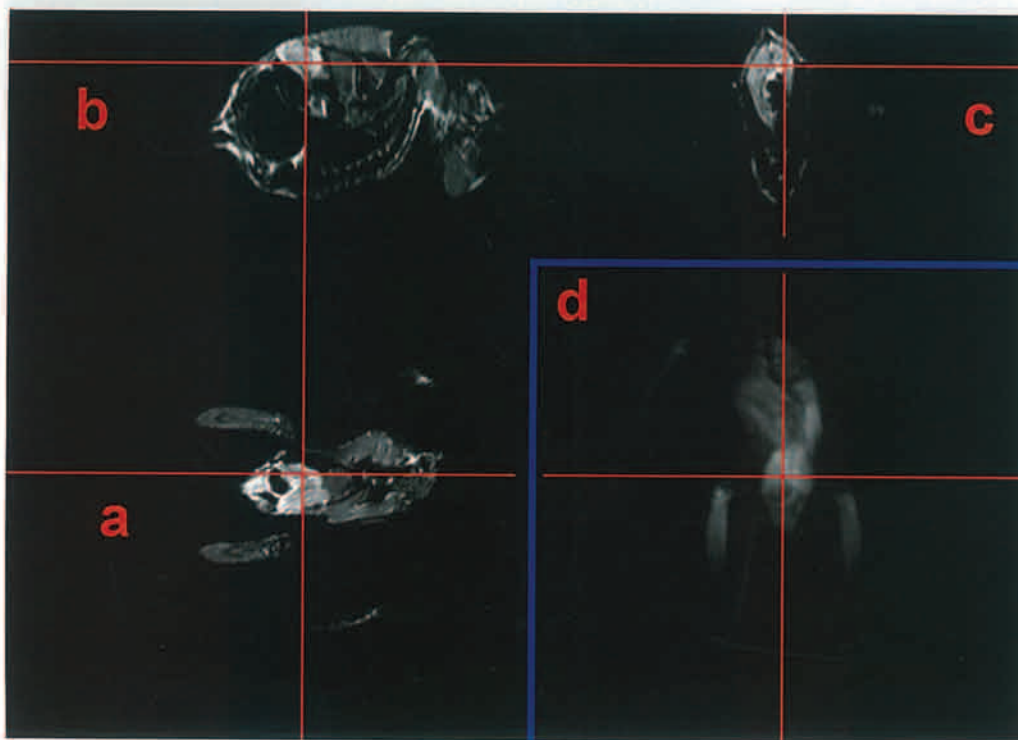


Fig. 6.8 Tawny owl (*Strix aluco*): MRI scan, liver, detail: a, b, c view of the same liver area in the three spatial positions; d, like 'a' with a different contrast.

SECTION 4 ADVANCED DIAGNOSTIC IMAGING TECHNIQUES

Acknowledgements

We would like to thank Mr Guido Comar, University of Trieste, Italy; Professor Maria Cova, Dr Matteo Coss and Mr Valter Amesich, Radiology Unit, Cattinara University Hospital, Trieste, Italy; Professor Giorgio Vallortigara, Department of Psychology, University of Trieste, Italy; Dr Gino D'Agnolo, Trieste, Italy and Dr Sara Tarabocchia, Trieste, Italy for the help and assistance given to us.

References

- Bartels T, Krautwald-Junghanns ME, Portmann S et al 2000 The use of conventional radiography and computer-assisted tomography as instruments for demonstration of gross pathological lesions in the cranium and cerebrum in the crested breed of the domestic duck (*Anas platyrhynchos*). *Avian Pathology* 29:101–108
- Burk RL, Ackerman N 1996 Small animal radiology and ultrasonography: a diagnostic atlas and text, 2nd edn. WB Saunders, Philadelphia
- Carrani F, Gelli D, Salvadori M et al 2003 A preliminary echocardiographic initial approach to diastolic and systolic function in medium and large parrots. *Proceedings of European Association of Avian Veterinarians*, April 22–26, Tenerife, Spain, pp. 145–149
- Fleming GJ, Lester NV, Stevenson R et al 2003 High field strength (4.7T) magnetic resonance imaging of hydrocephalus in an African grey parrot (*Psittacus erithacus*). *Veterinary Radiology Ultrasound* 44:542–545
- Garland MR, Lawler LP, Whitaker BR et al 2002 Modern CT applications in veterinary medicine. *Radiographics* 22:55–62
- Gumperberger M, Henninger W 2001 The use of computed tomography in avian and reptilian medicine. *Seminars in Avian and Exotic Pet Medicine* 10:174–180
- Gumperberger M, Korbel R 2001 Ultrasonographic and computer tomographic examinations of the avian eye. *Proceedings of European Association of Veterinary Diagnostic Imaging, EAVDI/ECVDI* July 18–21, Paris
- Higgins CB, Hricak H, Helms CA 1997 *Magnetic Imaging of the Body*, 3rd edn. Lippincott Raven, New York
- Krautwald-Junghanns ME, Enders F 1994 Ultrasound in birds. *Seminars in Avian and Exotic Pet Medicine* 3:140–146
- Krautwald-Junghanns ME, Schulz M, Hagner D et al 1995 Transcoelomic two-dimensional echocardiography in the avian patient. *Journal of Avian Medicine and Surgery* 9(1):19–31
- Krautwald-Junghanns ME, Kostka VM, Dorsch B 1998a Comparative studies on the diagnostic value of conventional radiography and computed tomography in evaluating the heads of psittacine and raptorial birds. *Journal of Avian Medicine and Surgery* 12(3):149–157
- Krautwald-Junghanns ME, Schuhmacher F, Sohn HG 1998b Examination of the lower respiratory tract of Psittacines and Amazoniae varieties by means of reconstructed computer x-ray tomography. 1: Examination of healthy parrots. *Tierarztl Praxis Ausg Klientiere Heimtiere* 26:61–70
- Orosz S, Toal R 1992 Tomographic anatomy of the golden eagle. *Journal of Zoo and Wildlife Medicine* 23:39–46
- Pees M, Straub J, Krautwald-Junghanns ME 2003 Echocardiographical examinations of healthy psittacine birds under special consideration of the African grey parrot (*Psittacus erithacus erithacus*). *Proceedings of European Association of Avian Veterinarians*, April 22–26, Tenerife, Spain, pp. 161–163
- Romvari R, Petrasi Z, Suto Z et al 2004 Noninvasive characterization of the turkey heart performance and its relationship to skeletal muscle volume. *Poultry Science* 83:696–700
- Schnelle GB 1945 Radiology in canine practice. The North American Veterinarian, Evanston, IL
- Silverman S 1993 Diagnostic imaging of exotic pets. *Veterinary Clinic of North American Small Animal Practice* 23:1287–1299
- Smith RD, Williams M 2000 Applications of informatics in veterinary medicine. *Bulletin of the Medical Library Association* 88:49–51
- Talbot RB 1991 Veterinary medical informatics. *Journal of the American Veterinary Medical Association* 199:52–57
- Tindemans I, Verhoye M, Balthazart J et al 2003 In vivo dynamic ME-MRI reveals differential functional responses of RA- and area X-projecting neurons in the HVC of canaries exposed to conspecific song. *European Journal of Neuroscience* 18:3352–3360
- Van der Linden A, Verhoye M, Van Audekerke J et al 1998 Noninvasive in vivo anatomical studies of the oscine brain by high resolution MRI microscopy. *Journal of Neuroscience Methods* 81:45–52
- Van der Linden A, Van Meir V, Tindemans I 2004 Applications of manganese-enhanced magnetic resonance imaging (MEMRI) to image brain plasticity in song birds. *NMR Biomedicine* 17:602–612
- Verhoye M, Van der Linden A, Van Audekerke J 1998 Imaging birds in a bird cage: in-vivo FSE 3D MRI of bird brain. *MAGMA* 6:22–27

Further reading

- NEMA Strategic Document, Version 4.0, Dec 29, 2004 Digital Imaging and Communications in Medicine (DICOM). National Electrical Manufacturers Association, Rosslyn, VA
- NEMA PS 3-10 Document 2004 Digital Imaging and Communications in Medicine (DICOM). Part 10: Media Storage and File Format for Media Interchange. National Electrical Manufacturers Association, Rosslyn, VA

Index

Page numbers in *italics* represent figures, those in **bold** represent tables.

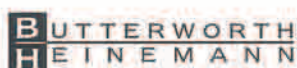
- Abdominal air sac
 - common barn owl, 162
 - Eurasian eagle owl, 180, 182
 - gyr falcon, 50
 - Northern goshawk, 124, 126
 - palm nut vulture, 88, 90, 96
 - red kite, 144, 146
 - saker falcon, 32
 - Steppe eagle, 70
- Accessory pygostyle, gyr falcon, 50, 52
- Advanced diagnostic imaging, 261–73
 - DICOM standard, 264, 265
 - importance of, 261
 - materials and methods, 262–4
 - techniques, 266–72
 - see also individual modalities
- Air sacs
 - abdominal, 32, 50, 70, 88, 90, 96, 124, 144, 146, 162, 180, 182
 - caudal thoracic, 32, 50, 70, 90, 96, 124, 126, 144, 146, 162, 180, 182
 - clavicular, 124, 162, 180
 - infection, 239
- Alular claw
 - gyr falcon, 54
 - saker falcon, 34
- Alular digit
 - common barn owl, 166
 - Eurasian eagle owl, 184, 186
 - Eurasian honey buzzard, 108, 110
 - gyr falcon, 54, 56, 57
 - Northern goshawk, 129, 131
 - palm nut vulture, 92, 94
 - red kite, 148, 150
 - saker falcon, 34, 36, 37
 - Steppe eagle, 75, 77
- American kestrel (*Falco sparverius*), musculoskeletal system, 21
- Amyloidosis, 249, 250
- Anatomy, 21–102
 - gastrointestinal system, 22
 - heart and vascular system, 24
 - liver, 23
 - musculoskeletal system, 21–2
 - reproductive system, 24
 - respiratory system, 23
 - spleen, 23
 - urinary system, 24
- Anesthesia, 3
- Angiography, contrast radiography, 15, 19
- Ansa iliofibularis, 22
- Arthritis
 - degenerative
 - elbow joint, 205
 - shoulder joint, 204
 - wings, 205
 - septic
 - intertarsal joint, 208
 - phalangeal joint, 207
- Artifacts, 256
- Aspergilloma, 237, 238
- Aspergillosis, 235, 237
- Barbary falcon (*Falco pelegrinoides*), musculoskeletal system, 21
- Barium sulphate, transit time, 15
- Barred owl (*Strix varia*), musculoskeletal system, 21
- Bill
 - common barn owl, 160, 161
 - Eurasian eagle owl, 176, 177, 178, 179
 - Eurasian honey buzzard, 104, 105, 107
 - gyr falcon, 47, 48, 49
 - Northern goshawk, 120, 121, 123
 - palm nut vulture, 84, 85, 87
 - red kite, 140, 141, 143
 - saker falcon, 26, 27, 29
 - Steppe eagle, 66, 69
- Black kite (*Milvus migrans*), musculoskeletal system, 21, 22
- Blaine see Bursitis
- Body
 - common barn owl, 162–5
 - Eurasian eagle owl, 180–3
 - gyr falcon, 50–3
 - northern goshawk, 124–7
 - palm nut vulture, 88–91
 - red kite, 144–7
 - saker falcon, 30–3
 - steppe eagle, 70–3
- Bonelli's eagle (*Hieraetus fasciatus*), metabolic bone disease, 228
- Bones, ingestion of, 226
- Bumblefoot
 - Eurasian eagle owl, 200
 - saker falcon, 197, 198
 - Steppe eagle, 199
- Bursitis (blaine), 251, 252
- Cardiohepatic waist
 - common barn owl, 162
 - Eurasian eagle owl, 180
 - gyr falcon, 50
 - palm nut vulture, 88
 - red kite, 144
 - Steppe eagle, 70
- Carpals
 - common barn owl, 166
 - Eurasian eagle owl, 184, 186
 - Eurasian honey buzzard, 108, 110
 - gyr falcon, 54, 56, 57
 - Northern goshawk, 129, 131
 - palm nut vulture, 92, 94
 - red kite, 148, 150
 - saker falcon, 36, 37
 - Steppe eagle, 75, 77
- Caseous mass, 239
- Caudal thoracic air sac
 - common barn owl, 162
 - Eurasian eagle owl, 180, 182
 - gyr falcon, 50
 - Northern goshawk, 124, 126
 - palm nut vulture, 90, 96
 - red kite, 144, 146
 - saker falcon, 32
 - Steppe eagle, 70
- Caudal vertebrae
 - common barn owl, 164, 168, 170
 - dislocations, 206
 - Eurasian eagle owl, 182, 190
- Eurasian honey buzzard, 112, 114
- gyr falcon, 50, 52, 60
- Northern goshawk, 124, 126, 134
- palm nut vulture, 88, 90, 96, 98
- red kite, 144, 146, 152, 154
- saker falcon, 30, 32, 40
- Steppe eagle, 70, 72
- Caudoplantar position, 6, 7
- Ceratobranchial bone
 - common barn owl, 160, 161
 - Eurasian eagle owl, 177, 178, 179
 - Eurasian honey buzzard, 105, 106
 - gyr falcon, 47, 49
 - Northern goshawk, 120, 121, 122
 - palm nut vulture, 84, 85, 86, 87
 - red kite, 141, 142
 - saker falcon, 26, 27, 28
 - Steppe eagle, 66, 67, 68, 69
- Cervical ribs
 - common barn owl, 161
 - Eurasian eagle owl, 178
 - Eurasian honey buzzard, 105, 106
 - gyr falcon, 48, 49
 - Northern goshawk, 121, 122
 - palm nut vulture, 85, 86
 - red kite, 141, 142
 - saker falcon, 28
 - Steppe eagle, 68
- Cervical vertebrae
 - common barn owl, 160, 161, 162, 164
 - Eurasian eagle owl, 176, 177, 178, 179, 180, 182
 - Eurasian honey buzzard, 104, 105, 106, 107
 - gyr falcon, 47, 48, 49, 50, 52
 - Northern goshawk, 120, 121, 122, 123, 124, 126
 - palm nut vulture, 84, 85, 86, 87, 88, 90
 - red kite, 140, 141, 142, 143, 144, 146
 - saker falcon, 26, 28, 29, 30, 32
 - Steppe eagle, 66, 67, 68, 69, 70
- Clavicle
 - common barn owl, 162, 164, 166
 - Eurasian eagle owl, 180, 182, 184
 - Eurasian honey buzzard, 108, 109
 - gyr falcon, 50, 52, 54
 - Northern goshawk, 126, 128
 - palm nut vulture, 88, 90, 92, 93
 - red kite, 144, 146, 148, 149
 - saker falcon, 34
 - Steppe eagle, 70, 72, 74
- Clavicular air sac
 - common barn owl, 162
 - Eurasian eagle owl, 180
 - gyr falcon, 50
 - Northern goshawk, 124
 - palm nut vulture, 88
 - saker falcon, 30
- Claws
 - Eurasian eagle owl, 193, 194
 - Eurasian honey buzzard, 116, 117, 118
 - gyr falcon, 62, 63
 - Northern goshawk, 136, 137, 138
 - palm nut vulture, 100, 101
 - red kite, 156, 157, 158
 - saker falcon, 40, 43, 44
- Cloaca, 22
- Common barn owl (*Tyto alba*), 159–72, 159
 - body, 162–5
 - foot, 172–4
 - musculoskeletal system, 21, 22
 - pelvic limb, 168–71
 - scoliosis, 227
 - skull, 160–3
 - wings, 166–7
- Common kestrel (*Falco tinnunculus*)
 - egg binding, 253
 - fractures
 - radius, 201
 - ulna, 201
- Computed tomography, 269, 270
- lanner falcon, 269–70
- tawny owl, 261, 264–5
- Contrast radiography, 12–19
 - angiography, 15, 19
 - gastrointestinal, 12, 13, 14, 15
 - interpretation, 17
 - myelography, 17, 19
 - positive pressure insufflation, 15, 16
 - urography, 15, 17, 18
- Conventional radiography, 8
 - exposure guidelines, 8
- Coracoid
 - common barn owl, 162, 164, 166
 - Eurasian eagle owl, 180, 182, 184, 185
 - Eurasian honey buzzard, 108, 109
 - fractures, 203
 - gyr falcon, 50, 52, 54, 55
 - Northern goshawk, 124, 126, 128, 130
 - palm nut vulture, 88, 90, 92, 93
 - red kite, 144, 146, 148, 149
 - saker falcon, 30, 34
 - Steppe eagle, 70, 72, 74, 76
- Cornea
 - common barn owl, 161
 - Eurasian eagle owl, 177, 178
- Cranial cavity
 - common barn owl, 160, 161
 - Eurasian eagle owl, 176, 177, 178, 179
 - Eurasian honey buzzard, 104, 105, 106, 107
 - gyr falcon, 47, 49
 - Northern goshawk, 120, 121, 122, 123
 - palm nut vulture, 84, 85, 86, 87
 - red kite, 140, 141, 142, 143
 - saker falcon, 26, 27, 28, 29
 - Steppe eagle, 66, 67, 68, 69
- Cranial cnemial crest
 - gyr falcon, 58
 - saker falcon, 38
- Craniocaudal position, 6
- Crop (ingluvies), 22
- Degenerative diseases, 249–50
- Dehydration, 218
- Diagnostic errors, 253–9
 - artifacts, 256
 - egg binding, 253
 - hepatomegaly, 254

- Diagnostic errors (*contd*)
 recent feeding, 258
 shotgun pellet location, 255
 static electricity, 259
 DICOM standard, 264, 265
 Digital pad
 Eurasian eagle owl, 192, 193, 194
 gyr falcon, 62, 63
 palm nut vulture, 96, 100, 101, 102
 red kite, 156
 saker falcon, 38, 42, 44, 45
 Dislocations, caudal vertebrae, 206
- Egg binding, 253
 Elbow joint
 arthritis, 205
 Northern goshawk, 128
 red kite, 150
 saker falcon, 36
 soft-tissue swelling, 252
 Steppe eagle, 74
 Epibranchial bone
 Eurasian eagle owl, 178
 Eurasian honey buzzard, 105, 106
 gyr falcon, 47, 48
 Northern goshawk, 121, 122
 palm nut vulture, 85, 86
 red kite, 141, 142
 saker falcon, 26, 27, 28
 Steppe eagle, 66, 67, 68, 69
 Esophagus, palm nut vulture, 90
 Eurasian buzzard (*Buteo buteo*)
 caudal vertebrae, dislocations, 206
 contrast angiography, 19
 fractures
 coracoid, 203
 mandible, 205
 ultrasound, 268
 wings, arthritis, 205
 Eurasian eagle owl (*Bubo bubo*)
 175–94, 175
 body, 180–3
 foot, 192–4
 bumlefoot, 200
 musculoskeletal system, 21, 22
 pelvic limb, 188–91
 skull, 176–9
 wings, 184–7
 Eurasian griffon vulture (*Gyps fulvus*)
 femoral fracture, 206
 Eurasian honey buzzard (*Pernis apivorus*)
 103–18, 103
 foot, 116–18
 musculoskeletal system, 21, 22
 pelvic limb, 112–15
 skull, 104–7
 wings, 108–11
 European kestrel, musculoskeletal system, 21
 Exposure guidelines
 conventional radiography, 8
 magnification radiography, 9, 11
- Femorotibial joint
 common barn owl, 168
 Eurasian eagle owl, 188
 gyr falcon, 58
 Northern goshawk, 132
 palm nut vulture, 96
 red kite, 152
 saker falcon, 38
 Femur
 common barn owl, 164, 168, 170
 common barn owl, 162
 Eurasian eagle owl, 180, 182, 188, 190
 Eurasian honey buzzard, 112, 114
 fractures, 201, 206, 214, 215
 gyr falcon, 50, 52, 58, 60
 Northern goshawk, 124, 126, 132, 134
 palm nut vulture, 88, 90, 96, 98
 red kite, 144, 146, 152, 154
 saker falcon, 38, 40
 Steppe eagle, 70, 78, 80
 Fibula
 common barn owl, 168, 170
 Eurasian eagle owl, 188, 190
 Eurasian honey buzzard, 112, 114
 gyr falcon, 60
 Northern goshawk, 134
 palm nut vulture, 88, 98
 red kite, 154
 saker falcon, 40
 Steppe eagle, 80
 Flexor digitorum longus, 22
 Foot
 common barn owl, 172–4
 Eurasian eagle owl, 192–4
 Eurasian honey buzzard, 116–18
 gyr falcon, 62–4
 Northern goshawk, 136–8
 palm nut vulture, 100–2
 red kite, 156–8
 saker falcon, 42–5
 Steppe eagle, 82, 199
 trauma, 197
 Fractures, 200–5, 206
 coracoid, 203
 femur, 201, 206, 214
 hallux, 207
 metacarpals, 213
 pathological, 228
 radius, 200, 201
 tarsometatarsus, 208
 tibiotarsus, 201, 206, 207, 216, 217
 ulna, 201, 205, 212
 wings, 203
 Fungal plaques, 234
 Gastroenteritis, 247
 Gastrointestinal system
 anatomy, 22
 contrast radiography, 12, 13, 14, 15
 Gizzard, 22
 Golden eagle (*Aquila chrysaetos*)
 musculoskeletal system, 21
 shotgun injury, 209
 Gout, 240
 Great horned owl (*Bubo virginianus*)
 musculoskeletal system, 21
 Gyr falcon (*Falco rusticolus*), 46–64, 46
 body, 50–3
 foot, 62–4
 subcutaneous abscess, 199
 fractures, wings, 203
 impaction, 223
 infections
 aspergillosis, 235
 septicemia, 245
 lead toxicosis, 223
 metabolic bone disease, 229
 musculoskeletal system, 21, 22
 pelvic limb, 58–61
 radiography
 caudoplantar position, 7
 craniocaudal position, 6
 magnification, 9
 ventrodorsal position, 4
 ventrodorsal 'stressed' position, 5
 skull, 47–9
 wings, 54–7
 fractures, 203
 Gyr-peregrine hybrid falcon (*Falco rusticolus-peregrinus*)
 aspergillosis, 235
 fractures
 coracoid, 203
 femur, 214
 tibiotarsus, 206
 musculoskeletal system, 21, 22
 Gyr-saker hybrid falcon (*Falco rusticolus-cherrug*)
 amyloidosis, 249
 diagnostic errors, 254
 infections, gastroenteritis, 247
 musculoskeletal system, 21, 22
- Hallus, red kite, 152
 Hallux
 common barn owl, 172, 173, 174
 Eurasian eagle owl, 193, 194
 Eurasian honey buzzard, 118
 fractures, 207
 gyr falcon, 64
 Northern goshawk, 132, 134, 136, 137, 138
 palm nut vulture, 96, 98, 100, 101, 102
 red kite, 154, 158
 Steppe eagle, 78, 80, 82
 Harris hawk (*Parabuteo unicinctus*)
 musculoskeletal system, 21, 22
 Head see Skull
 Heart and vascular system, 24
 common barn owl, 164
 Eurasian eagle owl, 180, 182
 gyr falcon, 50, 52
 Northern goshawk, 124, 126
 palm nut vulture, 88, 90, 96
 red kite, 144, 146, 152
 saker falcon, 30, 32
 Steppe eagle, 70, 72
 Hepatomegaly, 204
 diagnostic errors, 254
 Historical aspects, 1
 Humeroscapular bone
 Eurasian eagle owl, 185
 Eurasian honey buzzard, 109
 gyr falcon, 55
 Northern goshawk, 130
 red kite, 149
 Humerus
 common barn owl, 162, 164, 166
 Eurasian eagle owl, 180, 182, 184, 185, 186
 Eurasian honey buzzard, 108, 109, 110
 fractures, 202, 211
 gyr falcon, 50, 52, 54, 55, 56
 Northern goshawk, 124, 126, 128, 129, 130, 131
 palm nut vulture, 88, 90, 92, 93, 94
 red kite, 144, 146, 148, 149, 150
 saker falcon, 32, 34, 35, 36
 Steppe eagle, 70, 72, 74, 76
 Hyoid apparatus
 common barn owl, 160, 161
 Eurasian eagle owl, 177, 178, 179
 Eurasian honey buzzard, 104, 105, 106, 107
 gyr falcon, 47, 48
 Northern goshawk, 121, 122, 123
 palm nut vulture, 85, 86
 red kite, 141, 142, 143
 saker falcon, 26, 27, 28
 Steppe eagle, 66, 67, 68, 69
 Hypotarsus
 common barn owl, 168
 Eurasian eagle owl, 188
 Eurasian honey buzzard, 112
 Northern goshawk, 132
 palm nut vulture, 96
 red kite, 152
- Ilium
 common barn owl, 162, 164
 Eurasian eagle owl, 180, 182
 Eurasian honey buzzard, 114
 gyr falcon, 50, 60
 Northern goshawk, 124, 126, 134
 palm nut vulture, 88, 96, 98
 red kite, 144, 146, 154
 saker falcon, 30, 32, 38
 Steppe eagle, 70, 80
 Impaction, 221, 222, 223
 Infectious diseases, 230–48
 air sacs, 239
 aspergillosis, 237, 238
 aspergillosis, 235, 237
 caseous mass, 239
 fungal plaques, 234
 gastroenteritis, 247
 gout, 240
 liver, 241, 242, 244
 Newcastle disease, 243, 244
 parasitic infestation, 232
 pneumonia, 240
 septicemia, 245
Serratia pulchrum seuratii, 232, 233, 234
 splenomegaly, 246
Trichomonas gallinae, 230, 231
 trichomonosis, 231
 Infraorbital sinus, 21
 common barn owl, 160
 Eurasian eagle owl, 176
 Eurasian honey buzzard, 104
 gyr falcon, 47
 Northern goshawk, 120
 palm nut vulture, 84
 red kite, 140
 saker falcon, 26
 Steppe eagle, 66
 Interorbital septum
 common barn owl, 161
 Eurasian eagle owl, 177
 Interorbital sinus, Eurasian eagle owl, 179
 Intertarsal joint
 common barn owl, 168, 170
 Eurasian eagle owl, 188, 190
 Eurasian honey buzzard, 112
 gyr falcon, 58, 60, 64
 Northern goshawk, 132, 134
 palm nut vulture, 96, 98
 red kite, 152, 154
 saker falcon, 38, 45
 septic arthritis, 208
 Steppe eagle, 80
 Intertrochlear notch
 common barn owl, 173, 174
 Eurasian eagle owl, 193, 194
 Eurasian honey buzzard, 117, 118
 palm nut vulture, 101, 102
 red kite, 157, 158
 Steppe eagle, 80, 82
 Intestine
 common barn owl, 162, 164
 Eurasian eagle owl, 180, 182
 gyr falcon, 52
 Northern goshawk, 124
 palm nut vulture, 88, 90
 red kite, 144, 146

- Intestine (*cont'd*)
saker falcon, 30
Steppe eagle, 72
- Intracranial ossification, 21, 22
barn owl, 166
Eurasian eagle owl, 184, 186, 190
gyr falcon, 54, 58
saker falcon, 34, 38
- Iohexol, 15
- Ischium
common barn owl, 162, 170
Eurasian eagle owl, 180, 190
gyr falcon, 50
Northern goshawk, 124, 134
palm nut vulture, 88, 98
red kite, 144, 154
saker falcon, 30
Steppe eagle, 70, 80
- Jess
gyr falcon, 60, 62, 63
red kite, 152, 158
saker falcon, 40, 42, 43, 44
- Jugal arch
common barn owl, 160, 161
Eurasian eagle owl, 176, 177, 178, 179
Eurasian honey buzzard, 104, 105, 106, 107
gyr falcon, 47, 48, 49
Northern goshawk, 120, 121, 122, 123
palm nut vulture, 84, 85, 86, 87
red kite, 140, 141, 142, 143
saker falcon, 26, 27, 28, 29
Steppe eagle, 66, 67, 68, 69
- Kidney
Eurasian eagle owl, 180, 182
gyr falcon, 50, 52
Northern goshawk, 126
palm nut vulture, 90
red kite, 144, 146
saker falcon, 32
Steppe eagle, 72
- Lacrimal bone
Eurasian honey buzzard, 104, 105, 107
gyr falcon, 48, 49
Northern goshawk, 121, 122, 123
palm nut vulture, 85, 86, 87
red kite, 141, 142, 143
saker falcon, 27, 28, 29
Steppe eagle, 67, 68, 69
- Laggar falcon (*Falco jugger*),
musculoskeletal system, 22
- Lanner falcon (*Falco biarmicus*)
computed tomography, 269–70
musculoskeletal system, 21, 22
osteoarthritis, 204
ventrolateral 'stressed' position, 5
- Lappet-faced vulture (*Torgos traquelliotus*), mislocated
satellite transmitter, 224
- Lateral position, 3, 4
- Lead pellet ingestion, 219, 220, 248
- Lead toxicosis, 218, 223
- Ligamentum cartilago metatarsale
mediale, 22
- Lipoma, 251
- Liver, 23
common barn owl, 162, 164
Eurasian eagle owl, 180, 182
gyr falcon, 50, 52
infection, 241, 242, 244
- Northern goshawk, 124, 126
palm nut vulture, 88, 90, 96
red kite, 144, 146, 152
saker falcon, 30
Steppe eagle, 70, 72
- Lung
common barn owl, 162, 164
Eurasian eagle owl, 180, 182
gyr falcon, 50, 52
Northern goshawk, 124, 126
palm nut vulture, 88, 90, 96
red kite, 144, 146
saker falcon, 32
Steppe eagle, 70, 72
- Magnetic resonance imaging, 271, 272
tawny owl, 263, 271, 272
- Magnification radiography, 9–11
exposure guidelines, 9, 11
table-top technique, 9, 11
- Management-related diseases, 218–29
bone ingestion, 226
dehydration, 218
impaction, 221, 222, 223
lead pellet ingestion, 219, 220
lead toxicosis, 218, 223
metabolic bone disease, 228, 229
mislocated satellite transmitter, 224
pathological fractures, 228
sand ingestion, 220, 221
scoliosis, 227
stone ingestion, 225
- Mandible
common barn owl, 160, 161
Eurasian eagle owl, 176, 177, 178, 179
Eurasian honey buzzard, 104, 105, 106, 107
fractures, 205
gyr falcon, 47, 48, 49
Northern goshawk, 120, 121, 122, 123
palm nut vulture, 84, 85, 86, 87
red kite, 140, 141, 142, 143
saker falcon, 26, 27, 28, 29
Steppe eagle, 66, 67, 68, 69
- Mandibular symphysis
common barn owl, 160
Eurasian eagle owl, 176, 178, 179
Eurasian honey buzzard, 104, 106, 107
gyr falcon, 47, 49
Northern goshawk, 120, 122, 123
palm nut vulture, 86, 87
red kite, 140, 142, 143
saker falcon, 26, 29
Steppe eagle, 66, 69
- Maxilla
Eurasian honey buzzard, 105, 107
gyr falcon, 48, 49
Northern goshawk, 121
palm nut vulture, 84, 85, 87
red kite, 140, 141
saker falcon, 27, 29
- Medial hypotarsal crest
gyr falcon, 58
saker falcon, 38
- Metabolic bone disease, 228, 229
- Metacarpals
common barn owl, 166
Eurasian eagle owl, 184, 186
Eurasian honey buzzard, 110
fractures, 213
gyr falcon, 54, 56, 57
Northern goshawk, 129, 131
palm nut vulture, 92, 94
- red kite, 148, 150
saker falcon, 34, 36
Steppe eagle, 75, 77
- Metatarsal pad
Eurasian eagle owl, 192
gyr falcon, 64
Northern goshawk, 138
palm nut vulture, 96, 100
red kite, 152, 156
saker falcon, 38, 42, 45
- Metatarsals
common barn owl, 168, 170, 172, 173, 174
Eurasian eagle owl, 188, 190, 192, 193, 194
Eurasian honey buzzard, 116, 118
gyr falcon, 58, 60, 62
Northern goshawk, 132, 134, 136, 138
palm nut vulture, 96, 98, 100, 101, 102
red kite, 152, 154, 156, 157, 158
saker falcon, 43
Steppe eagle, 78, 80, 82
- Metatarsophalangeal joint
common barn owl, 172, 173, 174
Eurasian eagle owl, 192, 193, 194
Eurasian honey buzzard, 117, 118
gyr falcon, 63
Northern goshawk, 137
palm nut vulture, 101, 102
red kite, 157, 158
saker falcon, 44
Steppe eagle, 80, 82
- Musculoskeletal system, 21, 21–2
- Myelography, contrast radiography, 17, 19
- Nares
common barn owl, 160, 161
Eurasian eagle owl, 176, 179
Eurasian honey buzzard, 104, 107
gyr falcon, 47, 49
Northern goshawk, 120, 123
palm nut vulture, 84, 87
red kite, 140, 143
saker falcon, 26, 29
Steppe eagle, 66, 69
- Neoplastic disease, 251–2
Newcastle disease, 243, 244
- Northern goshawk (*Accipiter gentilis*),
119–38, 119
body, 124–7
foot, 136–8
musculoskeletal system, 21
pelvic limb, 132–5
skull, 120–3
wings, 128–31
- Northern long-eared owl (*Asio otus*)
contrast myelography, 19
shotgun injury, 210
- Notarium
common barn owl, 162, 164
Eurasian eagle owl, 180, 182
gyr falcon, 50, 52, 58
Northern goshawk, 124, 126
palm nut vulture, 88, 90, 96
red kite, 144, 146
saker falcon, 30, 32
Steppe eagle, 70, 72
- Olecranon
common barn owl, 166
Eurasian eagle owl, 184
Eurasian honey buzzard, 108
Northern goshawk, 128
palm nut vulture, 92
- red kite, 148
Steppe eagle, 74
- Orbit
Eurasian eagle owl, 176
Eurasian honey buzzard, 104, 105
gyr falcon, 47, 48
Northern goshawk, 120, 121
palm nut vulture, 84, 85
red kite, 140, 141
saker falcon, 26
Steppe eagle, 66
- Osteoarthritis, 204
- Osteomyelitis, 197, 198, 208
- Ostia pulmonare, mechanical
obstruction, 236
- Palatine bone
Eurasian honey buzzard, 105
gyr falcon, 48
Northern goshawk, 121
palm nut vulture, 85
red kite, 141
saker falcon, 27
Steppe eagle, 67
- Palm nut vulture (*Gypohierax
angolensis*), 83–102, 83
body, 88–91
foot, 100–2
musculoskeletal system, 21
pelvic limb, 96–9
skull, 84–7
wings, 92–5
- Parasitic infestation, 232
- Patella
common barn owl, 164, 168
Eurasian eagle owl, 182, 188, 190
Eurasian honey buzzard, 112
gyr falcon, 52, 58, 60
Northern goshawk, 126, 132
palm nut vulture, 90, 96
red kite, 146, 152
saker falcon, 38, 40
Steppe eagle, 72, 78
- Pectoral girdle, 6
- Pectoral muscles
common barn owl, 162, 166
Eurasian eagle owl, 180, 185
Eurasian honey buzzard, 109
gyr falcon, 50, 55
Northern goshawk, 124, 130
palm nut vulture, 88, 93
red kite, 144, 149
saker falcon, 30
Steppe eagle, 70, 76
- Pelvic limb, 6
common barn owl, 168–71
Eurasian eagle owl, 188–91
Eurasian honey buzzard, 112–15
gyr falcon, 58–61
Northern goshawk, 132–5
palm nut vulture, 96–9
red kite, 152–5
saker falcon, 38–41
steppe eagle, 78–81
- Peregrine falcon (*Falco peregrinus*)
arthritis of shoulder joint, 204
contrast radiography, 17, 18
humeral fracture, 202
hepatomegaly, 204
infections
aspergillosis, 237
caseous mass, 239
liver, 242, 244
osteomyelitis, 208
musculoskeletal system, 21, 22
sand ingestion, 220
scoliosis, 227

- Peregrine falcon (*Falco peregrinus*)
(cont'd)
 shotgun injury, 210
 stone ingestion, 225
- Phalangeal joint
 Eurasian eagle owl, 192, 193
 Eurasian honey buzzard, 116, 118
 gyr falcon, 60, 63
 palm nut vulture, 101
 red kite, 158
 saker falcon, 43, 44
 septic arthritis, 207
 Steppe eagle, 80, 82
- Phalanges
 common barn owl, 166, 172, 173, 174
 Eurasian eagle owl, 184, 186, 192, 193, 194
 Eurasian honey buzzard, 108, 110, 116, 117, 118
 gyr falcon, 54, 56, 57, 62, 63
 Northern goshawk, 131, 136, 137
 palm nut vulture, 94, 100, 101, 102
 red kite, 148, 150, 156, 157, 158
 saker falcon, 43, 44
 Steppe eagle, 75, 82
- Pneumonia, 240
- Positive pressure insufflation contrast radiography, 15, 16
- Postpatagium
 common barn owl, 166
 gyr falcon, 57
- Prairie falcon (*Falco mexicanus*), musculoskeletal system, 21
- Preacetabular ilium, gyr falcon, 52, 58
- Premaxilla
 common barn owl, 160
 Eurasian eagle owl, 176, 179
 Eurasian honey buzzard, 104
 gyr falcon, 47
 Northern goshawk, 120
 red kite, 140
 saker falcon, 26
- Propatagium
 common barn owl, 166
 gyr falcon, 54, 57
 Northern goshawk, 129
 red kite, 148
- Proventriculus
 common barn owl, 164
 Eurasian eagle owl, 182
 gyr falcon, 52
 Northern goshawk, 126
 palm nut vulture, 90, 96
 red kite, 146
 Steppe eagle, 72
- Pubis
 common barn owl, 162, 170
 Eurasian eagle owl, 180, 182, 190
 gyr falcon, 50, 52, 60
 Northern goshawk, 124, 126, 134
 palm nut vulture, 88, 90, 96, 98
 red kite, 144, 146, 154
 saker falcon, 30, 40
 Steppe eagle, 70, 72
- Pygostyle
 common barn owl, 164, 168
 Eurasian eagle owl, 182, 190
 Eurasian honey buzzard, 114
 gyr falcon, 50, 52, 60
 Northern goshawk, 126, 134
 palm nut vulture, 88, 90, 96, 98
 red kite, 144, 146, 152, 154
 saker falcon, 30, 40
 Steppe eagle, 70, 72
- Quadrates
 Eurasian eagle owl, 179
 Eurasian honey buzzard, 107
 gyr falcon, 49
 Northern goshawk, 123
 palm nut vulture, 87
 red kite, 143
 saker falcon, 29
- Quadratmandibular joint
 common barn owl, 161
 Eurasian eagle owl, 177, 178
 Eurasian honey buzzard, 105
 gyr falcon, 48
 Northern goshawk, 121
 palm nut vulture, 85
 red kite, 140, 141
 saker falcon, 27
 Steppe eagle, 67
- Radial carpal bone
 gyr falcon, 54, 56
 saker falcon, 34, 36
- Radiography, as diagnostic technique, 1
- Radius
 common barn owl, 166
 Eurasian eagle owl, 184, 185, 186
 Eurasian honey buzzard, 108, 109, 110
 fractures, 200, 201
 gyr falcon, 54, 55, 56, 57
 Northern goshawk, 128, 129, 130, 131
 palm nut vulture, 92, 93, 94
 red kite, 148, 150
 saker falcon, 34, 35, 36, 37
 Steppe eagle, 74, 75, 76, 77
- Red kite (*Milvus milvus*), 139–58, 139
 body, 144–7
 foot, 156–8
 musculoskeletal system, 21, 22
 pathological fractures, 228
 pelvic limb, 152–5
 skull, 140–3
 wings, 148–51
- Red-naped shaheen (*Falco peregrinoides babylonicus*), musculoskeletal system, 21, 22
- Red-tailed hawk (*Buteo jamaicensis*), musculoskeletal system, 21
- Reproductive system, 24
- Respiratory system, 23
- Restraint
 anesthesia, 3
 caudoplantar position, 6, 7
 craniocaudal position, 6
 lateral position, 3, 4
 'stressed' position, 5
 ventrodorsal position, 3, 4
- Röntgen, Wilhelm Conrad, 1
- Saker falcon (*Falco cherrug*), 25–45, 25
 amyloidosis, 250
 arthritis
 elbow joint, 205
 intertarsal joint, 208
 body, 30–3
 bursitis (blaine), 251
 dehydration, 218
 diagnostic errors, 253, 255
 foot, 42–5
 bumblefoot, 197, 198
 osteomyelitis, 197, 198
 trauma, 197
 fractures
 femur, 206, 215
 scapula, 202
 tarsometatarsus, 208, 217
 tibiotarsus, 207
 ulna, 205, 212
 GI contrast radiography, 12, 13, 14
 hallux, fracture, 207
 impaction, 221, 222
 infections
 air sacs, 239
 aspergilloma, 237, 238
 gout, 240
 liver, 241
 Newcastle disease, 243, 244
 parasitic infestation, 232
 pneumonia, 240
 Serratospiculum seaurati, 232, 233, 234
 splenomegaly, 246
 Trichomonas gallinae, 230, 231
 trichomonosis, 231
 lead pellet ingestion, 219, 220, 248
 lead toxicosis, 218
 lipoma, 251
 metabolic bone disease, 229
 musculoskeletal system, 21
 ostia pulmonare, mechanical obstruction, 236
 pelvic limb, 38–41
 radiography
 magnification, 9, 10, 11
 positive-pressure insufflation contrast, 16
 standing position, 7
 ventrolateral 'stressed' position, 5
 restraint, 3, 4
 sand ingestion, 221
 shotgun injury, 210
 skull, 26, 27, 28, 29
 soft tissue injury, 208
 spinal luxation, 209
 wings, 34–7
- Saker-peregrine hybrid falcon (*Falco cherrug-Falco peregrinus*)
 fractures
 humerus, 211
 metacarpals, 213
 tibiotarsus, 207, 216
 sand ingestion, 220, 221
 satellite transmitter, misplacement, 224
- Scapula
 common barn owl, 162, 164
 Eurasian eagle owl, 180, 182, 184, 185
 Eurasian honey buzzard, 108
 gyr falcon, 50, 52, 54, 55
 Northern goshawk, 124, 126, 128, 130
 palm nut vulture, 88, 90, 92, 93
 red kite, 144, 146, 148, 149
 saker falcon, 32, 35
 Steppe eagle, 70, 74, 76
- Scleral ring
 common barn owl, 160, 161
 Eurasian eagle owl, 176, 177, 178, 179
 Eurasian honey buzzard, 104, 105, 106, 107
 gyr falcon, 47, 48, 49
 Northern goshawk, 120, 121, 122, 123
 palm nut vulture, 84, 85, 86, 87
- red kite, 140, 141, 142, 143
 saker falcon, 26, 28, 29
 Steppe eagle, 66, 67, 68, 69
- Scoliosis, 227
- Screech owl (*Otus asio*), musculoskeletal system, 21
- Semicircular canals, Eurasian eagle owl, 177, 179
- Septicemia, 245
- Serratospiculum seaurati*, 232, 233, 234
- Sesamoids
 Eurasian honey buzzard, 110
 gyr falcon, 57, 58, 62, 64
 Northern goshawk, 129, 132
 saker falcon, 37, 42, 45
- Short-toed snake-eagle (*Circus gallicus*), bone ingestion, 226
- Shotgun injury, 209, 210
- Skull, 21
 common barn owl, 160–1
 Eurasian eagle owl, 176–9
 Eurasian honey buzzard, 104–7
 gyr falcon, 47–9
 Northern goshawk, 120–3
 palm nut vulture, 84–7
 red kite, 140–3
 saker falcon, 26, 27, 28, 29
 Steppe eagle, 66–9
- Soft tissue injury, 208
- Sparrowhawk (*Accipiter nisus*), musculoskeletal system, 21
- Spinal luxation, 209
- Spleen, 23
 common barn owl, 164
 Eurasian eagle owl, 180, 182
 Northern goshawk, 126
 palm nut vulture, 90
 red kite, 146
- Splenomegaly, 246
- Static electricity, 259
- Steppe eagle (*Aquila nipalensis*), 65–82, 65
 body, 70–3
 foot, 82
 bumblefoot, 199
 musculoskeletal system, 21
 pelvic limb, 78–81
 skull, 66–9
 wings, 74–7
- Sternal ribs
 common barn owl, 164
 Eurasian eagle owl, 182
 gyr falcon, 52
 palm nut vulture, 90
 red kite, 144, 146
 saker falcon, 30
 Steppe eagle, 72
- Sternum
 common barn owl, 162, 164
 Eurasian eagle owl, 180, 182
 gyr falcon, 50, 52, 58
 Northern goshawk, 124, 126
 palm nut vulture, 88, 90
 red kite, 144, 146
 saker falcon, 30
 Steppe eagle, 70, 72
- Stone ingestion, 225
- Subcutaneous abscess, 199
- Sun-burst effect, 234
- Synsacrum
 common barn owl, 162, 164
 Eurasian eagle owl, 180, 182
 Eurasian honey buzzard, 114
 gyr falcon, 50, 52, 58, 60
 Northern goshawk, 124, 126, 134
 palm nut vulture, 88, 90, 96, 98
 red kite, 144, 146, 154

- Synsacrum (*cont'd*)
 saker falcon, 30, 32, 38
 Steppe eagle, 70, 72
- Syrinx
 gyr falcon, 52
 palm nut vulture, 90
 saker falcon, 32
- Tail feather repair, 257
- Tarsometatarsus
 common barn owl, 168, 170, 172, 173, 174
 Eurasian eagle owl, 188, 190, 192, 193, 194
 Eurasian honey buzzard, 112, 114, 116, 117, 118
 fractures, 208
 gyr falcon, 60, 62, 63, 64
 Northern goshawk, 132, 134, 136, 137, 138
 palm nut vulture, 96, 98, 100, 101, 102
 red kite, 152, 154, 156, 157, 158
 saker falcon, 42, 43, 44, 45
 Steppe eagle, 78, 80, 82
- Tawny owl (*Strix aluco*)
 computed tomography, 261, 264–5, 270
 fractures
 femur, 201
 radius, 200
 tibiotarsus, 201
 ulna, 200
 magnetic resonance imaging, 263, 271, 272
 ultrasound, 267
- Tendo ossificans, 21
- Thoracic esophagus, gyr falcon, 52
- Tibiotarsus
 common barn owl, 164, 168, 170
 Eurasian eagle owl, 188, 190
 Eurasian honey buzzard, 112, 114
 fractures, 201, 206, 207, 216, 217
 gyr falcon, 52, 58, 60, 64
 Northern goshawk, 126, 132, 134
 palm nut vulture, 88, 90, 96, 98
 red kite, 144, 152, 154
 saker falcon, 38, 40, 45
 Steppe eagle, 70, 78, 80
- Tomial tooth, 22
- Tongue
 common barn owl, 160
 Eurasian honey buzzard, 104, 107
 Northern goshawk, 123
 red kite, 143
- Trachea
 common barn owl, 160, 161, 162, 164
 Eurasian eagle owl, 176, 177, 178, 179, 182
 Eurasian honey buzzard, 104, 105, 106, 107
 gyr falcon, 47, 48, 49, 52
 Northern goshawk, 120, 121, 122, 123, 126
 palm nut vulture, 84, 85, 86, 87, 90
 red kite, 140, 141, 142, 143, 146
 saker falcon, 26, 27, 28, 29
 Steppe eagle, 66, 67, 68, 69, 72
- Trauma-related conditions, 197–217
 arthritis, 204, 205, 207
 fractures, 200–8, 211–17
 shotgun injury, 209, 210
 soft tissue injury, 208
 spinal luxation, 209
- Trichomonas gallinae*, 230, 231
- Trichomonosis, 231
- Trochlea
 gyr falcon, 63, 64
 palm nut vulture, 102
- Tympanic area
 common barn owl, 160
 Eurasian eagle owl, 176
- Eurasian honey buzzard, 104
 gyr falcon, 47
 Northern goshawk, 120
 palm nut vulture, 84
 red kite, 140
 saker falcon, 26
 Steppe eagle, 66
- Ulna
 common barn owl, 166
 Eurasian eagle owl, 184, 185, 186
 Eurasian honey buzzard, 108, 109, 110
 fractures, 201, 205, 212
 gyr falcon, 54, 55, 56, 57
 Northern goshawk, 128, 129, 130, 131
 palm nut vulture, 92, 93, 94
 red kite, 148, 149, 150
 saker falcon, 35, 36, 37
 Steppe eagle, 74, 75, 76, 77
- Ultrasound, 266, 267, 268
 Eurasian buzzard, 268
 tawny owl, 267
- Undigested material, impaction of, 221
- Urinary system, 24
- Urography, contrast radiography, 15, 17, 18
- Uropygial gland
 common barn owl, 164, 168
 Eurasian eagle owl, 182
 gyr falcon, 52
 Northern goshawk, 126
 red kite, 146
 saker falcon, 32
- gyr falcon, 50, 52
 Northern goshawk, 124, 126
 palm nut vulture, 88, 90, 96
 red kite, 144, 146
 saker falcon, 38
 Steppe eagle, 70, 72
- Ventrodorsal position, 3, 4
 wings, 4, 5
- Vertebral ribs
 common barn owl, 162
 Eurasian eagle owl, 180
 Eurasian honey buzzard, 114
 gyr falcon, 50, 52
 Northern goshawk, 124
 palm nut vulture, 88
 red kite, 144, 146
 saker falcon, 32
- White-tailed eagle (*Haliaeetus albicilla*), phalangeal joint, septic arthritis, 207
- Wings
 common barn owl, 166–7
 Eurasian eagle owl, 184–7
 Eurasian honey buzzard, 108–11
 fractures, 203
 gyr falcon, 54–7
 Northern goshawk, 128–31
 palm nut vulture, 92–5
 radiography
 stressed position, 5
 ventrodorsal position, 4, 5
 red kite, 148–51
 saker falcon, 34–7
 steppe eagle, 74–7
- Zygomatic arch see Jugal arch
- Ventriculus
 common barn owl, 162, 164
 Eurasian eagle owl, 182



VETERINARY PUBLISHERS OF CHOICE FOR GENERATIONS

For many years and through several identities we have catered for professional needs in veterinary education and practice. Saunders and Mosby, the leading imprints for veterinary medicine and Butterworth Heinemann, the leading imprint for veterinary nursing, are now part of Elsevier. Our expertise spreads across both books and journals and we continue to offer a comprehensive resource for veterinary surgeons and veterinary nurses at all stages of their career.

As the leading international veterinary publisher we take our role seriously and are proud to offer, in association with the British Veterinary Nursing association, two annual bursaries to veterinary nursing students. For further details please contact BVNA at www.bvna.org.uk.

To find out how we can provide you with the right book at the right time, log on to our website, www.elsevier-health.com or request a veterinary catalogue from the Marketing Department, Elsevier, 32 Jamestown Road, Camden, London NW1 7BY, tel: +44 20 7424 4200, emarketing@elsevier-international.com.

We are always keen to expand our veterinary list so if you have an idea for a new book please contact either Rita Demetriou-Swanwick, Associate Editor for Veterinary Nursing/Technology (r.demetriou@elsevier.com) or Joyce Rodenhuis, Commissioning Editor for Veterinary Medicine (j.rodenhuis@elsevier.com). We can also be contacted at Elsevier, The Boulevard, Langford Lane, Kidlington, Oxford OX5 1GB, UK (tel +44 1865-843000).



Have you joined yet?

Sign up for e-Alert to get the latest news and information.

Register for eAlert at www.elsevierhealth.com/eAlert Information direct to your Inbox

ELSEVIER DVD-ROM LICENCE AGREEMENT

PLEASE READ THE FOLLOWING AGREEMENT CAREFULLY BEFORE USING THIS PRODUCT. THIS PRODUCT IS LICENSED UNDER THE TERMS CONTAINED IN THIS LICENCE AGREEMENT ("Agreement"). BY USING THIS PRODUCT, YOU, AN INDIVIDUAL OR ENTITY INCLUDING EMPLOYEES, AGENTS AND REPRESENTATIVES ("You" or "Your"), ACKNOWLEDGE THAT YOU HAVE READ THIS AGREEMENT, THAT YOU UNDERSTAND IT, AND THAT YOU AGREE TO BE BOUND BY THE TERMS AND CONDITIONS OF THIS AGREEMENT. ELSEVIER LIMITED ("Elsevier"), EXPRESSLY DOES NOT AGREE TO LICENSE THIS PRODUCT TO YOU UNLESS YOU ASSENT TO THIS AGREEMENT. IF YOU DO NOT AGREE WITH ANY OF THE FOLLOWING TERMS, YOU MAY, WITHIN THIRTY (30) DAYS AFTER YOUR RECEIPT OF THIS PRODUCT RETURN THE UNUSED PRODUCT AND ALL ACCOMPANYING DOCUMENTATION TO ELSEVIER FOR A FULL REFUND.

DEFINITIONS As used in this Agreement, these terms shall have the following meanings:

"Proprietary Material" means the valuable and proprietary information content of this Product including without limitation all indexes and graphic materials and software used to access, index, search and retrieve the information content from this Product developed or licensed by Elsevier and/or its affiliates, suppliers and licensors.

"Product" means the copy of the Proprietary Material and any other material delivered on DVD-ROM and any other human readable or machine-readable materials enclosed with this Agreement, including without limitation documentation relating to the same.

OWNERSHIP This Product has been supplied by and is proprietary to Elsevier and/or its affiliates, suppliers and licensors. The copyright in the Product belongs to Elsevier and/or its affiliates, suppliers and licensors and is protected by the copyright, trademark, trade secret and other intellectual property laws of the United Kingdom and international treaty provisions, including without limitation the Universal Copyright Convention and the Berne Copyright Convention. You have no ownership rights in this Product. Except as expressly set forth herein, no part of this Product, including without limitation the Proprietary Material, may be modified, copied or distributed in hardcopy or machine-readable form without prior written consent from Elsevier. All rights not expressly granted to You herein are expressly reserved. Any other use of this Product by any person or entity is strictly prohibited and a violation of this Agreement.

SCOPE OF RIGHTS LICENSED (PERMITTED USES) Elsevier is granting to You a limited, non-exclusive, non-transferable licence to use this Product in accordance with the terms of this Agreement. You may use or provide access to this Product on a single computer or terminal physically located at Your premises and in a secure network or move this Product to and use it on another single computer or terminal at the same location for personal use only, but under no circumstances may You use or provide access to any part or parts of this Product on more than one computer or terminal simultaneously.

You shall not (a) copy, download, or otherwise reproduce the Product or any part(s) thereof in any medium, including, without limitation, online transmissions, local area networks, wide area networks, intranets, extranets and the Internet, or in any way, in whole or in part, except for printing out or downloading nonsubstantial portions of the text and images in the Product for Your own personal use; (b) alter, modify, or adapt the Product or any part(s) thereof, including but not limited to decompiling, disassembling, reverse engineering, or creating derivative works, without the prior written approval of Elsevier; (c) sell, license or otherwise distribute to third parties the Product or any part(s) thereof; or (d) alter, remove, obscure or obstruct the display of any copyright, trademark or other proprietary notice on or in the Product or on any printout or download of portions of the Proprietary Materials.

RESTRICTIONS ON TRANSFER This Licence is personal to You, and neither Your rights hereunder nor the tangible embodiments of this Product, including without limitation the Proprietary Material, may be sold, assigned, transferred or sublicensed to any other person, including without limitation by operation of law, without the prior written consent of Elsevier. Any purported sale, assignment, transfer or sublicense without the prior written consent of Elsevier will be void and will automatically terminate the Licence granted hereunder.

TERM This Agreement will remain in effect until terminated pursuant to the terms of this Agreement. You may terminate this Agreement at any time by

removing from Your system and destroying the Product and any copies of the Proprietary Material. Unauthorized copying of the Product, including without limitation, the Proprietary Material and documentation, or otherwise failing to comply with the terms and conditions of this Agreement shall result in automatic termination of this licence and will make available to Elsevier legal remedies. Upon termination of this Agreement, the licence granted herein will terminate and You must immediately destroy the Product and all copies of the Product and of the Proprietary Material, together with any and all accompanying documentation. All provisions relating to proprietary rights shall survive termination of this Agreement.

LIMITED WARRANTY AND LIMITATION OF LIABILITY Elsevier warrants that the software embodied in this Product will perform in substantial compliance with the documentation supplied in this Product, unless the performance problems are the result of hardware failure or improper use. If You report a significant defect in performance in writing to Elsevier within ninety (90) calendar days of your having purchased the Product, and Elsevier is not able to correct same within sixty (60) days after its receipt of Your notification, You may return this Product, including all copies and documentation, to Elsevier and Elsevier will refund Your money. In order to apply for a refund on your purchased Product, please contact the return address on the invoice to obtain the refund request form ("Refund Request Form"), and either fax or mail your signed request and your proof of purchase to the address indicated on the Refund Request Form. Incomplete forms will not be processed. Defined terms in the Refund Request Form shall have the same meaning as in this Agreement.

YOU UNDERSTAND THAT, EXCEPT FOR THE LIMITED WARRANTY RECITED ABOVE, ELSEVIER, ITS AFFILIATES, LICENSORS, THIRD PARTY SUPPLIERS AND AGENTS (TOGETHER "THE SUPPLIERS") MAKE NO REPRESENTATIONS OR WARRANTIES, WITH RESPECT TO THE PRODUCT, INCLUDING, WITHOUT LIMITATION THE PROPRIETARY MATERIAL. ALL OTHER REPRESENTATIONS, WARRANTIES, CONDITIONS OR OTHER TERMS, WHETHER EXPRESS OR IMPLIED BY STATUTE OR COMMON LAW, ARE HEREBY EXCLUDED TO THE FULLEST EXTENT PERMITTED BY LAW.

IN PARTICULAR BUT WITHOUT LIMITATION TO THE FOREGOING NONE OF THE SUPPLIERS MAKE ANY REPRESENTATIONS OR WARRANTIES (WHETHER EXPRESS OR IMPLIED) REGARDING THE PERFORMANCE OF YOUR PAD, NETWORK OR COMPUTER SYSTEM WHEN USED IN CONJUNCTION WITH THE PRODUCT, NOR THAT THE PRODUCT WILL MEET YOUR REQUIREMENTS OR THAT ITS OPERATION WILL BE UNINTERRUPTED OR ERROR-FREE.

EXCEPT IN RESPECT OF DEATH OR PERSONAL INJURY CAUSED BY THE SUPPLIERS' NEGLIGENCE AND TO THE FULLEST EXTENT PERMITTED BY LAW, IN NO EVENT (AND REGARDLESS OF WHETHER SUCH DAMAGES ARE FORESEEABLE AND OF WHETHER SUCH LIABILITY IS BASED IN TORT, CONTRACT OR OTHERWISE) WILL ANY OF THE SUPPLIERS BE LIABLE TO YOU FOR ANY DAMAGES (INCLUDING, WITHOUT LIMITATION, ANY LOST PROFITS, LOST SAVINGS OR OTHER SPECIAL, INDIRECT, INCIDENTAL OR CONSEQUENTIAL DAMAGES ARISING OUT OF OR RESULTING FROM: (I) YOUR USE OF, OR INABILITY TO USE, THE PRODUCT; (II) DATA LOSS OR CORRUPTION; AND/OR (III) ERRORS OR OMISSIONS IN THE PROPRIETARY MATERIAL.

IF THE FOREGOING LIMITATION IS HELD TO BE UNENFORCEABLE, OUR MAXIMUM LIABILITY TO YOU IN RESPECT THEREOF SHALL NOT EXCEED THE AMOUNT OF THE LICENCE FEE PAID BY YOU FOR THE PRODUCT. THE REMEDIES AVAILABLE TO YOU AGAINST ELSEVIER AND THE LICENSORS OF MATERIALS INCLUDED IN THE PRODUCT ARE EXCLUSIVE.

If the information provided in the Product contains medical or health sciences information, it is intended for professional use within the medical field. Information about medical treatment or drug dosages is intended strictly for professional use, and because of rapid advances in the medical sciences, independent verification of diagnosis and drug dosages should be made. The provisions of this Agreement shall be severable, and in the event that any provision of this Agreement is found to be legally unenforceable, such unenforceability shall not prevent the enforcement of any other provision of this Agreement.

GOVERNING LAW This Agreement shall be governed by the laws of England and Wales. In any dispute arising out of this Agreement, you and Elsevier each consent to the exclusive personal jurisdiction and venue in the courts of England and Wales.

System Requirements for DVD-ROM

This DVD will run on both Windows and Mac:

Microsoft Windows Users

To function properly, your computer should support at least an 800 x 600 pixels screen resolution, 256 colours, 128 MB RAM, and operate on Windows 2000 or above. Additionally, be sure your browser has "Show pictures" enabled. For Internet Explorer users, you will find the "Show pictures" option by selecting the following from your menu: Tools, Internet Options, Advanced, multimedia. If the "Show pictures" box is not checked, do so.

"QuickTime player" and "MRlcro" are needed to view the Movie files and DICOM images respectively. If your computer does not already have QuickTime installed, the latest version can be downloaded from <http://www.apple.com/quicktime>.

This software is designed to run with Internet Explorer 6.0, Netscape 7 or later and Firefox 1.x.

Instructions

1. If your system does not support Autorun, navigate to your DVD drive and double click on Birdsofprey.exe to begin.
2. "MRlcro" ("mrinstall.exe") can be installed from the software folder of the DVD.

Mac Users

Your computer should meet the following minimum requirements: 800x600 pixels screen resolution, 256 colours, 128 MB RAM, and MAC OS 9.2 or later operating system.

"QuickTime player" is needed to view the Movie files. If your computer does not already have QuickTime installed, the latest version can be downloaded from <http://www.apple.com/quicktime>.

"MRlcro", which is needed to view the DICOM images, is not designed to work on Mac and is Windows only.

This software is designed to run with Safari 1.x or later and Firefox 1.x. Refer to the help files for problems specific to the browser.

Instructions

1. Click on the DVD icon that appears on your desktop, and then select Birdsofprey.exe to open the application.
2. If the browser does not launch after clicking on the 'I Agree' button from the Birdsofprey.exe, open 'Index.htm' to launch the Home page.

Technical Support

Technical support for this product is available between 7.30 a.m. and 7.00 p.m. CST, Monday through Friday.

Before calling, be sure that your computer meets the minimum system requirements to run this software.

Inside the United States and Canada, call 1-800-692-9010.

Inside the United Kingdom, call 0-0800-6929-0100.

Rest of World, call +1-314-872-8370.

You may also fax your questions to +1-314-523-4932,

or contact Technical Support through e-mail: technical.support@elsevier.com.